PALEOMAGNETISM AND GEOCHEMISTRY OF MESOZOIC DIKES AND SILLS IN WEST-CENTRAL MASSACHUSETTS

BY SUZANNE A. McENROE

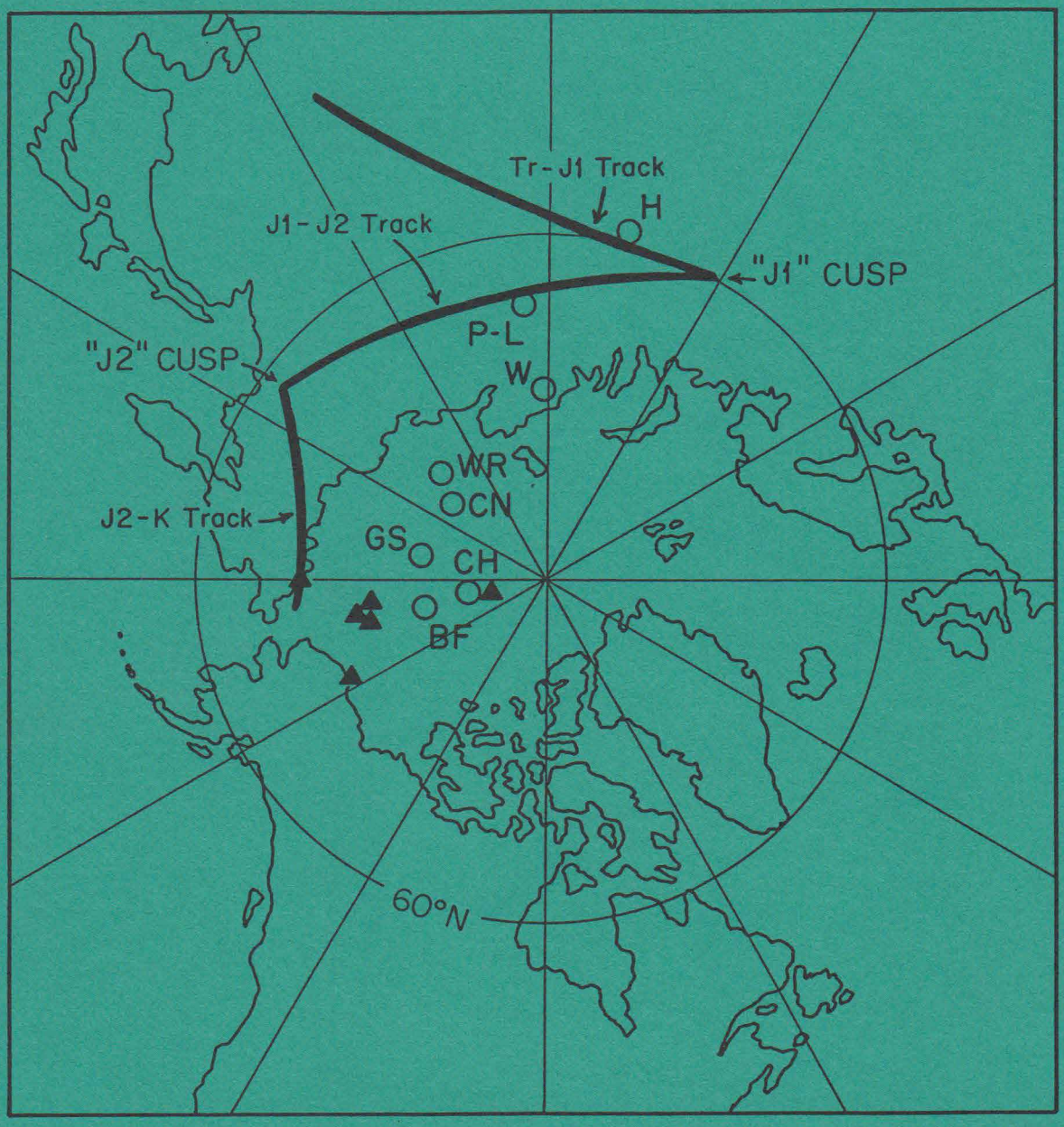

CONTRIBUTION NO. 64
DEPARTMENT OF GEOLOGY & GEOGRAPHY
UNIVERSITY OF MASSACHUSETTS
AMHERST, MASSACHUSETTS

PALEOMAGNETISM AND GEOCHEMISTRY OF MESOZOIC DIABASE DIKES AND SILLS IN WEST-CENTRAL MASSACHUSETTS

(M. S. Thesis)

by

SUZANNE A. McENROE

Contribution No. 64

Department of Geology and Geography

University of Massachusetts

Amherst, Massachusetts

September 1989

ACKNOWLEDGEMENTS

The author received assistance and support from numerous individuals. Professor L. Brown provided enthusiasm, guidance, field assistance even in rainy weather, and patience with long breaks for Irish coffee and sushi. Discussions with her helped develop this thesis and my understanding of paleomagnetism. Committee members Professors P. Robinson, J. M. Rhodes, and S. E. Haggerty contributed greatly by discussions and reviews of this manuscript. P. Robinson provided invaluable help in locating exposures of diabase dikes and sills, and with ground-magnetic traverses. Collection of oriented samples was assisted by I. Brown, L. Brown, P. Fallon, B. Martin, L. Reinen, P. Robinson, M. Roll, C. Shrady, K. Sioui, M. Valentine, and S. Berry. The following persons made specific contributions: M. Litterer, assistance with drafting; K. Hollocher and J. Sparks, help with the geochemical analyses; S. Field and T. Kudrikow, guidance and preparation of thin and polished sections; S. E. Haggerty, S. Field and K. Sioui, discussions and assistance in reflected-light microscopy; D. Elbert, microprobe analyses; N. Caffall, M. Shannon, and J. Leung, discussions on paleomagnetism; D. Scott, M. McEnroe, M. McPeak, A. McManamon, M. Nadakavukaren, M. Schmidt and my office mates for their friendship. Partial support for field work and thirty XRF analyses was provided by National Science Foundation grants EAR-84-10370 and EAR-86-08762 (to Peter Robinson) and Sigma Xi. J. M. Rhodes generously provided thirty XRF analyses, and maintained the analytical faculties of the Ronald B. Gilmore Memorial X-Ray Laboratory. Professor Kenneth Foland of Ohio State University generously provided thirteen K-Ar whole rock ages and one $^{40}Ar/^{39}Ar$ release spectrum. Major conclusions of this study would not have been possible without his contribution. Each of the above persons and institutions is gratefully acknowledged. This work is dedicated to my mother Mary. E. McEnroe and to my father, the late John H. McEnroe, without whose love and support this thesis would not have been possible.

TABLE OF CONTENTS

	Page
ACKNOWLEDGEMENTS	ii
TABLE OF CONTENTS	iii
LIST OF TABLES	iv
LIST OF FIGURES	v
ABSTRACT	viii

Chapter

1. INTRODUCTION	1
Tectonic Setting of Igneous Intrusions	1
Previous Work	5
Geology	5
Paleomagnetism	5
Geochemistry	5
Geochronology	6
Present Work	6
Massachusetts Geological Setting	6
Systems and Groups of Intrusions Studied	7
Holden System	10
Pelham-Loudville System	11
Loudville Group	11
Pelham Group, Millers Falls Area	12
Pelham Group, Isolated Intrusions	12
Pelham Group, Pelham Dike	13
Pelham Group, Southwest Quabbin Area	13
Ware System	14
Bliss Hill Group	15
Quabbin Reservoir Group	15
2. PETROGRAPHY	18
Introduction	18
Holden System	18
Pelham-Loudville System	21
Ware System	26
Bliss Hill Group	29
Quabbin Reservoir Group	31
Mineral Analyses	31
Holden System - Sample 1681-C	31
North Bliss Hill - Sample 4I4A	31
Chapman Island - Sample QB-4	36
3. GEOCHEMISTRY	38
Introduction	38
Major Elements	38
Trace Elements	53
Trace Element Spider Diagrams	69
Summary of Chemical Systems	74
4. PALEOMAGNETISM	77
Methods	77
Paleomagnetic Results	77
Alternating Field Demagnetization	78
Holden System	78

Pelham-Loudville System 78
Ware System 89
Bliss Hill Group. 89
Quabbin Reservoir Group 89
Thermal Demagnetization Studies 97
Magnetic Site Directions 97
Pole Positions 105
Polar Wander Paths 108
Rock Magnetic Properties. 108
IRM Acquisition Study 108
Methods 108
Results 110
Curie Temperature 110
Methods 110
Results 110

5. K-Ar RADIOMETRIC AGES. 114
Introduction 114
Results 114

6. COMMENTS ON DIABASE PETROGENESIS 119
Geochemical Discriminant Diagrams for Tectonic Settings 119
Major Element Concentrations in Relation to Petrography and Magma Evolution 127

7. CONCLUSIONS 129

REFERENCES 131

LIST OF TABLES

Page

2.1 Estimated modes of diabases from the Holden system 19
2.2 Estimated modes of diabases, Loudville group, Pelham-Loudville system. . . . 22
2.3 Estimated modes of diabases, Millers Falls area, Pelham group, Pelham-Loudville system. 23
2.4 Petrography of diabases, central area, Pelham group, Pelham-Loudville system 24
2.5 Estimated modes of diabases, southwest Quabbin area, Pelham group, Pelham-Loudville system. 25
2.6 Estimated modes of diabases from the Ware system. 27
2.7 Estimated modes of diabases of the Bliss Hill group. 30
2.8 Estimated modes of Chapman Island diabases, Quabbin Reservoir group 32
2.9 Estimated modes, Baffle Dam Island and south Baffle Dam diabases, Quabbin Reservoir group. 33
2.10 Representative electron probe analyses and structural formulae of plagioclase and pyroxenes in sample 1681C-1, a coarse interior sample from the Holden trap rock quarry in the Holden dike system. 34
2.11 Representative electron probe analyses and structural formulae of oscillatory-zoned orthopyroxene phenocryst in sample 4I4A-1 from the northern Bliss Hill dike, selected from 201 analyses. 35
2.12 Representative electron probe analyses and structural formulae of brown unknown inclusions in orthopyroxene phenocrysts in sample 4I4A-1 from the northern Bliss Hill dike. 37
3.1 Major- and trace-element analyses and CIPW norms of samples from the Holden system. 39

3.2 Major- and trace-element analyses and CIPW norms of samples from the Loudville group, Pelham-Loudville system 41
3.3 Major- and trace-element analyses and CIPW norms of samples from the Millers Falls area, Pelham-Loudville system 42
3.4 Major- and trace-element analyses and CIPW norms of samples from the Pelham dike and southwest Quabbin areas, Pelham Group, Pelham-Loudville system 44
3.5 Major- and trace-element analyses and CIPW norms of samples from the Ware system 46
3.6 Major- and trace-element analyses and CIPW norms of samples from the Bliss Hill and Quabbin Reservoir groups of intrusions and the Gassetts, Vermont, lamprophyre. 48
4.1 Summary of site mean directions and statistical parameters for Central Massachusetts Mesozoic diabases 99
4.2 Summary of virtual geomagnetic poles (VGP) and statistical parameters for the central Massachusetts Mesozoic diabases 102
4.3 Mean pole positions for the Mesozoic diabases in central Massachusetts 103
4.4 Pole positions for northern and southern Appalachian Mesozoic igneous rocks 107
5.1 Summary of whole-rock K-Ar results 115

LIST OF FIGURES

Page
1.1 Location map showing the distribution of exposed and covered Mesozoic basins of eastern North America 2
1.2 Paleotectonic reconstruction of the southern North Atlantic region at the Triassic-Jurassic boundary. 3
1.3 Time-stratigraphic correlation chart of Newark strata in eastern North America based on palynofloral zones and extrusive horizons. 4
1.4 Setting of Mesozoic basins in Massachusetts in relation to major tectonic features, mainly of Paleozoic age. 8
1.5 Map showing geographic grouping of Mesozoic dikes and sills in central Massachusetts 9
1.6 Ground-magnetic profiles over dike at Sawmill Hills with normal polarity (positive anomaly) and over sill at Chapman Island with reversed polarity (negative anomaly) 16
3.1 Diagram of weight percent Na_2O+ K_2O and weight percent SiO_2, showing the discriminant line for Hawaiian alkali olivine basalts and tholeiites established by Macdonald and Katsura (1964). 50
3.2 Diagram of weight ratio $Fe_2O_3/(Fe_2O_3+MgO)$ versus wt.% TiO_2. 51
3.3 Plot of wt.% TiO_2 versus wt.% MgO.. 52
3.4 Plot of wt.% Fe_2O_3 versus wt.% MgO.. 54
3.5 Plot of wt.% Al_2O_3 versus wt.% MgO 55
3.6 Plot of wt.% K_2O versus wt.% MgO 56
3.7 Plot of V ppm versus Zr ppm. 57
3.8 Plot of Y ppm versus Zr ppm 58
3.9 Plot of Y ppm versus Sr ppm. 60
3.10 Plot of wt.% P_2O_5 versus Y ppm. 61
3.11 Plot of Ti ppm versus Nb ppm. 62
3.12 Plot of Cr ppm versus Zr ppm 63
3.13 Plot of Cr ppm versus Ni ppm 64
3.14 Plot of Cr ppm versus wt.% MgO.. 65
3.15 Plot of Ni ppm versus wt.% MgO 66

3.16 Plot of Ni ppm versus Nb ppm 67
3.17 Plot of Zr ppm versus Nb ppm 68
3.18 Spider diagram of chondrite-normalized trace element concentrations in the Holden system 70
3.19 Spider diagram of chondrite-normalized trace element concentrations in the Pelham-Loudville system 71
3.20 Spider diagram of chondrite-normalized trace element concentrations in the Ware system 72
3.21 Spider diagram of chondrite-normalized trace element concentrations in the Bliss Hill and Quabbin Reservoir diabases 73
3.22 Spider diagram of chondrite-normalized trace element concentrations for all the central Massachusetts diabases 75
4.1 Normalized intensity plot for representative samples from the Holden system 79
4.2 Normalized intensity plot for representative samples from the Pelham-Loudville system 80
4.3 Normalized intensity plot for representative samples from the Ware system . . . 81
4.4 Normalized intensity plot for representative samples from the Quabbin Reservoir diabases 82
4.5 Vector end-point diagram of alternating field demagnetization study of a sample from the Holden system, site 1688, sample C. 83
4.6 Vector end-point diagram of alternating field demagnetization study of a sample from the Holden system, site Fiskdale, sample 2 84
4.7 Vector end-point diagram of alternating field demagnetization study of a sample from the Holden system, site 1683 85
4.8 Vector end-point diagram of alternating field demagnetization study of a sample from the Holden system, site Quinapoxet, sample 6 86
4.9 Vector end-point diagram of alternating field demagnetization study of a sample from the Holden system, site Quinapoxet, sample 3 87
4.10 Vector end-point diagram of alternating field demagnetization study of a sample from the Pelham-Loudville system, site Butterworth, sample 2 88
4.11 Vector end-point diagram of alternating field demagnetization study of a sample from the Pelham-Loudville system, site North Valley Rd., sample 6 90
4.12 Vector end-point diagram of alternating field demagnetization study of a sample from the Pelham-Loudville system, site Lake Pleasant 91
4.13 Vector end-point diagram of alternating field demagnetization study of a sample from the Pelham-Loudville system, site Laird 1, sample 7 92
4.14 Vector end-point diagram of alternating field demagnetization study of a sample from the Ware system, site Barre, sample 3 93
4.15 Vector end-point diagram of alternating field demagnetization study of a sample from the Ware system, site Ware, sample 4 94
4.16 Equal area net of alternating field demagnetization study of a sample from the Ware system, Fox Hill site, sample 1-2 95
4.17 Vector end-point diagram of alternating field demagnetization studies of samples from Cretaceous sites 96
4.18 Thermal demagnetization vector end-point diagram from the Ware system, site Fox Hill, sample 1-1 98
4.19 Equal area projections of site-mean magnetic directions from the central Massachusetts diabases studied 101
4.20 Mean magnetic directions of central Massachusetts diabase systems plotted on a equal area net with a_{95} cones of confidence shown 104
4.21 Mesozoic apparent polar wander path for North America, after May and Butler (1986) 106

4.22 Histogram of peak alternating field demagnetizations levels from the central Massachusetts diabases 109
4.23 IRM saturation study of samples from Baffle Dam Island 111
4.24 IRM saturation study of samples from Cape Neddick Gabbro, Maine 112
4.25 Curie determination curve of titanomagnetite from the Chapman Island diabase 113
5.1 Diagram showing the K-Ar ages from this study and others recently published by Foland et al. (1987) for New England and adjacent Quebec 116
5.2 Mesozoic igneous provinces in New England, modified from McHone and Butler (1984) 118
6.1 Ti-Zr-Y discriminant diagram, after Pearce and Cann (1973) with plot areas of Massachusetts diabase systems and groups shown 120
6.2 Discriminant diagram of Tippm/1000 versus V ppm, after Shervais (1985) . . . 121
6.3 Log-log plot of Ti ppm versus Cr ppm 123
6.4 Discriminant diagram of Zr/Y versus Zr ppm after Pearce and Norry (1979) modified by Pearce (1983) 124
6.5 Discriminant diagram for the trace elements Nb, Zr, and Y (after Meschede,1986) indicating tectonic settings for tholeiites and all types of within-plate basalts. 125
6.6 Comparison of compositions of central Massachusetts diabases against experimental liquidus phase relations using the method of Grove et al. (1982) 128

ABSTRACT

Diabases in central Massachusetts were investigated using paleomagnetic, geochemical, petrographic and radiometric techniques. Forty paleomagnetic sites and sixty geochemical samples were collected. These diabases, all previously considered to be Early Jurassic, range from Early Jurassic to Early Cretaceous.

The paleomagnetic sites were grouped according to geochemical signatures which indicate distinct magmatic sources for each chemical system. According to the major-element chemistry all the diabases are tholeiites. The C.I.P.W. norms show the rock compositions fall within the quartz-tholeiite and olivine-tholeiite volumes of the basalt tetrahedron. The three Jurassic diabase systems fall broadly into the fields of the three quartz-normative chemical types for eastern North American diabases of Wiegand and Ragland (1970). Of these three quartz-normative types, high TiO_2, low TiO_2 and high Fe_2O_3, only the high-TiO_2 quartz-normative type had previously been reported from Massachusetts. The Cretaceous diabases fall outside these fields. Trace-element chemistry further refines the subdivisions of the Massachusetts diabases into four chemical systems. The ratios of the incompatible elements Zr and Nb in the different systems are distinct: the Holden system has an average Zr/Nb ratio of 13, the Pelham-Loudville system of 19, the Ware system of 16, and the Cretaceous diabases of 7. These distinctions are repeated in other incompatible element diagrams. Each of these systems produces a distinct pattern on spider diagrams due to the enrichment or depletion of the elements plotted. Of the Jurassic systems, the Holden system is the most enriched in Sr, Ce, Zr, Cr, and Ni and has a positive Sr anomaly; the Pelham-Loudville is enriched in TiO_2, Y, and V but has a striking negative Sr anomaly; and the Ware system is lowest in Zr, Nb and has a striking negative TiO_2 anomaly. The Cretaceous Bliss Hill and Quabbin Reservoir diabases are chemically distinct, and are enriched in Ni, Cr, Sr, Ba, Zr, Nb and low in V compared to the Jurassic diabases and have a positive Sr anomaly.

All the paleomagnetic samples were subjected to alternating field demagnetization techniques. Representative samples from each system were cleaned thermally and the directions obtained confirmed the alternating field demagnetization directions. Of the forty sites sampled, thirty-two were found to be stable. Based on of the North American Apparent Polar Wander Path (APWP) of May and Butler (1986), the Early Jurassic Holden diabase system ($I = 28.1^0$, $D = 15.2^0$, $n = 4$, $a95 = 3.3^0$) plots on the Triassic-Jurassic track prior to the J1 cusp. The Pelham-Loudville system ($I = 32.9^0$, $D = 5.7^0$, $n=19$, $a95=2.2^0$) is interpreted to be younger and plots on the J1-J2 track after the J1 cusp. The Ware system is interpreted as Middle Jurassic ($I= 45^0$, $D = 5^0$, $n =5$, $a95 = 2^0$) but is displaced northward from May and Butler's APWP, but not from Irving and Irving's APWP (1982). The Early Cretaceous diabases, the Quabbin Reservoir diabases ($I= -61.6^0$, $D = 168.7^0$, $n=2$, $a95 = 4^0$) (136-119 m.y. by K-Ar), of reversed polarity, and the Bliss Hill north diabase of normal polarity (121 m.y.), are displaced north of the APWP. The Bliss Hill south diabase yields a transitional direction and is dated at 152 m.y. (K-Ar). These data, combined with the success of using the chemical signatures of the diabases as a means of grouping them, indicate that previous groupings of the Jurassic Newark Supergroup igneous rocks of eastern North America need to be reevaluated. More importantly, these data call attention to the critical need for reexamination of the Mesozoic APW path for North America.

The occurrence of Cretaceous magmatic activity in central Massachusetts extends the New England - Quebec igneous province of McHone and Butler (1984) south into Massachusetts. The Cretaceous diabases in Massachusetts are the first reported tholeiites from this province.

CHAPTER 1

INTRODUCTION

Tectonic Setting of Igneous Intrusions

The Mesozoic basins of eastern North America occur in a linear zone extending from Florida to the Grand Banks off Newfoundland (Hubert et al., 1978) (Figure 1.1). The basins were formed by the extensional forces related to the breakup of Pangea, the separation of North America from Africa and Europe, and the formation of the present day Atlantic Ocean (Figure 1.2). In some areas the rifting may have taken place along low angle detachment faults giving rise to half grabens along conjugate sets of lower and upper plate margins (Manspeizer, 1988). In other areas, such as the Newark basin, it has been suggested that Mesozoic faulting reactivated older Paleozoic low angle faults (Ratcliffe and Burton, 1984). Magmatism associated with this rifting produced numerous basalt flows, and intrusive dikes and sills. The flows are exposed in Mesozoic basins, but abundant dikes and sills intrude country rocks outside the basins. Dike swarms occur along the eastern margin of North America. The emplacement of some of the diabase dikes along the east coast coincides with the rifting of the supercontinent, Pangea. King (1961) first described the geographical distribution of these diabase dikes and noted a systematic change in orientation of the diabases along the coast. May (1971) proposed that the circum-Atlantic Mesozoic dikes were emplaced along radial fractures that are perpendicular to a minimum principle stress axis. Based on their reactivation model, Ratcliffe and Burton (1984) would suggest, that the dike and stress orientations are locally controlled by the configuration of master faults in the basement rocks. Diabases associated with rifting can provide important evidence as to the nature and sequence of these processes, and about the crust and mantle conditions during rifting.

The temporal sequence of events that led to the formation of the Atlantic Ocean has been difficult to constrain accurately. The onshore northern Newark basins were filled with fluvial sandstones, interbedded lavas and lacustrine sediments limited to the Triassic and early Jurassic. At this time offshore there was a major unconformity as documented in the COST G-2 well (Manspeizer and Cousminer, 1988) (Figure 1.3). This major unconformity marks the change from synrift to postrift deposition. The transition from rifting to drifting, based on the sea-floor spreading record, was at approximately 175 m.y., assuming a constant spreading rate prior to the Tithonian. The end of rifting is believed to have coincided with the final igneous event in the onshore rift basins (Klitgord and Schouten,1986).

Offshore late middle Jurassic igneous activity at 140 m.y. was restricted to Georges Bank. The main period of offshore igneous activity was concentrated in the Aptian/Barremian, at 120 m.y. This activity consisted of dike swarms in the Baltimore canyon, dikes, sills and strato volcanoes in the Scotia shelf, and strato volcanoes in the Grand Banks (Jansa and Pe-Piper, 1988).

Regional tectonic events that were synchronous with major phases of igneous activity in the Mesozoic are: the initial rifting of Pangea at 200-195 m.y., the beginning of sea-floor spreading between North America and Africa at about 175 m.y., the initiation of the rifting in the Labrador-Greenland region 140 m.y., the separation of the continental plates between Iberia and the Grand Banks 115 m.y., and the separation of the Greenland and European continental plates 83-92 m.y (Jansa and Pe-Piper, 1988; Klitgord,1988). The majority of igneous activity occurred along old fracture zones that appear to have been reactivated, and/or along new fractures or fracture zones in the continental crust. The new fracture zones resulted from the changes in stress patterns caused by a change in plate motion direction.

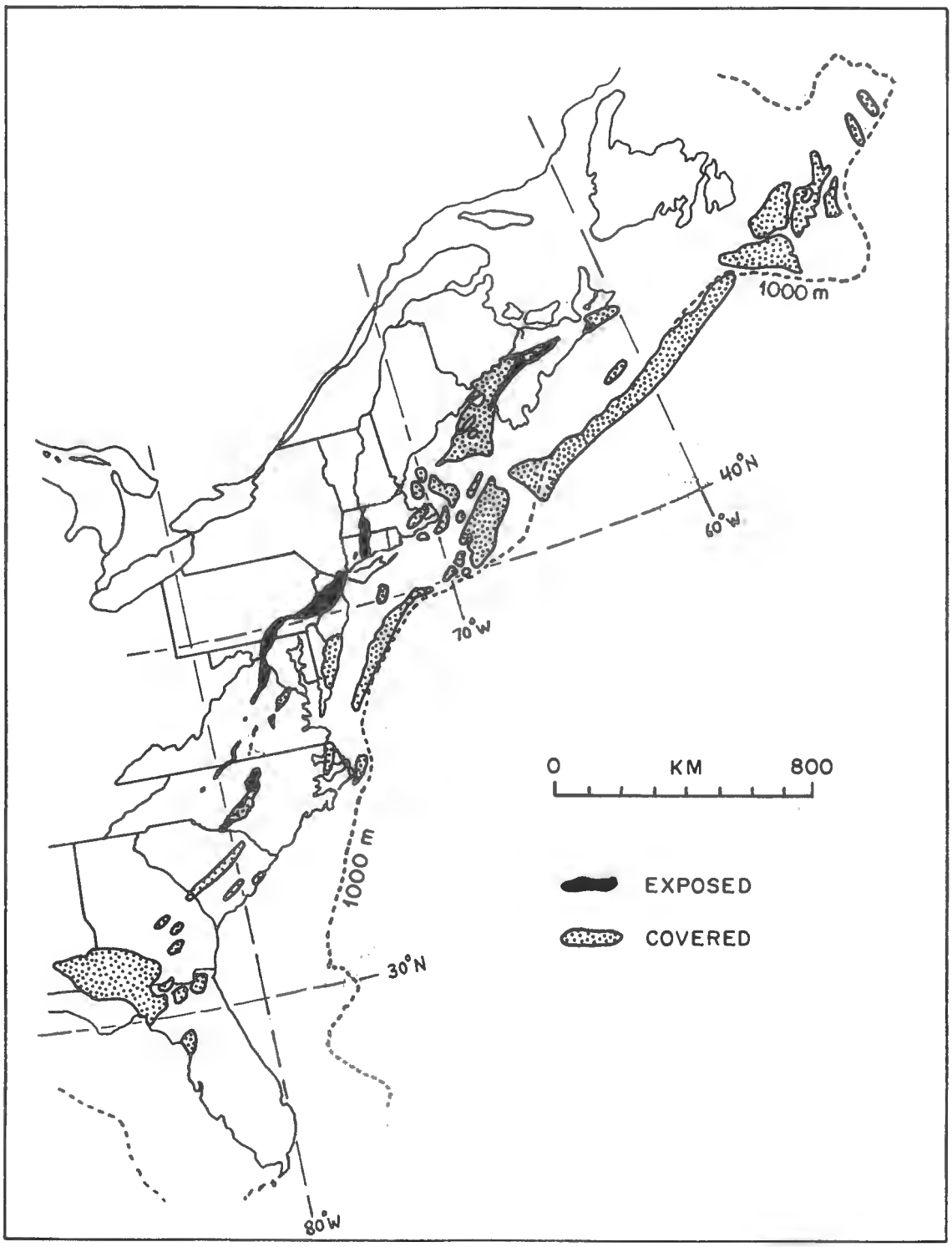

Figure 1.1 Location map showing the distribution of exposed and covered Mesozoic basins of eastern North America. From Hubert (1978).

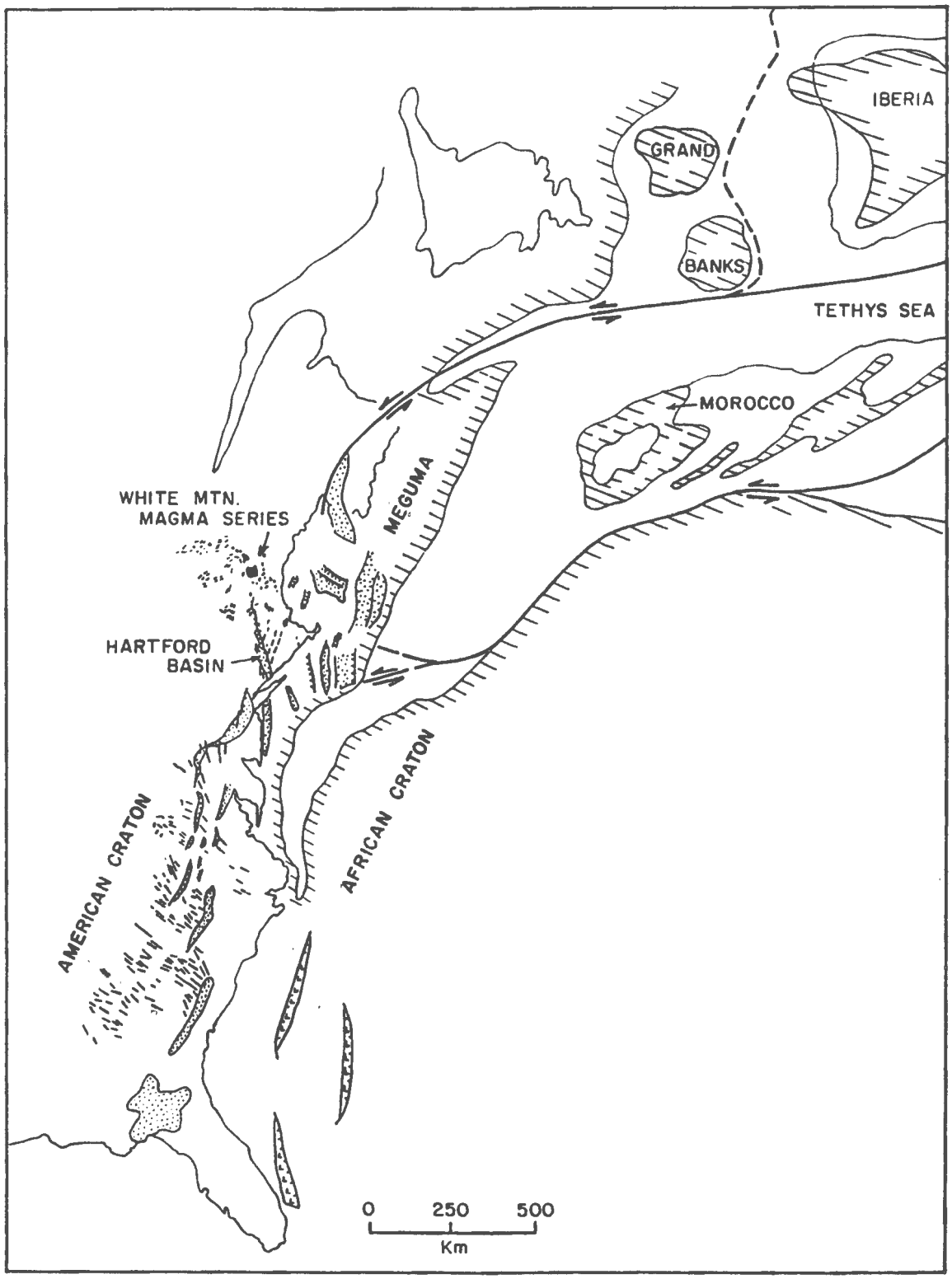

Figure 1.2 Paleotectonic reconstruction of the southern North Atlantic region at the Triassic-Jurassic boundary. Boundary between land and sea marked by ruled pattern. Dotted pattern shows North American Mesozoic basins. Dikes and other intrusions in fine black patterns. From Manspeizer (1988).

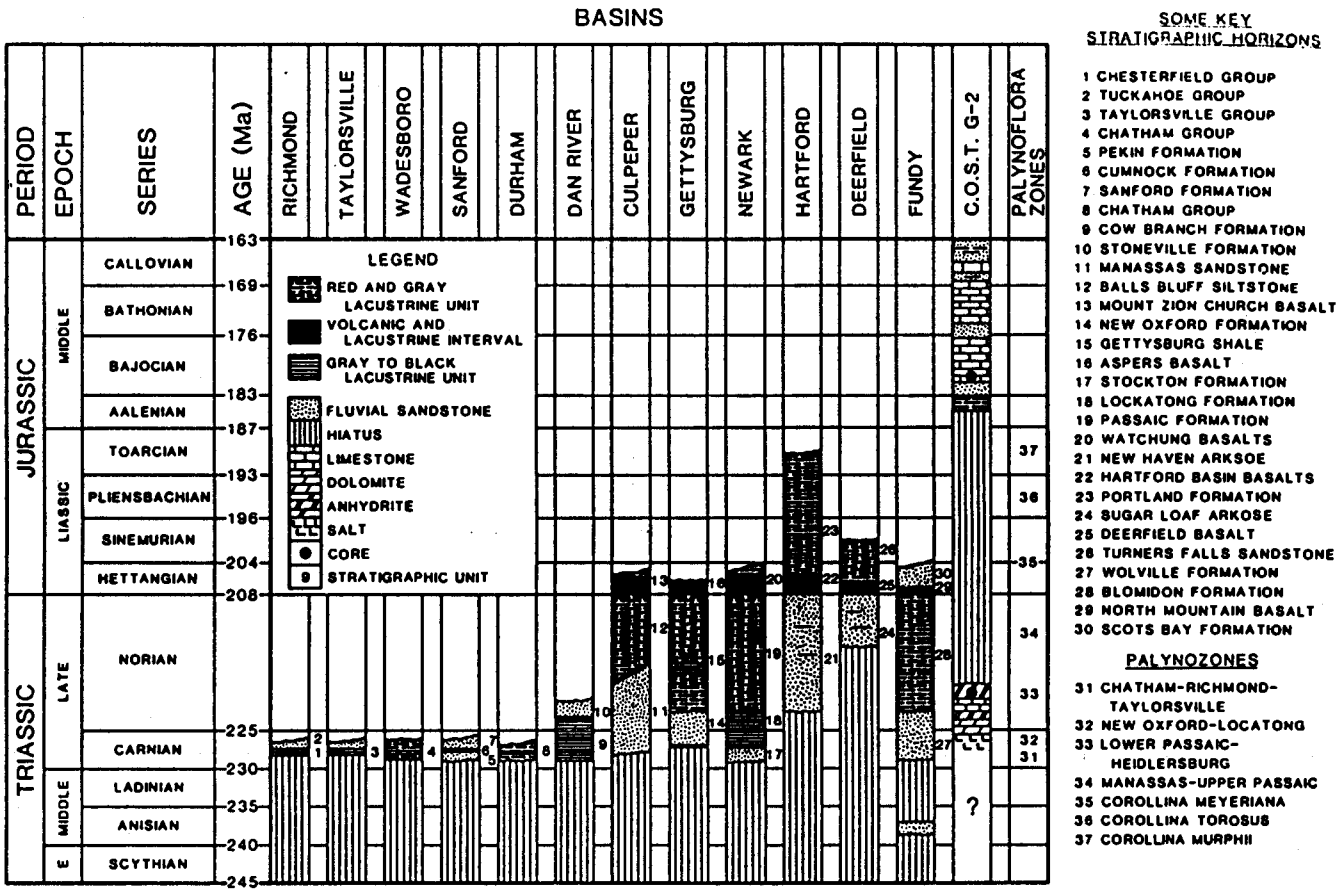

Figure 1.3 Time-stratigraphic correlation chart of Newark strata in eastern North America based on palynofloral zones and extrusive horizons. From Manspeizer and Cousminer (1988).

Previous Work

Geology

Geological and structural mapping of the dikes and sills of this study was done by a wide variety of workers, and was compiled and referenced by Zen et al. (1983). Rather than give a summary here, references are given with the detailed locality descriptions below.

Paleomagnetism

The eastern North America diabases and basalts of the Newark Supergroup have been an object of paleomagnetic studies for the last thirty years. The magnetic research on these rocks includes that of Bowker (1960); Opdyke (1961); deBoer (1967, 1968); Beck (1972); Smith (1976); Smith and Noltimier (1979); Brown (1979,1988); and Smith (1986). Some have produced conflicting results, and certain studies, particularly the older ones, are no longer considered valid. Others have produced acceptable and consistent information. To date there has been surprisingly little paleomagnetic work on the intrusive diabases in west-central Massachusetts, even though there are abundant outcrops. To the south, in Connecticut, excellent paleomagnetic work on the diabase intrusions by Smith and Noltimier (1979) produced valuable data that is widely used in calculating a polar wander path for North America in the Mesozoic. Smith and Noltimier investigated possible groupings of virtual geomagnetic pole (VGP) data. The paleomagnetic data combined with $^{40}Ar/^{39}Ar$ age determinations (Sutter and Smith, 1979) led them to suggest that there were two pulses of igneous activity at 190 m.y. and 175 m.y. Using their own results and other published data, Smith and Noltimier (1979) calculated an older Newark I pole and a younger Newark II pole. The Newark Trend I and II poles have become widely accepted as representative pole positions for the Early Jurassic. There are some inherent problems with the Newark groupings. Smith and Noltimier (1979) grouped all the lava flows and most of the large intrusions together, based on similar pole positions for the units in Connecticut. This forms the basis for the older Newark I pole. All the "narrow" dikes and sills in Connecticut, Pennsylvania and Maryland constitute the younger Newark II pole. The present study has produced both confirmations of and disagreements with their interpretations.

Geochemistry

Weigand and Ragland (1970) characterized the diabases throughout the eastern North American province as tholeiites. In New England the diabases were studied in Rhode Island, New Hampshire and Maine by Peirce (1970), McHone and Trygstad (1982) and Hermes et al. (1982). The diabases from the central Newark basin in west-central New Jersey and eastern Pennsylvania were studied by Husch et al. (1984) and Husch and Roth (1988). The Watchung basalts of the Newark basin were studied by Puffer and Lechler (1980). Puffer et al. (1981) did a limited reconnaissance study (39 samples) of the Talcott, Holyoke, and Hampden flows of Massachusetts and Connecticut, of which only 23 samples were found to be unaltered. Philpotts and Reichenbach (1983), based on melting experiments, concluded that there are successively lower liquidus temperatures for the Talcott, Holyoke and Hampden flows respectively, and that these flows are related by fractional crystallization. Philpotts and Martello (1986) concluded that the intrusives in Connecticut are feeder dikes for the three flows, the Talcott, Holyoke, and Hampden. Based on the number of oscillations in the lacustrine sediments between the Talcott, Holyoke, and Hampden flows, Olsen, in a personal communication cited by Puffer and Phlipotts (1988), concluded that the Holyoke flow is 138,000 years younger than the Talcott Basalt and the Hampden is 345,000 years younger than the Holyoke Basalt. If this is true, then it is unlikely that the Newark I and II poles can be correct, because they would represent magnetic directions that are about 15 m.y. apart. The most extensive geochemical

study on the Holyoke flow in Massachusetts was by Heinrich (1980). Peachy (1983) studied five diabase outcrops from the Pelham group. The temporal and genetic relationships between the diabase intrusions and the flows are not yet adequately understood and appear to be more complex than earlier thought.

Geochronology

Geochronological studies of these basalts and diabases by K/Ar and Ar/Ar methods have met with mixed results along the entire length of the Appalachians. The ages range from greater than 1 b.y. to 119 m.y. though generally the range is from 225 to 165 m.y. Sutter (1985) in a progress report on the Mesozoic diabases and basalts states that, other than being a subject of geochronological research for two decades " they have also proven to be among the most difficult crystalline rocks of the earth's crust to date accurately." Numerous interpretations of the complex problem of excess Ar have been given by many authors (e.g. Sutter, 1985). To complicate this problem there are suggestions that there has been Ar loss to the systems (Armstrong and Besancon, 1970) due to zeolite facies burial metamorphism. It is probable that more than one cause exists for the anomalous behavior of the K-Ar isotopic system in these rocks.

The age dating on the flows in the Connecticut Valley has been inconclusive Recent work by Seidemann et al. (1984) yielded the oldest date on the stratigraphically youngest flow, with tens of millions of years between flows. Olsen (1986), based on correlation of lake cycles in the Newark Supergroup sections to the Milankovitch cycles seen in Quaternary sediments, suggests all magmatic activity took place in less than 2 m.y. Given the present state of geochronological research in these basalts and diabases, accurate paleomagnetic studies are increasingly important in our understanding of the Mesozoic tectonics and igneous activity of the Appalachians.

Present Work

Field collecting of cores and oriented blocks for paleomagnetic and geochemistry work was begin in summer 1985 and completed in July 1987. Sites were located on the basis of the Bedrock Geologic Map of Massachusetts (Zen et al., 1983) and detailed field maps and notes kindly supplied by various geologists in the region. Field observations, pace and compass maps and structural measurements were supplemented in a few areas by ground-magnetic profiles done with a Sharp total-intensity nuclear-precession magnetometer. Supplemental collecting of lamprophyres in Vermont and gabbros in Maine was done in June and July 1987. Paleomagnetic and rock magnetism studies were done at the University of Massachusetts throughout the collecting, with final checking extending to January 1988. Geochemical samples for X-ray fluorescence analysis were prepared in fused glass discs and run for major elements periodically from 1987 through February 1988. Pressed powder samples for trace element analyses were prepared in July 1987, run for molybdenum-tube traces in September 1987 through January 1988, and for gold-tube traces in April 1988. Samples for K-Ar dating were selected for Prof. K. E. Foland in June 1987 and November 1988, and were run in his mass spectrograph and chemistry labs at Ohio State University. The details of the various techniques are given in appropriate chapters below.

Preliminary results of this work, summaries of results, and implications for future research were presented at one regional meeting, two national meetings, and one national symposium (McEnroe and Brown, 1987; McEnroe et al., 1987; McEnroe, 1988; McEnroe and Brown, 1988).

Massachusetts Geological Setting

Forty sites from diabase outcrops in west-central Massachusetts were sampled for paleomagnetic and geochemical studies. These diabase dikes and sills intruded highly deformed metamorphic rocks of Late Precambrian through Devonian age (Zen et al.,1983).

The metamorphic rocks (Figure 1.4) are arranged in three north-northeast trending belts, from west to east, the Connecticut Valley synclinorium, the Bronson Hill anticlinorium, and the Merrimack synclinorium. The Connecticut Valley synclinorium is dominated by metamorphosed sedimentary and volcanic rocks of Cambrian through Devonian age (Zen et al.,1983). The Bronson Hill anticlinorium is an en echelon series of gneiss domes exposing late Precambrian to Middle Ordovician feldspathic gneisses and related rocks, mantled by Middle Ordovician to Early Devonian stratified cover. It extends from Maine to Long Island Sound. The Merrimack synclinorium includes Silurian to Lower Devonian metamorphosed sedimentary rocks that have been intruded by Devonian tonalite, granite, and smaller bodies of gabbro and diorite.

In Massachusetts the eastern margin of the Connecticut Valley synclinorium and the western margin of the Bronson Hill anticlinorium are unconformably overlain by Upper Triassic and Lower Jurassic sedimentary rocks and basaltic volcanics of the Connecticut Valley Mesozoic basins, which are localized mainly along the west side of the Connecticut Valley border fault, (Figure 1.5). This major west-dipping listric normal fault is estimated to have had about 5 km of vertical displacement in northern Massachusetts (Robinson et al., 1986) and as much as 10 km near the Connecticut State line. In matching the metamorphic rocks on opposite sides of the listric normal fault, Elbert (1986) suggests a 16 degree rotation of the western block relative to the eastern block. Based on slickensides the net slip was approximately down the dip of the fault (Ashenden, 1973) and the rotation axis essentially horizontal and trending N30 E parallel to the fault trace. This appears to be the maximum Mesozoic rotation that has been proposed for any large block of basement rock in this part of New England. In view of the north-trending rotation axis, which is subparallel to the magnetic declinations of most of the Mesozoic intrusions, this rotation has only a minor effect on paleomagnetic orientations, particularly those with low inclinations. Indeed, this geometric combination has so far prevented paleomagnetism from successfully being used to measure fault rotations. Knowing that this represents an extreme example, it is probable that the Jurassic dikes and sills away from this major fault have not been rotated by any major amount that would be significant to the paleomagnetic studies, and the Cretaceous intrusions would have been affected even less. Rotation along the border fault, which is the extreme condition, results in a difference in magnetic directions of 2^0 to 3^0, which is negligible. Therefore all paleomagnetic directions are reported in situ.

Systems and Groups of Intrusions Studied

On the basis of geography, geochemistry, paleomagnetism and radiometric ages the diabase intrusions cutting crystalline metamorphic and igneous rocks in west-central Massachusetts have been divided into systems and groups. By a system is meant a series of intrusions that can be inferred to have formed more or less synchronously, under similar conditions from chemically related magmatic sources. The justification for the grouping is based on detailed data given later in the thesis.

In collecting samples for this study several numbering systems were used. Some localities were assigned the same field numbers used by previous regional mappers Peter Robinson, R.D. Tucker, and Robert Balk. The Robinson numbers are all a combination of one letter and two digits or three digits such as C26, 8C9, 4I4, or 126. The Tucker locations all have four digits such as 1681, commonly followed by a letter suffix. The single Balk locality, Balk's original hand sample is B44 at south Baffle Dam. For the remaining localities, the author applied her own system of two letters and one digit, or three letters, thus BH-1, NF, SMW2, QP, EDH, and QX-3 (Figure 1.5).

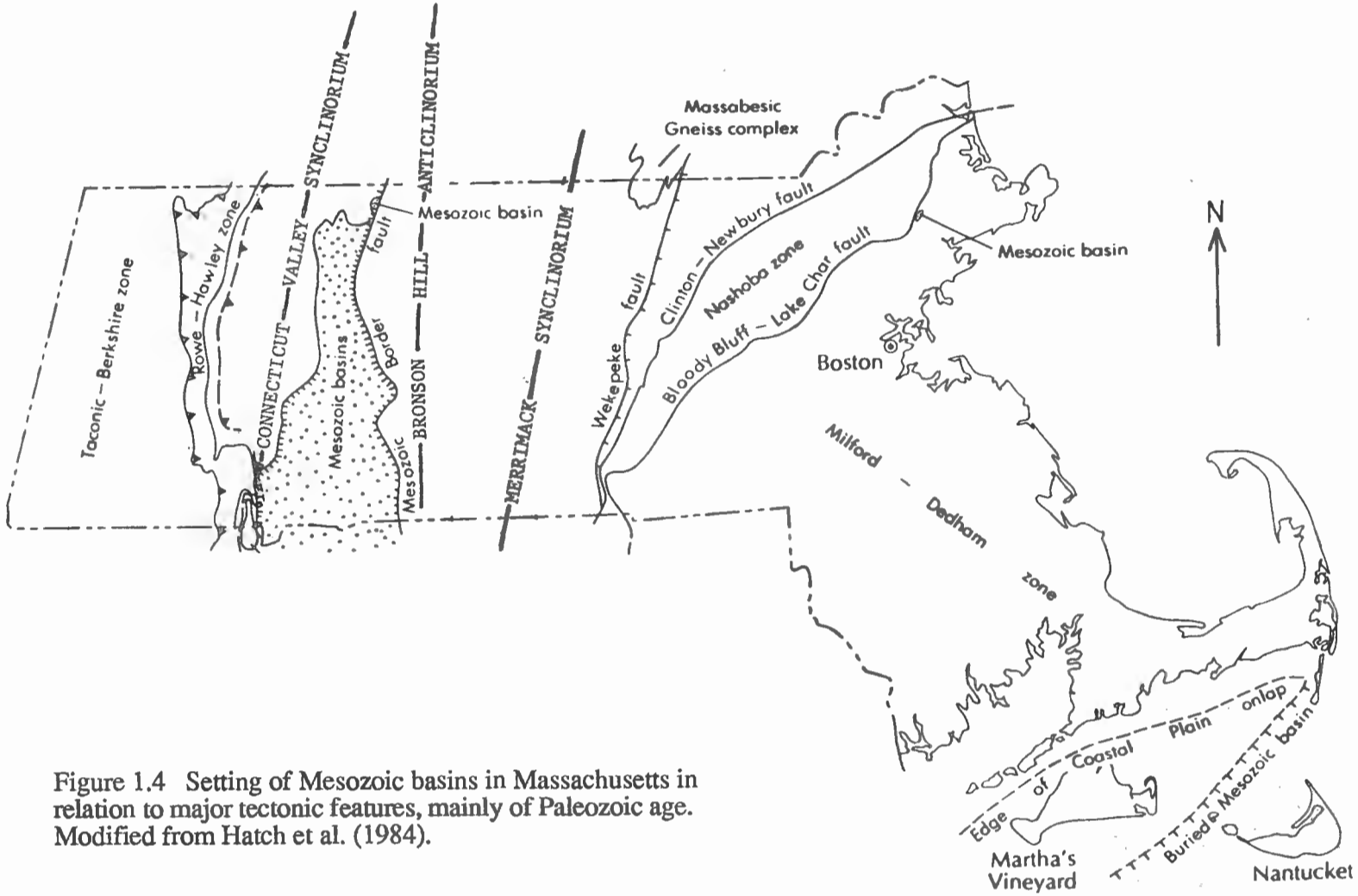

Figure 1.4 Setting of Mesozoic basins in Massachusetts in relation to major tectonic features, mainly of Paleozoic age. Modified from Hatch et al. (1984).

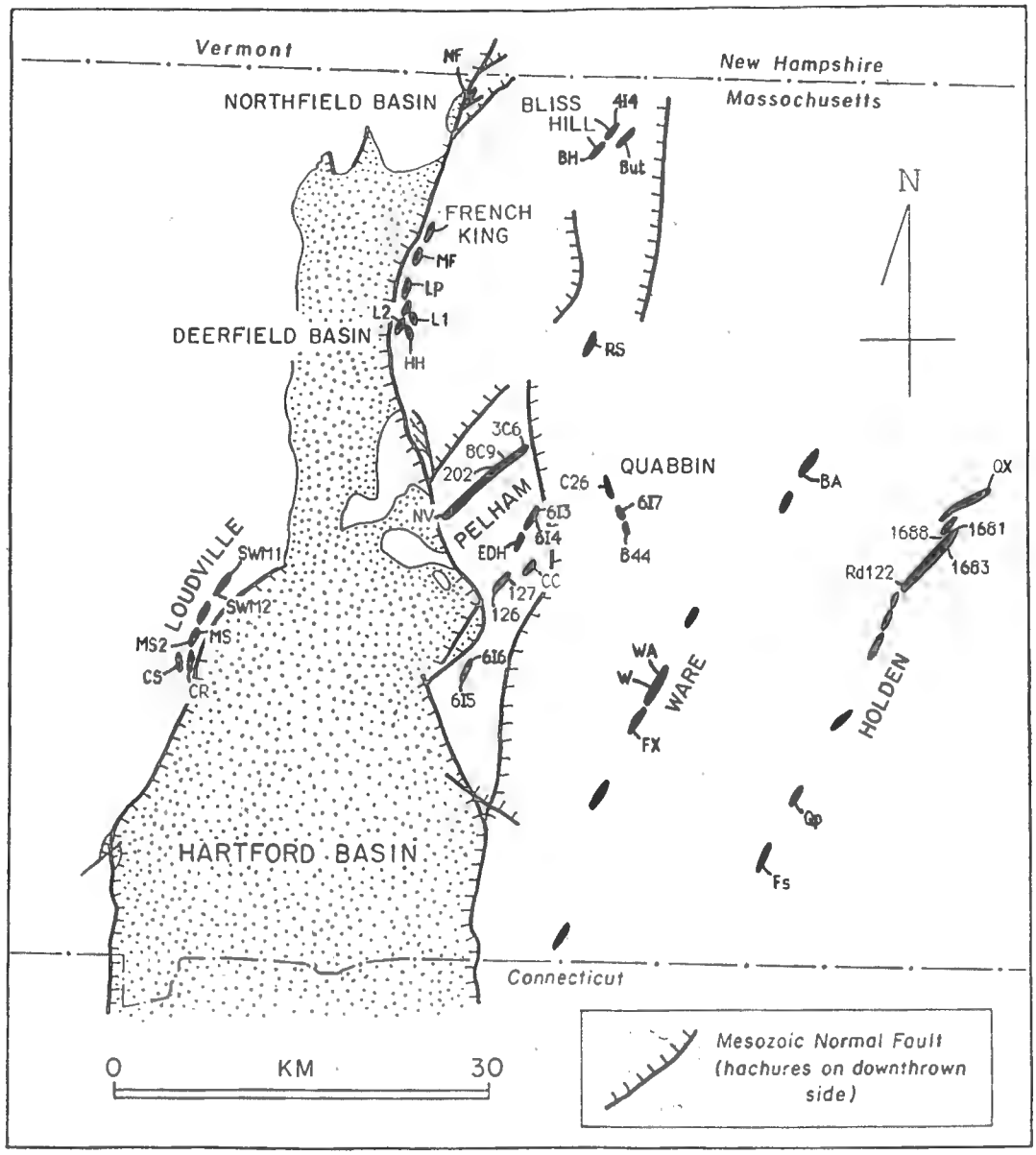

Figure 1.5 Map showing geographic grouping of Mesozoic dikes and sills in central Massachusetts. Individual diabase localities are labelled as given in text and tables.

Holden System

The dikes of the Holden system in Massachusetts extend in a NE-SW trending en echelon pattern for 175 km from the Connecticut border to the New Hampshire border. These intrude the crystalline metamorphic and igneous rocks of the Merrimack synclinorium and are located in the easternmost part of the study area (Figure 1.5). Numerous internal chilled contacts were observed in the field indicating that there were multiple igneous pulses. In hand sample the interiors of the dikes are ophitic orthopyroxene-plagioclase-clinopyroxene diabases or gabbros. From paleomagnetic studies the dikes are at least as old as earliest Jurassic (McEnroe, 1988). The dike localities that were sampled in this study are described below in order from northeast to southwest.

Quinapoxet Reservoir Spillway (Samples labelled QX): The dike intrudes vertically into the granulite member of the Paxton Formation and trends N49E. Only the southeast contact is exposed and there is a minimum thickness of 24 m of diabase. There is a 0.5 m screen of country rock separating the main dike from a 1.2 m dike to the southeast. All the samples were obtained by drilling the outcrop. Samples QX-1 and QX-2 are from the thin southeast dike, QX-1 at 0.28 m and QX-2 at 0.76 m from the southeast contact. Sample QX-3 was taken at the chilled contact of the main dike, and samples QX-4, 5, 6, 7, and 8 were taken at distances of 0.9 m, 1.8 m, 6.1 m, 9.7 m, and 13.1 m northwest of the contact of the main dike.

Holden Traprock Quarry: The main dike (samples numbered 1681 and 1683) and a dikelet (sample 1688) were sampled. Sample locations were based on a pit map prepared by Peter Robinson and R. D. Tucker on December 15, 1976. According to the pit map the dike trends approximately north at the northeast end of the pit where it has a measured thickness of 39 m. In the central part of the pit the dike turns to a trend of about N45E and reaches a maximum thickness of about 55 m. In the southern part of the pit the dike bends back to a more northerly trend and thins to about 25 m. The overall exposure along the length of the dike is 180 m and the contact attitudes are highly irregular. Individual attitudes measured along the northwest contact include N1E 85E, N67E 86E, N10E 87W and N5E 73E; along the southeast contact N15E 60W, N6E 50W, N47E 79W, and N62E 79SE. The country rocks on the northwest side of the main dike include the granulite member of the Paxton Formation containing a separately mapped layer of rusty mica schist and an overlying sill of foliated biotite granitic gneiss. Country rock contacts dip gently to the northeast. The country rock on the southeast side of the main dike is the rusty quartzite member of the Paxton also dipping gently. These relations combined with regional geology suggest there is a normal fault, down on the northwest, along the dike. This is confirmed in the northeast corner of the quarry where slickensided fault surfaces in the diabase itself close to the southeast contact show attitudes of N9E 60W with slickensides plunging N80W, and N18E 57W with deep slickensides plunging N67W and later fine slickensides plunging 9S. Within the main dike there appear to be multiple internal chilled contacts, away from which the diabase texture coarsens to that of an ophitic gabbro. All samples were taken from oriented blocks. Samples 1681 were all collected near the northwest contact of the main dike near the north end of the quarry. 1681B was at the contact, 1681A was 0.2-0.5 m east of the contact, and 1681C was 6 m east of the contact. An internal chill was observed in this vicinity 10 meters from the dike contact but no sample was obtained east of the chill. Sample 1683 consisted of coarse diabase collected 23 m east from the west contact at the south end of the pit, and probably lies east of the internal chilled contact described above. Site 1688 is from a newly located fine-grained dikelet 0.41 m thick, with an attitude N 29W 70SW, that has intruded the biotite granitic gneiss in the northwestern part of the quarry.

Route 122: Site Rd 122 is from a road cut exposure on Route 122 northwest of the village of Paxton. The diabase intrudes the rusty quartzite member of the Paxton Formation. In hand sample the diabase has gabbroic texture.

Quacumquasit: Site Qp is on a powerline just southwest of Quacumquasit Pond. The diabase intrudes the sulfidic schist of the Rangeley Formation (H. Berry pers. comm. 1988) The dike is poorly exposed, but appears to be vertical and with a trend of N50E. It has an approximate thickness of 10 m. The diabase is coarse-grained and has a late-stage quartz-feldspar segregation texture.

Fiskdale: Site Fs is exposed on the Quinebaug River in Fiskdale. The dike is 50 m thick and intrudes sulfidic schist of the Rangeley Formation (H. Berry pers. comm., 1988) The trend is N17E and the dip is vertical.

Pelham-Loudville System

The diabases of the Pelham-Loudville system crop out in the western half of the field area. This system is subdivided into two distinct geographic groups. The Pelham group crops out east of the Northfield, Deerfield and Hartford Mesozoic basins, and the Loudville group crops out west of the Hartford Basin. These diabases (Figure 1.5) intrude the metamorphic and igneous rocks of the Connecticut Valley synclinorium and Bronson Hill anticlinorium, which are dominated by metamorphosed sedimentary and volcanic rocks of late Proterozoic through early Devonian age, and Ordovician and Devonian intrusions (Zen et al., 1983). Few dikes and sills are exposed in the Mesozoic basins in Massachusetts. Those that are, are clustered close to outcrops of the Hampden Basalt and Granby Basaltic Tuff, and were not included in the present study. In hand sample the diabases of the Pelham-Loudville system are fine-grained with phenocrysts of plagioclase and clinopyroxene. From paleomagnetic studies these diabases appear to be Early Jurassic (McEnroe, 1988).

Loudville Group. On the bedrock geologic map of Massachusetts (Zen et al., 1983) only two diabase localities are shown west of the Hartford Basin in Massachusetts, near Loudville. During the present study altogether seven areas of exposure were found, and a series of ground-magnetic profiles (report in progress) shows that they belong to a dike set trending N25E and extending over a distance of at least 6.7 km. The exposures of the Loudville diabases represent a shallower level of intrusion than those of the Pelham group, in that they are on the downthrown side of the Connecticut Valley border fault and close to the unconformity at the base of the Triassic strata. Based on the middle cross section of the bedrock geologic map of Massachusetts, this difference in level of intrusion is estimated at about 5 km. From north to south, the sampled localities of the Loudville group are as follows:

Sawmill Hills (Samples labelled SWM1, SWM2): Two exposures of diabases were found that intrude the Littleton Formation and the Willamsburg Granodiorite. Sawmill 1 consists of dikelets exposed on a southeast-facing wall of silicified granitic pegmatite. Three dikelets with a general attitude of N35E dip 82SE were sampled. Based on magnetic traverses there is a dike in the adjacent valley 9 m wide with approximately the same trend. Sawmill 2 lies 150 m southwest of Sawmill 1. The outcrop consists of about 1 m of medium- to fine-grained diabase with columnar cooling joints that trend N53W and plunge 16SE, suggesting a dike that strikes N37E and dips 74NW.

Mineral Springs, Loudville (Samples labelled MS, MS2): Two areas of exposure of a diabase dike that intrudes the Waits River Formation and the Williamsburg Granodiorite were found in this vicinity. Two outcrops were sampled. In a roadcut on Mineral Springs Road the northwest contact strikes N36E and dips 82NW, the southeast contact strikes N20E and dips 87NW, and the dike has a maximum thickness of 17 m. A second locality (MS2) west of the roadcut on the eastern bank of the north branch of

Manhan River shows both contacts of the dike as well as a dikelet along the southeast side. Here the northwest contact of the dike strikes N38E, dips 79NW, and the dike has a thickness of 15 m.

Cold Spring (Samples labelled CR, CS): Two areas of exposure occur near Southampton Road in the Town of Westhampton, which is an extension of Cold Spring Road in Southampton. These sites are located where an unnamed tributary of Manhan River cuts Southampton Rd. The diabase intrudes the Waits River Formation and Willamsburg Granodiorite, here dominated by pegmatite. The Cold River locality (CR) lies just east of the middle of three culverts where Southampton Road crosses the tributary. Here the width of the dike varies from 6.7 m to 14 m as mapped by magnetometer. It has a general trend N25E and appears to be vertical. The Cold Spring locality (CS) is 50 meters northwest of the Cold River locality in the bed of the tributary. Here two contacts of a different dike 13 m thick are exposed. Also an irregular dikelet that is exposed 3.6 m west of the northwest contact of the main dike, has a strike of N23E, dip is vertical and is approximately 0.3 m thick.

Pelham Group, Millers Falls Area. The Pelham group of the Pelham-Loudville system includes most of the diabase intrusions exposed in Massachusetts immediately east of the Northfield, Deerfield and Hartford Mesozoic basins, over a distance of 50 km north-south and as much as 15 km east of the Connecticut Valley border fault (Figure 1.5). This group is exposed in several distinct geographic areas. The Millers Falls area includes intrusions to the east of the Northfield and Deerfield basins from Northfield (NF) in the north through Harvey Hill (HH) in the south.

Northfield (Samples labelled NF): The exposure is about 3 m across. Ground-magnetic profiles suggest that the intrusion is a west-dipping sill parallel to the foliation of the enclosing granulite member of the Erving Formation and that the intrusion has a thickness of about 10 m.

Millers Falls (Samples labelled MF): This outcrop is located in the Village of Millers Falls on the northern bank of the Millers River. The sill is subparallel to foliation of the Hornblende Member of the Dry Hill Gneiss, striking N56E and dipping 20NW. The thickness of the sill is approximately 30 m. The chilled contact at the top of the sill is perfectly exposed west of the northern bridge abutment.

Lake Pleasant (Samples labelled LP): This diabase, 4.8 km southwest of Millers Falls, is poorly exposed and presumed to be a sill (Laird, 1974). The outcrop is approximately 1.5 m wide and the diabase apparently intrudes the Fourmile Gneiss.

Laird1, Laird 2, and Harvey Hill (Samples labelled L, LA and HH): These are diabases that were mapped by Scott Laird (1974). He interpreted these to be an inter-connected intrusive complex of dikes and sills. Numerous small dikelets splay out into the country rocks. The best exposures of the five diabase intrusions are located 1 mile north of Harvey Hill in Montague. These diabases are well exposed for 1500 m along strike on the west limb of the Pelham dome. The diabase at locality Laird 1 is a dike that intrudes the Poplar Mountain Quartzite. It has a maximum width of 30 m and strikes N5W. The diabase at locality Laird 2 is a sill that intrudes the Fourmile Gneiss. It has an approximate width of 5 m, strikes N30E, and displays abundant sheeting joints parallel to the contacts. The Harvey Hill locality is a dike eroded to form a narrow gully, on the sides of which are rare exposures of chilled diabase. The dike intrudes the Dry Hill Gneiss and the Poplar Mountain Quartzite. It has an approximate width of 2 m, strikes N15W, and is vertical.

Pelham Group, Isolated Intrusions. East of the Millers Falls area are two isolated intrusions at Butterworth Ridge and at Rattlesnake Hill.

Butterworth Ridge (Samples labelled But): Although the intrusion at Butterworth Ridge is locally sill-like and parallel to the foliation of the enclosing Ammonoosuc Volcanics, it is locally cross-cutting. It was originally recognized in 1960 (Robinson, 1963) and was extended in this study for a distance of 230 m along strike. Along this distance the following contact attitudes were measured: N9E 83W; N52E 68NW; N15E 85NW; N20E 76NW. In this distance the thickness of the intrusion varies irregularly from 0.8 m to 1.1 m.

Rattlesnake Hill, Quabbin Reservoir (Samples labelled RS): On the southeast slope of Rattlesnake Hill a dike of varying thickness intrudes the Monson Gneiss. The dike strikes N25E, has a vertical dip, and a maximum thickness of about 5.5 m and can be traced for 32 m in the field.

Pelham Group, Pelham Dike. Directly east of the Amherst arch that separates the Deerfield and Hartford basins is the Pelham dike proper, with a total exposed length of 9.5 km. This was sampled at four localities described from northeast to southwest (samples labelled 3C6, 8C9, 2O2, NV).

Cobb Brook (Samples labelled 3C6): This is the northern extension of the Pelham dike. The exposure sampled is near the mouth of the Cobb Brook on the Quabbin Reservoir. The dike intrudes an amphibolite of the Partridge Formation. Based on a ground-magnetic profile, the width of the dike appears to be 20 m. The strike appears to be N63E and the dip vertical.

Atherton Brook (Samples labelled 8C9): This exposure is on the south ridge of hill 1012 northwest of Atherton Brook and is the largest exposure of the Pelham dike. The dike intrudes the Fourmile Gneiss perpendicular to foliation, and is 20 m thick. The strike is N60E, and the dip is vertical. Sample 8C9A is from a 10 cm dikelet adjacent to the northwest contact of the main dike, sample 8C9B is from the northwest contact of the main dike, sample 8C9C is 8 m from the northwest contact, and sample 8C9D is at the southeast contact about 30 m due east from 8C9B.

Route 202 (Samples labelled 202): A commonly visited exposure of the Pelham dike is the road cut on Route 202. Here it intrudes the Mt. Mineral Formation. The strike is N56E, the dip is vertical, and the approximate width is 15 m. In the woods 150 m northwest of route 202 the dike is exposed where it intrudes the basal quartzite member of the Mt. Mineral Formation. Here there is strong evidence that there is no fault displacement across the dike because the sharp lower contact of the basal quartzite member shows no offset. A sample from a 18 cm dikelet in the quartzite was obtained for geochemistry.

North Valley Rd., Pelham (Samples labelled NV): This outcrop shows both contacts of the dike against Dry Hill Gneiss. The thickness of the dike is 19 m. All samples were drilled within 1.2 m of the northwest contact. The diabase is cut by younger quartz veins.

Pelham Group, Southwest Quabbin Area. South of the Pelham dike is the southwest Quabbin area of isolated intrusions from Gulf Brook (6I3, 6I4) through Turkey Hill (6I5, 6I6). The Pelham dike and the southwest Quabbin area all lie within a Mesozoic horst between the border fault on the west and a fault along the west arm of Quabbin Reservoir to the east. The dikes exposed in the southwest Quabbin area are described from northeast to southwest as follows:

Gulf Brook (Samples labelled 6I3, 6I4): This dike intrudes members of the Partridge formation on the summit and steep east slope of the ridge north of Gulf Brook in the Quabbin Reservoir area. As mapped by Michener (1983) the dike is in two segments, a southwest segment trending N53E and a northeast segment trending N25E. The present study, based on field relations suggests there may be a direct connection between them. All

samples for the present study were taken from the northeast segment. Here the dike is 11 m thick and can be traced for 200 m. The southeast contact at 6I3 is N12E 61SE; at 6I4, N18E 72 SE. Samples were obtained from the chilled southeast contact to 8.5 m into the dike.

Hill East of Dodge Hill (Samples labelled EDH): This diabase is best exposed on the west slope of the hill east of Dodge Hill in the Belchertown quadrangle. It is the southwestern-most and best exposed of four small lens-like intrusions portrayed on the Massachusetts bedrock map that intrude the Fourmile Gneiss on the east limb of the Pelham dome. The other three lenses were mapped on the basis of ground-magnetic anomalies and very low outcrops (P. Robinson, pers. comm., 1986). At the sample locality the northwest contact was measured. The strike is N47E, and dip 69NW. The dike has a thickness of approximately 14 meters. The chilled contact on the northwest side is very well exposed and shows small xenoliths of Fourmile Gneiss.

Cadwell Creek, Quabbin Reservoir (Samples labelled CC): There are three diabase dikes that intrude the Fourmile Gneiss located in the bed of Cadwell Creek near Quabbin Reservoir. The northernmost dike is 1.2 m thick, strikes N65E and dips 67NW. The second dike 2.4 m to the south is 18 cm thick, strikes N60E, and dips 75NW. The third dike about 1 m further south is also 18 cm thick, strikes N70E, and dips 87NW. The southern dike has been fractured and weathered, and appears to have been hydrothermally altered. All paleomagnetic and geochemical samples were from the northern dike.

Jabish Brook (Samples labelled 126,127): Two diabase dikes intrude the Pelham Quartzite in an en echelon pattern. At locality 126, 134 m east of Jabish Brook, the strike is N32E, the dip is vertical, and the maximum thickness is 12 m. At locality 127, 61 m northeast of 126, the strike of the dike is N34E, the dip is vertical, and the maximum thickness is 14 m. A ground-magnetic anomaly map of these two diabases produced by D.U. Wise and K. W. Blake shows that these two exposures belong to two en echelon dikes.

Turkey Hill, Belchertown (Samples labelled 6I5, 6I6): These diabase dikes located near the summit of Turkey Hill intrude the Belchertown Quartz Monzodiorite (Guthrie, 1972; Ashwal et al., 1979). Eight outcrops of diabase can be traced for 61 m. The maximum exposed thickness is 17 m and the dike thins north and south to about 11 m. The trend is N17E and the dip is vertical.

Ware System

The diabases of the Ware system in Massachusetts extend in a northeast-southwest trending en echelon pattern for 50 km from the Connecticut border of Massachusetts to the eastern part of Barre. These diabases intrude the metamorphic and igneous rocks of the Merrimack synclinorium as well as the Bronson Hill anticlinorium (Figures 1.4, 1.5). Thirty-five km northwest of Barre, at the French King Bridge locality, a sill of this system intrudes the Fourmile Gneiss of the Bronson Hill anticlinorium. This sill crops out in the geographic region of the Millers Falls area of the Pelham group. In hand sample the interior of the dikes and sills are subophitic plagioclase and clinopyroxene diabases. The sample localities from the Ware system are described in order from northeast to southwest.

Barre (Samples labelled BA): This area of exposures is in Barre State Forest, northeast of the village of White Valley. The dike intrudes the Partridge Formation , Littleton Formation, and the sulfidic schist and quartzite member of the Paxton Formation (Tucker, 1977; Zen et al., 1983). It strikes N56E, has a vertical dip, and a maximum estimated thickness of 40 m. During field work of the present study, outcrops were found southwest of those described by Tucker (1977), so that this diabase can now be traced in the field for one km along strike. Southwest 2.5 kilometers from this locality a diabase dike 40 m thick was exposed in the Quabbin tunnel (Fahlquist, 1935, section 78).

Ware (Samples labelled W and WA): There is very good exposure south on the powerline from the point where it intersects Route 9. The dike intrudes the Rangeley Formation, Fitch Formation, and Coys Hill Granite. The strike of the dike is N25E, the dip is vertical, and the width is 30 m. This dike has been traced in the field for a distance of 5.4 km (Field, 1975). This dike has been sampled at two localities 1 km - 2 km south on the powerline from Route 9 and a small dikelet, less than 0.3 m thick that strikes N6E, and dips 74E near site WA.

North of Fox Hill (Samples labelled PC): There are exposures on a powerline 200 m north of Fox Hill but no diabase contacts are visible. This area is mapped as the northern extension of the Fox Hill dike that intrudes the Coys Hill Granite in the Palmer quadrangle. This dike is shown as separate from but close to the Ware dike by Peper (1966), but as part of the Ware dike by Field (1975).

Fox Hill (Samples labelled FX): The dike is exposed on the west slope of Fox Hill in the Palmer quadrangle east of the powerline and intrudes the Coys Hill Granite. It strikes N33E, has a vertical dip, and is 21 m thick. Samples FX-1 and FX-2 were collected 9 m from the southeastern contact of the dike. Sample FX-3 was collected 3.7 m from the southeastern contact. Samples FX-5 were collected for geochemistry only from a dikelet 0.33 m thick in a block displaced less than one meter adjacent to the southeast contact.

French King Bridge (Samples labelled FK): This sill lies 37 km northeast of the Barre locality, in the Millers Falls quadrangle, on the east side of the Connecticut River, northeast of French King Bridge, on a powerline that crosses the Connecticut River at French King Rock. This sill is 0.2 m thick and intrudes parallel to foliation in the Fourmile Gneiss that strikes northeast and dips gently northwest.

Bliss Hill Group

The two diabases of the Bliss Hill group intrude the rocks of the Bronson Hill anticlinorium (Figure 1.5). These are separated from the geographically overlapping Pelham-Loudville system because of distinct chemistry, paleomagnetism and ages. In hand sample these are fine-grained with abundant small amygdules.

Bliss Hill North (Samples labelled 4I4): A dike 1.2 m wide intrudes the Clough Quartzite and Rangeley Formation on the southern slope of Bliss Hill in the Mt. Grace Quadrangle (Figure 1.6). The strike is N40E, and the dip is 70N.

Bliss Hill South (Samples labelled BH): The exposure is in a large excavation ditch on Athol Rd 100 m west of the town line between Warwick and Orange, in the Mount Grace quadrangle. The dike intrudes the sulfidic schist of the Rangeley Formation. The strike is N16E, the dip is 81NW, and the thickness is 1 m.

Quabbin Reservoir Group

Three sills intrude the rocks of the Bronson Hill anticlinorium (Figure 1.5) in the eastern part of the Quabbin Reservoir area. These are separated from the Pelham-Loudville system because of the distinct chemical and paleomagnetic signatures, and Cretaceous ages. In hand sample these are fine grained diabases with olivine phenocrysts and abundant amygdules.

Chapman Island (Samples labelled C26): This sill, 1 m thick, on the east coast of Chapman Island intrudes migmatitic schist of the Partridge Formation (Figure 1.5). It was discovered in 1965 by Peter Robinson (pers. comm.) and is shown on the bedrock map of Massachusetts (Zen et al., 1983). The sill strikes N5W and dips 42W. Ground-magnetic profiles measured over the sill show unusual negative anomalies consistent with the strong reversed polarity of the remanent magnetization (Figure 1.6).

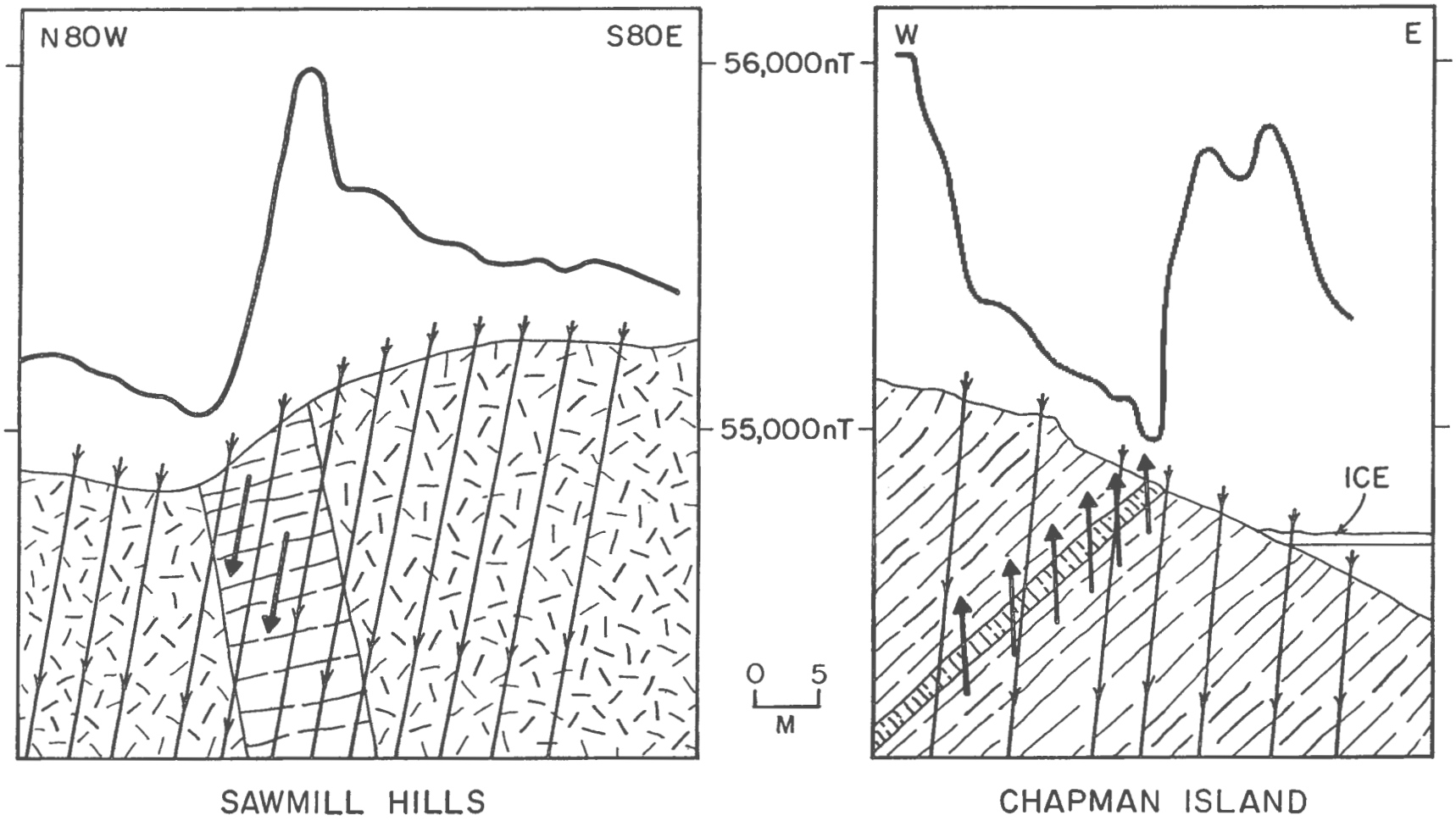

Figure 1.6 Ground-magnetic profiles over dike at Sawmill Hills with normal polarity (positive anomaly) and over sill at Chapman Island with reversed polarity (negative anomaly). Light arrows indicate present magnetic vector, heavy arrows indicate remanent magnetic vector, both projected into plane of section.

Baffle Dam Island (Samples labelled BF): A sill 0.3 m thick intrudes Monson Gneiss at elevation 655' on the east facing cliffs near the summit of the island (Figure 1.5). This was discovered in the present study during field search for Balk's South Baffle Dam locality. The sill strikes N27E and dips 55SE. It has been traced along strike for a distance of 100 m, and where last exposed at the north end, turns into a dike striking N62W and dipping 63SW.

South Baffle Dam: This locality, originally mapped by Robert Balk (1940) during construction of Quabbin Reservoir, is no longer exposed. It lies where the road from South Baffle Dam follows the southeast shore of Baffle Dam Island. Ground-magnetic profiles indicate a sill 1 m thick with strong reversed polarity. A sample from Balk's collection housed at the University of Massachusetts was analyzed geochemically and for K-Ar. Additional samples of a thinner chilled dikelet were obtained from rubble adjacent to the road.

CHAPTER 2

PETROGRAPHY

Introduction

In central Massachusetts the Mesozoic systems of intrusions into pre-Mesozoic crystalline rocks are distinct in their petrographic character. Each system is discussed separately in order of relative age as determined by paleomagnetism. Sixty-eight thin sections of the diabase dikes and sills were examined using petrographic microscope techniques. The phases present, textural relationships, and character and amount of alteration were noted. Plagioclase compositions were determined using the Michel-Levy method or estimated on the basis of CIPW norms calculated from chemical analyses (Chapter 3,Tables 3.1 to 3.6).

Twenty-four polished-thin sections and nine polished cores 2.5 cm in diameter were examined using oil immersion with a reflected light microscope. Crystal form, exsolution, oxidation and alteration of the opaque minerals were noted. The classification system of Haggerty (1976) was used to describe the extent of oxidation exsolution of magnetite-ulvospinel solid solution members.

C1: optically homogeneous ulvospinel-rich magnetite$_{ss}$.
C2: Magnetite-enriched$_{ss}$ with a small number of "exsolved" ilmenite lamellae parallel to {111} spinel parting planes.
C3: Ulvospinel-poor magnetite$_{ss}$ with densely crowded "exsolved" ilmenite along {111} parting planes of the cubic host.

The results of petrographic examination are presented in Tables 2.1 through 2.9. These contain estimated modes and estimates of maximum grain size in millimeters in each category, indicated by square brackets.

Holden System

Seventeen diabase samples from the Holden system were studied petrographically. These included eleven thin sections, two from chilled margins and nine from well crystallized interiors; and six polished cores, two from chilled margins and six from well crystallized interiors. The estimated modes are listed in Table 2.1.

The average chilled margins contain 5% normally zoned plagioclase phenocrysts An$_{59-64}$, 1.3 to 1.6 mm long; 3% Mg-rich orthopyroxene phenocrysts (2V=-80-85), 0.8 to 1.5 mm long, altered up to 20% along the edges and in cracks; and 8% clinopyroxene phenocrysts, including both augite and pigeonite of 0.8mm average length, commonly occurring in aggregates of crystals. The matrix is composed of 36% plagioclase, 38% clinopyroxene, red-brown biotite, 10% skeletal to euhedral grains of titanomagnetite classified from C1 to C2, and discrete grains of ilmenite. The sulfides are pyrite and chalcopyrite. The pyrite occurs as euhedral grains, filigree, and as an intergrowth with titanomagnetite.

The interiors of the diabases are well crystallized and in some samples it is difficult to distinguish phenocrysts from matrix minerals. The major minerals include 41-50% normally zoned plagioclase, An$_{58-72}$, ranging from 8.0 to 2.0 mm long; 2-10% of Mg-rich orthopyroxene (2V=-80-85), 1.4 to 2.2 mm long; 22-42% clinopyroxene, including augite and pigeonite, 0.8-2.0 mm long and 3% of red-brown biotite rimmed by green biotite, up to 0.7 mm long. The titanomagnetites have abundant "exsolution" lamellae of ilmenite and are classified as C2 to C3 with increasing ilmenite. These show greater alteration than in the chilled samples, to Fe-Ti amorphous oxides, to titanomaghemite, and possibly to sphene in some samples. Discrete grains of ilmenite are common. Pyrite varies in texture from droplets and filigree to euhedral grains. Chalcopyrite occurs in trace amounts, and

Table 2.1 Estimated modes of diabases from the Holden system. Sample numbers indicate type of specimen studied: **FK** - polished thin section, FK - normal thin section, *FK* - polished core.

	QX-3	*QX-3*	*QX-2*	*QX-8*	1681A	1681A3	1681B	1681B3
Phenocrysts								
Plagioclase	10 [1.6]				3 [2.0]	10 [1.5]	7 [1.5]	4 [2.0]
Augite-Pigeonite	7 [0.7]				5 [1.0]	10 [1.3]	5 [0.8]	4 [1.2]
Orthopyroxene	2 [0.8]				4 [1.8]	3 [2.2]	3 [1.4]	3 [2.2]
Matrix								
Plagioclase	37 [0.1]				40 [1.0]	40 [0.8]	38 [0.2]	40 [0.2]
Augite-Pigeonite	30 [0.04]				40 [0.6]	27 [0.6]	34 [0.15]	40 [0.1]
Biotite	4 [0.05]				2 [0.7]	2 [0.3]	3 [0.05]	3 [0.2]
Titanomagnetite	10 [0.8]	10 [0.8]	9 [0.7]	7 [0.5]	6 [0.3]	6 [0.3]	10 [0.15]	6 [0.1]
(Class)		C1-2	C3	C3				
Ilmenite		1 [0.1]		1 [0.2]				
Amorph. FeTi			tr	tr [0.3]				
Pyrite		1 [0.05]	1	1 [0.05]				
Filigree		5 [3.0]						
Sulfide Droplets		5 [0.5]		tr				
Chalcopyrite		tr		tr				
Alteration								
Calcite							tr	tr
Chlorite					tr	2	tr	tr
Sericite	tr				tr	tr		
Xenoliths								
Feldsp. Granulite	X							

Table 2.1 (continued).

	1681C	1681C-1	1683	*1683*	1688	*1683*	QP	*QP*	F2AR
Phenocrysts									
Plagioclase			5 [1.8]		5 [1.3]		10 [1.5]		15 [1.7]
Augite+Pigeonite			5 [2.0]		8 [0.8]		5 [0.6]		10 [1.4]
Orthopyroxene			10 [1.5]		3 [1.5]				6 [1.5]
Matrix									
Plagioclase	45 [1.4]	48 [1.7]	51 [0.8]		33 [0.2]		40 [0.8]		37 [0.4]
Augite+Pigeonite	42 [1.1]	41 [1.2]	22 [1.0]		43 [0.2]		32 [0.4]		25 [0.3]
Orthopyroxene	5 [1.7]	2 [0.9]							
Biotite	1 [0.2]	1 [0.3]	2 [0.5]				2 [0.7]		1 [0.15]
Apatite	tr								tr
Orthoclase+Quartz	tr	tr	tr				2		tr
Titanomagnetite	4 [0.6]	6 [0.8]	4 [0.8]	4 [0.7]	8 [0.2]	8 [0.2]	5 [1.0]	5 [0.7]	5 [0.4]
(Class)		C3		C3		C2		C3	C3
Ilmenite		tr [0.5]		1 [0.5]		tr		1 [0.7]	tr [0.5]
Amorph. FeTi		?		?		?		?	?
Pyrite		tr	tr	1		tr		tr	
Chalcopyrite		tr		tr					tr
Pentlandite		tr							
Sulfide Filigree						tr		1 [0.6]	1 [0.5]
Alteration									
Calcite	tr	tr	tr		tr		1		1
Chlorite	3	2	1		tr		3		
Sphene	tr							?	tr
Hematite							?	tr	

pentlandite is present in one section. Micrographic intergrowths of alkali feldspar and quartz are common and trace amounts of apatite and calcite are present in most samples. Chlorite is present as an alteration product in the matrix of 80% of the sections. Orthopyroxene is altered around the edges and about 15% of the plagioclase is sericitized.

The dikes of the Holden system contain certain petrographic features of particular interest to petrogenetic interpretations. In the interiors of the diabases there are grains of pigeonite rimmed by augite, probably indicating a peritectic relationship. These augite rims contain exsolution lamellae, that are probably pigeonite, and are indicative of relatively slow cooling. This is also suggested by local augite lamellae in the orthopyroxenes. The orthopyroxenes are rimmed by a mineral of a more Fe-rich composition, that in most cases has been replaced by a sheet silicate. This rim, before alteration, could have been olivine which was produced on orthopyroxene as it reacted during decompression, in which the field of primary crystallization of olivine expanded at the expense of the orthopyroxene field (Philpotts and Reichenbach, 1985). The clinopyroxene phenocrysts in the chilled margins have ragged edges which may indicate that they were also out of equilibrium with the liquid at the time of intrusion. There are late stage pyrites that surround the titanomagnetites, and pyrite and titanomagnetite intergrowths. The local micrographic intergrowths of quartz and alkali feldspar, common to all the interior samples, probably represent interstitial residual liquid of granitic composition.

Pelham-Loudville System

The diabases of the Pelham-Loudville system were the most extensively studied in thin section. Eight thin sections from chilled margins and twenty-two well crystallized interior samples were examined in transmitted light. Eighteen specimens were examined in reflected light. The estimated modes are in Tables 2.2 to 2.5.

The chilled margins contain 5-10% phenocrysts of plagioclase, An_{55-70}, 0.8 to 2.0 mm long; 3-5% microphenocrysts of olivine (2V=-80-85), Fo_{75-85}, 0.16 to 0.25mm in diameter; and 2-7% clinopyroxene phenocrysts including augite and pigeonite that range in length from 0.6 to 4mm. The plagioclase phenocrysts are commonly normally zoned and approximately 3% of the plagioclase phenocrysts appear to have crystallized in supersaturated conditions (Lofgren, 1974) as shown by the interiors of grains that have a coalescing finger- like texture that evolve to a single grain. Dungan and Rhodes (1978), alternatively, suggest that this texture in plagioclase may be produced by resorption during magma mixing. Inclusions of pyroxenes (0.04 mm) are common in the large plagioclase grains. The microphenocrysts of olivine are rimmed by augite and pigeonite. The widths of the reaction rims on the olivine crystals increase from the contact inward toward the interiors of the diabases until all the olivine is reacted out.

The matrix is composed of 39-47% plagioclase (0.1-0.2mm); 40-45% clinopyroxene, augite (2V=+30-50) and pigeonite (2V=+0-10) average size 0.12mm; 10-20% titanomagnetite (C1-C3), ranging from skeletal arrangements with herring-bone texture to euhedral grains; 3% fine-grained titanomagnetite dust; 1% sulfides including pyrite as sulfide droplets and euhedral crystals, and chalcopyrite; less than 1% biotite; and discrete grains of ilmenite. Trace amounts of apatite, and zircon are also present. Quartz xenoliths with reaction rims of pyroxene, ilmenite, and micrographic K-feldspar and quartz are common in most thin sections. Secondary alteration is less than 10%, including sericitized plagioclase that is more abundant in this system than in the Holden and Ware systems, and the Quabbin Reservoir and Bliss Hill groups. 1-3% Fe-chlorite, possibly replacing olivine is common. In some sections the titanomagnetites have been altered to an amorphous Fe-Ti oxide. Trace amounts of secondary calcite, Fe and Mg-chlorite, biotite and hematite occur in the matrix. In some sections there are thin veins or dikelets containing red-brown high-temperature biotite and olive-green hornblende.

Table 2.2 Estimated modes of diabases, Loudville group, Pelham-Loudville system. Sample numbers indicate type of specimen studied: FK - polished thin section, FK - normal thin section.

	SWM2A	MS2A	CR8	CS7	CS7A	CS9
Phenocrysts						
Plagioclase	2 [1.8]	5 [2.0]	4 [1.8]	4 [2.0]	2 [1.5]	4 [1.5]
Augite+Pigeonite	1 [0.8]	1 [0.8]		2 [0.8]	1 [0.2]	3 [1.2]
Olivine	?3 [0.5]	?2 [0.2]	?2 [0.3]	?3 [0.3]	?1 [0.3]	?1 [0.4]
Matrix						
Plagioclase	44 [0.4]	43 [0.5]	43 [0.6]			43 [0.3]
Augite+Pigeonite	37 [0.25]	40 [0.25]	40 [0.3]			36 [0.2]
Biotite		1 [0.15]				
Titanomagnetite	7 [0.2]	5 [0.5]	7 [0.2]			10 [0.15]
(Class)	C2		C2	C3		
Ilmenite	tr		tr			
Amorph. FeTi	tr		tr			
Pyrite	tr		tr			
Chalcopyrite			tr			
Sulfide Droplets	tr					
Apatite		tr	tr			
Groundmass						
Silicates				72	72	
Magnetite Dust	3		2	15	20	
Alteration						
Calcite		tr				tr
Chlorite	3	3	2	3	2	3
Sericite	tr		tr	tr	tr	tr
Hematite	tr			1	2	tr
Rutile			tr			
Xenoliths						
Quartz						X [0.8]

Table 2.3 Estimated modes of diabases, Millers Falls area, Pelham group, Pelham-Loudville system. Sample numbers indicate type of specimen studied: **FK** - polished thin section, FK - normal thin section.

	NF2	NF3	L154	LP	L7	LA	HH	But4
Phenocrysts								
Plagioclase	4 [1.2]	5 [1.4]	5 [1.5]	5 [1.7]	5 [2.0]	1 [2.2]	8 [1.5]	6 [1.2]
Augite+Pigeonite		1 [0.3]	3 [0.5]	1 [0.5]	1 [0.8]	3 [0.6]	6 [0.6]	3 [0.9]
Olivine	?1 [0.2]	1 [0.2]	?1 [0.2]				1 [0.2]	
Matrix								
Plagioclase	45 [0.6]	42 [0.4]	41 [0.1]	46 [0.3]	45 [0.4]	45 [0.6]		43 [0.4]
Augite+Pigeonite	42 [0.2]	40 [0.2]	39 [0.05]	43 [0.2]	44 [0.2]	45 [0.2]		40 [0.3]
Biotite	tr	tr						
Titanomagnetite	7 [0.2]	7 [0.25]	8 [0.02]	4 [0.15]	5 [0.3]	5 [0.4]		5 [0.4]
(Class)	C3	C3		C2-3	C2-3	C2-3		C1-3
Magnetite Dust								2
Titanomaghemite	tr	tr		tr				
Ilmenite	tr	tr		tr	tr	tr		
Amorph. FeTi				tr				
Pyrite	tr	tr		tr	tr			
Chalcopyrite					tr			
Apatite	tr	tr		tr		tr		tr
Devitirified Glass			1	tr	tr	1		
Groundmass								
Silicates							70	
Magnetite Dust							12	
Alteration								
Calcite								1
Chlorite		1	1				tr	1
Sericite	1	3		1				tr
Hematite			1					
Xenoliths								
Quartz		X [0.8]	X [0.2]	X [5.0]			X [3.0]	

Table 2.4 Petrography of diabases, central area, Pelham group, Pelham-Loudville system. Sample numbers indicate type of specimen studied: FK - polished thin section, FK - normal thin section.

	RS	RS1C	3C6	8C9A	202	NV-6	6I3-C1	6I3-C2
Phenocrysts								
Plagioclase	5 [1.8]	5 [1.8]	8 [1.8]	7 [1.2]	5 [1.9]	3 [1.5]	6 [1.5]	5 [1.6]
Augite+Pigeonite	2 [1.8]	2 [0.9]	3 [0.8]	5 [1.3]	3 [1.4]	2 [0.8]	3 [0.4]	2 [0.6]
Olivine				?1 [0.2]	1 [0.2]			
Matrix								
Plagioclase	42 [0.5]	42 [0.4]	43 [0.8]	41 [0.2]	41 [0.2]	45 [0.4]	39 [0.2]	42 [0.5
Augite+Pigeonite	41 [0.3]	42 [0.3]	40 [0.4]	32 [0.1]	38 [0.15]	41 [0.2]	40 [0.05]	39 [0.2]
Biotite			1 0.15]		2 [0.15]			1 [0.05]
Titanomagnetite	6 [0.2]	7 [0.15]	4 [0.6]	9 [0.05]	10 [0.1]	7 [0.15]	11 [0.05]	9 [0.01]
(Class)		C2		C1-2		C3		
Magnetite Dust	3	2				1 [0.1]		
Ilmenite		tr		tr [0.1]		tr		
Pyrite		1 [0.08]		1 [0.1]		1 [0.1]		
Chalcopyrite		tr [0.07]		tr [0.06]				
Sulfide Droplets		tr		tr [0.2]		tr [0.1]		
Apatite	tr	tr	tr	tr		tr		tr
Alteration								
Calcite				1				
Chlorite	1	tr	1	1	tr	1	1	1
Sericite	tr	tr	tr	tr		tr		
Sphene				1		tr		
Hematite		tr	tr	tr	tr			1
Vein								
Biotite				1	tr	1 [0.15]		
Hornblende				1				
Xenoliths								
Quartz			X [1.0]	X [1.0]	X [0.9]	X [1.8]		

Table 2.5 Estimated modes of diabases, southwest Quabbin area, Pelham group, Pelham-Loudville system. Sample numbers indicate type of specimen studied: FK - polished thin section, FK - normal thin section.

	6I4-2	EDH	EDH-X	127A	126A	CCA	6I5	6I6
Phenocrysts								
Plagioclase	7 [1.5]	5 [1.2]	5 [1.5]	4 [1.7]	7 [1.7]	5 [1.8]	4 [0.8]	4 [1.0]
Augite+Pigeonite	3 [0.6]	2 [0.8]	2 [0.6]	2 [0.8]	3 [0.7]	3 [0.8]	2 [1.2]	2 [0.8]
Matrix								
Plagioclase	40 [0.6]	40 [0.6]	42 [0.6]	42 [0.6]	40 [0.8]	40 [0.4]	41 [0.8]	44 [0.4]
Augite+Pigeonite	41 [0.3]	42 [0.4]	43 [0.2]	42 [0.3]	43 0.3]	38 [0.3]	43 [0.25]	40 [0.2]
Hornblende								1 [0.2]
Biotite	1 [0.1]	1 [0.1]	1 [0.1]	1 [0.1]	1 [0.1]		1 [0.1]	2 [0.2]
Titanomagnetite	6 [0.3]	7 [0.2]	6 [0.2]	6 [0.5]	5 [0.3]	10 [0.2]	5 [0.3]	5 [0.2]
(Class)	C2		C3	C2-3	C2-3	C3	C3	C3
Magnetite Dust						2		
Ilmenite			tr		tr	tr	tr	
Amorphous FeTi	tr		tr	tr	tr			tr
Pyrite	tr		tr	tr	tr	tr	tr	tr
Chalcopyrite						tr		
Sulfide Droplets	tr				tr	tr	tr	tr
Apatite	tr	tr	tr	tr	tr	tr	tr	
Alteration								
Chlorite	1	1	1	1	1	1	1	1
Sericite	1	2	tr	2				
Hematite						1	1	1
Xenoliths								
Quartz			X [0.4]			X [0.8]		

There are certain petrographic distinctions for each geographic area within the Pelham-Loudville system. The Loudville group (Table 2.2) contains up to 5% skeletal phenocrysts of olivine in the chilled contact zone that are recognized with difficulty due to alteration. In the interior of the diabases there is commonly an unidentified yellow-green sheet silicate that appears to be a replacement of olivine. Titanomagnetite is more abundant and on average is less oxidized (C1-C2). There is abundant very fine-grained titanomagnetite dust in the matrix.

Chilled margins in the Millers Falls area and the Pelham dike (Tables 2.3 and 2.4) contain microphenocrysts of olivine surrounded by augite. Phenocrysts of plagioclase and pyroxene contain abundant inclusions of trapped liquid that has crystallized glass or fine-grained crystals and oxides. Some plagioclase phenocrysts also contain inclusions of pyroxene. Titanomagnetite grains range in oxidation from C1 to C3. The texture varies from ultra-fine dust, skeletal herring-bone, to coarse-grained. Present in some of the tiatnomagnetites is an internal lit-par-lit texture. Pyrite is abundant in these groups, and texturally ranges from droplets to euhedral grains to titanomagnetite and pyrite intergrowths.

The diabases of the southwest Quabbin area (Table 2.4, 6I3; and Table 2.5) have red-brown biotite (0.2mm) in the matrix usually rimmed by secondary green biotite. The titanomagnetites range texturally, from skeletal crystals to coarse grain crystals. In some grains there are internal textures from lit-par-lit to "vermiform". The vermiform texture is restricted to the southwest Quabbin area. This texture is a product of exsolution (senso stricto) and high temperature oxidation and produces a titanomagnetite with a higher Curie temperature than the original starting composition (Haggerty, pers. comm., 1988).

The diabases of the Pelham-Loudville system fall into two geochemical classifications, olivine and quartz tholeiites. It should be noted that only small amounts ofeither olivine or quartz respectively, are present in the norms. This is confirmed petrographically in that microphenocrysts of olivine, where present, are out of equilibrium with the liquid, as demonstrated by the pyroxene rims. The Pelham-Loudville diabases differ from the other central Massachusetts diabases in that augite is the abundant clinopyroxene.

Ware System

Eleven samples were studied from the Ware system of diabases, three from chilled margins, and eight from well crystallized interiors. The sections studied are relatively fresh with less than 5% alteration. Three samples, two chilled margins, and one interior sample were examined in reflected light. The estimated modes are in Table 2.6.

The chilled margins contain 5% phenocrysts of plagioclase, An_{70}, 1.2 to 2.2mm long, and 2% microphenocrysts of olivine (2V=-80-85), Fo_{65-75}, up to 0.16mm in diameter. The plagioclase phenocrysts are commonly normally zoned. Olivines are rimmed by clinopyroxene, indicating a reaction relationship between olivine and liquid. About 3% of the clinopyroxene phenocrysts, including both augite and pigeonite, are present, with an average length of 0.6 mm. The matrix is composed of 35% plagioclase, 40% clinopyroxene, including both augite and pigeonite, 10% devitrified glass, 2% straw-colored oxidized glass and 10% fine-grained herring-bone skeletal titanomagnetite. Because the titanomagnetite lacks exsolution lamellae, it is classified as Cl.

Due to the interlocking texture of the grains from the interior specimens of the diabase, it is impossible to determine whether the clinopyroxenes and plagioclase grains are phenocrysts or matrix crystals. These rocks consist of 45 to 50% plagioclase, 0.2 to 1.2mm long; 40 to 50% clinopyroxene, including both augite (2V=+40-50) and pigeonite (2V=+0-5), 0.4 to l.7 mm long; and 3% titanomagnetite, 0.6mm in diameter. Most of the titanomagnetite grains have abundant lamellae of ilmenite and are classified as C3.

Table 2.6 Estimated modes of diabases from the Ware system. Sample numbers indicate type of specimen studied: **FK** - polished thin section, FK - normal thin section, ***FK*** - polished core.

	FK2I	FK2C	*FK*	BA-2	W4	WA-1	WA-3
Phenocrysts							
Plagioclase	5 [1.8]	7 [1.7]					
Augite+Pigeonite	3 [1.2]	3 [1.0]					
Olivine	1?	1 [0.2]					
Matrix							
Plagioclase	38 [0.6]	35 [0.1]		50 [1.6]	54 [1.0]	46 [0.8]	48 [1.0]
Pigeonite+Augite	40 [0.2]	25 [0.8]		45 [1.8]	43 [0.6]	50 [0.4]	47 [0.6]
Biotite				tr			
Titanomagnetite	9 [0.15]	15 [0.05]	10 [0.05]	5 [0.5]	3 [0.2]	4 [0.3]	4 [0.25]
(Class)			C1-2		C3		
Ilmenite					tr		
Amorph. FeTi			?		?		
Pyrite					tr		
Chalcopyrite					tr		
Filigree			tr				
Apatite	tr			tr	tr		tr
Oxidized Glass			1				
Devitrified Glass	2	12					
Alteration							
Calcite							tr
Chlorite				tr			1
Sericite		tr		tr			tr
Hematite	3	2	tr		tr		
Xenoliths							
Quartz	X [0.8]						

Table 2.6 (continued)

	PC3	FX5A	FX5B	FX3
Phenocrysts				
Plagioclase	5 [1.5]	1 [1.0]	1 [1.0]	1 [1.8]
Augite+Pigeonite	3 [1.0]			
Olivine		1 [0.5]	1 [0.6]	
Microphenocrysts				
Plagioclase		10 [0.2]	12 [0.3]	
Olivine		6 [0.15]	5 [0.15]	
Matrix				
Plagioclase	42 [0.5]	38 [0.04]	39 [0.1]	50 [0.8]
Augite+Pigeonite	45 [0.4]	30 [0.05]	30 [0.08]	42 [0.7]
Biotite	tr		tr	1 [0.3]
Titanomagnetite	5 [0.2]	12 [0.01]	12 [0.04]	5 [0.4]
(Class)	C2-3			
Ilmenite	tr			
Pyrite	tr			
Chalcopyrite	?			
Filigree	tr			
Apatite				tr
Alteration				
Calcite	tr			
Chlorite	tr	2	tr	1
Sericite	tr			
Hematite	tr		tr	
Xenoliths				
Feldspar			X	

Superimposed on the titanomagnetites are a high-temperature deuteric oxidation or possibly a much later post-emplacement alteration, in which the grains were modified to an amorphous Fe-Ti oxide. It is considered unlikely that this high-temperature alteration of the titanomagnetites is later than the cooling of the diabases, because little alteration of the plagioclases and pyroxenes was observed in these samples. This lack of alteration of the silicate minerals would support deuteric alteration of the titanomagnetites rather than a much later alteration by high temperature fluids. There are rare discrete grains of ilmenite. Sulfides are common, typically making up 1% of the rock. Pyrite varies in texture from droplets and filigree to euhedral crystals. Chalcopyrite is present in trace amounts. A red-brown biotite commonly rimmed by green biotite is present in amounts up to 1% in the interstitial matrix. Associated with this are trace amounts of apatite, quartz, K-feldspar and calcite. Ten percent of the plagioclase is sericitized and secondary Fe-chlorite and an oxychlorite are present in amounts less than 1%. Minor cracks are filled with late hematite. Pigeonite is preferentially altered, typically along the circular cracks believed to have been produced by structural contraction during the C to P inversion, whereas augite is less commonly altered. Locally an unidentified greenish-brown sheet silicate has replaced euhedral grains that may have been olivine.

In summary, based on petrographic characteristics, including the reaction relationship between early olivine microphenocrysts and liquid, and later interstitial quartz and alkali feldspar, the Ware system diabases are classified as tholeiites (Yoder and Tilley 1962). A distinguishing feature of this system, as compared to other systems is the marked abundance of pigeonite relative to augite.

Bliss Hill Group

Five thin sections and one polished core from the two Bliss Hill diabases were studied petrographically. The estimated modes are listed in Table 2.7. The northern diabase, 1.2 meters thick intrudes Clough Quartzite; the southern diabase, 0.5 meters thick, intrudes sulfidic schist of the Silurian Rangeley Formation. These dikes are petrographically distinct and are discussed separately.

The northern dike (4I4) contains 3% phenocrysts of plagioclase, An_{52-55}, 1.2-1.8 mm long; 3% of augite 1.0 mm long; 2% orthopyroxene, En_{75-81}, (2V=-70-75), 0.8 mm long with red-brown inclusions that are possibly kaersutite; and 1% altered olivine, 0.8 mm long. The matrix consists of 42% plagioclase, 0.4-1.0 mm long; 36% clinopyroxene, 0.2-0.3 mm long; 11% titanomagnetite, C2 to C3; 1% oxide-charged devitrified glass; and 1-2% amygdules, filled with calcite or devitrified glass. There are trace amounts of ilmenite and pyrite. Minor alteration minerals include sericite and chlorite, replacing olivine, and as trace amounts in the matrix, and up to 3% calcite.

The southern dike (BH) contains 3% plagioclase phenocrysts, An_{55-57}, 1.8 -2.2 mm long; and 1 % of augite, 0.8-1.2 mm long, and orthopyroxenes, En_{80-85} (2V=-80-90), 0.6-1.0 mm long. The matrix consists of 38% plagioclase, 0.1-0.9 mm long, 34% clinopyroxene, 0.05-0.5 mm long; 10% skeletal herring-bone and euhedral crystals of titanomagnetite, C1 to C2; 2-5% devitrified glass, 5 % amygdules up to 2.0 mm in diameter; and trace amounts of pyrite, pyrrhotite, and ilmenite. Alteration is minor. Secondary minerals include calcite, chlorite, hematite. Amygdules are locally filled with analcime, calcite. On the walls of the amygdules that are not filled by a secondary mineral devitrified glass is present.

The orthopyroxenes are abraded at the edges and appear to be out of equilibrium with the liquid. The presence of amygdules in these diabases, as contrasted to the more abundant Jurassic diabases, may be characteristic of a shallower level of intrusion in the Cretaceous than in the Jurassic.

Table 2.7 Estimated modes of diabases of the Bliss Hill group. Sample numbers indicate type of specimen studied: **FK** - polished thin section, FK - normal thin section, *FK* - polished core.

	4I4A-1	4I4	BH-2C1	BH-2C2	BH-2I	*BH-2I-4*
Phenocrysts						
Plagioclase	3 [1.2]	2 [1.8]	3 [1.8]	3 [2.0]	3 [2.2]	
Augite	3 [1.0]	1 [1.0	1 [0.8]	1 [1.2]	1 [0.8]	
Orthopyroxene	2 [0.8]		2 [0.8]	2 [1.0]	1 [0.6]	
Olivine	1 [0.8]					
Amygdules						
	1 [0.2]	2 [1.2]	5 [0.15]	3 [2.0]	5 [0.7]	
Matrix						
Plagioclase	40 [0.4]	42 [1.0]	35 [0.1]	38 [0.2]	40 [0.9]	
Augite+Pigeonite	34 [0.2]	38 [0.3]	32 [0.5]	34 [0.05]	36 [0.4]	
Titanomagnetite	12 [0.1]	10 [0.1]	12 [0.05]	10 [0.1]	8 [0.2]	8 [0.15]
(Class)	C3					C2
Ilmenite	tr					
Pyrite	tr					tr [0.08]
Pyrrhotite						tr [0.08]
Chalcopyrite						tr
Devitrified Glass	1	2	5	3	2	
Alteration						
Calcite	3	2	1	1	1	
Chlorite	tr	1	2	2	2	
Sericite	tr					
Analcime					1	
Hematite			1	3		

Quabbin Reservoir Group

Twelve thin sections from the Quabbin Cretaceous sills and one polished core were studied petrographically. The estimated modes are listed in Tables 2.8, and 2.9. These sills are less than 1 meter thick at any point, consequently most of the samples examined are fine-grained.

The chilled margins contain 1-2% phenocrysts of plagioclase, An_{51-62}, 0.6 to 1.6 mm long; and 2-5% partially altered skeletal olivines, Fo_{65-75} (2V=-80-85), 0.5 to 1.7 mm long. The matrix consists of 40-50% plagioclase laths, 0.04-0.8 mm long; and 22-40% clinopyroxenes, 0.05-0.2 mm long. Magnesium-rich titanomagnetites of several generations make up 7-15% of the sections in morphologies that include euhedral grains, some with blue-gray chrome spinel cores, skeletal coarse herring-bone crystals, and ultra fine grains. Very few oxidation exsolution lamellae are present and the titanomagnetites are classified C1 to C2. There is up to 6% devitrified glass and trace amounts of pyrite and chalcopyrite. Abundant amygdules, 0.04mm in diameter, are filled by devitrified glass, or secondary sheet silicates. Alteration is limited to the olivines, of which 45% are altered to chlorite. There are traces of late hematite and calcite in the sections.

Petrographically these diabases are distinct from the other Massachusetts diabases in the presence of abundant phenocrystic olivine, and the chrome spinel cores in titanomagnetites. The titanomagnetite rims result from the reaction chrome spinel + liquid = titanomagnetite. Based on the classification of Yoder and Tilley (1962) and Macdonald and Katsura (1964) these diabases are olivine tholeiites. The presence of amygdules indicates a shallow level of intrusion, similar to the Bliss Hill diabases.

Mineral Analyses

Although quantitative study of mineral chemistry was not an objective of this thesis, a limited number of electron microprobe analyses of minerals were carried out on two polished thin sections by David C. Elbert, using the Jeol microprobe at Rensselaer Polytechnic Institute. Selected analyses and structural formulae of minerals based on these analyses are presented here and discussed briefly as a supplement to the petrography. Electron back-scatter images were obtained from a third polished thin section.

Holden System - Sample 1681-C

This sample is from the coarse-grained interior of the dike at the Holden Trap Rock Quarry. Representative analyses and structural formulae are listed in Table 2.10. One analysis of plagioclase gives a composition An_{71}. Seven analyses represent relatively homogeneous orthopyroxene grains with Mg/(Mg+Fe) consistently between 0.785 and 0.795. These occur in two slightly different populations, one Al-poor (analysis 48) and the other Al-rich (analysis 33). Eight analyses are of relatively homogeneous augite with Mg/(Mg+Fe) of 0.757 to 0.764, and Ca/(Ca+Mg+Fe+Mn) of 0.427 to 0.421 (analysis 23). Seventeen analyses are of a wide range of low-Ca augites, pigeonites, or unresolved mixtures of the two, that are all more Fe-rich than the discrete orthopyroxene and augite. These show a wide range in Mg/(Fe+Mg) from 0.65 to 0.39 and in Ca/(Ca+Mg+Fe+Mn) 0.38 to 0.10. This scatter is represented by three analyses in Table 2.10, a low-Ca augite (analysis 57), a pigeonite (analysis 38), and the most Fe-rich pigeonite (analysis 36). The wide scatter in interstitial augite and pigeonite compositions could indicate local coarse crystallization of trapped liquid.

North Bliss Hill - Sample 4I4A

Electron back scatter images of orthopyroxene phenocrysts from this well crystallized interior sample indicate the presence of oscillatory zoning. A traverse of 201 spot analyses across a single phenocryst was made. Table 2.11 lists four representative analyses selected from moderate to extreme compositions. This traverse shows that the

Table 2.8 Estimated modes of Chapman Island diabases, Quabbin Reservoir group. Sample numbers indicate type of specimen studied: **FK** - polished thin section, FK - normal thin section.

	C26N-1	C26N-2	C26O-1	C26O-2	C26O-5	OB4
Phenocrysts						
Plagioclase		1 [1.8]	1 [1.2]			2 [0.6]
Olivine	4 [1.2]	3 [1.7]	3 [1.8]	3 [1.3]	2 [1.2]	3 [1.3]
Amygdules	1 [0.7]	2 [0.8]	2 [0.6]	1 [0.7]	1 [0.8]	1 [0.5]
Matrix						
Plagioclase	45 [0.8]	42 [0.6]	42 [0.6]	45 [0.7]	44 [0.6]	44 [0.4]
Augite(+Pigeonite?)	36 [0.06]	38 [0.2]	37 [0.2]	40 [0.4]	38 [0.4]	37 [0.6]
Titanomagnetite	10 [0.1]	7 [0.1]	7 [0.1]	7 [0.1]	10 [0.1]	7 [0.08]
(Class)						C1-2
Pyrite						tr
Devitrified Glass	1	4	1	1	2	3
Alteration						
Calcite						tr
Chlorite	3	3	2	3	3	3

Table 2.9 Estimated modes, Baffle Dam Island and south Baffle Dam diabases, Quabbin Reservoir group. Sample numbers indicate type of specimen studied: FK - normal thin section, *FK* - polished core.

	6I7-1	6I7-2	6I7-3	6I7-4	6I7-5	*6I7*	B44
Phenocrysts							
Plagioclase	1 [0.8]	1 [0.6]	1 [1.0]	1 [1.0]	1 [1.6]		1 [0.8]
Olivine	5 [1.0]	5 [1.0]	5 [1.7]	5 [1.5]	5 [1.7]		5 [1.7]
Amygdules	3 [0.2]	3 [0.2]	2 [0.3]	3 [0.4]	3 [0.4]		1 [0.2]
Matrix							
Plagioclase	40 [0.2]	40 [0.04]	44 [0.3]	45 [0.4]	40 [0.2]		44 [0.2]
Augite(+Pigeonite?)	28 [0.06]	26 [0.06]	25 [0.04]	22 [0.08]	29 [0.04]		26 [0.04]
Titanomagnetite (Class)	15 [0.05]	15 [0.05]	15 [0.08]	16 [0.05]	14 [0.05]	15 [0.1] C1-2	14 [0.05]
Ilmenite							
Pyrite						tr [0.1]	
Chalcopyrite						tr [0.05]	
Devitrified Glass	5	5	5	6	5		6
Alteration							
Calcite			tr				
Chlorite	3	5	3	2	3		3
Hematite	tr	tr					

Table 2.10 Representative electron probe analyses and structural formulae of plagioclase and pyroxenes in sample 1681C-1, a coarse interior sample from the Holden trap rock quarry in the Holden dike system. David C. Elbert, analyst.

	Plagioclase	48 Opx Al-poor	33 Opx Al-rich	23 Augite	57 Augite Ca-poor	38 Pigeonite	36 Pigeonite Fe-rich
SiO_2	50.69	55.24	54.60	52.55	50.78	51.33	49.01
Al_2O_3	31.32	1.03	1.81	2.31	2.04	1.06	1.48
TiO_2		0.12	0.23	0.38	0.64	0.51	0.39
MgO		27.73	27.76	15.04	11.43	16.93	1.48
FeO		13.19	12.73	8.35	17.31	23.01	29.51
MnO		0.31	0.29	0.26	0.52	0.55	0.86
CaO	14.63	2.35	2.43	20.82	17.13	6.15	8.50
Na_2O	3.05	0.03	0.03	0.25	0.23	0.05	0.14
K_2O	0.25						
Total	99.94	100.00	99.88	99.96	100.08	99.59	100.37

Structural formulae

	8 oxygens		6 oxygens					
Si	2.310	Si	1.977	1.954	1.947	1.945	1.963	1.941
Al	1.682	Al	.023	.046	.053	.055	.037	.059
Sum	3.992	Sum	2.000	2.000	2.000	2.000	2.000	2.000
Ca	.714	Al	.020	.030	.048	.037	.011	.010
Na	.270	Ti	.003	.006	.011	.018	.015	.012
K	.015	Mg	.976	.963	.831	.653	.965	.619
Sum	.998	Fe			.111	.292	.009	.360
		Sum	1.000	1.000	1.000	1.000	1.000	1.000
Ab	27.0							
An	71.6	Mg	.503	.518				
Or	1.5	Fe	.395	.381	.148	.262	.727	.618
		Mn	.009	.009	.008	.017	.018	.029
		Ca	.090	.093	.827	.703	.252	.361
		Na	.002	.002	.018	.017	.004	.011
		Sum	.999	1.003	1.001	.999	1.000	1.018
Mg/(Mg+Fe)			.789	.795	.763	.541	.567	.388
Ca/(Ca+Mg+Fe+Mn)			.046	.047	.430	.365	.128	.182
(Al+Ti+Na)/2			.024	.042	.065	.064	.033	.046

Table 2.11 Representative electron probe analyses and structural formulae of oscillatory-zoned orthopyroxene phenocryst in sample 4I4A-1 from the northern Bliss Hill dike, selected from 201 analyses. David C. Elbert, analyst.

	187 Mg-rich	44 Typical	101 Al-rich	11 Al-poor
SiO_2	54.64	53.64	52.96	54.73
Al_2O_3	2.04	3.39	4.78	1.39
TiO_2	0.25	0.30	0.32	0.21
MgO	28.67	27.97	27.52	28.51
FeO	11.33	11.60	11.98	12.03
MnO	0.36	0.24	0.33	0.32
CaO	1.99	2.14	2.28	2.13
Na_2O	0.06	0.04	0.03	0.00
Total	99.34	99.32	100.20	99.32
Structural formulae based on 6 oxygens				
Si	1.952	1.920	1.884	1.962
Al	.048	.080	.116	.038
Sum	2.000	2.000	2.000	2.000
Al	.038	.063	.085	.021
Ti	.007	.008	.009	.006
Mg	.956	.929	.907	.973
Sum	1.000	1.000	1.000	1.000
Mg	.571	.563	.553	.550
Fe	.338	.347	.356	.361
Mn	.011	.007	.010	.010
Ca	.076	.082	.087	.082
Na	.004	.003	.002	.000
Sum	1.001	1.002	1.008	1.003
Mg/(Mg+Fe)	.812	.811	.804	.809
Ca/(Ca+Mg+Fe+Mn)	.044	.043	.045	.041
(Al+Ti+Na)/2	.036	.077	.106	.032

oscillatory zoning is due mainly to the variation in Al content in orthopyroxene with a limited ratio of Mg/(Fe+Mg) from 0.804 to 0.812. This is expressed as a variation in weight % Al_2O_3 from 1.39 to 4.78, or by the ratio (Al+Ti+Na)/2 from 0.032 to 0.106, a measure of the total non-quadrilateral component. Based on optical properties, the orthopyroxene in the southern Bliss Hill dike is richer in Mg (2V=-85-90) than in this northern dike (4I4A).

Some of the orthopyroxene phenocrysts contain fine red-brown inclusions that are tentatively identified as kaersutite on the basis of the analyses in Table 2.12. These are presented as averages of 5 point analyses, 4 other point analyses, and an average of all 9 analysis points. The ratio Mg/(Mg+Fe) is 0.37, a kaersutite composition that is much too rich in Fe to have formed in equilibrium with the enclosing orthopyroxene. This ratio could theoretically be raised if a substantial part of the Fe were recalculated as Fe^{3+} in the structural formula. However, such a Fe^{3+} calculation would have the effect of raising the calculated content of Na in the M4 site to values even higher than the present values, that are already very high for a calcic amphibole. The most likely origin of the kaersutite grains is that they were xenoliths in the melt that were encased in orthopyroxene early in the crystallization history.

Chapman Island - Sample QB-4

Back scatter images were taken of some of the titanomagnetites in samples from the Chapman Island sill. These images show high peaks (the height of the peak is related to the abundance of the element), for chromium and magnesium. A number of these titanomagnetites have chrome spinel cores, and ilmenite exsolution is rarely observed in the titanomagnetite. The high magnesium content may stabilize the titanomagnetite solid-solution under conditions where a normal titanomagnetite solid solution would undergo oxidation-exsolution (Haggerty, 1976).

Table 2.12 Representative electron probe analyses and structural formulae of brown unknown inclusions in orthopyroxene phenocrysts in sample 4I4A-1 from the northern Bliss Hill dike. Structural formulae calculated as amphibole on the basis of 23 oxygens per formula unit. David C. Elbert, analyst.

	Average of 5 analysis points	Average of 4 analysis points	Average of all 9 points
SiO_2	41.51	37.79	39.65
Al_2O_3	16.00	16.56	16.28
TiO_2	4.14	6.01	5.08
MgO	6.42	6.64	6.53
FeO	19.26	20.18	19.72
MnO	0.20	0.23	0.22
CaO	8.50	9.48	8.99
Na_2O	2.04	2.27	2.16
K_2O	0.35	0.31	0.33
Total	98.42	99.47	98.96
Structural formulae based on 23 oxygens			
Si	6.232	5.673	5.953
Al	1.768	2.327	2.047
Sum	8.000	8.000	8.000
Al	1.063	.603	.833
Ti	.467	.679	.573
Mg	1.437	1.486	1.461
Fe	2.033	2.232	2.132
Sum	5.000	5.000	5.000
Fe	.385	.302	.343
Mn	.025	.029	.027
Ca	1.367	1.525	1.446
Na	.222	.144	.183
Sum	2.000	2.000	2.000
Na	.372	.517	.444
K	.067	.059	.063
Sum	.439	.576	.507
Mg/(Mg+Fe)	.373	.370	.371

CHAPTER 3
GEOCHEMISTRY

Introduction

Sixty samples from the diabases collected in this paleomagnetic study were selected for chemical analysis. These were chosen for freshness, and position in the dike. Whenever possible both interiors and chilled contacts of intrusions were analyzed. Commonly analyses were made from the same cores used for paleomagnetic studies, or at least from the same blocks from which paleomagnetic cores were drilled. Generally, freshness was easier to judge in broken samples than in cores, but was confirmed with thin section studies. Fresh samples of chilled contacts were not easy to obtain, because these zones are apparently more susceptible to weathering.

Approximately 20-50 grams of material were coarse-crushed in a steel percussion mortar. Coarse-crushed material was hand picked to avoid obvious weathered surfaces and rare secondary veins. This was followed by grinding in a tungsten carbide shatterbox. Aliquats of powder were sampled for X-ray fluoresence analysis at the University of Massachusetts using a modification of the methods of Norrish and Chappell (1967) and Norrish and Hutton (1969). For major element analyses the samples were first ignited at 1000°C for at least six hours, to remove all volatile constituents and to oxidize all Fe to Fe_2O_3. Samples were then fused into glass discs using a lithium tetraborate flux. Major elements are reported in weight percent of the oxides of the ignited material, with total Fe reported as Fe_2O_3. Pressed powder pellets were made for trace element analyses, which are reported in ppm. CIPW Norms in weight percent were calculated using an assumed constant amount of 90% of Fe_2O_3 as FeO (J.M. Rhodes, personal communication, 1988). The analytical results are listed in Tables 3.1 through 3.6 in which analyses are arranged according to major geochemical distinctions and geography. .Within each Table samples are listed geographically from north to south as shown in Figure 1.5. Petrography of the samples is given in Chapter 2.

The purpose of this geochemical study is to use major and trace elements as a means to classify the diabases, and to determine whether there is more than one chemical system. If more than one system exists, are the systems related by magmatic processes, such as crystal fractionation or melting, or do the melts represent different magmatic sources?

Major Elements

The major elements analyzed were Si, Ti, Al, Fe, Mn, Mg, Ca, Na, K, P. According to major element chemistry these diabases are tholeiites. This is shown in Figure 3.1 in which analyses are plotted on the alkali vs silica plot of Macdonald and Katsura (1964). All samples lie in the tholeiitic field except sample 6I6 of the Pelham-Loudville System. The C.I.P.W. norms (Tables 3-1 through 3-6) show that the rock compositions fall within the quartz tholeiite and olivine tholeiite volumes of the basalt tetrahedron (Yoder and Tilley, 1962). The diabases fall into all four of the chemical types for eastern North American diabases, as defined by Weigand and Ragland (1970). This is shown in Figure 3.2, in which the weight ratio $Fe_2O_3/(Fe_2O_3+MgO)$ is plotted against weight percent TiO_2. Three of these types , the high TiO_2 quartz-normative, low TiO_2 quartz-normative, and the high Fe_2O_3 quartz-normative were reported from Connecticut diabases by Weigand and Ragland (1970). They found a positive correlation for SiO_2 and $Fe_2O_3/(Fe_2O_3+MgO)$, but this has not been observed in the present study.

The chemical groups of the central Massachusetts diabases are particularly well shown on a plot of weight percent TiO_2 versus weight percent MgO in Figure 3.3. The Pelham-Loudville system, the Ware system, the Bliss Hill group and Quabbin Reservoir

Table 3.1 Major- and trace-element analyses and CIPW norms of samples from the Holden system.

	OX-1	OX-3	OX-6	1681A	1681B	1681C	1683	1688	Rd122	QUAC	QP-B	F2AR
SiO_2	52.19	51.97	52.15	52.15	52.13	51.80	52.34	52.24	52.06	52.22	52.97	52.48
TiO_2	1.03	1.17	.80	1.13	1.19	.88	1.32	1.11	1.54	1.21	1.43	1.24
Al_2O_3	14.13	14.50	15.89	13.84	14.39	14.34	14.76	13.79	14.99	14.69	14.61	14.66
Fe_2O_3	10.62	11.12	9.17	11.11	11.44	10.22	11.55	11.00	11.94	11.72	11.97	11.46
MnO	0.17	0.23	0.15	0.17	0.17	0.16	0.17	0.19	0.17	0.18	0.17	0.18
MgO	7.94	7.16	7.97	7.58	7.06	8.52	6.30	8.04	5.74	6.75	5.77	6.90
CaO	11.64	10.85	11.71	11.30	11.01	11.67	10.34	11.27	10.33	10.99	9.88	10.60
Na_2O	2.01	2.31	1.72	2.47	2.45	2.30	2.38	1.84	2.69	1.73	2.18	1.97
K_2O	0.30	0.52	0.40	0.36	0.46	0.38	0.71	0.57	0.75	0.43	0.89	0.71
P_2O_5	0.11	0.14	0.09	0.14	0.14	0.10	0.17	0.12	0.21	0.13	0.17	0.14
Total	100.14	99.97	100.05	100.25	100.44	100.37	100.04	100.17	100.42	100.05	100.04	100.34
Mg/(Mg+Fe)[1]	.597	.560	.633	.583	.550	.623	.519	.591	.488	.533	.488	.544
Ca/(Ca+Na)[1]	.762	.722	.790	.717	.713	.737	.706	.772	.680	.778	.715	.748
Trace Elements (ppm)												
Y	19	22	15	21	22	16	24	19	27	21	26	22
Sr	169	174	189	166	169	172	200	174	188	189	227	195
Rb	11	19	16	14	16	13	26	38	26	17	31	24
Th	3	1	1	1	2	2	2	1	1	2	3	1
Pb	6	7	5	6	6	4	8	5	5	5	7	5
Ga	16	18	17	17	18	16	20	16	16	18	19	17
Nb	7	9	5	7	8	6	9	7	10	7	10	8
Zr	89	106	66	102	105	71	119	95	128	101	136	108
Zn	81	95	64	90	94	77	86	82	101	87	92	88
Ni	94	85	91	88	81	104	68	93	66	73	65	76
Cr	362	211	270	321	242	372	211	360	166	111	106	183
V	240	268	182	250	262	210	230	254	272	275	263	250
Ce	25	32	23	31	27	16	37	29	32	28	28	30
Ba	92	149	121	97	125	114	198	137	201	147	230	164
La	7	13	6	3	9	3	11	5	11	10	15	8

Table 3.1 (continued).

CIPW Norms[2]

	OX-1	OX-3	OX-6	1681A	1681B	1681C	1683	1688	Rd122	QUAC	QP-B	F2AR
Qz	2.04	1.21	2.81	0.43	0.75		2.20	2.31	0.94	4.52	4.43	3.17
Or	1.77	3.09	2.35	2.13	2.72	2.25	4.20	3.37	4.42	2.52	5.24	4.18
Ab	17.03	19.51	14.56	20.90	20.73	19.46	20.14	15.57	22.79	14.65	18.42	16.70
An	28.64	27.67	34.64	25.62	26.91	27.68	27.50	27.70	26.60	31.06	27.48	29.06
Di	23.28	20.80	18.82	24.28	22.11	24.20	18.82	22.50	19.33	18.72	16.98	18.66
Hy	23.63	23.53	23.99	22.82	22.98	21.07	22.61	24.72	21.20	24.29	22.61	24.21
Ol						2.34						
Mt	1.54	1.61	1.33	1.61	1.65	1.48	1.68	1.59	1.73	1.70	1.73	1.66
Ilm	1.95	2.22	1.52	2.15	2.26	1.67	2.51	2.12	2.92	2.30	2.71	2.36
Ap	0.26	0.32	0.20	0.33	0.33	0.22	0.38	0.28	0.49	0.30	0.39	0.33
Total	100.14	99.97	100.03	100.25	100.44	100.37	100.04	100.17	100.42	100.06	99.99	100.33
An[3]	63	59	70	55	56	59	58	64	54	68	60	64

[1] Atomic ratio.

[2] Assuming 90% of Fe_2O_3 as FeO, 10% as Fe_2O_3.

[3] Molar anorthite content of normative plagioclase.

Table 3.2 Major- and trace-element analyses and CIPW norms of samples from the Loudville group, Pelham-Loudville system.

Sample	SWM2B	MS4	MS2B	CR7	CS5	CS9
SiO_2	50.40	50.04	50.46	50.65	50.29	50.28
TiO_2	1.33	1.29	1.34	1.26	1.30	1.37
Al_2O_3	13.49	13.56	13.16	13.56	13.70	13.25
Fe_2O_3	15.82	15.68	16.22	15.80	15.54	16.13
MnO	0.23	0.23	0.24	0.25	0.26	0.24
MgO	5.71	5.77	5.88	6.19	5.93	5.74
CaO	9.95	9.64	10.17	10.21	10.22	9.91
Na_2O	2.09	2.77	2.07	1.22	2.06	2.82
K_2O	0.60	0.94	0.52	0.55	0.40	0.55
P_2O_5	0.16	0.16	0.15	0.14	0.15	0.16
Total	99.78	100.08	100.21	99.83	99.85	100.45
Mg/(Mg+Fe)[1]	.417	.422	.418	.437	.430	.413
Ca/(Ca+Na)[1]	.725	.658	.731	.822	.733	.666

Trace Elements (ppm)

Y	36	34	35	33	32	34
Sr	105	134	102	106	233	108
Rb	26	49	21	25	54	24
Th	1	1	1	2	1	1
Pb	6	7	7	7	3	5
Ga	19	20	21	19	19	19
Nb	6	5	5	4	5	6
Zr	103	100	102	95	94	99
Zn	127	130	120	130	105	86
Ni	68	75	67	71	81	68
Cr	66	67	62	74	85	64
V	376	358	370	355	354	365
Ce	21	23	17	18	19	23
Ba	124	159	126	120	265	82
La	1	2	7	1	6	4

CIPW Norms[2]

Sample	SWM2B	MS4	MS2B	CR7	CS5	CS9
Qz	0.95		0.80	4.39	0.99	
Or	3.55	5.54	3.07	3.26	2.39	3.27
Ab	17.69	23.44	17.47	10.32	17.39	23.83
An	25.66	21.79	25.11	30.20	26.97	21.87
Di	19.07	21.02	20.46	16.39	19.33	22.12
Hy	27.69	12.94	28.06	30.37	27.77	16.45
Ol		10.25				7.61
Mt	2.29	2.27	2.35	2.29	2.25	2.34
Ilm	2.53	2.45	2.54	2.40	2.47	2.60
Ap	0.37	0.36	0.35	0.32	0.35	0.36
Total	99.78	100.06	100.21	99.94	99.91	100.45
An[3]	59	48	59	75	61	48

[1] Atomic ratio.

[2] Assuming 90% of Fe_2O_3 as FeO, 10% as Fe_2O_3.

[3] Molar anorthite content of normative plagioclase.

Table 3.3 Major- and trace-element analyses and CIPW norms of samples from the Millers Falls area, Pelham-Loudville system.

Sample	NF	NF	MF2	MF3	LP	L7	LA1	HH	BUT2	RS	RSG
SiO_2	50.64	50.33	50.62	50.62	50.66	50.74	50.74	50.49	50.47	50.39	50.72
TiO_2	1.34	1.33	1.37	1.32	1.36	1.24	1.36	1.44	1.33	1.31	1.32
Al_2O_3	13.48	13.28	13.01	13.60	13.43	13.67	13.54	13.11	13.44	13.36	13.53
Fe_2O_3	15.95	15.93	16.04	15.76	16.04	15.40	16.03	16.55	15.89	15.87	15.99
MnO	0.24	0.23	0.24	0.24	0.24	0.24	0.24	0.24	0.24	0.23	0.24
MgO	5.80	5.82	5.72	5.87	6.01	6.24	5.98	5.55	5.71	5.89	5.78
CaO	9.54	10.08	9.86	10.12	10.10	10.32	10.13	9.86	10.11	10.10	9.52
Na_2O	2.40	2.15	2.79	2.20	1.96	1.96	1.95	2.31	2.52	2.56	2.24
K_2O	0.84	0.45	0.51	0.52	0.50	0.45	0.49	0.52	0.58	0.43	0.87
P_2O_5	0.15	0.15	0.16	0.15	0.15	0.14	0.15	0.16	0.16	0.15	0.15
Total	100.38	99.75	100.32	100.40	100.45	100.40	100.61	100.23	100.45	100.29	100.36
Mg/(Mg+Fe)[1]	.419	.420	.414	.425	.426	.445	.425	.399	.416	.424	.417
Ca/(Ca+Na)[1]	.687	.722	.661	.718	.740	.744	.742	.702	.689	.686	.701
Trace Elements (ppm)											
Y	36	36	35	35	35	32	35	39	36	36	36
Sr	112	122	102	101	105	103	103	99	106	99	98
Rb	36	39	20	20	19	17	18	19	18	15	15
Th	2	1	3	3	1	2	2	2	1	1	3
Pb	5	6	8	6	7	6	8	8	6	5	9
Ga	19	20	20	20	20	20	19	19	19	19	20
Nb	6	5	6	5	5	4	5	7	6	6	6
Zr	101	101	110	100	99	88	99	112	102	100	102
Zn	128	122	148	136	115	108	118	151	129	132	136
Ni	69	65	70	67	65	67	65	69	65	68	69
Cr	69	66	66	69	61	70	64	56	60	68	70
V	375	360	395	374	346	344	359	400	360	377	380
Ce	20	18	28	16	21	17	25	20	25	22	23
Ba	153	182	119	127	118	112	119	116	110	115	105
La	5	5	6	2	6	3	6	8	8	2	6

Table 3.3 (continued).

CIPW Norms[2]

	NF	NF2	MF2	MF3	LP	L7	LA1	HH	BUT2	RS	RSG
Qz		0.82		0.43	1.43	1.30	1.56	0.35			
Or	4.96	2.65	3.01	3.07	2.93	2.65	2.90	3.07	3.37	2.56	5.13
Ab	20.31	18.15	23.61	18.62	16.58	16.59	16.47	19.54	21.28	21.6	18.97
An	23.53	25.29	21.47	25.70	26.38	27.18	26.75	23.87	23.71	23.69	24.30
Di	19.19	19.97	22.23	19.77	19.10	19.38	18.94	20.21	21.40	21.40	18.43
Hy	24.65	27.70	19.70	27.67	28.81	28.40	28.75	27.69	22.31	22.46	28.00
Ol	2.53		5.01						3.22	3.31	0.33
Mt	2.32	2.31	2.32	2.29	2.33	2.23	2.33	2.40	2.30	2.29	2.32
Ilm	2.54	2.53	2.60	2.51	2.58	2.35	2.58	2.73	2.52	2.49	2.59
Ap	0.35	0.34	0.36	0.35	0.35	0.32	0.34	0.38	0.36	0.34	0.35
Total	100.38	99.75	100.32	100.40	100.48	100.39	100.61	100.23	100.45	100.29	100.41
An[3]	54	58	48	58	61	62	62	55	53	52	56

[1] Atomic ratio.

[2] Assuming 90% of Fe_2O_3 as FeO, 10% as Fe_2O_3.

[3] Molar anorthite content of normative plagioclase.

Table 3.4 Major- and trace-element analyses and CIPW norms of samples from the Pelham dike and southwest Quabbin areas, Pelham Group, Pelham-Loudville system.

Sample	3C6	8C9	202W	NV6	6I3	6I4	EDH	CC	126A	JD	6I6
SiO_2	50.41	50.65	50.72	50.86	50.31	50.44	50.05	50.67	50.56	50.54	48.90
TiO_2	1.35	1.35	1.31	1.38	1.36	1.34	1.34	1.36	1.32	1.34	1.21
Al_2O_3	13.24	13.35	13.57	13.48	13.15	13.43	13.13	13.37	13.51	13.48	13.96
Fe_2O_3	16.02	15.99	15.64	16.01	16.38	15.92	16.09	16.02	15.69	15.97	15.11
MnO	0.24	0.25	0.23	0.24	0.25	0.24	0.24	0.24	0.23	0.25	0.21
MgO	5.70	5.69	5.78	5.83	5.73	5.79	5.80	5.70	5.88	5.75	5.79
CaO	10.02	9.98	10.06	9.92	10.02	10.04	10.02	9.81	10.11	10.11	10.64
Na_2O	2.32	2.53	2.33	2.02	2.50	2.40	2.55	2.16	2.34	2.29	2.83
K_2O	0.52	0.53	0.48	0.53	0.51	0.50	0.55	0.67	0.48	0.48	1.13
P_2O_5	0.16	0.16	0.15	0.16	0.16	0.15	0.15	0.16	0.15	0.15	0.13
Total	99.98	100.48	100.27	100.43	100.37	100.25	99.92	100.16	100.27	100.36	99.91
Mg/(Mg+Fe)[1]	.413	.413	.423	.419	.409	.419	.417	.413	.426	.416	.431
Ca/(Ca+Na)[1]	.705	.686	.705	.731	.689	.698	.685	.715	.705	.709	.675
Trace Elements (ppm)											
Y	36	36	35	36	37	36	35	37	35	36	37
Sr	101	96	96	99	100	98	97	103	99	103	106
Rb	19	23	17	21	17	19	19	28	19	26	21
Th	3	2	3	2	1	2	1	3	2	2	1
Pb	7	8	6	6	6	7	5	5	8	8	7
Ga	21	20	20	20	20	19	19	20	20	19	19
Nb	5	6	5	5	5	5	5	5	6	6	6
Zr	101	107	103	106	107	102	99	105	100	101	105
Zn	123	143	142	130	132	134	126	129	129	146	145
Ni	65	68	70	68	64	70	66	65	68	72	72
Cr	63	63	70	61	69	66	66	60	71	66	66
V	357	379	379	368	371	378	364	376	370	371	385
Ce	24	23	17	22	23	22	22	16	19	24	23
Ba	124	97	112	124	125	113	112	131	117	111	128
La	5	6	6	7	8	6	4	8	5	5	3

Table 3.4 (continued).

CIPW Norms[2]	3C6	8C9	202W	NV6	6I3	6I4	EDH	CC	126A	JD	6I6
Qz	0.05		0.34	1.73				0.95	0.42	0.18	
Or	3.07	3.13	2.82	3.15	3.01	2.95	3.24	3.94	2.84	2.85	6.67
Ab	19.63	21.41	19.69	17.08	21.15	20.31	21.60	18.07	18.90	19.35	23.01
An	24.18	23.51	25.18	26.16	23.15	24.40	22.75	24.92	25.42	25.08	22.05
Ne											0.52
Di	20.60	21.00	19.96	18.51	21.48	20.54	21.83	19.13	19.99	20.25	25.05
Hy	27.19	24.03	27.17	28.50	22.91	25.53	20.38	27.82	27.47	27.42	
Ol		2.12			3.32	1.31	4.89				17.81
Mt	2.32	2.32	2.27	2.32	2.38	2.32	2.33	2.32	2.27	2.31	2.19
Ilm	2.56	2.56	2.48	2.61	2.58	2.54	2.54	2.59	2.50	2.54	2.31
Ap	0.37	0.37	0.35	0.37	0.37	0.35	0.36	0.37	0.35	0.3	50.31
Total	99.98	100.45	100.26	100.43	100.37	100.25	99.92	100.10	100.26	100.35	99.92
An[3]	52	52	56	61	52	55	51	58	57	56	49

[1] Atomic ratio.

[2] Assuming 90% of Fe_2O_3 as FeO, 10% as Fe_2O_3.

[3] Molar anorthite content of normative plagioclase.

Table 3.5 Major- and trace-element analyses and CIPW norms of samples from the Ware system.

Sample	FK	BA3	W4	WA-D	WA-3	PC3	FX-5	FX-3
SiO_2	51.89	51.86	52.26	51.67	51.46	52.10	51.70	51.86
TiO_2	0.83	0.78	0.81	0.82	0.79	0.78	0.79	0.83
Al_2O_3	14.61	14.84	15.09	15.12	15.04	14.87	14.92	14.77
Fe_2O_3	11.80	11.78	11.55	11.60	11.59	11.63	11.50	11.70
MnO	0.19	0.20	0.19	0.20	0.20	0.19	0.19	0.19
MgO	7.29	7.35	7.28	7.33	7.19	7.47	7.54	7.04
CaO	10.60	10.49	10.77	11.07	11.07	10.69	10.87	10.69
Na_2O	2.35	2.07	1.64	2.15	1.98	2.25	2.49	2.62
K_2O	0.48	0.37	0.49	0.41	0.41	0.40	0.42	0.50
P_2O_5	0.11	0.10	0.10	0.10	0.10	0.10	0.10	0.11
Total	100.15	99.84	100.18	100.47	99.83	100.48	100.52	100.31
Mg/(Mg+Fe)[1]	.550	.553	.555	.556	.551	.561	.565	.548
Ca/(Ca+Na)[1]	.714	.737	.784	.740	.755	.724	.707	.693

Trace Elements (ppm)

Y	22	21	22	22	21	21	21	22
Sr	139	133	132	132	130	136	128	139
Rb	15	11	17	17	17	13	13	14
Th	1	1	0	0	1	1	1	1
Pb	7	6	4	4	6	4	5	5
Ga	17	17	17	17	17	18	17	16
Nb	4	5	4	4	4	4	5	5
Zr	70	65	70	67	68	65	66	72
Zn	93	91	86	98	88	88	94	95
Ni	61	62	55	64	58	57	64	59
Cr	178	182	156	205	181	168	198	176
V	258	250	238	257	252	237	253	265
Ce	21	26	18	15	17	14	12	18
Ba	121	104	128	95	112	114	110	112
La	7	4	5	6	7	4	8	8

Table 3.5 (continued).

CIPW Norms[2]	FK	BA3	W4	WA-D	WA-3	PC3	FX-5	FX-3
Qz	0.35	1.84	3.79	0.54	1.40	0.82		
Or	2.79	2.19	2.92	2.42	2.42	2.39	2.48	2.95
Ab	19.87	17.52	13.88	18.19	16.75	19.02	21.07	22.17
An	27.93	30.11	32.34	30.40	30.94	29.28	28.30	27.07
Di	19.81	17.60	16.86	19.70	19.25	19.06	20.60	20.88
Hy	25.86	27.17	26.93	25.75	25.64	26.51	21.80	21.39
Ol							2.87	2.32
Mt	1.71	1.71	1.67	1.68	1.68	1.69	1.67	1.70
Ilm	1.58	1.48	1.54	1.56	1.50	1.49	1.50	1.58
Ap	0.24	0.22	0.24	0.24	0.24	0.23	0.23	0.26
Total	100.15	99.84	100.18	100.47	99.83	100.49	100.52	100.31
An[3]	58	63	70	63	65	61	57	55

[1] Atomic ratio.

[2] Assuming 90% of Fe_2O_3 as FeO, 10% as Fe_2O_3.

[3] Molar anorthite content of normative plagioclase.

Table 3.6 Major- and trace-element analyses and CIPW norms of samples from the Bliss Hill and Quabbin Reservoir groups of intrusions and the Gassetts, Vermont, lamprophyre.

	Bliss Hill				Quabbin Reservoir							
Sample	4I4	4I4A	BH2C	BH2I	C26N	C26Q	QB4	QBS	6I7-3	6I7-4	B44	GS
SiO_2	50.30	51.12	52.45	51.96	51.70	51.80	51.97	51.94	51.24	51.45	51.50	47.37
TiO_2	1.50	1.52	1.62	1.49	1.33	1.27	1.26	1.33	1.33	1.34	1.28	3.10
Al_2O_3	14.96	15.17	15.55	15.05	14.58	14.71	14.73	15.32	14.60	14.65	14.70	17.73
Fe_2O_3	12.67	12.56	12.13	12.27	12.25	12.15	12.16	12.12	12.37	12.40	12.37	11.25
MnO	0.17	0.18	0.13	0.17	0.16	0.16	0.16	0.17	0.16	0.17	0.16	0.18
MgO	6.97	6.71	5.75	6.39	7.75	7.75	8.13	6.74	7.93	7.61	8.31	5.84
CaO	9.64	9.51	8.86	9.45	8.78	8.71	8.70	8.98	9.04	9.18	9.01	7.68
Na_2O	2.84	2.63	2.73	2.53	3.00	2.85	2.12	2.95	2.78	2.85	2.59	4.55
K_2O	0.63	0.63	0.54	0.52	0.61	0.60	0.59	0.60	0.51	0.57	0.43	2.01
P_2O_5	0.21	0.22	0.20	0.19	0.19	0.17	0.16	0.18	0.18	0.17	0.17	0.93
Total	99.89	100.25	99.96	100.02	100.35	100.19	99.98	100.33	100.14	100.39	100.52	100.64
Mg/(Mg+Fe)[1]	.521	.514	.484	.508	.556	.558	.570	.524	.559	.549	.571	.507
Ca/(Ca+Na)[1]	.652	.666	.642	.674	.618	.628	.694	.627	.642	.640	.658	.483
Trace Elements (ppm)												
Y	19	20	20	20	17	18	17	20	18	18	17	30
Sr	265	270	252	277	215	216	218	227	220	225	217	808
Rb	16	17	13	13	23	18	18	18	16	26	27	45
Th	2	2	2	2	2	2	2	1	2	1	2	6
Pb	5	4	4	5	4	5	4	5	3	4	2	7
Ga	18	18	20	20	19	19	18	19	18	19	18	16
Nb	20	20	16	16	18	18	18	18	18	18	18	81
Zr	111	114	116	111	104	104	103	111	103	103	102	236
Zn	116	120	129	116	119	120	113	125	122	124	123	112
Ni	161	167	164	155	219	234	222	192	223	223	253	23
Cr	163	176	156	143	279	285	273	257	279	279	290	33
V	182	179	189	183	176	170	163	184	175	174	172	189
Ce	30	39	27	31	27	26	24	31	27	26	27	101
Ba	212	183	167	177	174	170	169	225	146	156	152	757
La	11	14	7	8	8	10	8	15	11	12	12	56

Table 3.6 (continued).

CIPW Norms[2]	4I4	4I4A	BH2C	BH2I	C26N	C26O	QB4	QBS	6I7-3	6I7-4	B44
Q			2.98	1.99			2.06	1.68			
Or	3.72	3.72	3.19	3.07	3.60	3.54	3.48	3.55	3.00	3.39	2.55
Ab	24.03	22.25	23.10	21.41	25.37	24.15	17.92	21.10	23.50	24.12	21.91
An	26.21	27.73	28.58	28.18	24.54	25.57	28.93	28.83	25.88	25.49	27.20
Di	16.76	14.96	11.70	14.48	14.65	13.62	10.81	12.04	14.65	15.63	13.48
Hy	16.19	25.09	25.11	25.83	22.05	25.63	32.23	27.97	23.72	22.10	28.85
Ol	7.80	1.29			5.40	3.11			4.64	4.93	1.73
Mt	1.84	1.83	1.75	1.78	1.78	1.76	1.76	1.76	1.79	1.80	1.79
Ilm	2.85	2.89	3.08	2.83	2.52	2.42	2.39	2.52	2.52	2.54	2.43
Ap	0.49	0.50	0.46	0.44	0.44	0.40	0.38	0.41	0.41	0.40	0.39
Total	99.89	100.25	99.96	100.02	100.34	100.19	99.96	99.86	100.12	100.40	100.34
An3	52	55	55	57	49	51	62	58	52	51	55

[1] Atomic ratio.

[2] Assuming 90% of Fe_2O_3 as FeO, 10% as Fe_2O_3.

[3] Molar anorthite content of normative plagioclase.

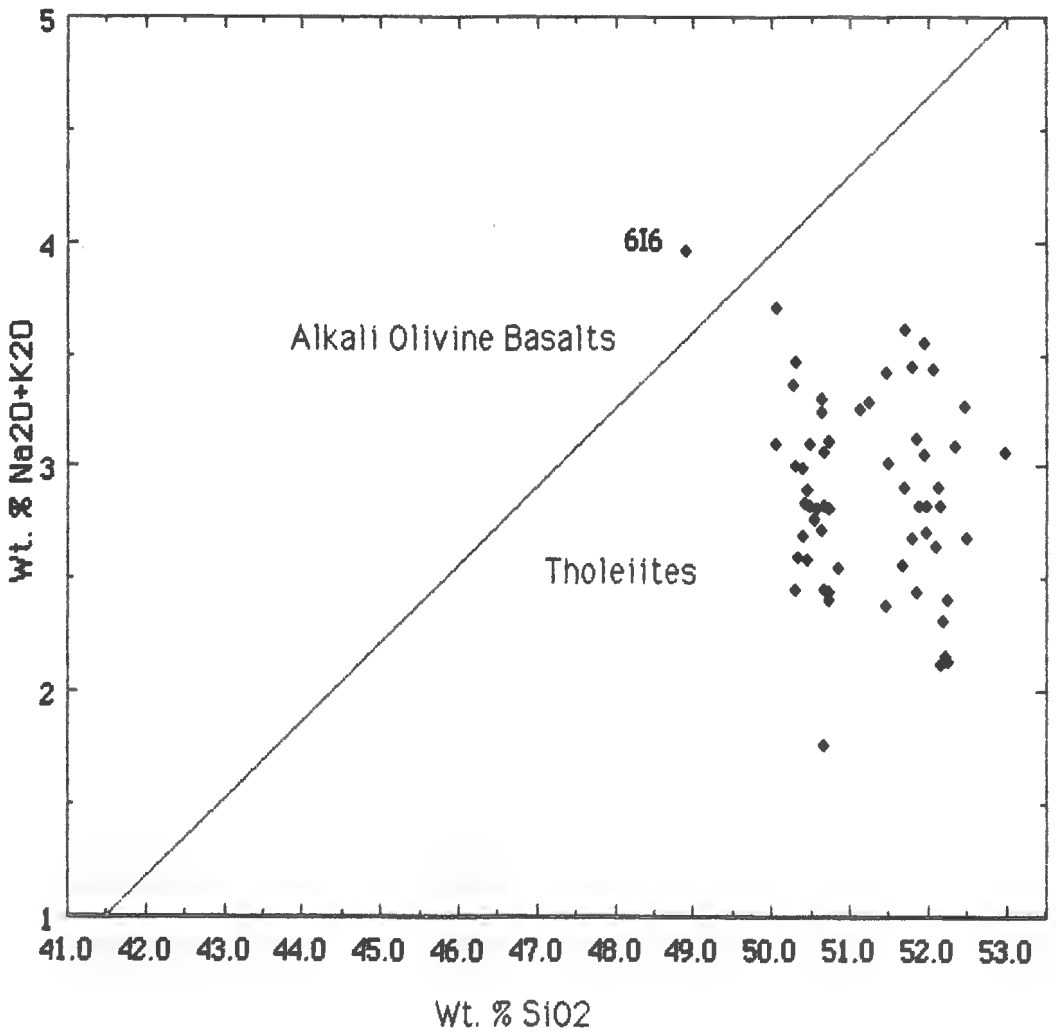

Figure 3.1 Diagram of weight percent $Na_2O+ K_2O$ and weight percent SiO_2, showing the discriminant line for Hawaiian alkali olivine basalts and tholeiites established by Macdonald and Katsura (1964). All analyses of Massachusetts diabases from this study are plotted.

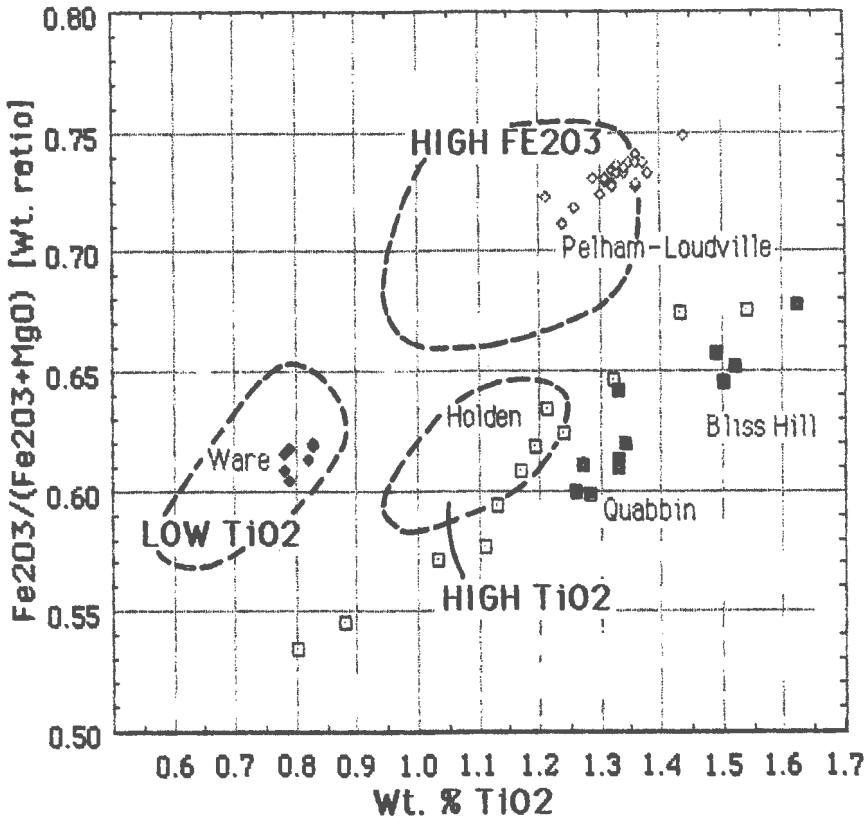

Figure 3.2 Diagram of weight ratio $Fe_2O_3/(Fe_2O_3+MgO)$ versus wt.% TiO_2. Dashed lines indicate fields of low TiO_2, high TiO_2, and high Fe_2O_3 quartz-normative diabases as defined by Weigand and Ragland (1970). All analyses of Massachusetts diabases from this study are plotted. Symbols: Holden - open squares; Pelham-Loudville - open diamonds; Ware - closed diamonds; Bliss Hill Quabbin Reservoir diabases - closed squares.

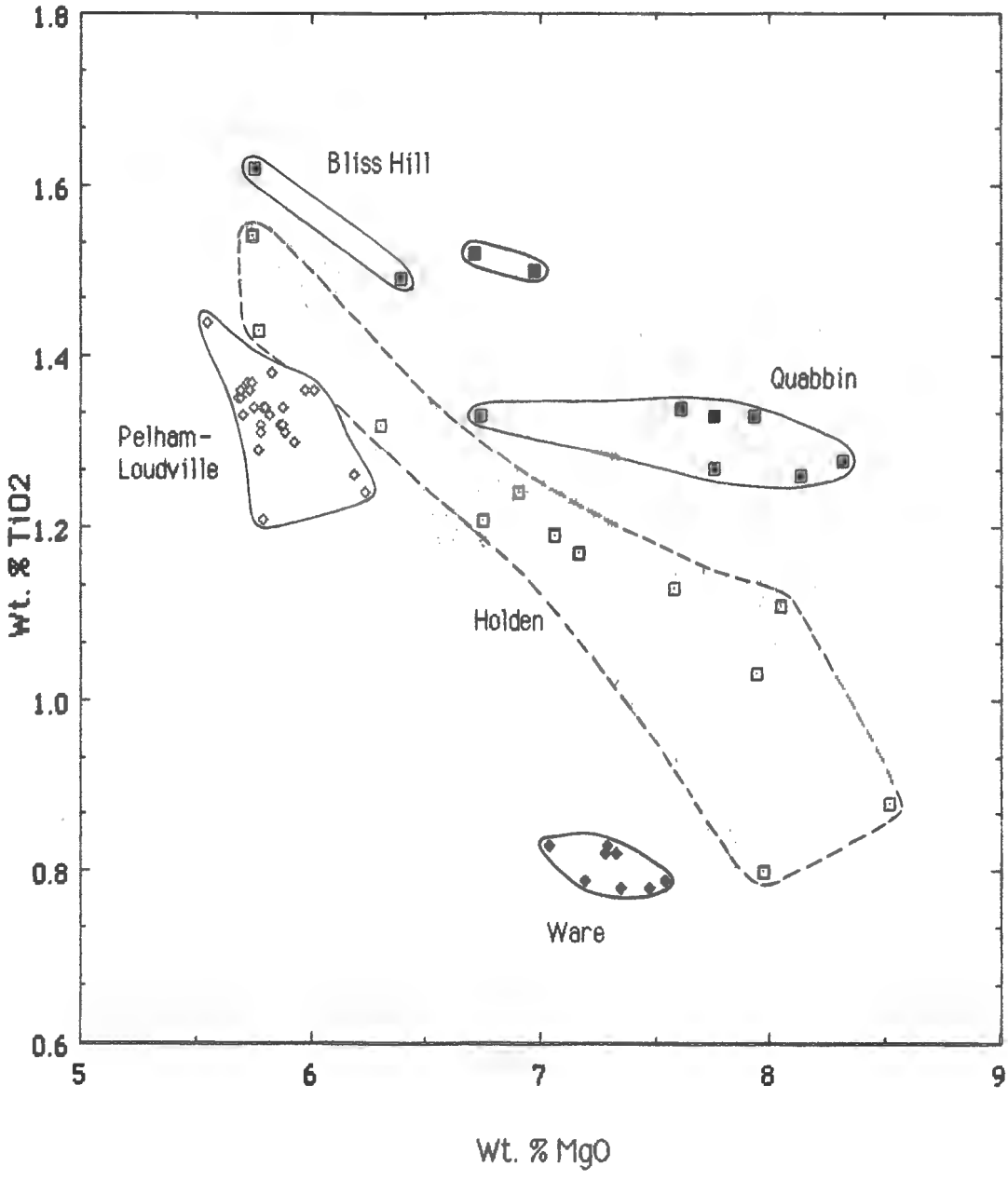

Figure 3.3 Plot of wt.% TiO_2 versus wt.% MgO. All diabase analyses from this study are plotted. Symbols: Holden - open squares; Pelham-Loudville - open diamonds; Ware - closed diamonds; Bliss Hill Quabbin Reservoir diabases - closed squares.

group are each tightly clustered. However, the analyses from the Holden system show a large variation in TiO_2 and MgO. The MgO, from 5.7 - 8.5 wt.% and TiO_2 from 1.54 - 0.80 wt.% show a good negative correlation on Figure 3.3. This large variation in major elements is characteristic of the Holden System. The MgO content of the Pelham-Loudville system is low at 5.9 wt.% and has normally higher TiO_2 near 1.3 wt.%. The Ware system clusters tightly in MgO about 7.0 wt.% and has markedly lower TiO_2 up to 0.8 wt.%, distinguishing it from the other systems. The Bliss Hill dikes have the highest TiO_2 contents of all the diabases, near 1.5 wt.%, with a range of MgO. The Quabbin Reservoir sills are rich in MgO, near 8.0 wt.%, and have TiO_2 close to 1.3 wt.%.

As shown in a plot of weight percent Fe_2O_3 versus MgO in Figure 3.4, the Holden system ranges in Fe_2O_3 from 9.2 to 12 wt.%. In the Pelham-Loudville system, the Fe_2O_3 is markedly higher from 15.4 to 16.6 wt.%, a distinct feature of this system. Surprisingly the TiO_2 content is not higher, as would be expected, if this were a FeTi basalt and the amount of Fe_2O_3 were taken as a measure of how evolved the system was. The Pelham-Loudville system is in the low range of Mg/(Mg+Fe) values, 0.399-0.445, for the Massachusetts diabases. These values indicate an evolved magma. The Ware system varies very slightly in Fe_2O_3 content from 11.5 to 11.8 wt.% . The Bliss Hill and Quabbin Reservoir diabases are similar in Fe_2O_3 contents of approximately 12 wt.%.

The range in Al_2O_3 in the Holden system is from 13.8 to 15.9 wt.% with a weak linear relationship to MgO, as shown in Figure 3.5. The Pelham-Loudville system is the lowest in Al_2O_3, from 13 to 13.7 wt.%, and shows little variation. The Ware system varies by only 0.5 wt.% in Al_2O_3. .The Bliss Hill diabases are the highest in Al_2O_3 and this decreases linearly with MgO content. The Quabbin Reservoir samples have a slight variation in Al_2O_3 content of 14.7-15.3 wt.%.

The range in K_2O content in the Holden system is from 0.3 to 0.9 wt.%, with some trend of decreasing K_2O with increasing MgO (Figure 3.6). The variation in the K_2O in the Pelham-Loudville system is quite large, from 0.4 to 1.13 wt.%, and appears not to be a function of MgO content. This could be related to the sericitic alteration of plagioclase. Sample 6I6 is sericitized. This might account from for the large increase in K_2O content in this sample compared to the average of 0.5 wt.% in the Pelham-Loudville system. In the Ware system there is a slight increase in K_2O with decreasing MgO content. The Bliss Hill and Quabbin Reservoir diabases have K_2O values from O.43-O.61 wt.%, that do not vary linearly with MgO.

Trace Elements

The trace elements analyzed in this study were Nb, Zr, Zn, Y, Sr, Rb, Ga, Ni, Cr, V, Pb, Ce, Th, Ba, and La. The trace elements provide further support for the subdivision of the central Massachusetts diabases into four chemical systems.

The trace elements Zr and V are plotted in Figure 3.7. In this diagram there is no clear trend in the Holden system, and Zr overlaps with the Pelham and Ware systems, and the Bliss Hill and Quabbin Reservoir groups. The range in Zr is large in the Holden system from 65 to 135 ppm, and V varies from 175 to 275 ppm. The Pelham-Loudville system is the richest in V with up to 400 ppm that varies relatively linearly with Zr. In the Ware system V and Zr vary only slightly from 250 ppm and 65 ppm, respectively. The Bliss Hill and Quabbin Reservoir diabases are the lowest of the systems in V with approximately 185 ppm and 175 ppm, respectively but are separated by Zr content. In the plot of Y versus Zr in Figure 3.8 the same relationships are present, except that the Holden system is more coherent in Y, which increases linearly with Zr, and plots in a distinct region. The Pelham-Loudville system is the richest in Y with 32 to 39 ppm, and the Ware system is tightly clustered with Y contents of 22 ppm. On average, Bliss Hill and Quabbin Reservoir diabases differ by about 2 ppm in Y, well within the determinative errors.

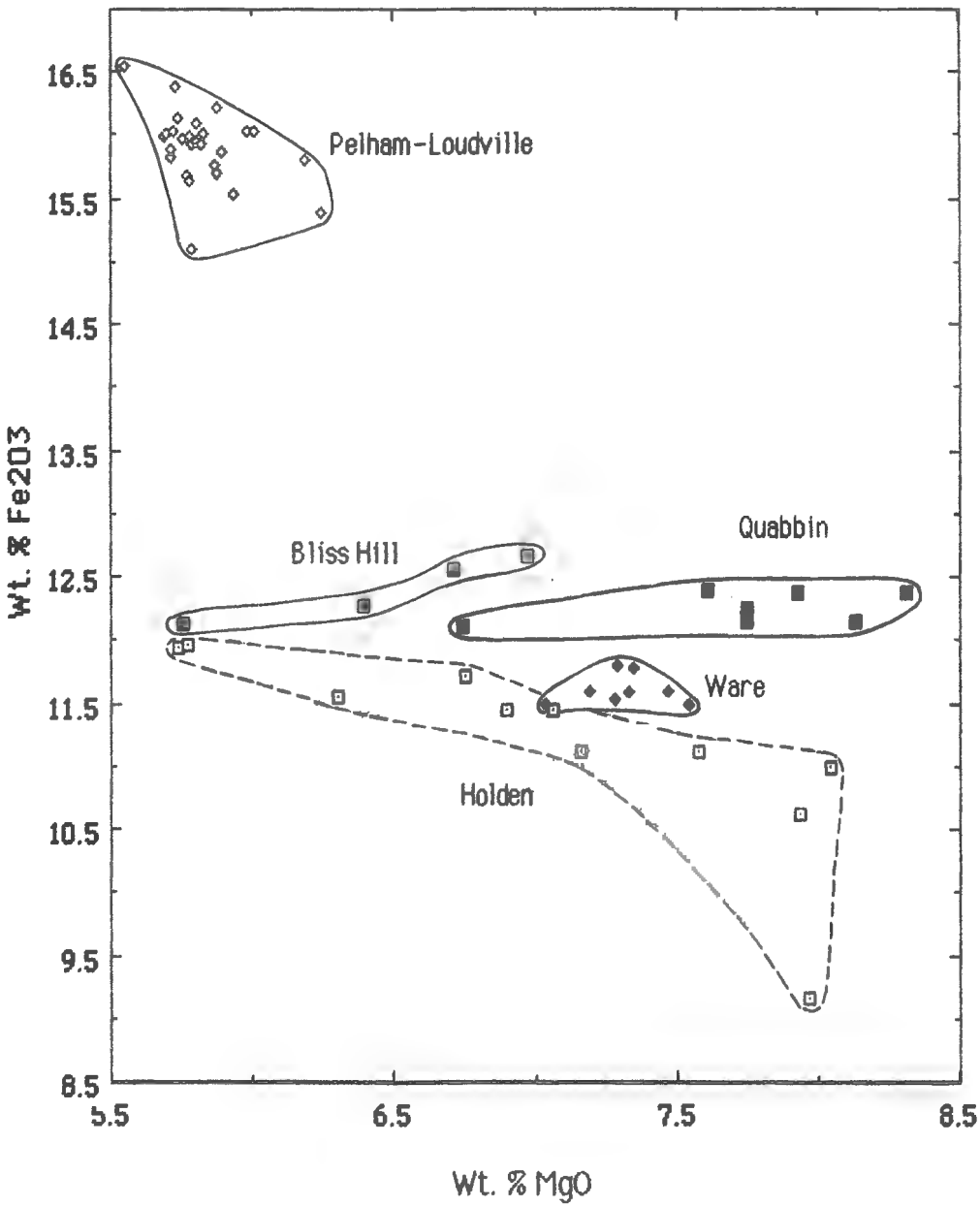

Figure 3.4 Plot of wt.% Fe_2O_3 versus wt.% MgO. All diabase analyses from this study are plotted. Symbols: Holden - open squares; Pelham-Loudville - open diamonds; Ware - closed diamonds; Bliss Hill Quabbin Reservoir diabases - closed squares.

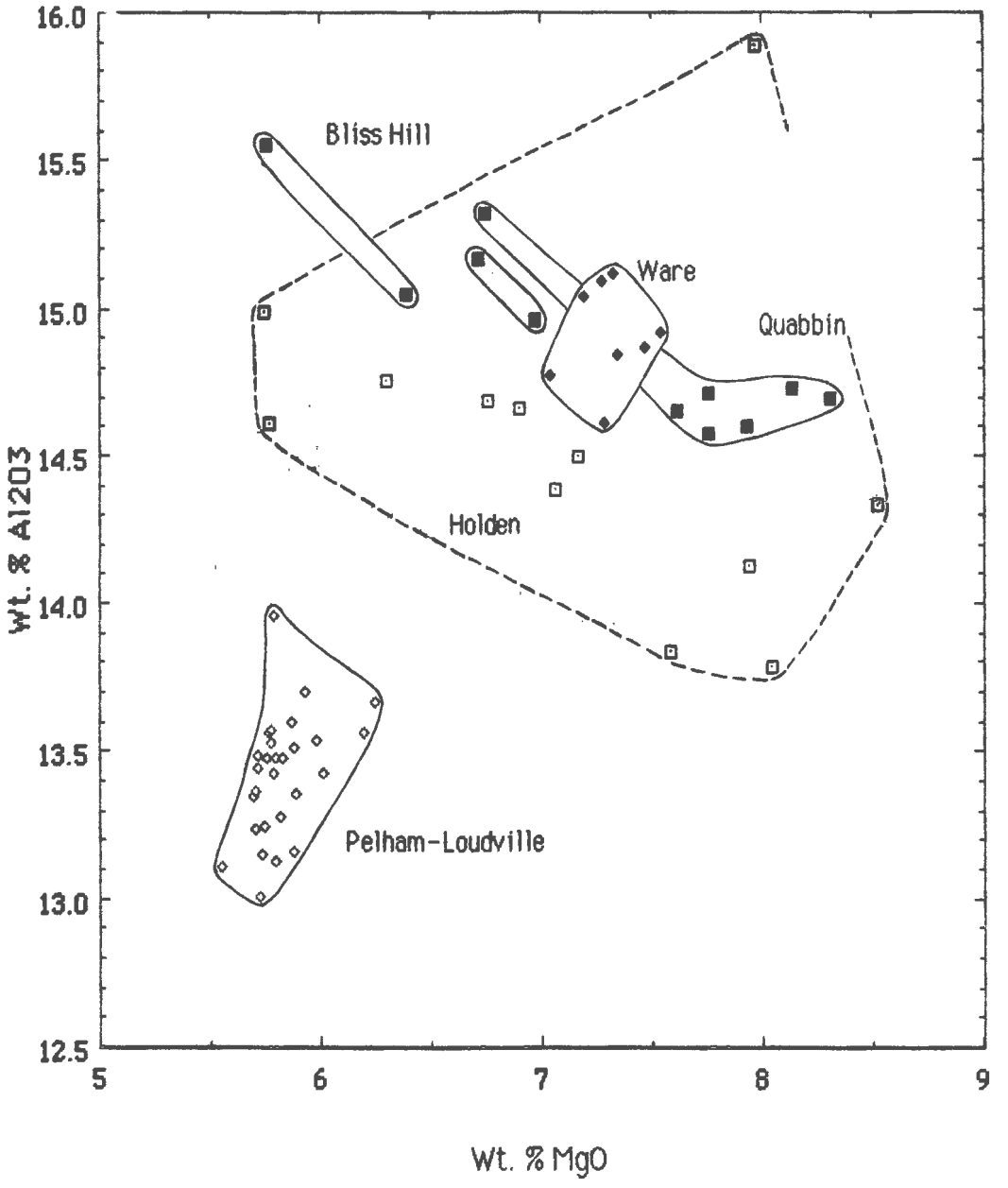

Figure 3.5 Plot of wt.% Al_2O_3 versus wt.% MgO. All diabase analyses from this study are plotted. Symbols: Holden - open squares; Pelham-Loudville - open diamonds; Ware - closed diamonds; Bliss Hill Quabbin Reservoir diabases - closed squares.

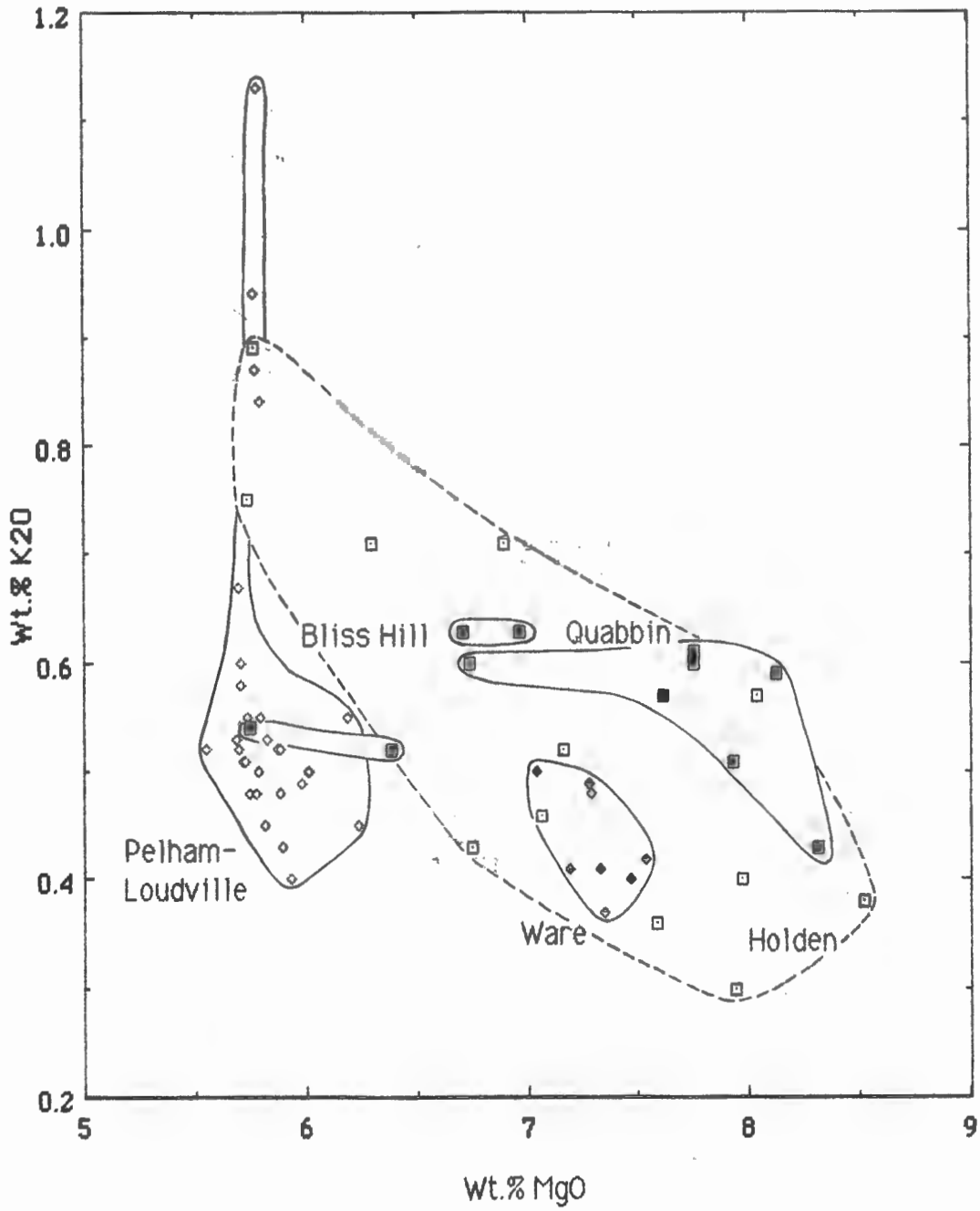

Figure 3.6 Plot of wt.% K_2O versus wt.% MgO. All diabase analyses from this study are plotted. Symbols: Holden - open squares; Pelham-Loudville - open diamonds; Ware - closed diamonds; Bliss Hill Quabbin Reservoir diabases - closed squares.

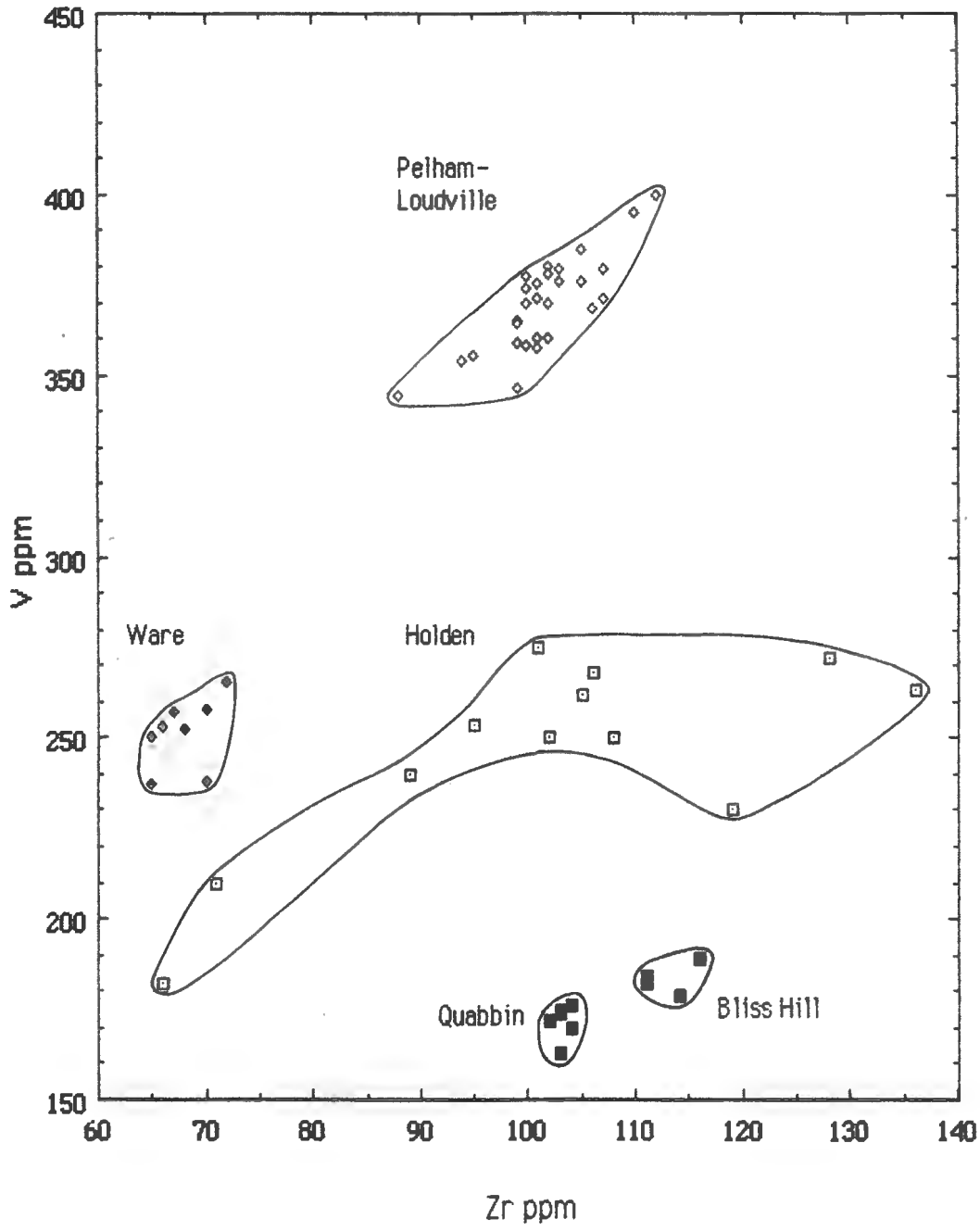

Figure 3.7 Plot of V ppm versus Zr ppm. All diabase analyses from this study are plotted. Symbols: Holden - open squares; Pelham-Loudville - open diamonds; Ware - closed diamonds; Bliss Hill Quabbin Reservoir diabases - closed squares.

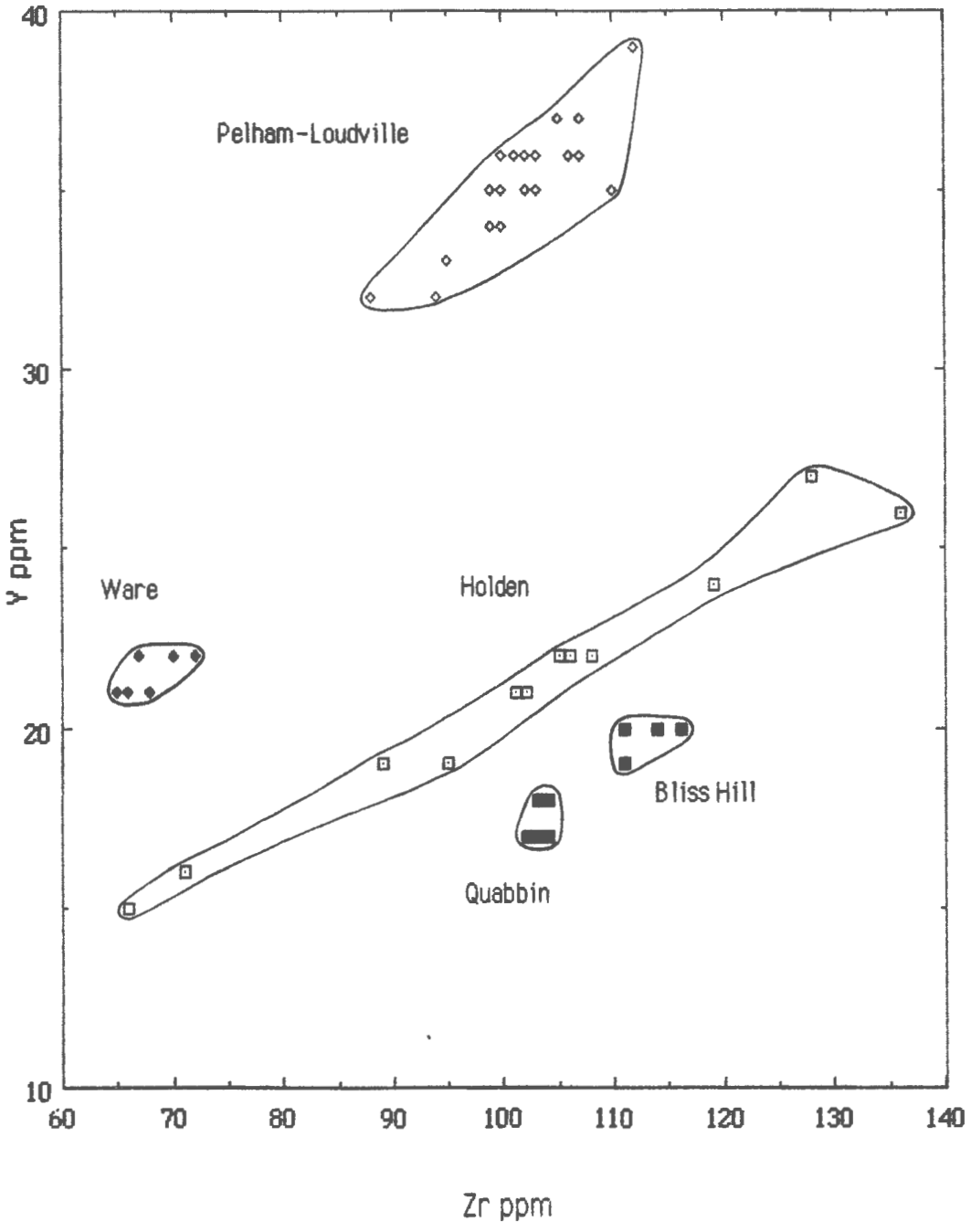

Figure 3.8 Plot of Y ppm versus Zr ppm. All diabase analyses from this study are plotted. Symbols: Holden - open squares; Pelham-Loudville - open diamonds; Ware - closed diamonds; Bliss Hill Quabbin Reservoir diabases - closed squares.

In a plot of Y versus Sr, Figure 3.9, the Holden system shows a significant spread in Y, with little correlation to Sr. It is a surprise that, given this variation, there is no overlap of the Holden system with any other system on this plot. The Pelham-Loudville system varies only slightly in Sr content near 100 ppm, except for one isolated sample, Cold Springs, with 230 ppm. The Ware system is again tightly clustered in Sr as well as in Y. The Bliss Hill and Quabbin Reservoir diabases are the richest in Sr with about 220 ppm and 250 ppm, respectively, falling into two groups. In a graph of TiO_2 versus Y there is a strong positive correlation in the Holden and Pelham systems, whereas the Ware system shows no variation but a very tight clustering.

With P_2O_5, or Zr is plotted against Y, distinct chemical systems should form linear trends radiating from the origin, if simple fractionation is the cause of variation within the system. In Figure 3.10, with P_2O_5, there is no clear single grouping in the Holden system but possibly two trends. These two trends are also noted in a plot of P_2O_5 versus MgO. The Pelham-Loudville system clusters quite well, as does the Ware system, and neither of these overlap with the other systems. The Bliss Hill and Quabbin Reservoir diabases on average are relatively enriched P_2O_5 compared to the other intrusions and plot in a distinct region on this diagram.

Ti is plotted against Nb in Figure 3.11. The trends here are very similar to those in a plot of P_2O_5 versus MgO. The Holden system shows a 50% variation in both Ti and Nb. The Pelham-Loudville system shows a minor increase in Ti and Nb, and the Ware system is tightly clustered in both of these elements. The Bliss Hill and Quabbin Reservoir diabases have significantly higher Nb contents, near 18 ppm, and plot distinctly away from the other intrusions.

The compatible element Cr, is plotted against a relatively incompatible element Zr in Figure 3.12. There appears to be no coherent relationship between these elements in the Holden system. But with Cr plotted against another compatible element, Ni, in Figure 3.13, there is a coherent linear trend with a steep slope for all the systems except for the Bliss Hill and Quabbin Reservoir diabases. The Quabbin Reservoir samples are saturated in olivine. Most of the chromium in the Quabbin samples is probably in the Cr spinels. Cr is plotted against MgO in Figure 3.14. The Holden system appears to plot on two separate trends. However, only a single very tight trend is shown in a plot of Ni versus MgO in Figure 3.15. In the Pelham-Loudville and Ware systems there is a small range in Cr, Ni and MgO (Figures 3.14, 3.15). In plots of Ni versus Zr, or Ni versus Nb in Figure 3.16, the Holden system decreases in Ni and increases in Zr and Nb. The chilled contact samples from the Holden system do not plot as end points. The samples richest in Ni, Cr and poorest in incompatible elements are interior well crystallized samples. The Pelham-Loudville system plots between the Holden and the Ware systems with relatively constant Ni near 70 ppm, Zr about 100 ppm, Nb about 6 ppm. The Ware system has the lowest values of these elements, Ni about 60 ppm, Zr about 68 ppm Nb about 4 ppm. The Bliss Hill and Quabbin Reservoir diabases have higher contents of Ni, and Nb and plot well away from the other intrusions, with no obvious direct relationship.

With Zr plotted against Nb in Figure 3.17, each system occupies distinct areas, with no overlap. The Zr and Nb in the Holden system show the largest spread, but behave quite systematically, showing a strong positive correlation. The Pelham-Loudville system is low in Nb, and shows little variation in either element . The Ware system is low in Zr and Nb. The Bliss Hill and Quabbin Reservoir diabases are significantly enriched in Nb compared to the other diabases with 18-20 ppm. The Zr/Nb ratios for the Holden, Pelham-Loudville and Ware systems range from 12 to 20, whereas in the Bliss Hill and Quabbin Reservoir diabases are less than 8.

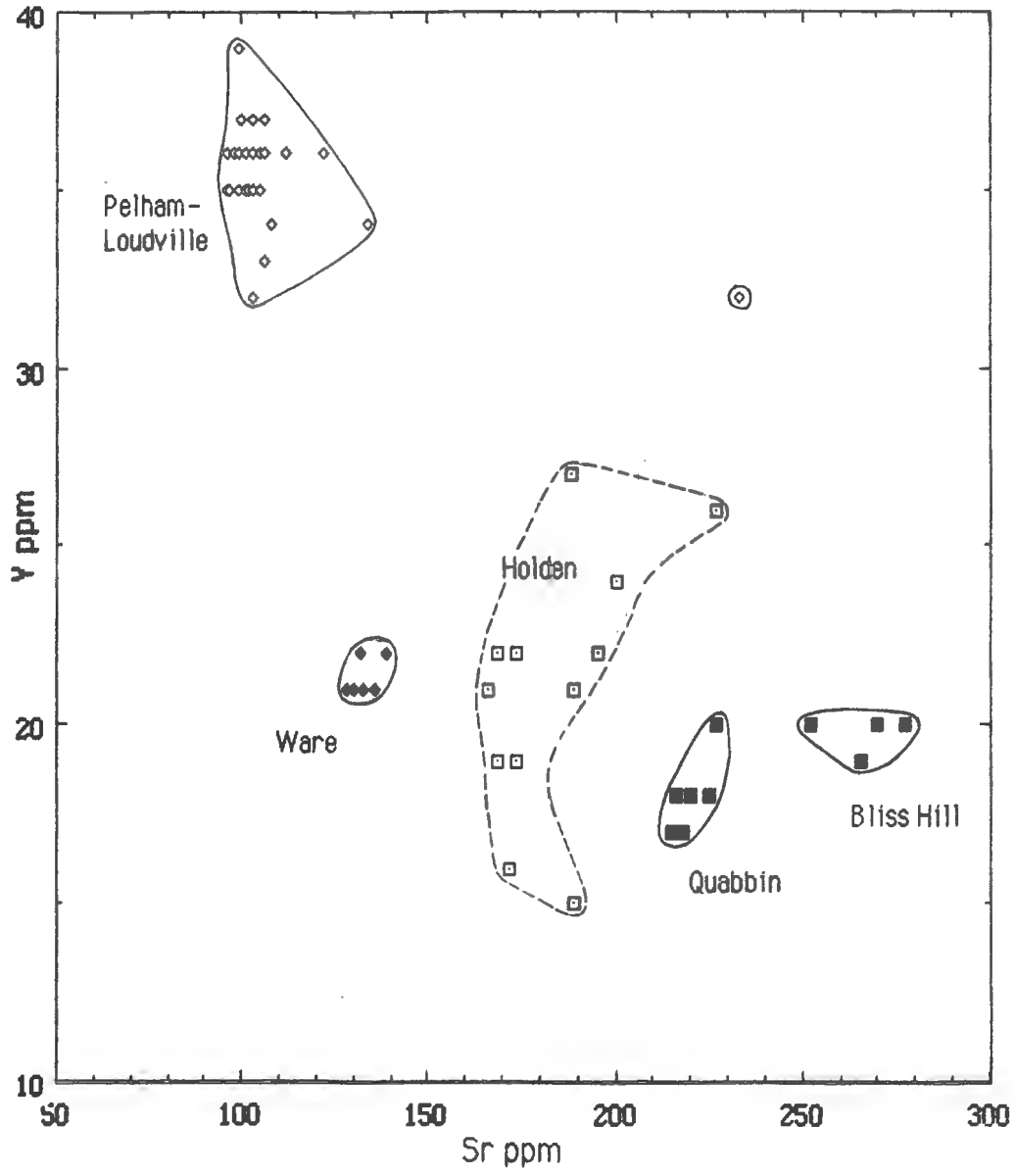

Figure 3.9 Plot of Y ppm versus Sr ppm. All diabase analyses from this study are plotted. Symbols: Holden - open squares; Pelham-Loudville - open diamonds; Ware - closed diamonds; Bliss Hill Quabbin Reservoir diabases - closed squares.

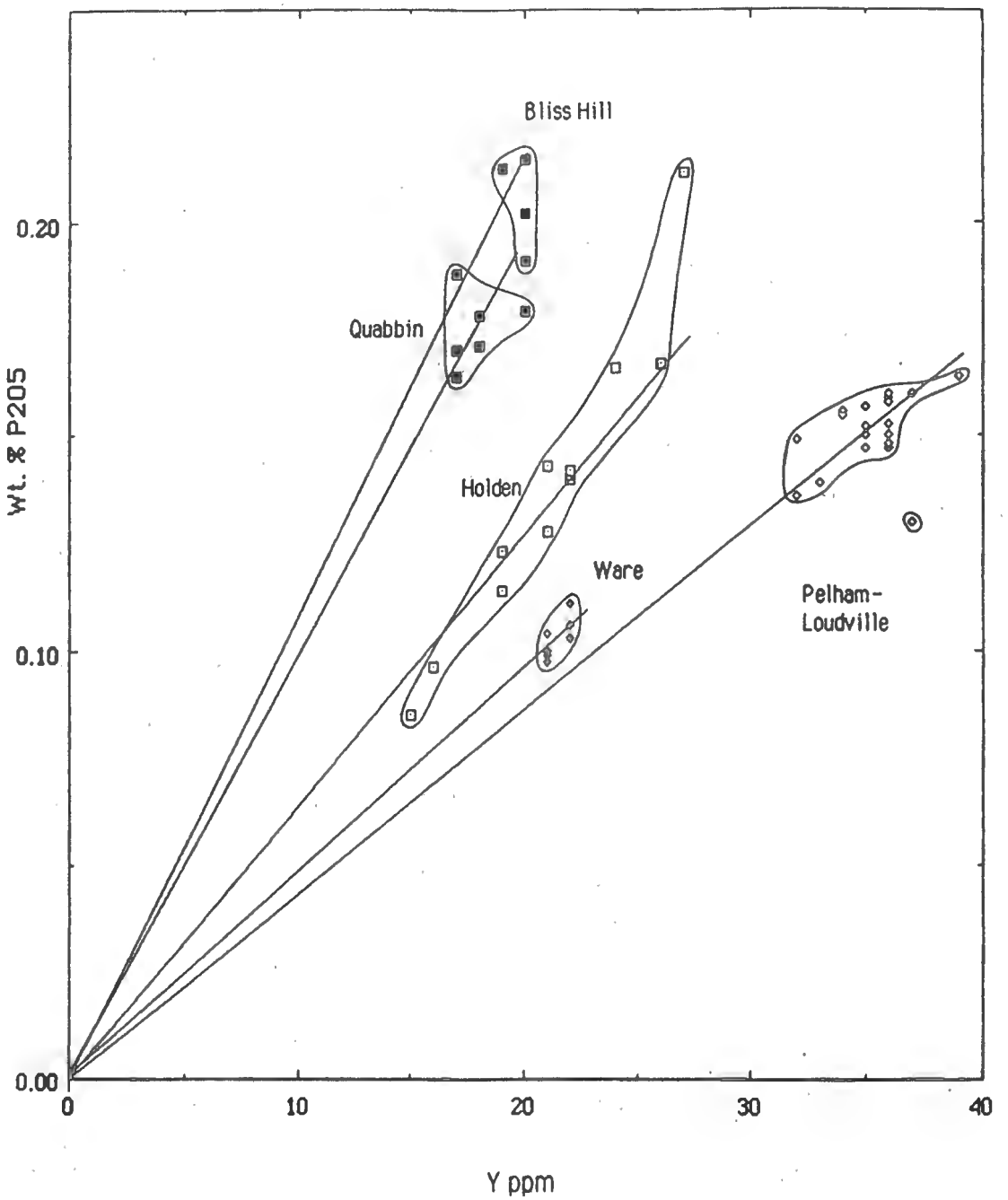

Figure 3.10 Plot of wt.% P_2O_5 versus Y ppm. All diabase analyses from this study are plotted. Symbols: Holden - open squares; Pelham-Loudville - open diamonds; Ware - closed diamonds; Bliss Hill Quabbin Reservoir diabases - closed squares.

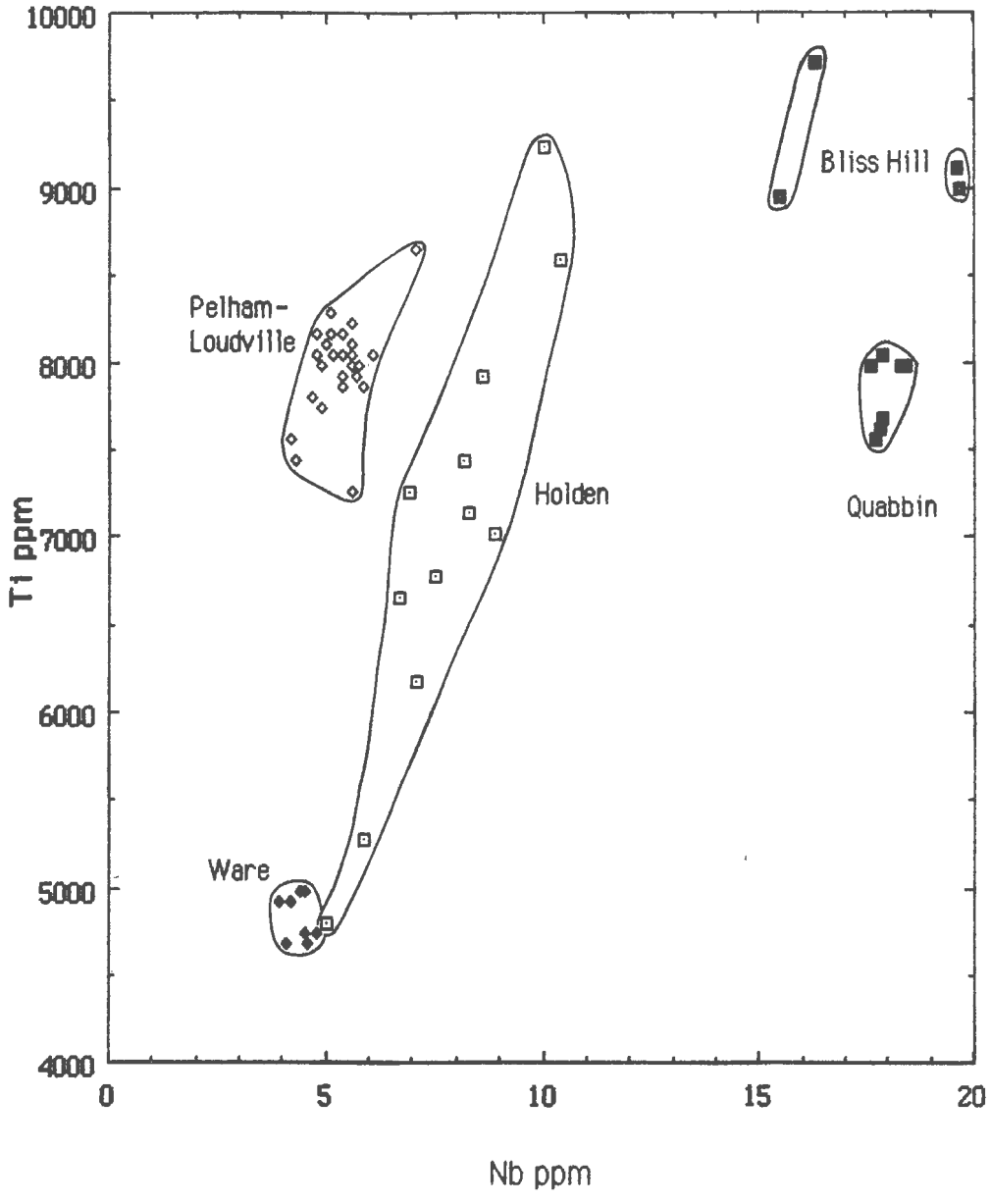

Figure 3.11 Plot of Ti ppm versus Nb ppm. All diabase analyses from this study are plotted. Symbols: Holden - open squares; Pelham-Loudville - open diamonds; Ware - closed diamonds; Bliss Hill Quabbin Reservoir diabases - closed squares.

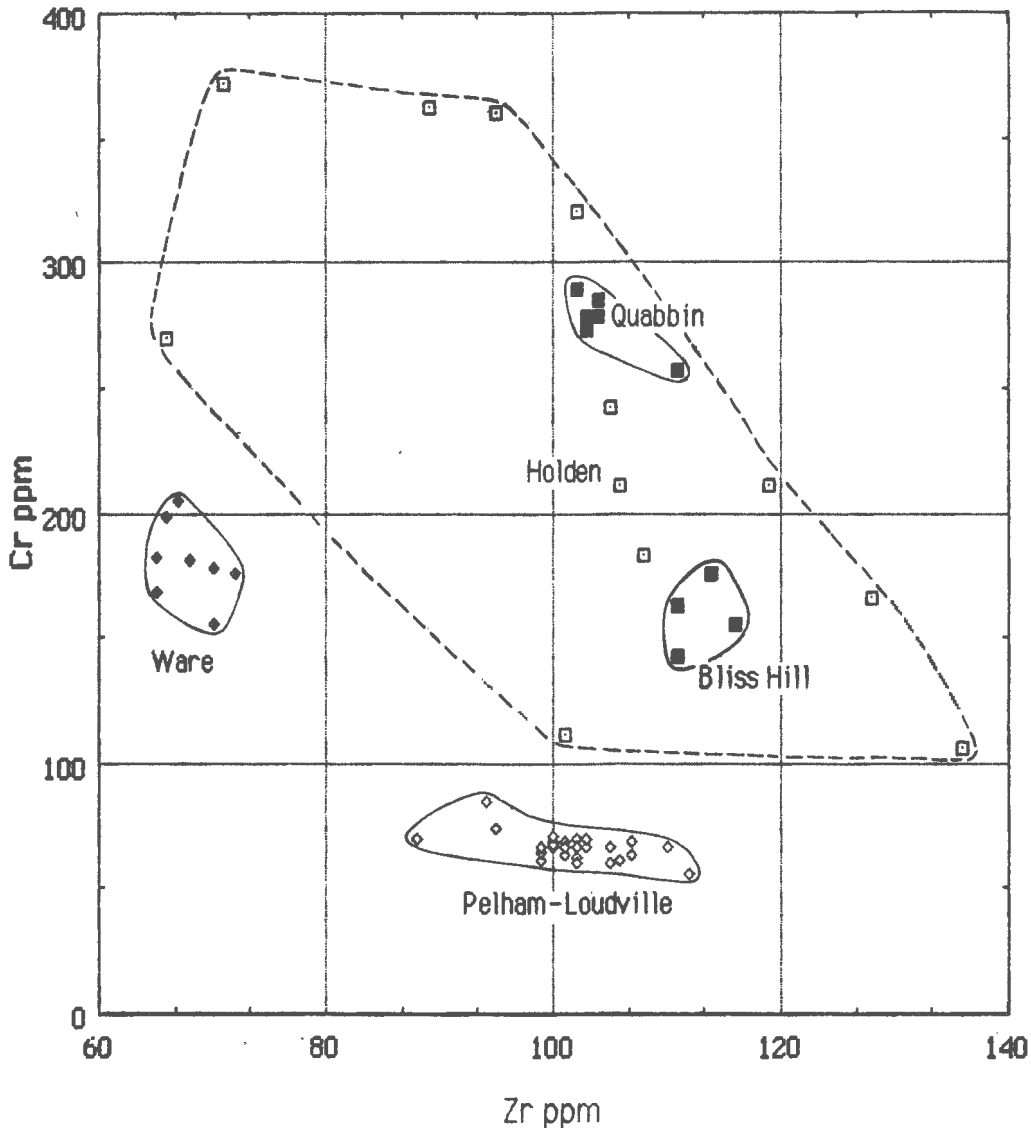

Figure 3.12 Plot of Cr ppm versus Zr ppm. All diabase analyses from this study are plotted. Symbols: Holden - open squares; Pelham-Loudville - open diamonds; Ware - closed diamonds; Bliss Hill Quabbin Reservoir diabases - closed squares.

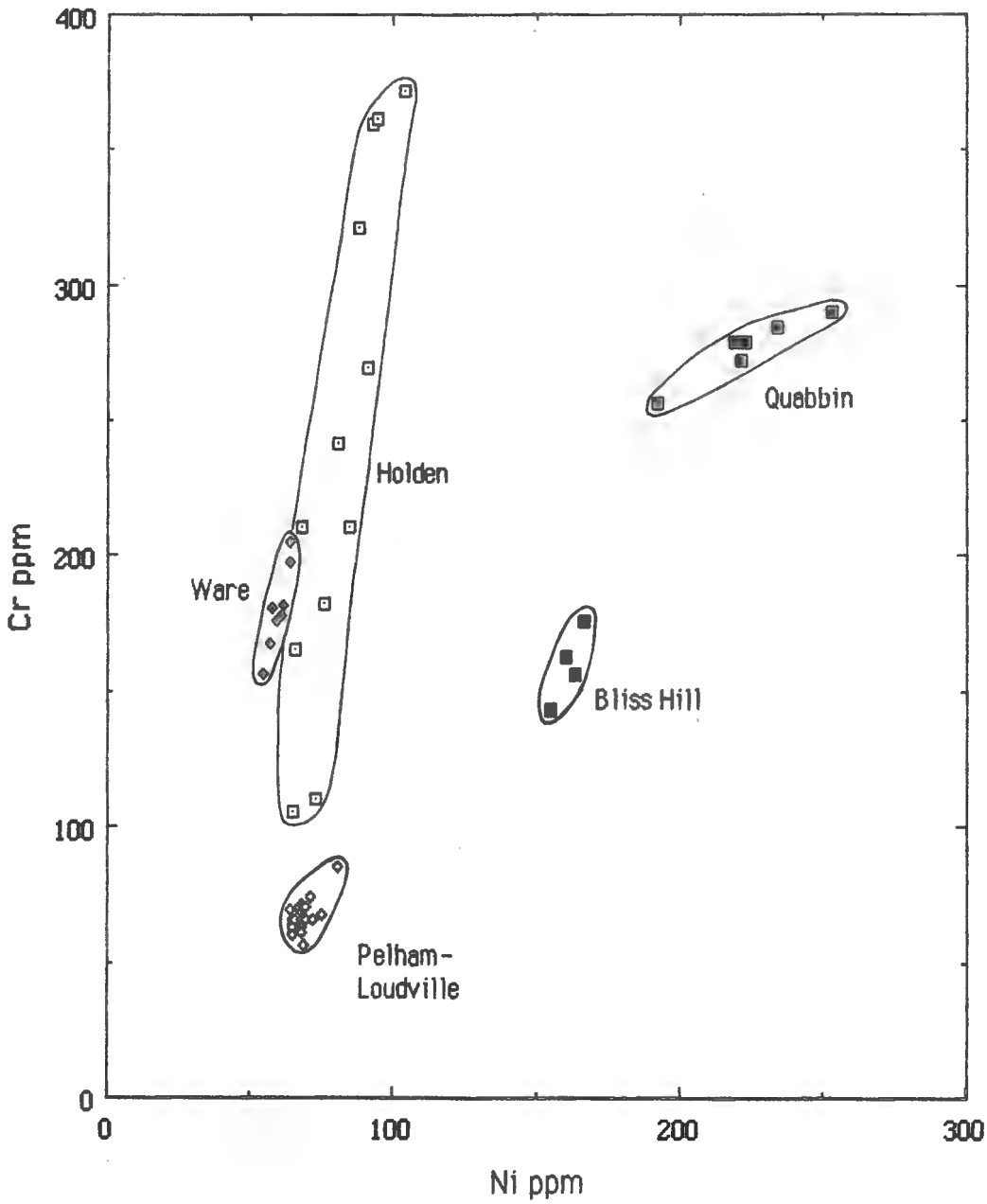

Figure 3.13 Plot of Cr ppm versus Ni ppm. All diabase analyses from this study are plotted. Symbols: Holden - open squares; Pelham-Loudville - open diamonds; Ware - closed diamonds; Bliss Hill Quabbin Reservoir diabases - closed squares.

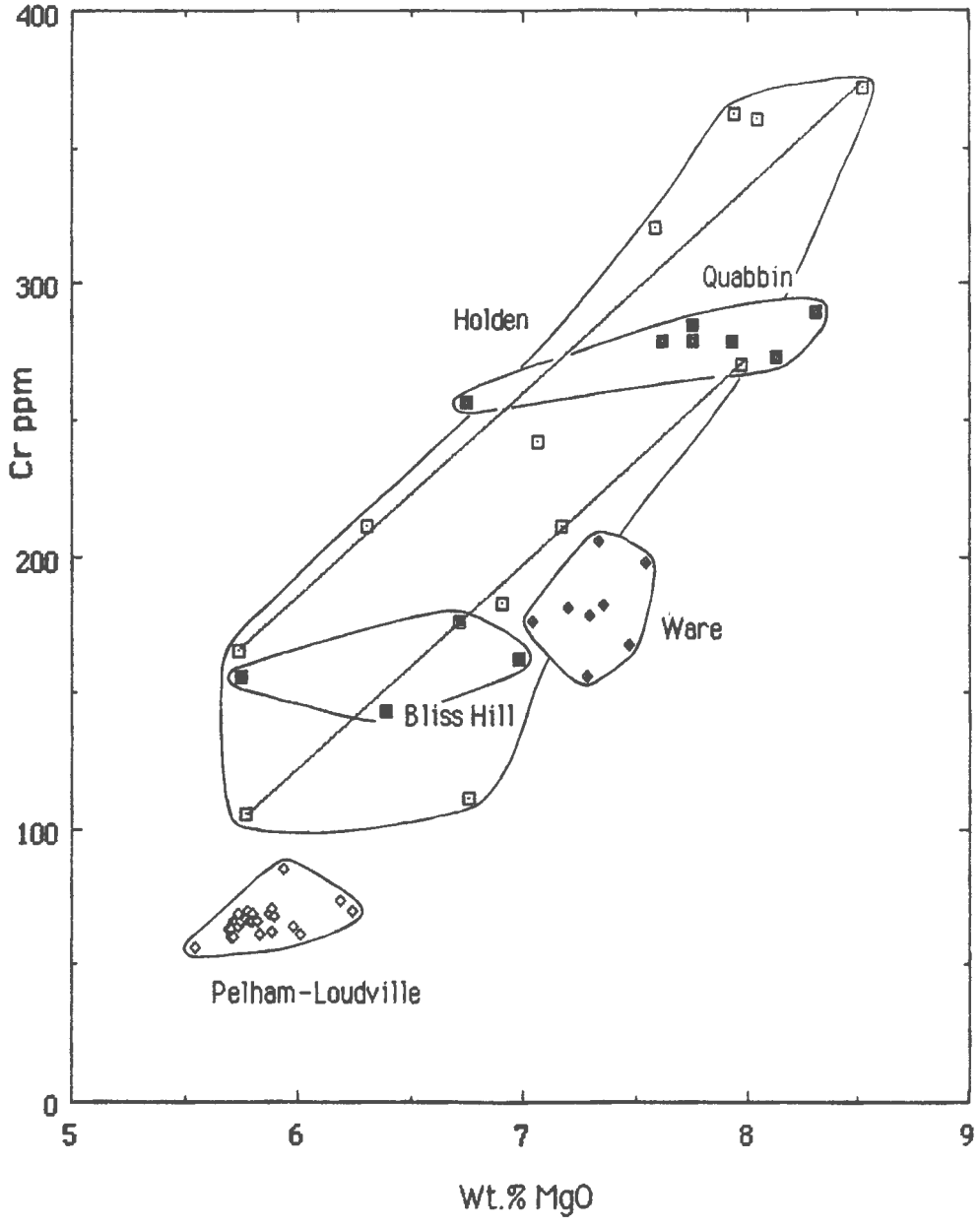

Figure 3.14 Plot of Cr ppm versus wt.% MgO. All diabase analyses from this study are plotted. Symbols: Holden - open squares; Pelham-Loudville - open diamonds; Ware - closed diamonds; Bliss Hill Quabbin Reservoir diabases - closed squares. Straight lines indicate two possible separate trends within the Holden system.

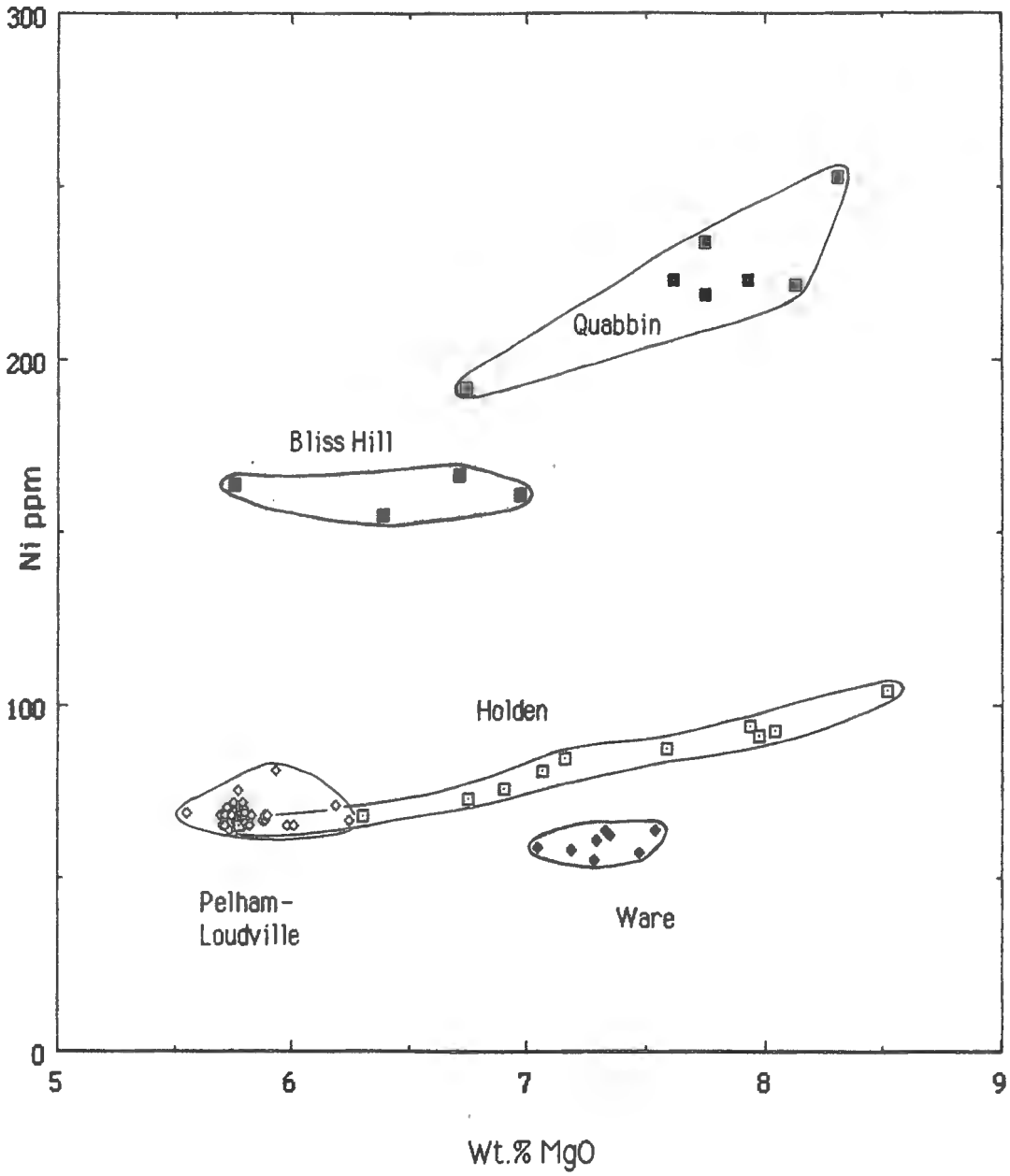

Figure 3.15 Plot of Ni ppm versus wt.% MgO. All diabase analyses from this study are plotted. Symbols: Holden - open squares; Pelham-Loudville - open diamonds; Ware - closed diamonds; Bliss Hill Quabbin Reservoir diabases - closed squares.

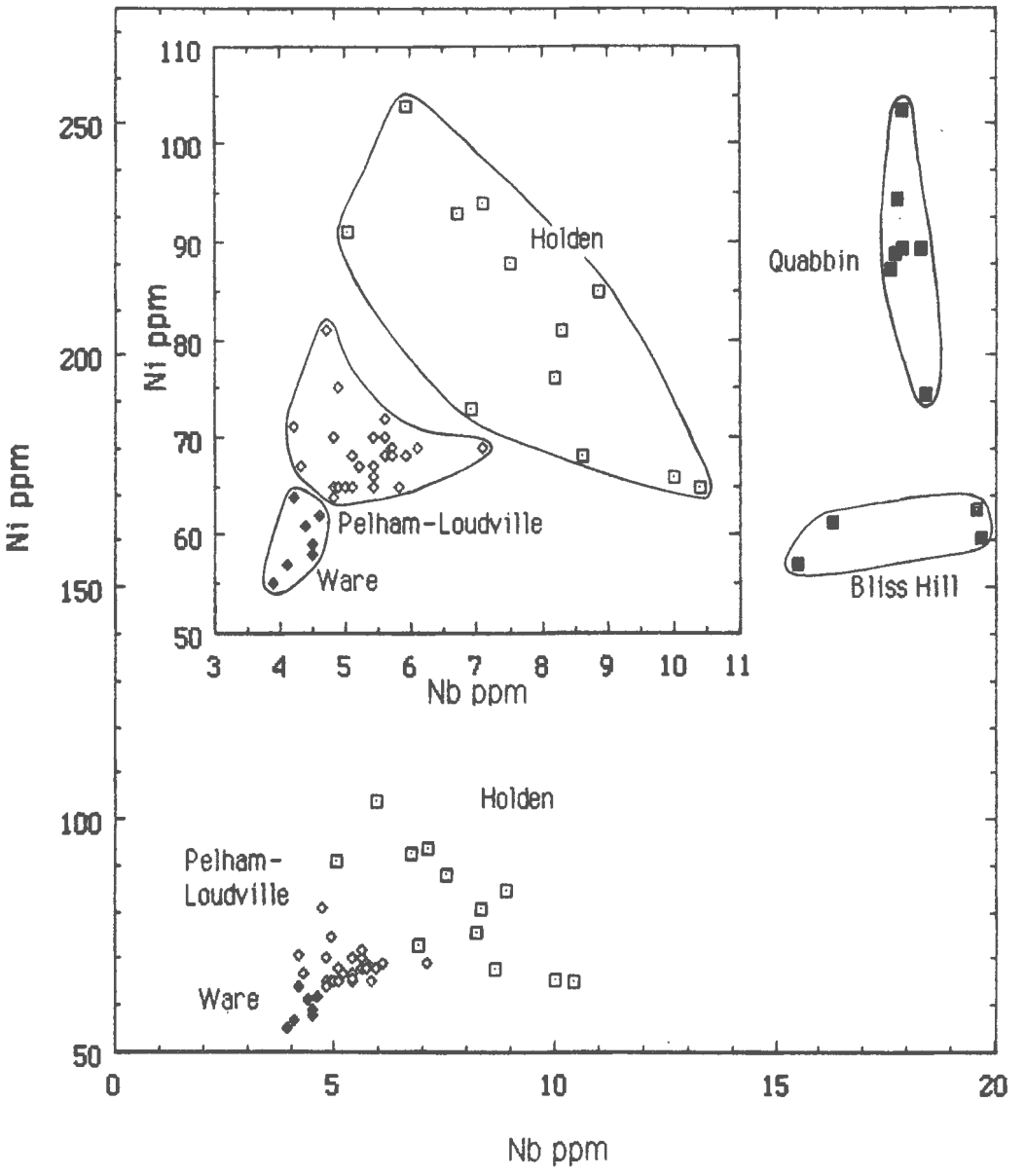

Figure 3.16 Plot of Ni ppm versus Nb ppm. All diabase analyses from this study are plotted. Symbols: Holden - open squares; Pelham-Loudville - open diamonds; Ware - closed diamonds; Bliss Hill Quabbin Reservoir diabases - closed squares.

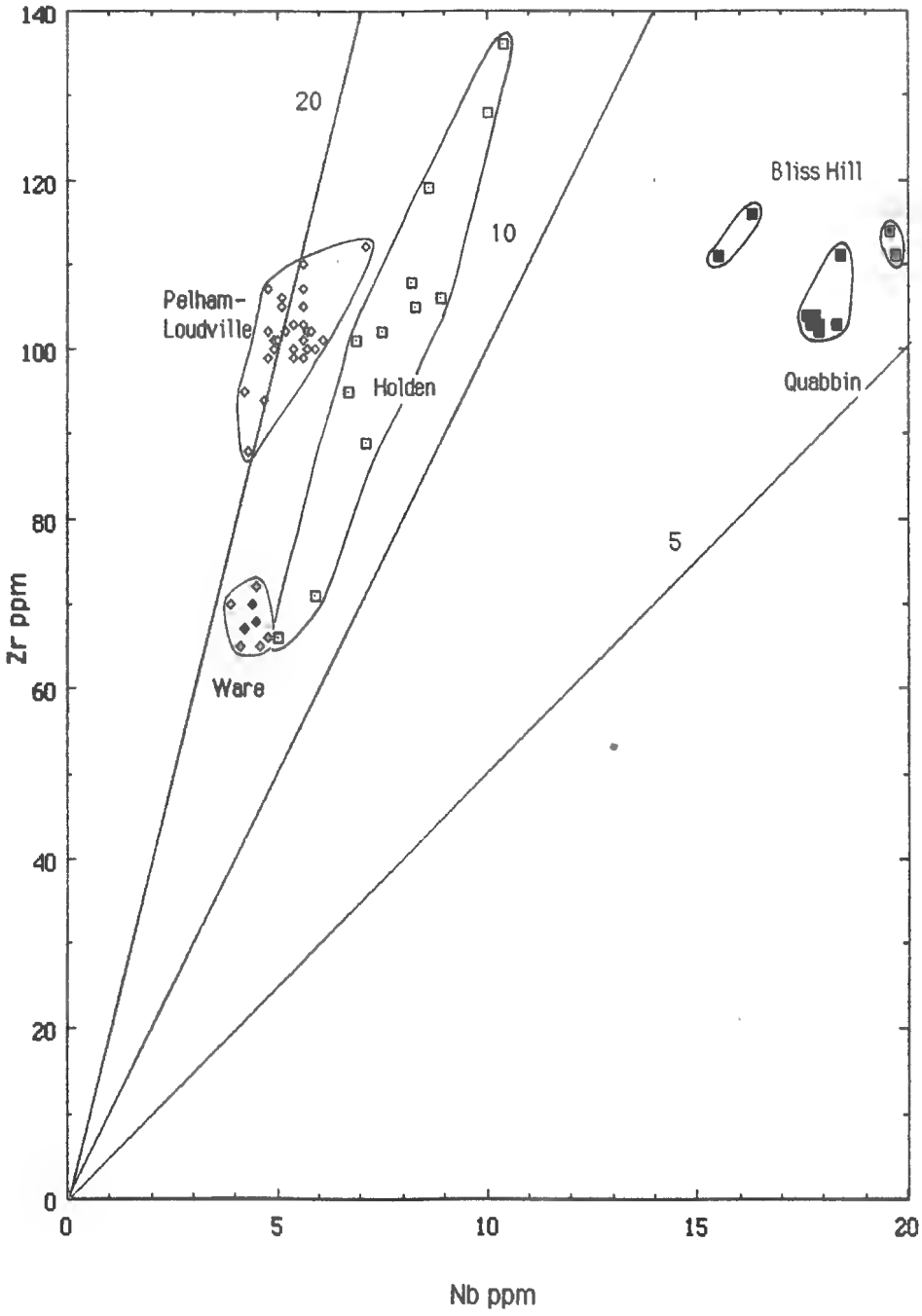

Figure 3.17 Plot of Zr ppm versus Nb ppm. All diabase analyses from this study are plotted. Symbols: Holden - open squares; Pelham-Loudville - open diamonds; Ware - closed diamonds; Bliss Hill Quabbin Reservoir diabases - closed squares.

Trace Element Spider Diagrams

Rare earth element contents of igneous rocks are relatively resistant to changes during alteration. Changes should not be expected except under the most extreme conditions (Hanson, 1980), though subtle variations in REE, K, Nb, and Zr are reportedly produced by high-temperature metasomatism (Menzies and Hawkesworth). The rare earth element patterns give a key to the origin of an igneous body. " Poor man's rare earth element" (PMREE) analyses are a relatively inexpensive way to obtain an analog to the REE (Bougault, 1980; Bougault and Treuil, 1980), because most of the elements that were originally selected for this method are routinely analyzed by XRF. Bougault selected Ti, V, Y, Zr, Hf, Ta, and Th. The elements used are incompatible ($Kd \leq 1$), belong to a transition series, and are not volatile under planetary accretion. Ce, a rare earth element, has been added to this list because it is analyzed by XRF, and Hf and Ta are removed because they are not. Sr is substituted for Eu because of similar ionic radii, and behavior. All the PMREE diagrams are chondrite-normalized, and all data from this study are plotted in these figures. The terms "LREE" and "HREE", though not strictly applicable to the PMREE diagram, because few REE elements were analyzed, are used here in quotation marks to describe element behavior on the left and right sides of the diagrams, respectively. The patterns in these diagrams can be thought of as fingerprints of the different magmatic systems, each quite distinct. Genetic relationships among the systems can be dismissed or proposed, but there is insufficient evidence here to directly relate one system to another.

The slope of the PMREE pattern for the Holden dikes in Figure 3.18 is the steepest of the Jurassic intrusions. From Ce to V the elemental abundances decrease in order of REE position, except for the positive Sr anomaly. This anomaly probably is due to plagioclase accumulation in the melt. Nb although depleted, is the least depleted in all of the systems.

The Pelham-Loudville system produces a very gentle almost flat slope, except for the negative Sr anomaly, as seen on Figure 3.19. This anomaly may represent a source depleted in Sr for this system, as noted by Philpotts (1986), since the system is saturated in plagioclase. The relatively enriched ""HREE"" and depleted "LREE" could indicate that the magma evolved form a source that had been melted more extensively than the source for the Holden system. This is supported by the lower Nb content of this system.

The Ware system produces a PMREE pattern in Figure 3.20 that is moderately depleted in the "LREE" compared to the Pelham-Loudville system. Sr, Zr, and Y are nearly constant in this system but Zr and Y are more depleted in comparison to the Pelham-Loudville system and Sr is higher. The striking difference is the negative Ti anomaly. Three possible explanations for this anomaly are that there is a residual Ti-rich mineral in the source, that the melt had magnetite and ilmenite on the cotectic and that crystal settling of these Ti-rich minerals occurred, or possibly that the melt was from a low-Ti source. The average Nb in the Ware system is lower than all the other systems, indicating that the magma melted from a more-depleted source.

The pattern for the Bliss Hill and Quabbin Reservoir diabases in Figure 3.21 is completely different from any pattern produced by the other diabase systems. This pattern is far more enriched in the "LREE", and more depleted in the "HREE". The Nb content, which is 4 to 5 times higher than the other diabases systems, argues for a small degree of melting of a source to produce this magma. Compatible elements Ni and Cr, which are enriched in this system agree with a small degree of melting from a source rich in these elements, and little crystal settling of olivine or spinel that would have removed Ni and Cr respectively.

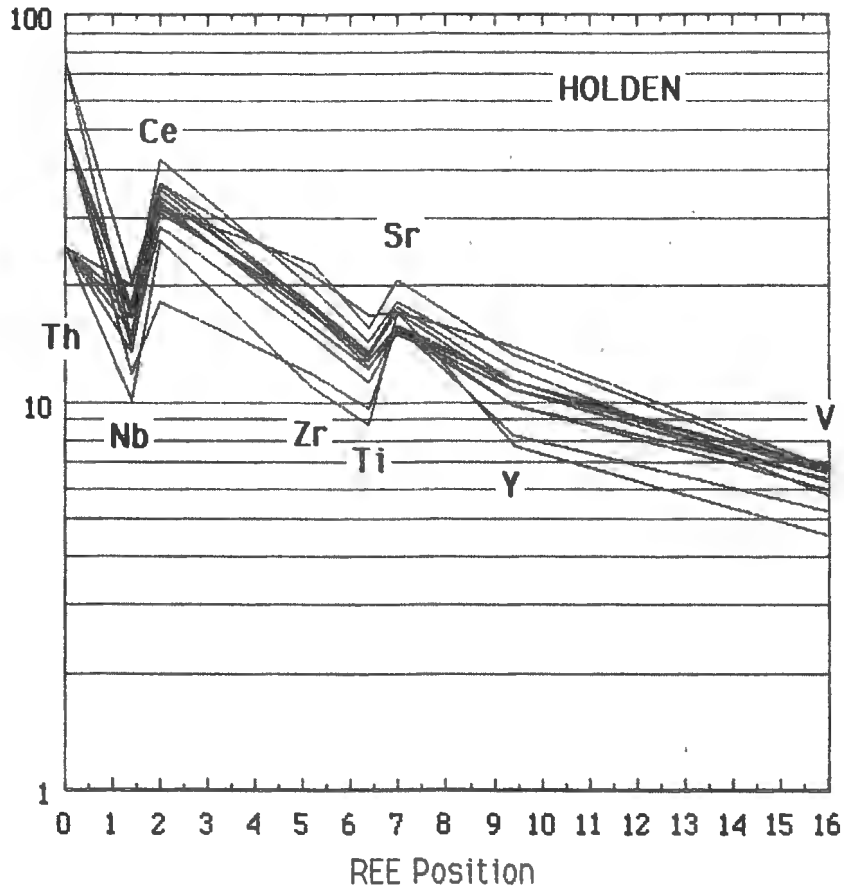

Figure 3.18 Spider diagram of chondrite-normalized trace element concentrations in the Holden system. Elements are arranged according to the theoretical REE position by the method of Bougault (1980).

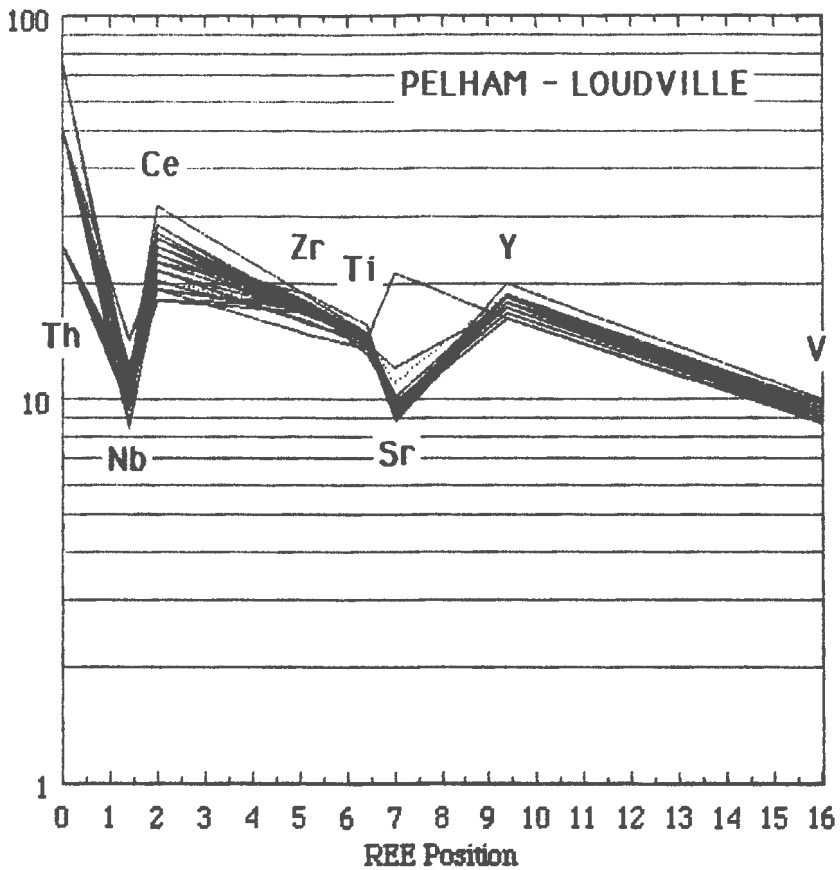

Figure 3.19 Spider diagram of chondrite-normalized trace element concentrations in the Pelham-Loudville system. Elements are arranged according to the theoretical REE position by the method of Bougault (1980).

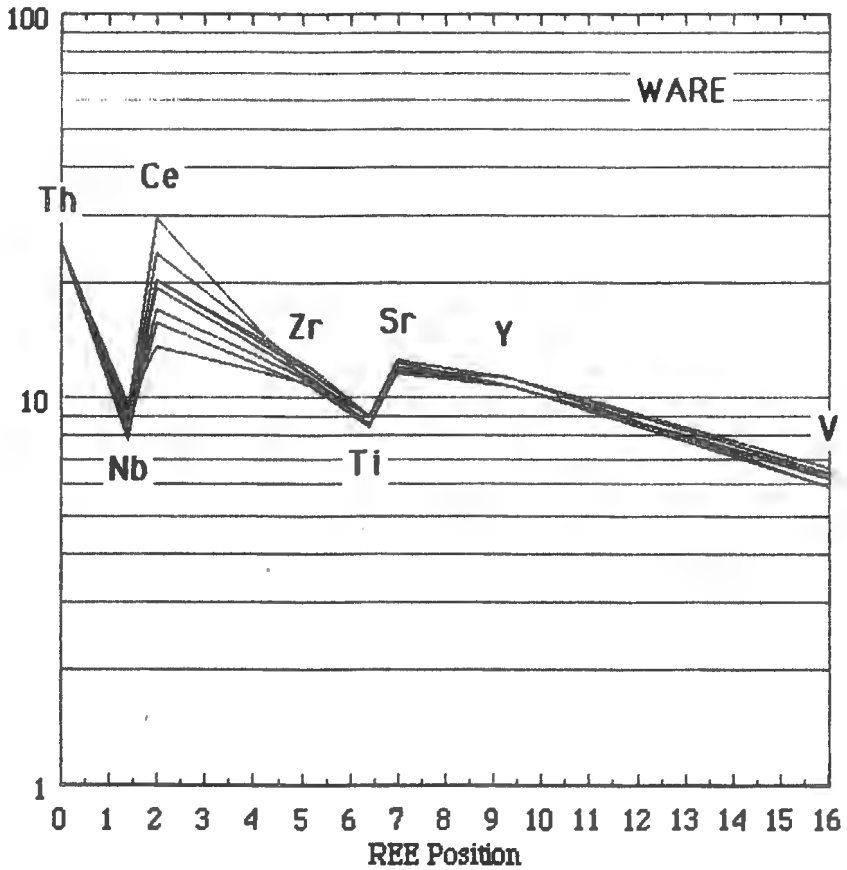

Figure 3.20 Spider diagram of chondrite-normalized trace element concentrations in the Ware system. Elements are arranged according to the theoretical REE position by the method of Bougault (1980).

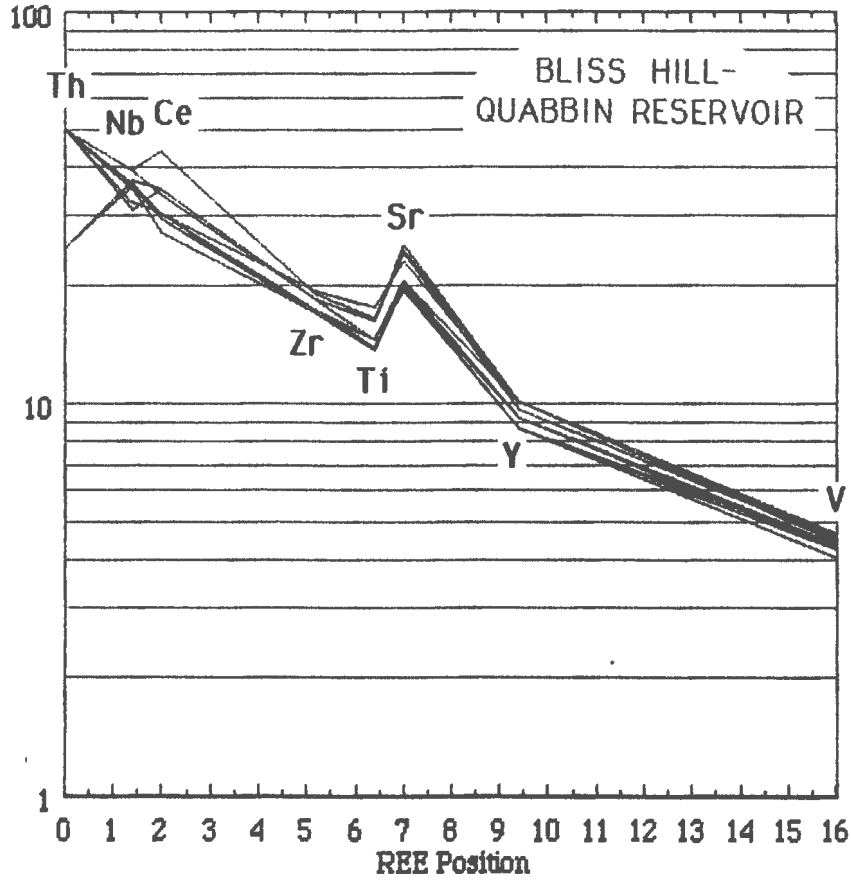

Figure 3.21 Spider diagram of chondrite-normalized trace element concentrations in the Bliss Hill and Quabbin Reservoir diabases. Elements are arranged according to the theoretical REE position by the method of Bougault (1980).

Contrasts among the spider diagrams of the four major geochemical systems of dikes in central Massachusetts are shown in Figure 3.22, where the total range of PMREE elements for each system is portrayed directly (omitting for this purpose the odd Sr value of sample CS-5 of the Loudville group). The Holden system and the Bliss Hill and Quabbin Reservoir diabases are similar in showing "LREE" enrichment and "HREE" depletion, and in having pronounced negative Sr anomalies. They differ dramatically in that the Holden system shows a pronounced negative Nb anomaly, whereas the Bliss Hill and Quabbin Reservoir diabases show virtually no Nb anomaly at all. The Pelham-Loudville and Ware systems also show similarities in being less "LREE" enriched and less "HREE" depleted than the other two groups, and also show strong negative Nb anomalies as found in the Holden system. Further, the Pelham-Loudville system shows greater "HREE" values than any other system. However, the Pelham-Loudville system shows a strong negative Sr anomaly unlike any of the other systems, whereas the Ware system shows a negative Ti anomaly unlike any other system. When more complete and precise trace-element data become available on the Mesozoic lavas, these PMREE "fingerprints" will become a powerful tool for testing magmatic correlations, in the same way that it already has been in the present study for correlating isolated occurrences of diabase dikes.

Summary of Chemical Systems

The Holden system consistently shows a large range in major elements, MgO, TiO_2, Al_2O_3, K_2O, P_2O_5, and in trace elements Zr, Y, Nb, Cr, and Sr. This system is more enriched in Sr, Ce, Zr, Cr, and Ni than the Pelham-Loudville and Ware systems. There is some indication that the variation in elements is a result of crystal fractionation, but other patterns of elements would argue against this inference and support a mixing model or multiple intrusions of slightly different magmatic compositions. There is field evidence of at least two magmatic pulses in a number of the Holden system localities sampled. No significant differences in the phenocrystic assemblages are observed along the dikes, indicating that there is probably is a genetic relationship between the two pulses of intrusion. Although there is a considerable range in the chemistry of this system, there is little overlap between the Holden system and the other systems. The range in elements indicates a more complex history to these diabase intrusions than has previously been postulated (Philpotts and Martello,1986). As shown in the spider diagram there is a definite chemical pattern that differs markedly from the other Jurassic and Cretaceous systems. The Zr/Nb ratios fall in the relatively narrow range of 11.7 to 14.6, suggesting a consistent magmatic source for all the intrusions in the Holden system.

The Pelham-Loudville system is characterized by very high iron content (greater than 15 wt.% Fe_2O_3), and V. The TiO_2, Y, and V contents are the highest of the diabases, and the system is poorest in MgO, Al_2O_3, Cr, and Sr. The V and Y contents are particularly striking. All V analyses lie between 340 and 400 ppm whereas no analyses from other systems exceeds 280 ppm. All Y analyses lie between 32 and 39 ppm, whereas all analyses of other systems lie between 15 and 20 ppm. The negative Sr anomaly in the spider diagram is characteristic and is markedly different from the diagrams of the other systems. The Zr/Nb ratio varies from 16 to 22.

The chemistry of the Ware system is tightly clustered. The striking negative TiO_2 anomaly in the spider diagram is indicative of the low TiO_2 contents of all samples from this system regardless of geographic location. The average MgO content of this system is the highest of the Jurassic intrusions. The iron content is markedly lower than the Pelham-Loudville system but is the same as the Holden system. Like the Pelham system, the Ware system is consistently low in Sr, tightly clustered between 128 and 139 ppm, and is slightly higher than typical for the Pelham-Loudville system. The average Zr and Nb contents are lower than all the other systems. Zr in the Ware system is consistently

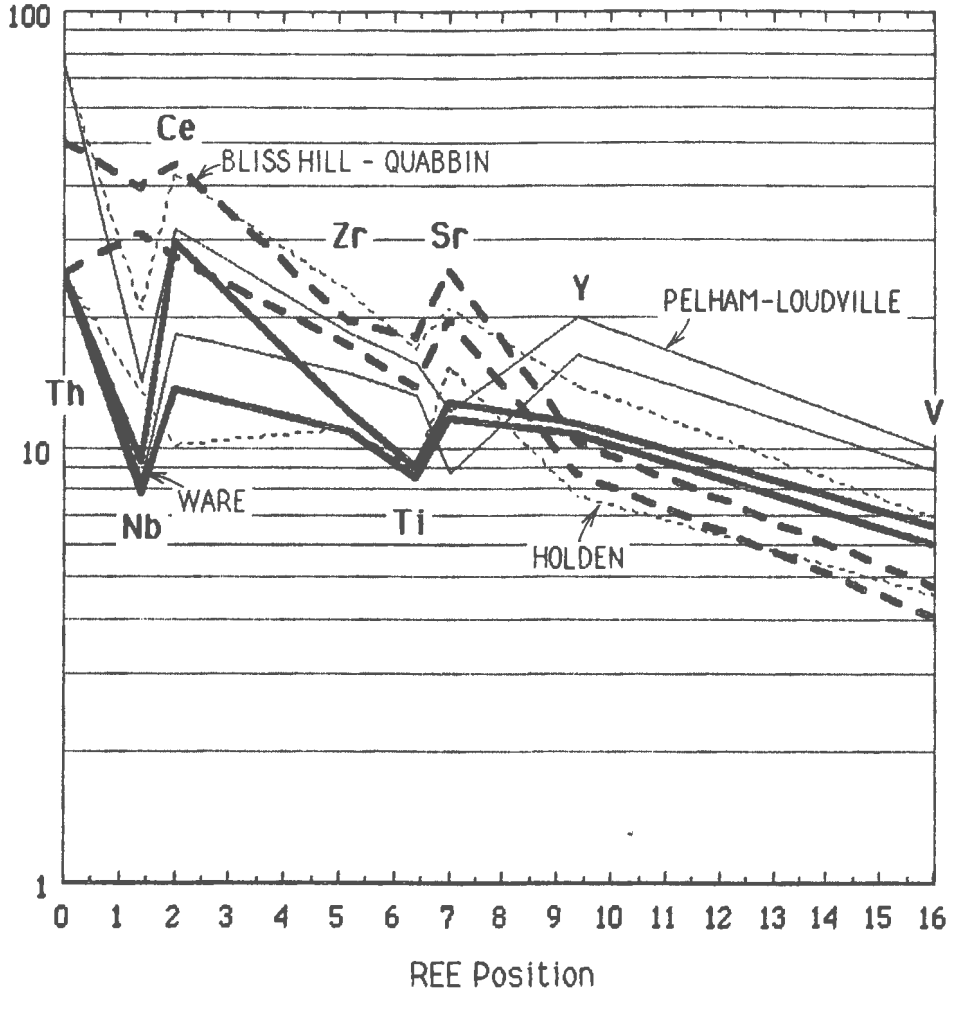

Figure 3.22 Spider diagram of chondrite-normalized trace element concentrations for all the central Massachusetts diabases. Elements are arranged according to the theoretical REE position by the method of Bougault (1980).

between 65 and 72 ppm, whereas only two other analyses fall as low as this and most fall between 90 and 120 ppm. The Zr/Nb ratio ranges from 14.4 to 17.5.

The Bliss Hill and Quabbin Reservoir diabases are distinct chemically from all the other intrusions. The Bliss Hill group is the highest in TiO_2 and Al_2O_3, whereas the Quabbin diabases are the most enriched in MgO. These diabases are also enriched in Ni, Cr, Sr, Ba, Zr, and Nb and low in V compared to the other diabases. For example, Bliss Hill and Quabbin Reservoir intrusions have less than 200 ppm V, whereas only one analysis from the other diabases falls in this category. Further, all the Bliss Hill and Quabbin Reservoir diabases have between 15 and 20 ppm Nb, whereas all the other diabases have between 4 and 11 ppm. The Zr/Nb ratios in the Bliss Hill and Quabbin Reservoir diabases range from 5.6 to 7.9, considerably different from the Zr/Nb ratios in the other systems which range from 11.7 to 22.

On the basis of the major- and trace-element analyses described above, it is concluded that the Holden, Pelham-Loudville, Ware systems and the Bliss Hill and Quabbin Reservoir diabases were probably produced from different upper mantle sources, or at least produced from the upper mantle under different conditions. The geochemical grouping of the diabases demonstrated here is consistent with paleomagnetic characteristics described in the next chapter.

CHAPTER 4

PALEOMAGNETISM

Oriented samples for paleomagnetic study were collected from forty sites in west-central Massachusetts shown in Figure 1.5. Thirty-six sites are Jurassic intrusions representing the three major chemical systems discussed previously. Of these, seven sites are from the Holden system, five sites from the Ware system, and twenty-four sites from the Pelham-Loudville system. The twenty-four sites of the Pelham-Loudville system include eighteen from the Pelham group and six from the Loudville group. Three sites are considered Cretaceous, two from the Quabbin Reservoir group, and one from the Bliss Hill group (Bliss Hill north). The other member of the Bliss hill group (Bliss Hill south) may represent the only late Jurassic site, as indicated by a K-Ar date, Table 5.1. At the moment the paleomagnetic direction at Bliss Hill south is considered preliminary and additional demagnetization studies are needed.

Methods

Sixteen sites were drilled in the field with a gas-powered rock drill, then oriented with a brass or aluminum orienter and a brunton compass. At the remaining sites, oriented blocks were collected in the field, drilled, and oriented with a non-magnetic orienter in the laboratory at the University of Massachusetts. Cores 2.54 cm in length and diameter were cut for paleomagnetic analyses. Natural remanent magnetization (NRM) directions were determined for each core using a Molspin fluxgate magnetometer. At least one core per site was selected for step-wise alternating field (AF) demagnetization in progressive steps of 2.5, 5.0, 10, 20, 40, 60, and 80 mT, or 5, 10, 20, 30, 50, 70, and 80 mT on a Schonstedt AC Geophysical Specimen Demagnetizer. In some cases the overprinting was complex and the entire site was stepwise AF demagnetized. After a stable remanent direction was determined from the AF studies, the remaining cores were AF demagnetized at the appropriate level. Mean coercivities are variable from site to site. Pilot specimens from each system were selected for thermal demagnetization studies at 200^0C, 300^0C, 400^0C, 500^0C, and 550^0C. These were compared to the directions obtained from the AF studies. Site mean directions were calculated from AF data at the milliTesla (mT) level where the stable remanent direction was reached and where the least in-site scatter was determined. Fisherian statistics were then applied to the data (Fisher, 1953). Sites were grouped on the basis of the chemical signature of the site, and not by geographical location or general trend of the diabase as previous workers had done by averaging data.

A Curie temperature was determined for a Cretaceous Baffle Dam Island sample using the Curie balance at the University of Massachusetts. An IRM acquisition study for the Baffle Dam Island sample, as well as for a comparison sample from the Cretaceous Cape Neddick Gabbro, Maine, was run at the University of Massachusetts.

Paleomagnetic Results

The natural remanent directions (NRM)of the Jurassic sites show considerable scatter, whereas the Cretaceous sites cluster well in NRM directions. The NRM intensities vary within each chemical system. The intensities for the Holden system range from 0.4 to 2.4 A/M, in the Pelham-Loudville system from 0.8 to 4.0 A/M, and in the Ware system from 0.3 to 2.4 A/M. Two unusual sites from the Pelham-Loudville system have NRM intensities above 200 A/M. These sites showed considerable scatter in NRM directions and after demagnetization. As a consequence these were excluded from the statistical analysis. Based on the extremely high intensities these sites probably developed an isothermal remanence from lightning strikes. The NRM intensities in the Cretaceous diabases range from 1.7 to 5.0 A/M.

Normalized intensity plots for representative samples from the Holden system are shown in Figure 4.1. Approximately 20% of the average original NRM intensity is removed by 20 mT and 50% is removed by 40 mT. The characteristic magnetic direction appears after 50% of the NRM has been removed in these sites between 20 mT and 40 mT. The diabases of the Pelham-Loudville system are diverse in their coercivity as shown in Figure 4.2. Fifty percent of the NRM intensity is removed in a range from 10 mT to 40 mT. In the Ware system as shown in Figure 4.3, 40% of the average NRM is removed by 20 mT and 80% is removed by 30 mT. In general the normalized intensity plots of the Jurassic diabases compare well with other Jurassic tholeiitic diabases from eastern north America (Smith, 1987). The reversed Cretaceous Quabbin Reservoir diabases show a different decay curve on a normalized intensity plot as shown in Figure 4.4. These samples increase in intensity at low mT levels, as a soft component, in the opposite direction is removed. This soft component is probably related to the present-day normal field. Fifty percent of the original NRM is removed by 20 mT. In the Bliss hill diabases, the magnetic carrier is highly viscous, with 50% of the NRM intensity removed by 10 mT in site BH and, in site 4I4, 90% is removed by 10 mT.

Alternating Field Demagnetization

Holden System. Progressive AF demagnetization studies on selected samples in the Holden system indicate the presence of several components of magnetization. In most samples there was a low-coercivity present-field overprint. These soft magnetic components are considered to be a viscous remanence gained in the present-day field. By 40 mT the stable remanence was obtained in most samples. Based on the results of the AF studies samples were subjected to AF demagnetization levels of 40 mT. Representative individual sites are discussed below.

Vector end-point diagrams from sites 1688 and Fiskdale in the Holden system are shown in Figures 4.5 and 4.6. These both show an overprinting of soft components in different directions; 1688 in a northwest direction, and F2AR in a southeast direction. By 40 mT, all secondary components are removed in sample 1688 and there is a linear decay towards the origin, indicating that the stable remanent direction was reached by 40 mT. There is still a very small secondary component in F2AR that is not removed until 60 mT, after which there is a linear decay towards the origin, indicating that the stable remanent direction was reached. Site 1683 (Fig. 4.7) shows the removal of a secondary component in a northwesterly direction at low fields, 20 mT, then an orderly decay to the origin. Sample QX-6 (Figure 4.8) QX6 indicates a soft viscous component that is removed at low fields that is steeper than the remanent direction and in a northeast direction . In QX3, as shown in Figure 4.9, little overprinting is seen, and there is an orderly decay pattern to the origin. The stable remanent directions obtained from this site are similar to other sites in this system as listed in Table 4.1. Most secondary and/or viscous components are removed by 20 mT or 40 mT.

Pelham-Loudville System. Progressive AF demagnetization studies on selected samples in the Pelham-Loudville system in general, show the presence of two components of magnetization. A minor viscous secondary component due to post-solidification alteration and/or a low-coercivity present field overprint is present. Based on petrographic work the main magnetic carrier is titanomagnetite. There is fine-grained pseudo-single-domain titanomagnetite in the contact samples and multidomain titanomagnetites in the interiors that are less altered than in the Holden or Ware systems.

The magnetic decay patterns from the Pelham-Loudville system show the largest variety. Twenty-four sites represent this system, and a number of minor secondary components are identified. These vector end-point diagrams are difficult to observe because the north component dominates the east-west components. A vector end-point diagram from the Butterworth site represents the most complex path (Figure 4.10). There

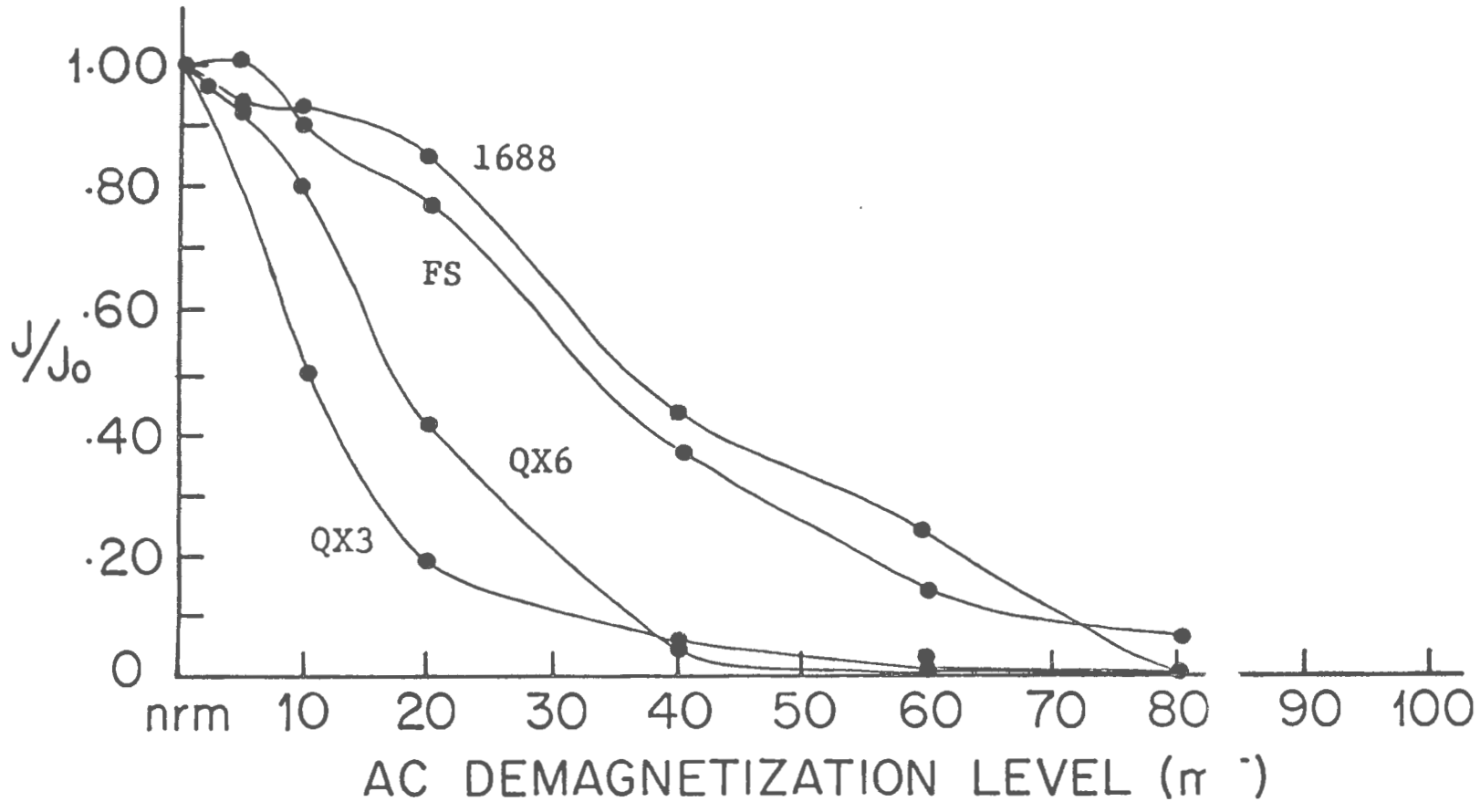

Figure 4.1 Normalized intensity plot for representative samples from the Holden system.

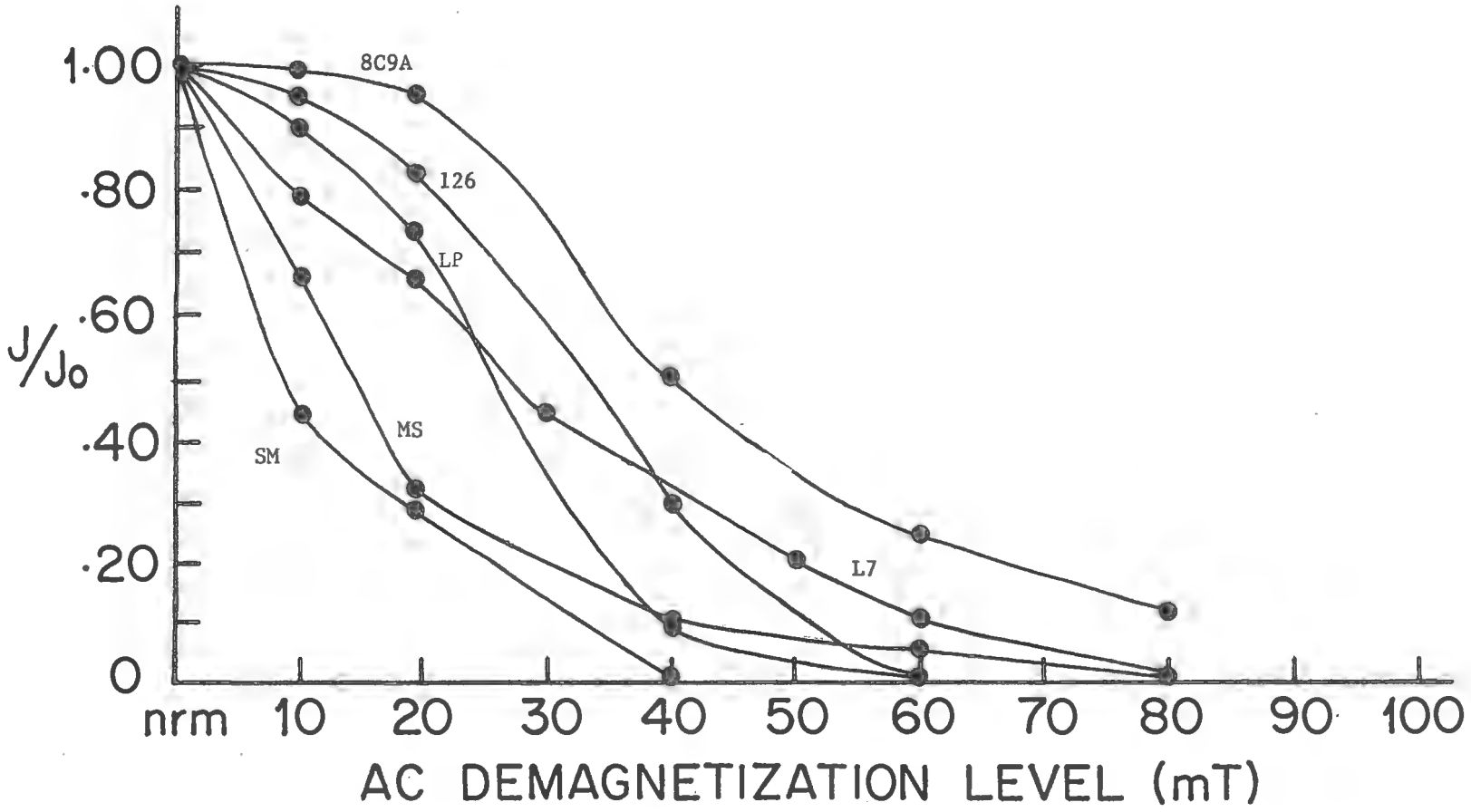

Figure 4.2 Normalized intensity plot for representative samples from the Pelham-Loudville system.

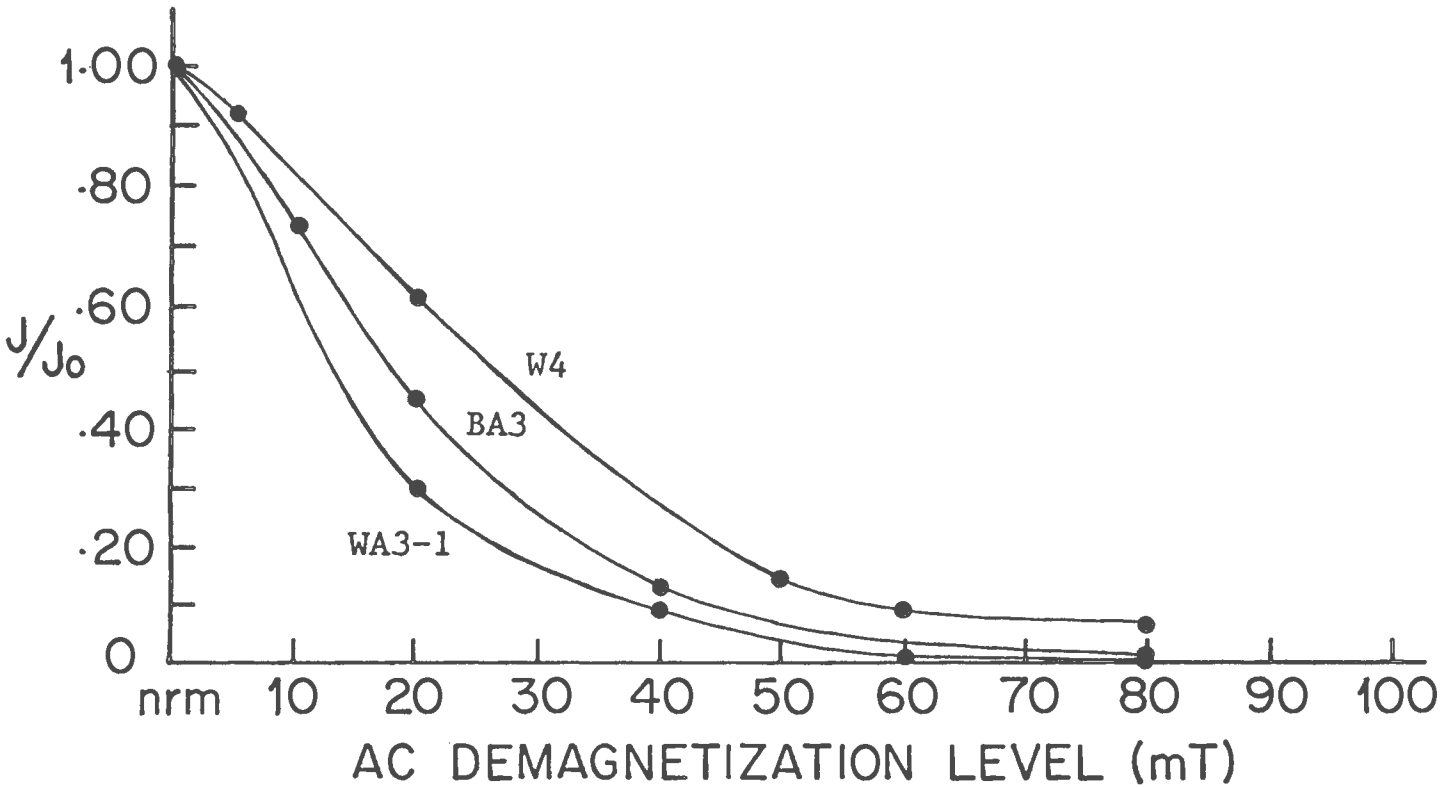

Figure 4.3 Normalized intensity plot for representative samples from the Ware system.

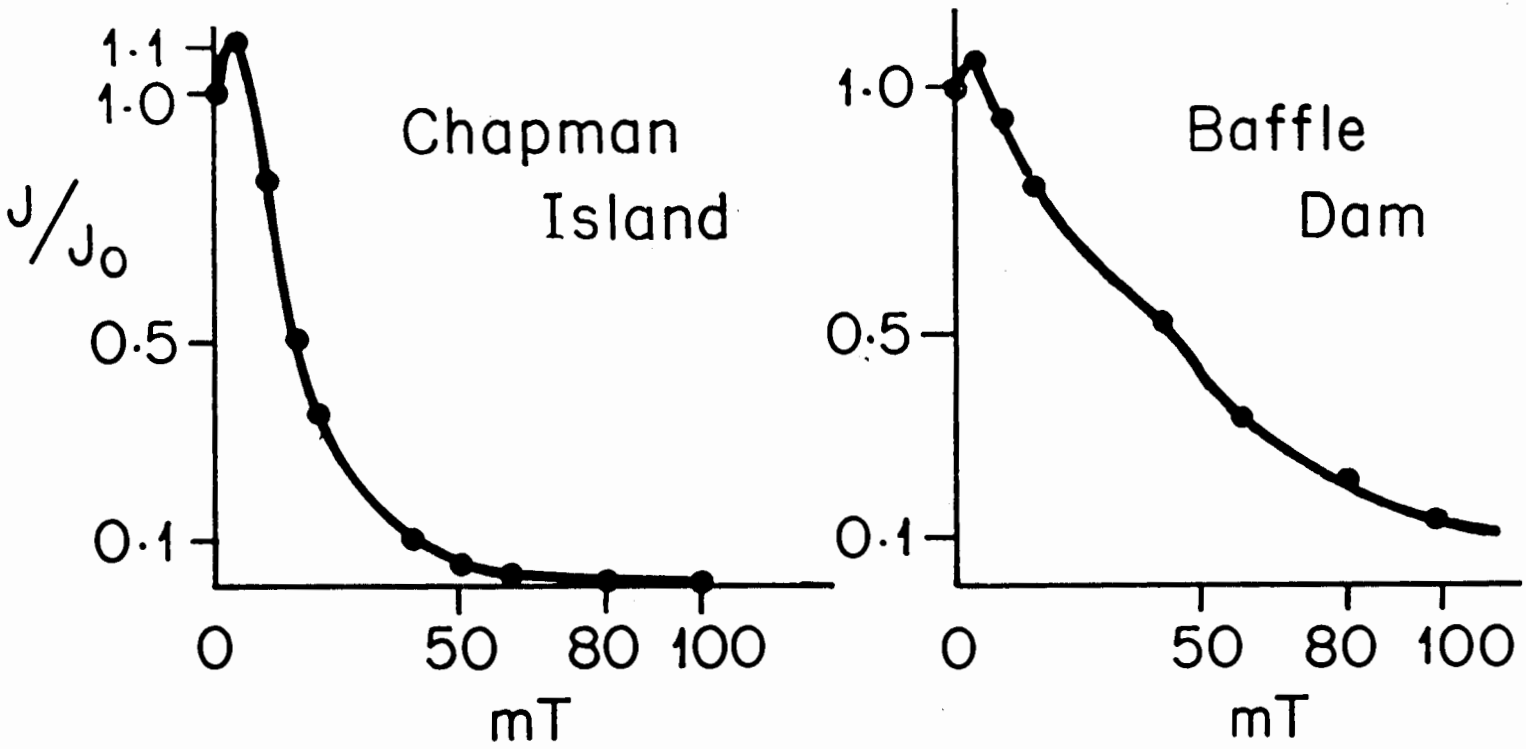

Figure 4.4 Normalized intensity plot for representative samples from the Quabbin Reservoir diabases.

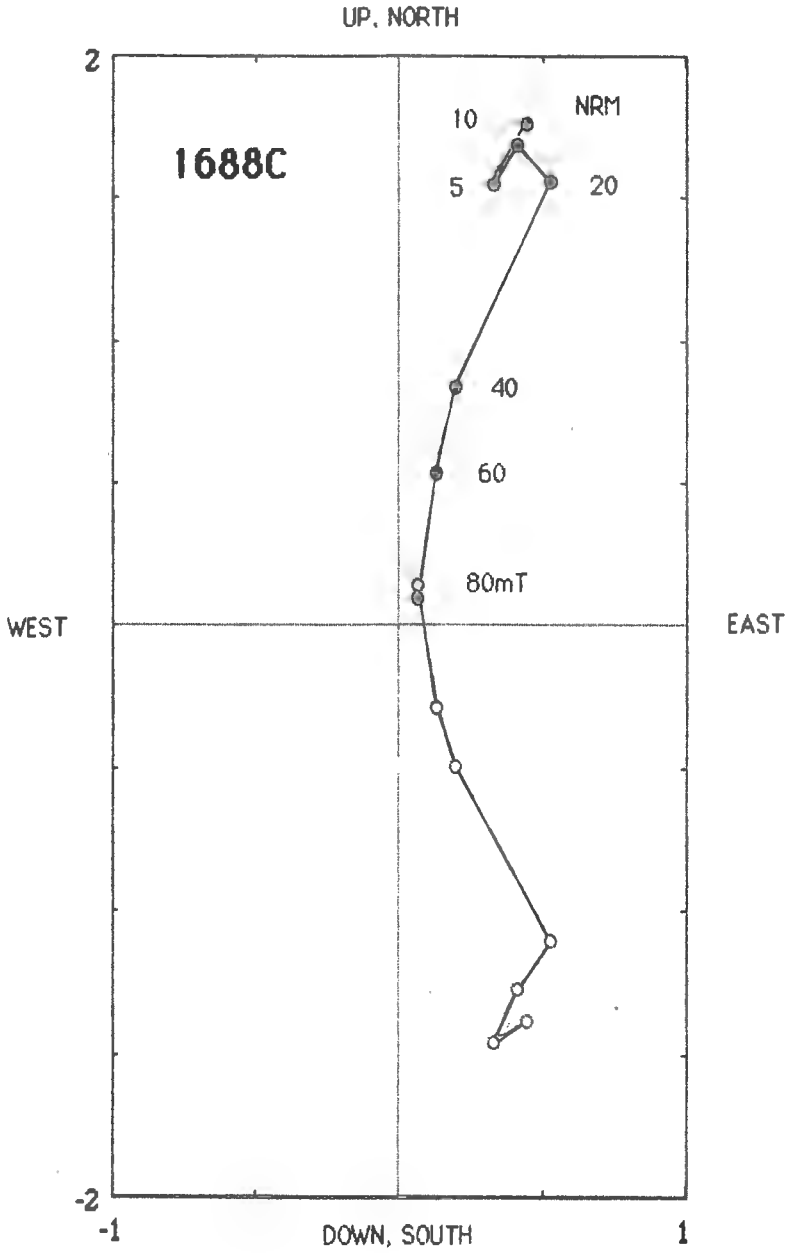

Figure 4.5 Vector end-point diagram of alternating field demagnetization study of a sample from the Holden system, site 1688, sample C. Open circles are projections on the vertical plane, closed circles are on the horizontal plane. Scales in A/m.

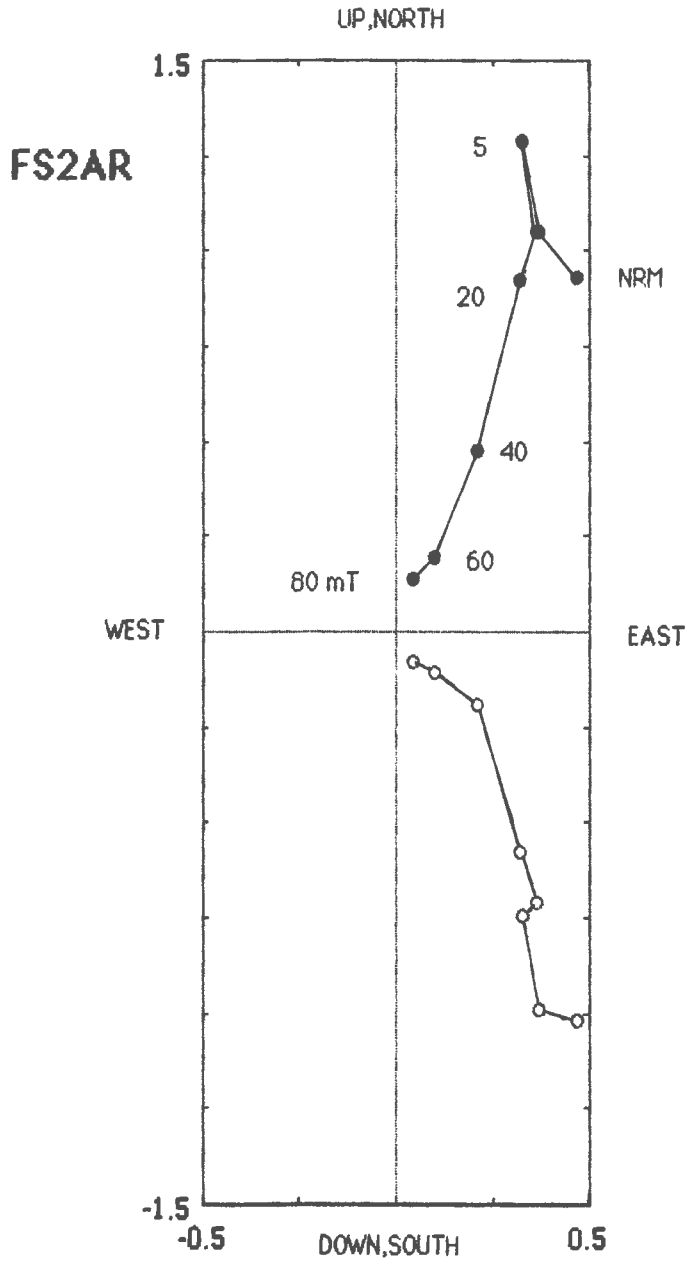

Figure 4.6 Vector end-point diagram of alternating field demagnetization study of a sample from the Holden system, site Fiskdale, sample 2. Open circles are projections on the vertical plane, closed circles are on the horizontal plane. Scales in A/m.

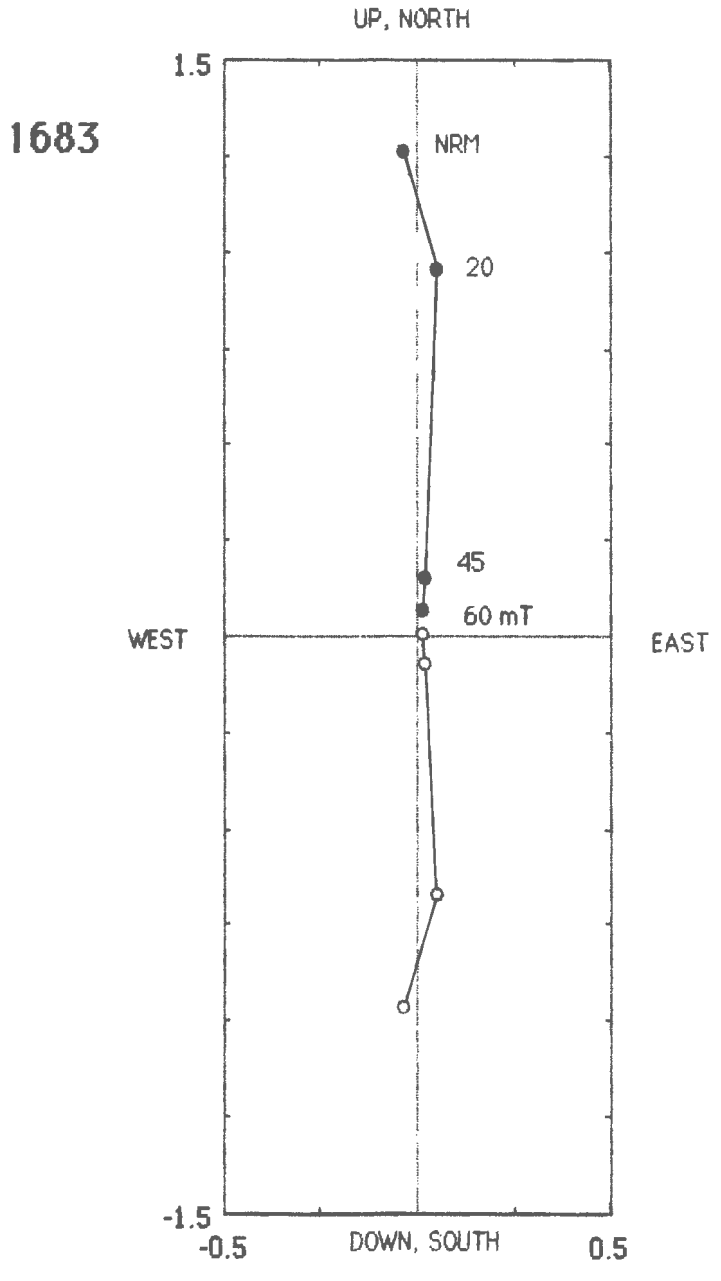

Figure 4.7 Vector end-point diagram of alternating field demagnetization study of a sample from the Holden system, site 1683. Open circles are projections on the vertical plane, closed circles are on the horizontal plane. Scales in A/m.

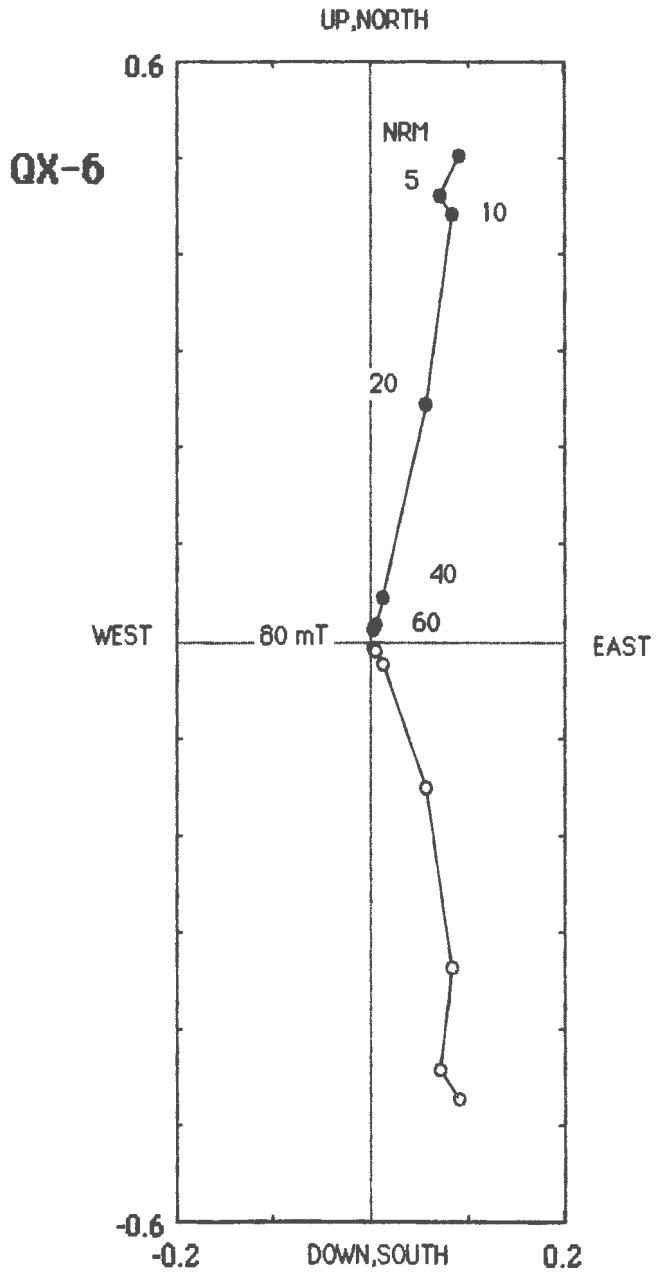

Figure 4.8 Vector end-point diagram of alternating field demagnetization study of a sample from the Holden system, site Quinapoxet, sample 6. Open circles are projections on the vertical plane, closed circles are on the horizontal plane. Scales in A/m.

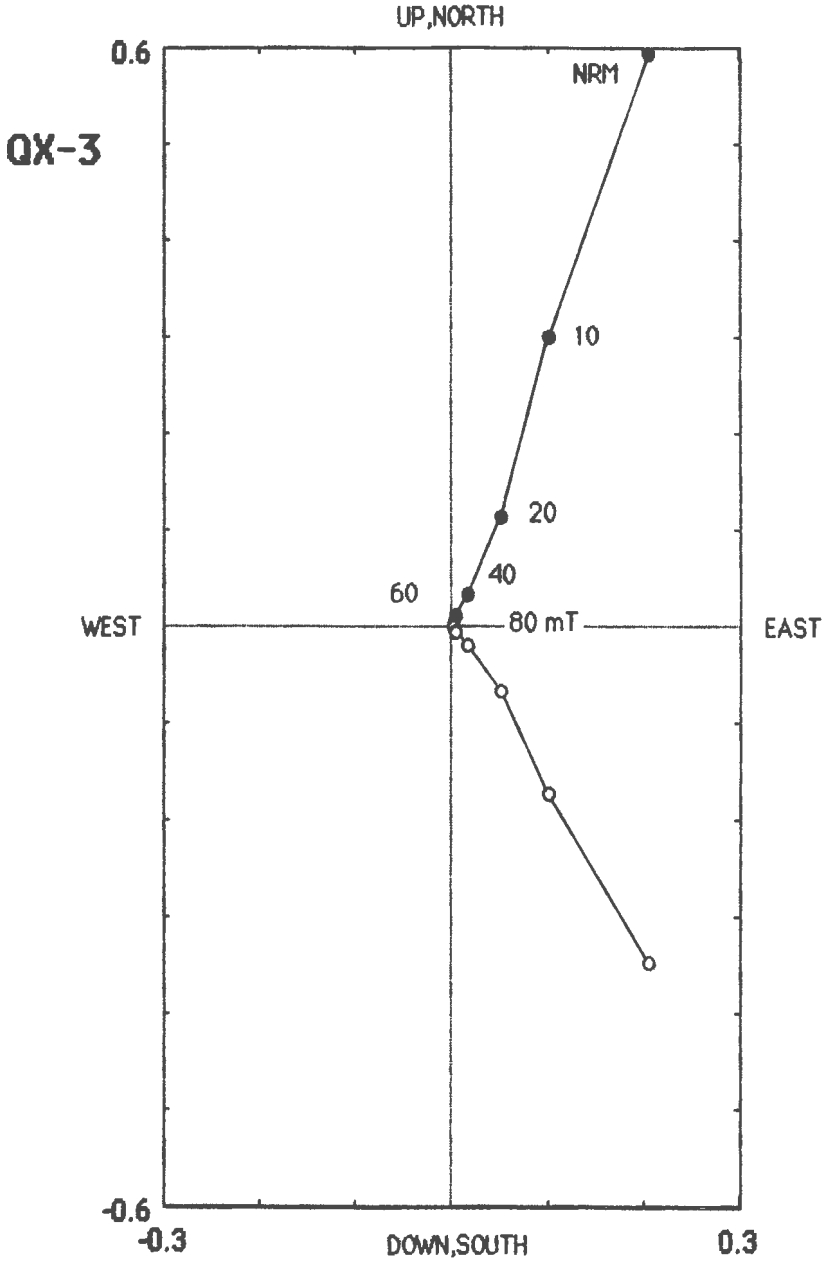

Figure 4.9 Vector end-point diagram of alternating field demagnetization study of a sample from the Holden system, site Quinapoxet, sample 3. Open circles are projections on the vertical plane, closed circles are on the horizontal plane. Scales in A/m.

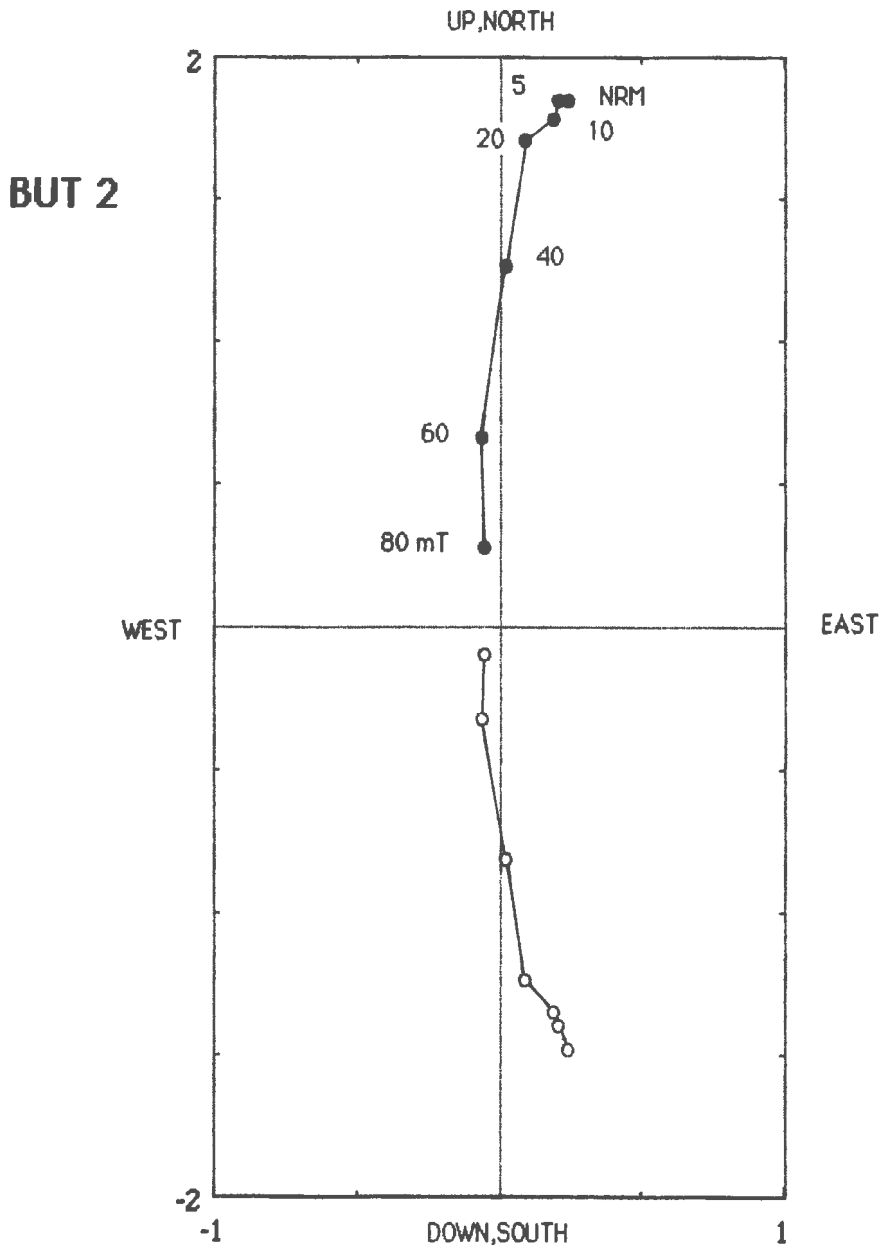

Figure 4.10 Vector end-point diagram of alternating field demagnetization study of a sample from the Pelham-Loudville system, site Butterworth, sample 2. Open circles are projections on the vertical plane, closed circles are on the horizontal plane. Scales in A/m.

is a change from northeast to northwest for the horizontal component. This is due to the dominant north component which is significantly larger than the east-west component. There is a secondary component that is not removed until 60 mT, then a linear decay to the origin. Note that the intensities in this system are an order of magnitude greater than in the Holden or Ware systems. In Figures 4.11 and 4.12, both the North Valley and Lake Pleasant both sites show a removal of a small viscous component at low fields (10 mT), above which a stable remanent direction is reached and there is a linear decay to the origin. In Figure 4.13, Laird 1 site, a larger soft component in the northwest direction is seen but is removed by 30 mT. In the Pelham-Loudville system there is a variation in overprint directions. These are easily removed and the majority of the sites indicate stable remanent directions with good in-site, and site-to-site agreement after AF demagnetization.

Ware System. Progressive AF demagnetization studies on selected samples in the Ware system show the presence of two components of magnetization. A small component is removed at low fields. Based on petrographic work the main magnetic carrier is titanomagnetite. There is fine-grained unaltered pseudo-single-domain titanomagnetite in the contact samples. The euhedral multidomain titanomagnetite grains in the interior samples are altered to an Fe-Ti amorphous oxide. This alteration was probably deuteric because the same remanent direction is obtained from the contact samples as the interior samples. Individual vector end-point diagrams for three Ware sites are discussed below.

Vector end-point diagrams of interior sites from the Ware system diabases show similar overprintings. In Figures 4.14 and 4.15, representative samples from Barre and Ware sites are plotted. Both show a soft secondary component that is removed by 10 mT in Ware and by 20 mT in Barre, and a stable direction results at higher fields. An equal area net of a sample from the Fox Hill site in Figure 4.16, shows the removal of a secondary component in a northwestward direction, then a clustering of directions after 40 mT, indicating that the stable remanent direction has been reached. The decay pattern from the French King Bridge site shows little overprinting. Less than fifty percent of the original NRM has been removed by 80 mT. There are abundant pseudo-single-domain grains of titanomagnetite and single domain grains are inferred to be present. Very little hematite was noted. The direction obtained from the French King Bridge site is the same as the directions from the other diabases in the Ware system exposed 35 km to the southeast.

Bliss Hill Group. The Cretaceous diabases in Massachusetts record both normal and reversed polarity. The Bliss Hill north diabase (site 4I4) records cooling in a field of normal polarity. This site shows the removal of a secondary component that is steeper than the remanent direction. This may be a present-day overprint. The magnetic component is quite soft and after 10 mT, less than ten percent of the original direction is left. This direction is similar to one obtained on the lamprophyre at Gassetts, Vermont (McEnroe et al., 1987). The Bliss Hill south diabase (site BH) also shows a soft magnetic signature. The direction in this diabase is not yet understood and additional paleomagnetic work is needed. A series of magnetometer traverses were run over the diabase and it is definitely in place and not rotated, so the paleomagnetic direction is correct. It may be representative of cooling during a transition of the earths field either in the late Jurassic or early Cretaceous.

Quabbin Reservoir Group. The intrusions recording reversed polarity are located in the Quabbin Reservoir area. These magnetic directions were compared to other New England Cretaceous intrusions of approximately the same age. Progressive AF demagnetization studies of selected cores from the reversed sites show the presence of a normal secondary component as shown in Figure 4.17. This component is removed in all sites by 10 mT, with stable remanence above this level. The Chapman Island sill, the West Rutland, Vermont, dikes, and the Baffle Dam island sill all show a small normal overprint,

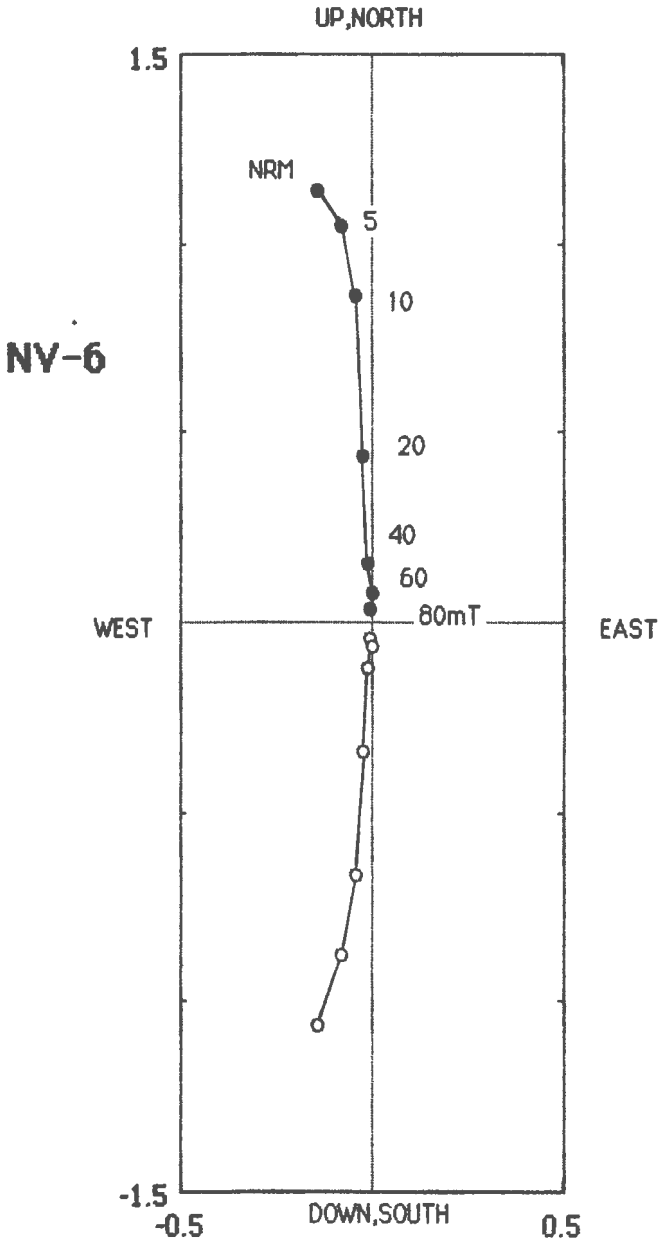

Figure 4.11 Vector end-point diagram of alternating field demagnetization study of a sample from the Pelham-Loudville system, site North Valley Rd., sample 6. Open circles are projections on the vertical plane, closed circles are on the horizontal plane. Scales in A/m.

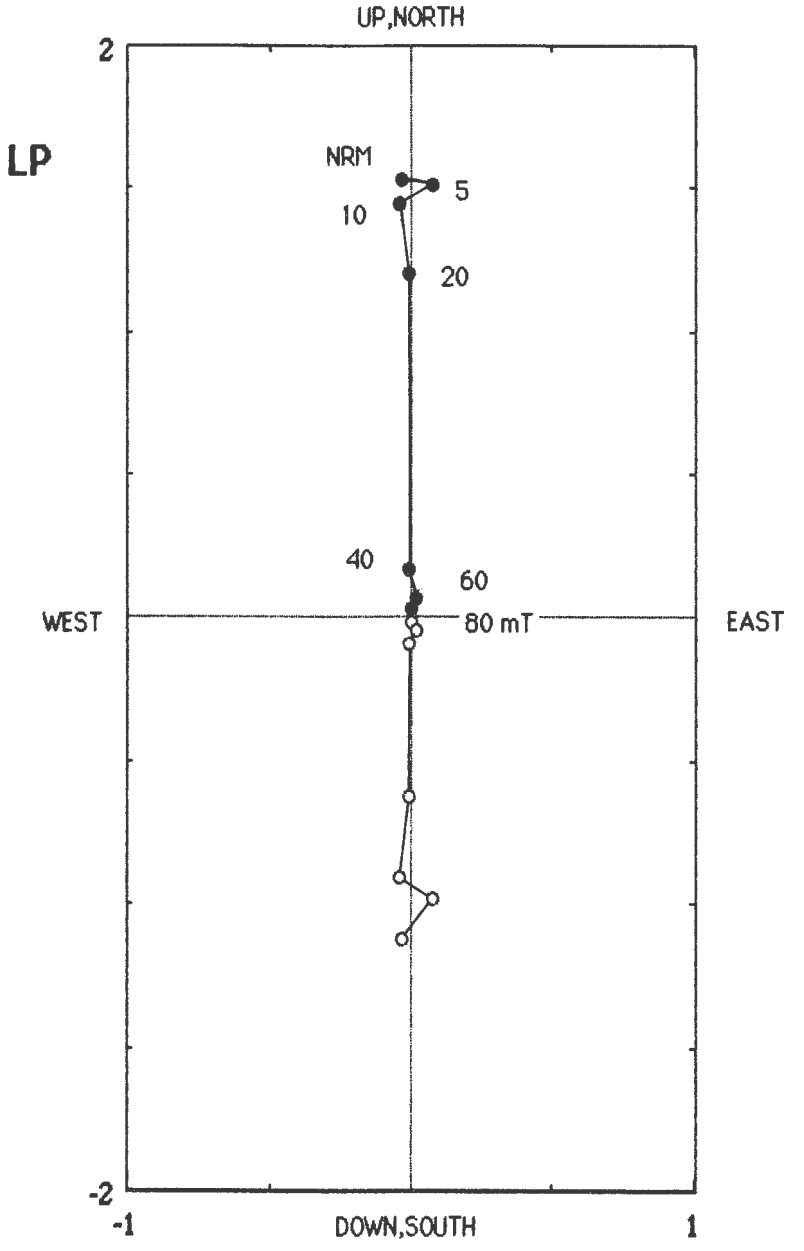

Figure 4.12 Vector end-point diagram of alternating field demagnetization study of a sample from the Pelham-Loudville system, site Lake Pleasant. Open circles are projections on the vertical plane, closed circles are on the horizontal plane. Scales in A/m.

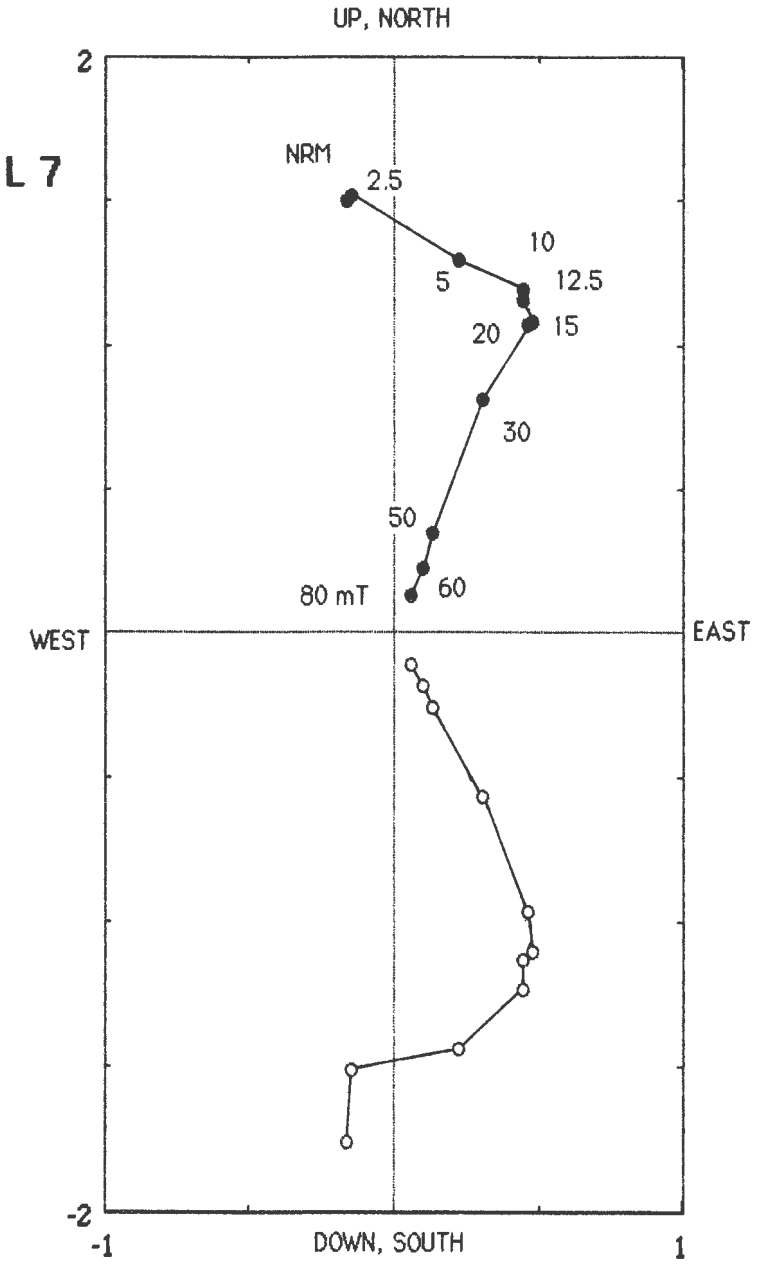

Figure 4.13 Vector end-point diagram of alternating field demagnetization study of a sample from the Pelham-Loudville system, site Laird 1, sample 7. Open circles are projections on the vertical plane, closed circles are on the horizontal plane. Scales in A/m.

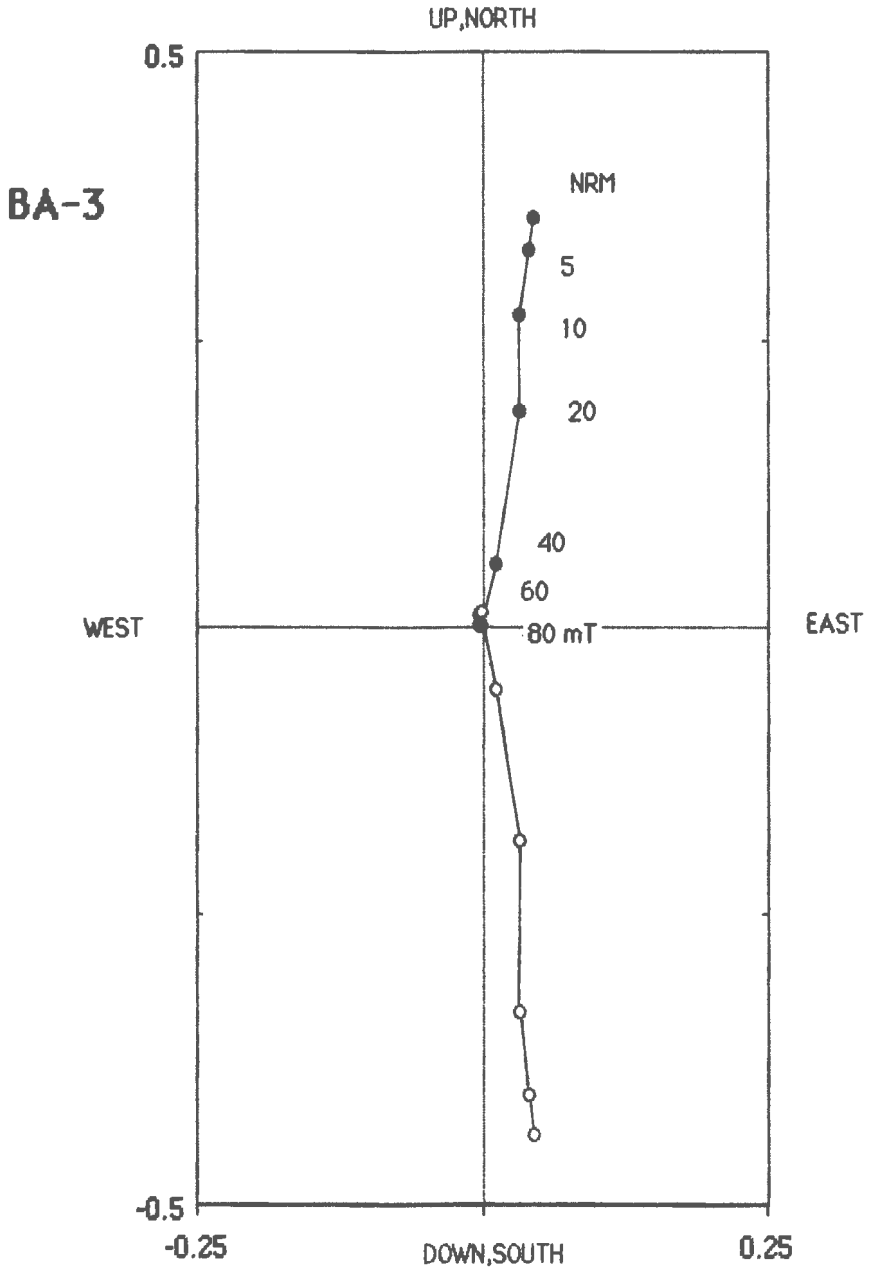

Figure 4.14 Vector end-point diagram of alternating field demagnetization study of a sample from the Ware system, site Barre, sample 3. Open circles are projections on the vertical plane, closed circles are on the horizontal plane. Scales in A/m.

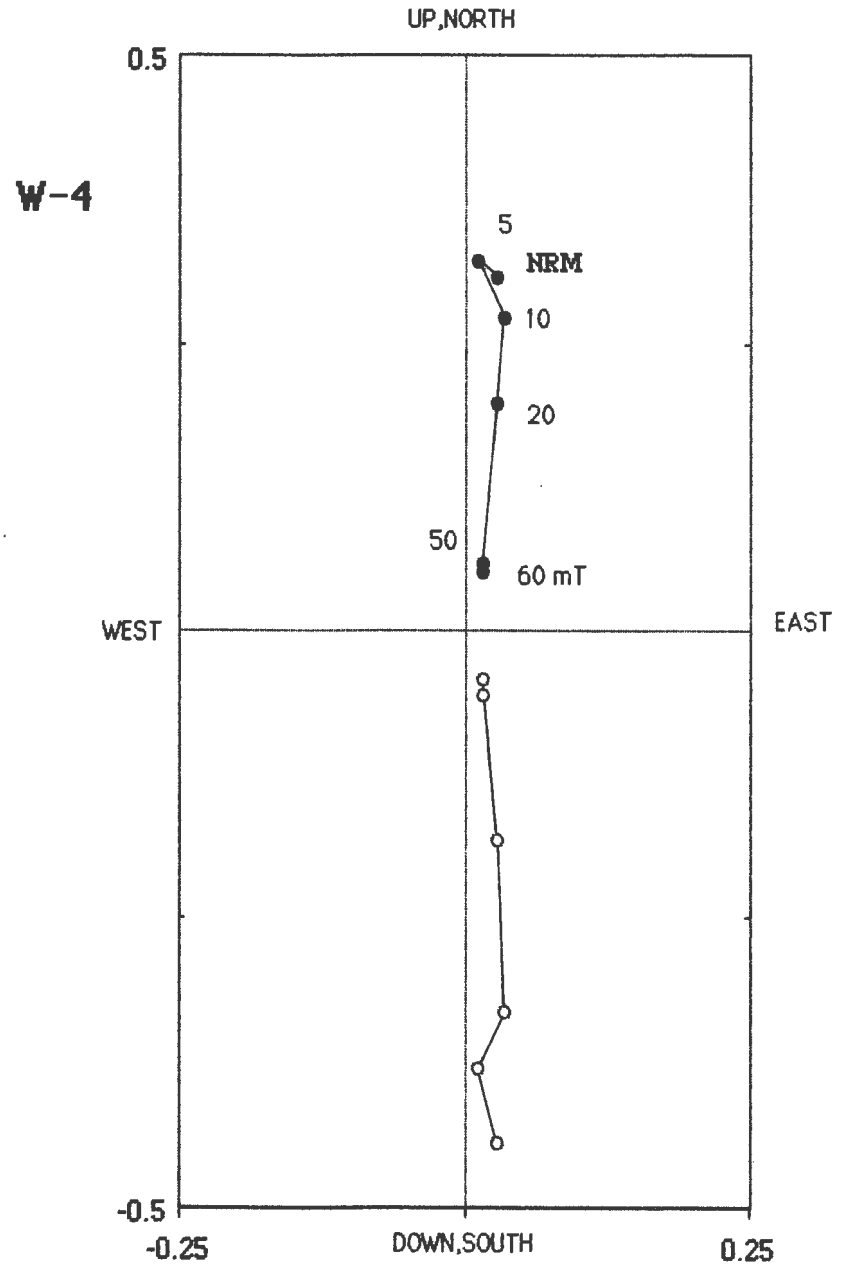

Figure 4.15 Vector end-point diagram of alternating field demagnetization study of a sample from the Ware system, site Ware, sample 4. Open circles are projections on the vertical plane, closed circles are on the horizontal plane. Scales in A/m.

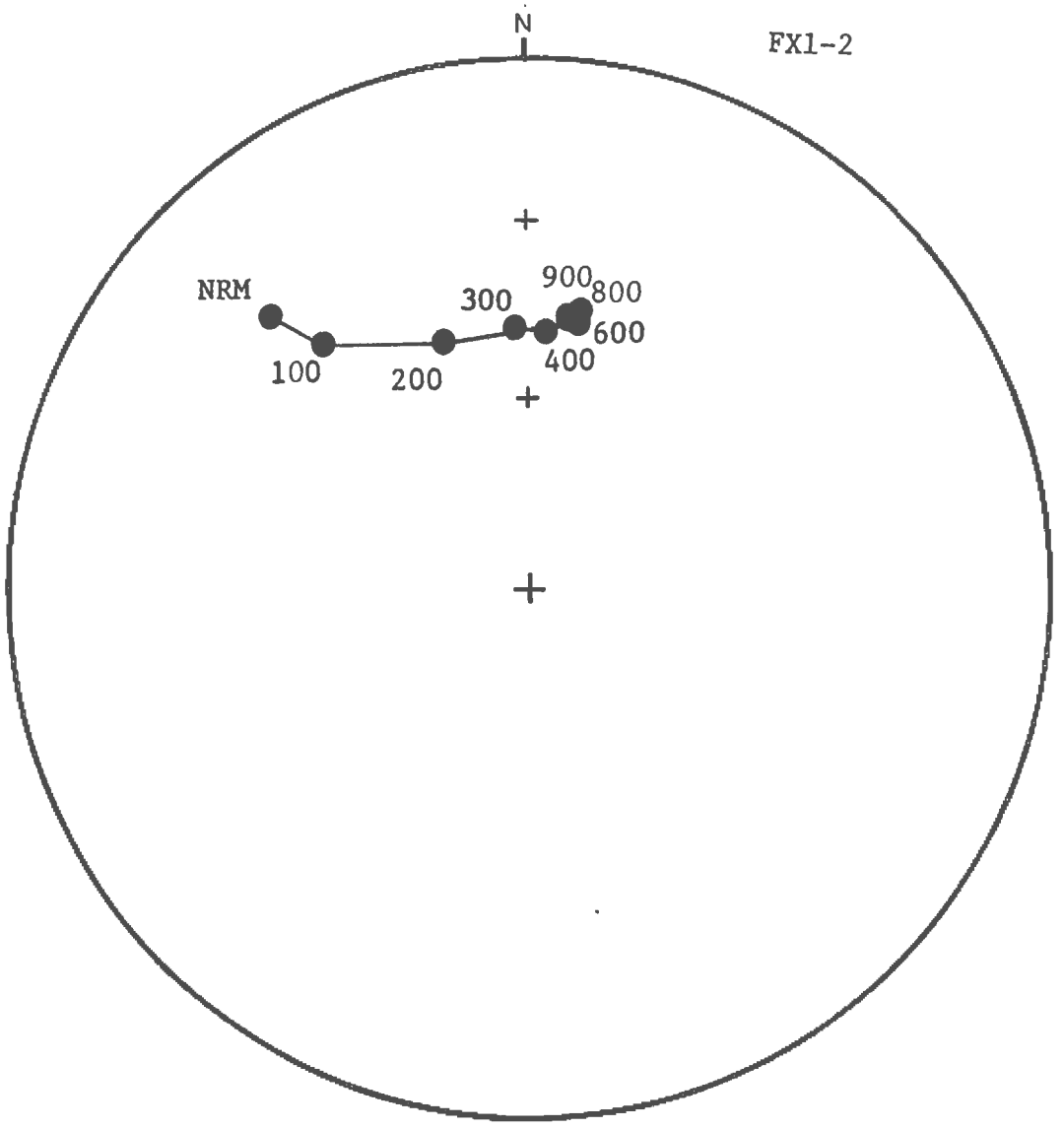

Figure 4.16 Equal area net of alternating field demagnetization study of a sample from the Ware system, Fox Hill site, sample 1-2. Open circles are projections on the vertical plane, closed circles are on the horizontal plane.

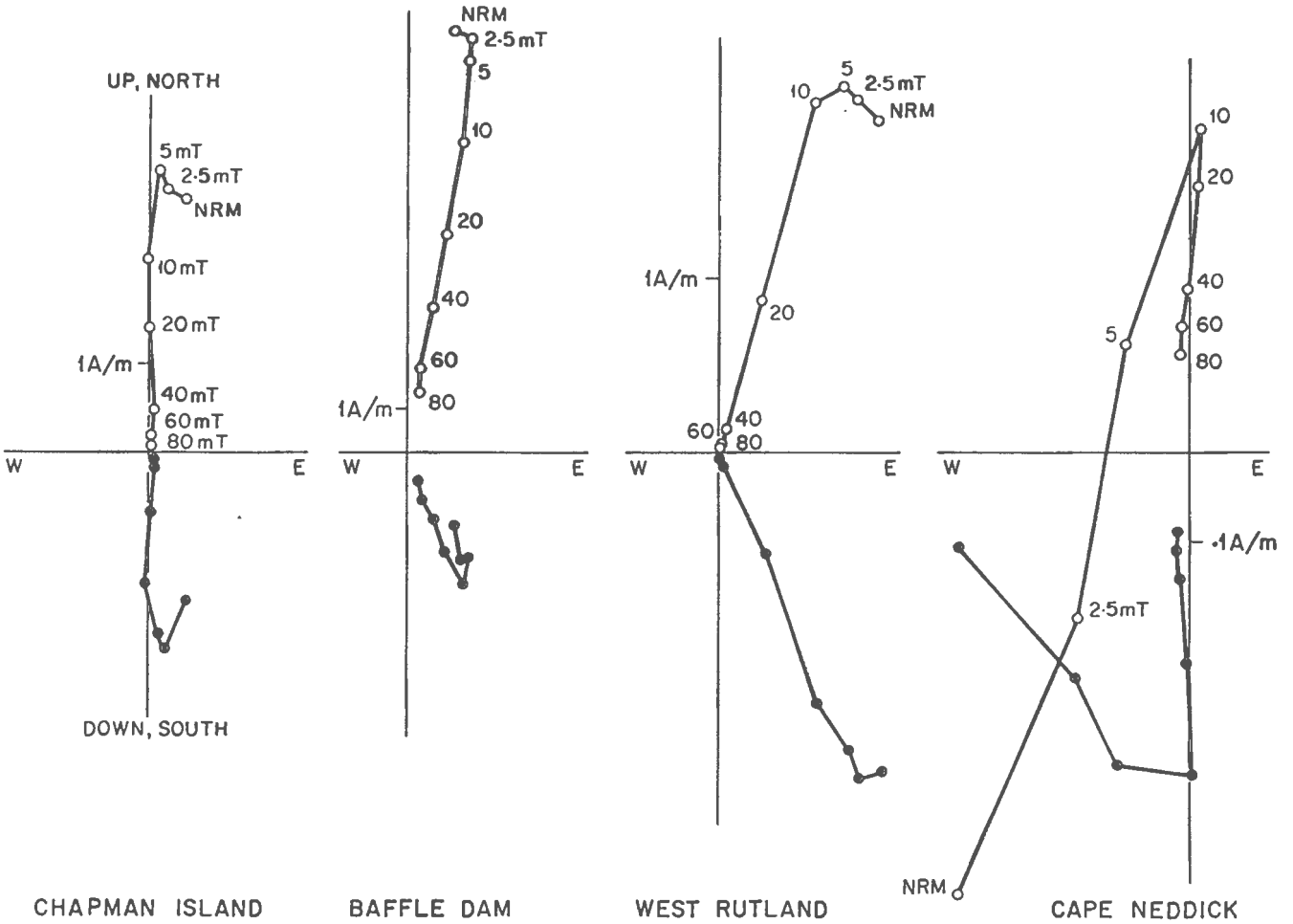

Figure 4.17 Vector end-point diagram of alternating field demagnetization studies of samples from Cretaceous sites. Quabbin Reservoir diabases, Chapman Island and Baffle Dam Island sites, are compared to the Cretaceous Cape Neddick intrusion in Maine and West Rutland, Vermont, lamprophyre. Open circles are projections on the vertical plane, closed circles are on the horizontal plane. Scales in A/m.

then a stable direction that is southerly and with a steep negative inclination. There is a larger secondary component of normal direction in the Cape Neddick Gabbro but it is easily removed at low fields and a similar reversed direction is present. It is believed that the stable remanent direction obtained in these studies is the primary remanence obtained by the intrusions upon cooling. A thermal demagnetization study confirms the direction obtained in the AF demagnetization, though the magnetite behaves viscously.

Thermal Demagnetization Studies

Thermal demagnetization studies on ten selected samples of Jurassic diabase, at least three from each chemical system were run. The directions obtained confirm the directions recorded from the AF studies. Figure 4.18, shows a vector-end point diagram for a sample from the Ware system. This thermal demagnetization pattern shows stable remanent directions that are identical to those produced by the alternating field decay studies. In one of the Holden sites, 1681C, the dominant magnetic carrier appears to be a later hematite, because it is stable at temperatures greater than 580^0C and the original intensities are very low. The steep and varying inclination obtained from this site in the AF studies agrees with the thermal studies that suggest hematite is the main magnetic carrier. This magnetic direction was acquired at a later post-solidification stage or possibly even in the present field because the magnetic vector streaks toward a present-day direction under AF and thermal demagnetization. The magnetites from this site are highly altered, in some instances to non-magnetic sphene. The other Holden site selected for a thermal study from this system, 1688, confirms the AF directions obtained. The thermal demagnetization directions obtained in samples from the Pelham-Loudville system, from Mineral Spring, Sawmill Hills, Laird 1, and Turkey Hill all confirm the trends and directions obtained in the alternating field studies

Magnetic Site Directions

Table 4.1 is a summary of the mean magnetic directions and statistical parameters determined for the forty sites studied. The reliable mean site directions are plotted on an equal area diagram (Figure 4.19). Each diabase system is indicated by a separate symbol. The Jurassic diabases are all of normal polarity, hence plotted in the lower hemisphere. The Cretaceous diabases are of mixed polarity and plot in the upper (reversed) and lower hemisphere (normal). The virtual geomagnetic poles (VGP) for the diabase determined in this study, are given in Table 4.2.

The average paleomagnetic directions for each chemical system was then calculated. Pole positions were calculated by averaging the virtual geomagnetic poles obtained for the different chemical systems. These are listed in Table 4.3. Each chemical system records statistically different pole positions. Three sites from the Holden system were omitted from the average, either because a stable remanent direction could not be adequately obtained through AF cleaning or thermal techniques, or because of large within-site scatter. Two sites were eliminated from the Pelham-Loudville system due to extreme within-site scatter, presumably due to lightning strikes. Two other sites were removed from the study due to large within-site scatter, as indicated by large values of a95. The removal of sites with $a95 > 17^0$ is consistent with rejection criteria values from 10^0 to 25^0 used in previous studies of the eastern North America diabases (Smith,1987).

The mean paleomagnetic directions for the Jurassic systems are of normal polarity. These are: Holden system D=15.2, I=28.1, $a95=3.3^0$; Pelham-Loudville system $D=5.7^0$, $I=32.9^0$, $a95=2.2^0$; Ware system $D=5.4^0$, $I=44.8^0$, $a95=2.3^0$. These mean system paleomagnetic directions are shown in Figure 4.20 with 95% confidence circles. The three Jurassic groups are statistically distinct, with no overlap of the a95. This indicates that each Jurassic system recorded a different magnetic direction. The paleomagnetic directions obtained for the Cretaceous diabases are of mixed polarity. The Bliss Hill north site (4I4,

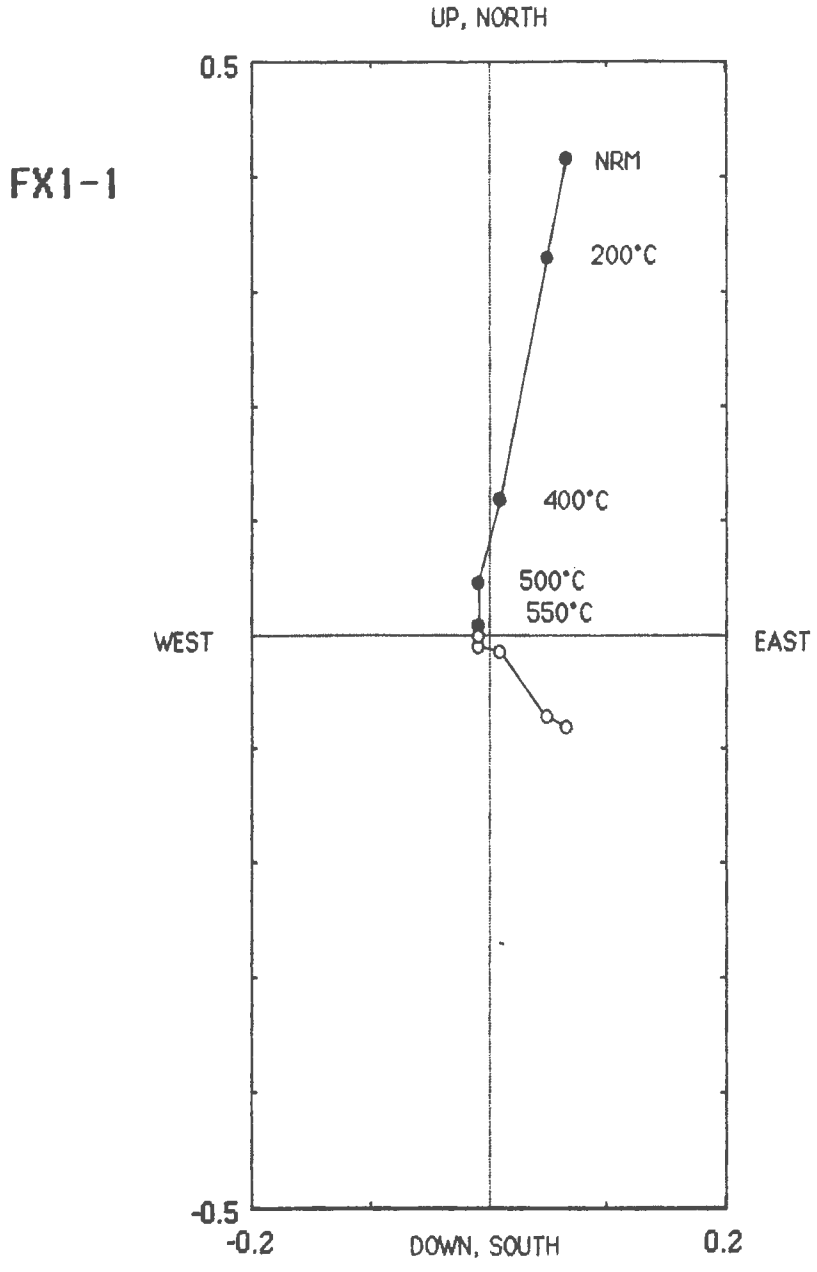

Figure 4.18 Thermal demagnetization vector end-point diagram from the Ware system, site Fox Hill, sample 1-1. Open circles are projections on the vertical plane, closed circles are on the horizontal plane. Scales in A/m.

Table 4.1 Summary of site mean directions and statistical parameters for Central Massachusetts Mesozoic diabases.

JURASSIC DIABASES

Site	n/N	D	I	a95	K	R	Site Lat.N	Site Long. E	Demag
HOLDEN									
Qx. Res	7/8	18.7	33.4	4.9	154	6.96	42.4	288	20mT
1688	7/7	19.3	29.9	4.8	160	9.96	42.2	289	40mT
1683	9/9	10.3	26.5	4.7	120	8.93	42.2	289	40mT
Fiskdale	8/8	14.3	23.6	10.0	32	7.78	42.1	288	40mT
1681*	6/6	3.6	53.8	34.0	5	4.99	42.2	288	40mT
Rd122*	5/9	346.0	15.3	18.5	19	4.78	42.2	288	40mT
Qp*	7/8	345.9	27.6	20	10	6.41	42.1	288	25mT
WARE									
Bare	6/6	13.3	45.8	5.5	151	5.97	42.4	288	20mT
Ware	6/7	7.6	46.3	7.1	90	5.94	42.2	288	25mT
WA3	8/8	1.5	46.9	4.5	154	7.95	42.2	288	30mT
Foxhill	8/10	4.2	43.8	3.2	308	7.98	42.2	288	40mT
FK- B.	5/6	1.7	39.4	7.1	116	4.97	42.6	288	60mT
PELHAM									
NV	6/6	353.2	41.3	4.2	259	5.98	42.2	288	20mT
202	4/6	9.8	28	11.1	69.6	3.96	42.3	288	30mT
8C9A	7/7	353.1	29.6	5.4	126	6.95	42.3	288	40mT
8C9C	3/3	10.0	30.1	6.9	316	2.99	42.3	288	40mT
3C6*	6/9	-	-	-	-	-	42.3	288	--
NF	6/6	0.4	28.3	5.6	143	5.97	42.7	288	20mT
MF	7/7	12.1	28.1	7.8	64	6.91	42.3	288	40mT
LP	8/8	7.1	25.6	5.2	113	7.94	42.3	288	30mT
LairdI	6/7	14.1	24.6	12.3	40	4.9	42.3	288	40mT
LairdII	7/7	2.1	31.3	4.1	220	6.97	42.3	288	40mT
6I4,3	5/5	6.3	34.4	16.9	22	4.81	42.2	288	40mT
EDH	6/7	6.3	35.2	8.5	64	5.92	42.2	288	40mT
CC	6/6	9.5	32.8	5.6	142	5.96	42.2	288	50mT
126	9/10	357.6	34.2	7.1	53	8.85	42.2	288	40mT
6I6	3/3	25.1	41.2	20.1	38	2.95	42.2	288	40mT
6I5	4/4	6.2	34.6	4.8	373	3.99	42.2	288	40mT
RS*	9/9	-	-	-	-	-	42.	288	--
BUT	8/8	356.3	32	3.7	225	7.96	42.7	288	40mT
LP-B	17/17	4.3	26	4.1	78	16.8	42.3	288	40mT
LOUDVILLE									
Mineral	7/7	1.2	35.7	7.9	60	6.99	42.17	288	40mT
MS-2	5/5	39.4	33.8	12.3	40	4.99	42.17	287.6	60mT
Cold R.	6/10	18.9	36.8	14.2	23	5.78	42.28	287.3	40mT
Cold S.*	10/10	-	-	-	-	-	42.28	287.3	--
SMH1	5/6	7.5	44	8.7	78.3	4.95	42.33	287.3	30mT
SWM II	4/5	228.1	44.2	13.6	47	3.94	42.33	287.3	15mT

Table 4.1 (continued)

LATE JURASSIC - CRETACEOUS DIABASES

Site	n/N	D	I	a95	K	R	Site Lat.N	Site Long.E	Site Demag
QUABBIN									
Chapman	10/11	175.2	-61.8	5.5	79	9.89	42.24	287.8	20mT
Baffle	8/8	165.1	-60.0	2.3	557	7.99	42.24	287.8	40mT
BLISS HILL									
4I4	6/6	7.6	63.9	12.2	31	5.84	42.68	287.7	20mT
BH	5/6	105.7	20.1	9.1	71	4.93	42.68	287.7	20mT

n/N, number of samples/number collected; D, mean declination; I, mean inclination; a_{95}, radius of cone of confidence at the 95% level around site mean; K and R, statistical parameters of Fisher(1953); Latitude and Longitude of sites, peak demagnetization level.

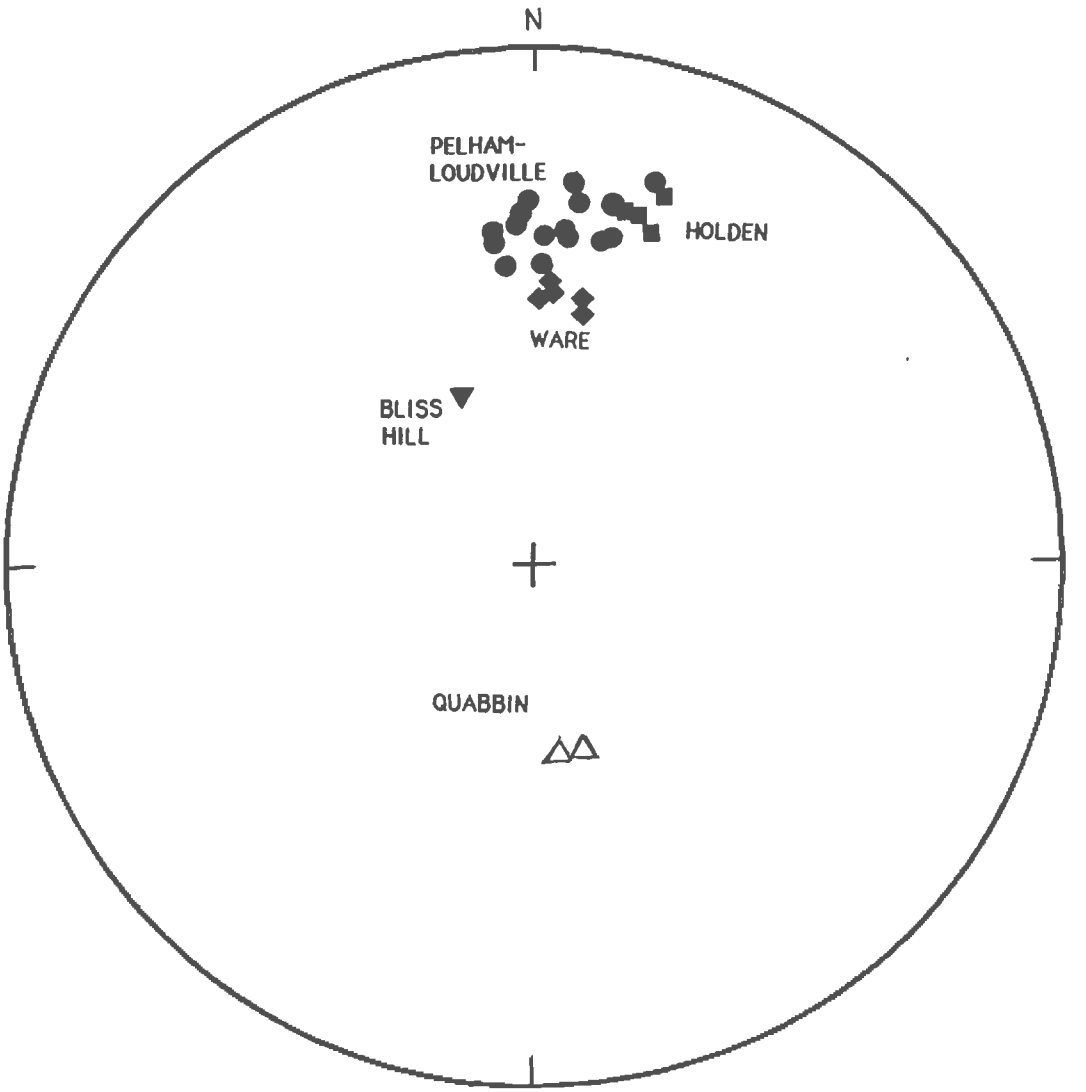

Figure 4.19 Equal area projections of site-mean magnetic directions from the central Massachusetts diabases studied. Closed symbols are projections on the lower hemisphere, open symbols are on the upper hemisphere.

Table 4.2 Summary of virtual geomagnetic poles (VGP) and statistical parameters for the central Massachusetts Mesozoic diabases.

Site	Lat.	Long.	dp	dm
Jurassic Diabases				
HOLDEN				
Qx. Res.	61.1	69.1	3.2	5.6
1688	59.9	74.3	1.5	2.7
1683	60.0	84.9	2.5	4.6
Fiskdale	57.8	81	5.7	10.7
WARE				
Barre	71.3	68.2	4.5	7.0
Ware	74.2	82.4	5.8	9.1
Wa3	74.7	114.6	4.7	7.4
Foxhill	73.0	94.7	2.5	4.0
French K. B.	69.7	103.0	5.1	8.5
PELHAM				
NV	70.6	126.6	3.1	5.1
202	61.4	87.7	6.7	12.1
8C9A	62.5	86.6	4.3	7.7
8C9A	62.5	86.6	4.3	7.7
NF	62.4	106.7	3.4	6.1
MF	60.7	83.3	4.6	8.3
LP	60.5	93.6	3.0	5.6
Laird 1	59.3	80.5	7.1	13.2
Laird II	64.5	103.0	2.6	4.6
EDH	66.6	92.7	5.7	9.8
CC	64.3	86.5	3.6	6.3
126	66.9	112.1	6.2	10.8
6I5	66.3	94.5	5.0	8.7
6I6*	62.1	51.5	15.0	24.6
BUT	64.8	116.1	2.3	4.2
LP-B	59.0	121.7	10.9	20.5
LOUDVILLE				
MS	67.6	104.6	5.3	9.2
MS2	49.1	40.7	8.0	14.0
CR	63.0	65.2	9.7	16.6
SWM1	70.3	88.2	5.9	9.7
SWM2	-8.6	244.7	10.7	17.1
LATE JURASSIC - CRETACOUS DIABASES				
BLISS HILL				
4I4	83.8	347.1	15.5	19.4
BH	-4.2	359.4	5.0	9.5
QUABBIN				
Chapman Island	-86.4	31.6	6.6	-8.5
Baffle Dam Island	-88.7	227.7	9.4	-3.5

Latitude in degrees north; Longitude in degrees east; dp and dm, semi-minor and semi-major axis, respectively, of ellipse at the 95% confidence level around the pole.

Table 4.3 Mean pole positions for the Mesozoic diabases in central Massachusetts.

Site	n/N	D	I	a95	K	Pole Position Lat.N	Long.	dp	dm
JURASSIC DIABASES									
HOLDEN	4/7	15.2	28.1	3.3	62	59.7	77.9	2.0	3.6
PELHAM	19/24	5.7	32.9	2.2	35.2	65.2	95.0	1.4	2.5
WARE	5/5	5.4	44.8	2.3	119.4	73.3	90.8	2.9	2.3
LATE JURASSIC - CRETACEOUS DIABASES									
BLISS H. S.	1/1	105.7	20.1	9.1	71.0	-4.2	359.4	5.0	9.5
BLISS H. N.	1/1	5.4	57.6	9.6	29.6	83.9	63.2	0.3	14.1
QUABBIN	2/2	168.7	-61.6	4.0	77.1	-81.7	25.2	4.8	6.2

n/N, number of sites used in computation of the mean (n), over total sites(N); D, mean declination; I, mean inclination; a95, radius of 95% confidence circle; K, a statistical parameter of Fisher (1953); dp and dm, semi-minor axis and semi-major axis, respectively, of ellipse at the 95% confidence limit around the pole.

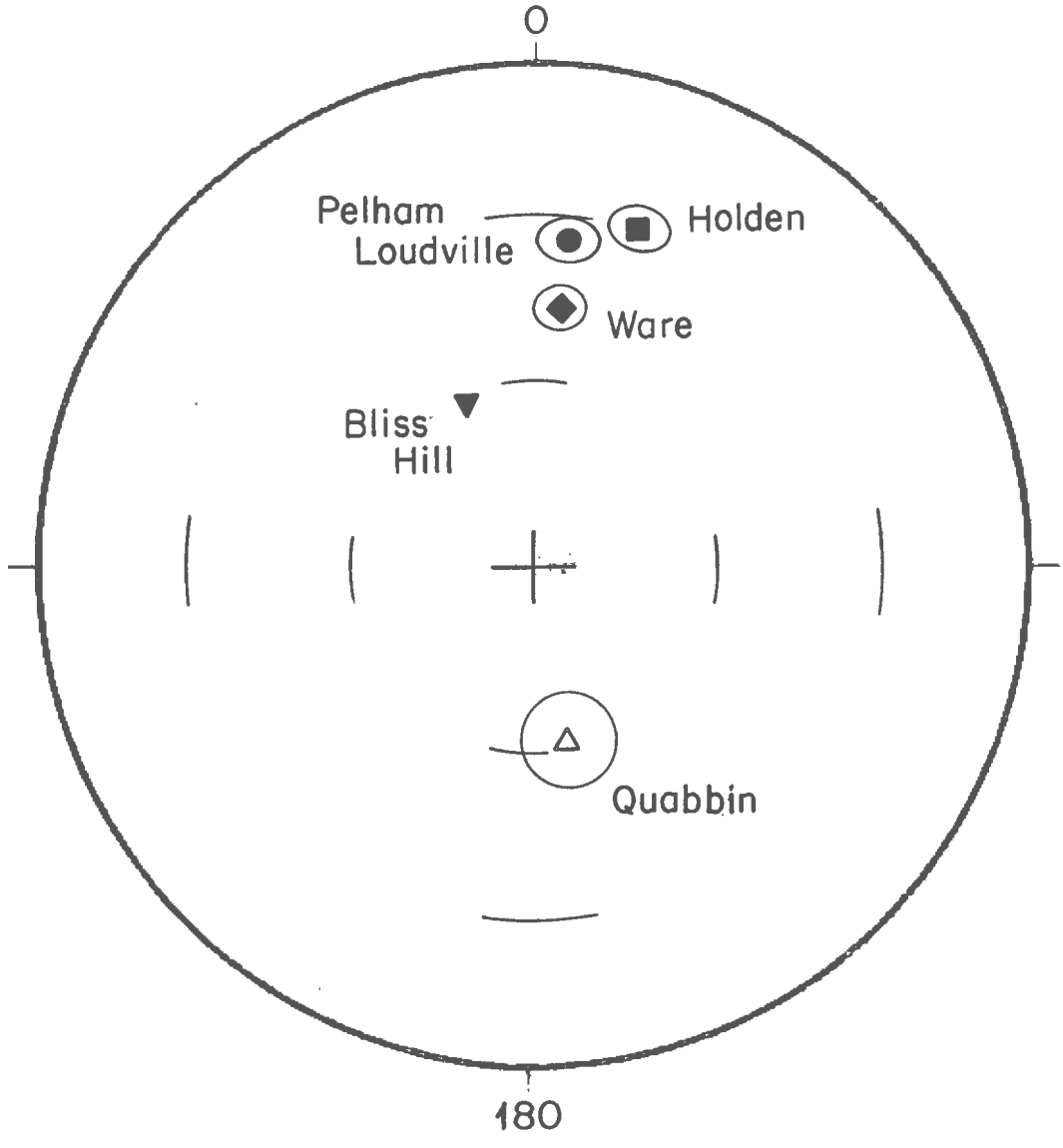

Figure 4.20 Mean magnetic directions of central Massachusetts diabase systems plotted on an equal area net with a_{95} cones of confidence shown. Closed symbols are projections on the lower hemisphere, open symbols are on the upper hemisphere.

normal polarity) and the Quabbin Reservoir group (reversed polarity) show expected steeper inclinations than the Jurassic diabases. These directions are: .Bliss Hill north (4I4), $D=5.4^0$, $I=57.6^0$, $a95=9.6^0$; Quabbin, $D=168.7^0$, $I=-61.6^0$, $a95=4.0^0$.

If the groups are listed in order of progressive steepening of the magnetic inclination in the mean magnetic directions, it may be considered as a list ordered in decreasing age. Steeper mean magnetic directions translate into higher paleopole latitudes, and hence younger pole positions. Under normal behavior of the earth's magnetic field over time this relationship between paleopole latitudes and inclination is valid. Such a list of inclinations gives the Jurassic Holden system at 28.1^0, the Jurassic Pelham-Loudville at 32.9^0, the Jurassic Ware system at 44.8^0, site 4I4 of the Bliss Hill group at 57.6^0 and the Cretaceous Quabbin group at -61.6^0

Pole Positions

These paleopoles suggest a difference in time for the emplacement of the diabase systems. The paleopoles from this study are plotted on Figure 4.21, and are compared to the polar wander curve for North America in the Mesozoic by May and Butler (1986). The Holden paleopole plots near the Triassic-Jurassic track prior to the J1 cusp. The Pelham-Loudville system, interpreted as intermediate in age, plots near the J1-J2 track, and the Ware system, the youngest of the Jurassic dike systems, has a high latitude pole plotting north of the J1-J2 track. The Massachusetts Cretaceous diabases plot well north and east of the J2-K track. As a comparison, other Mesozoic pole positions for the Appalachians are listed in Table 4.4. Smith and Noltimier (1979) did paleomagnetic work on the Newark Supergroup intrusive rocks and basalt flows in Connecticut and related this to $^{40}Ar/^{39}Ar$ age determinations (Sutter and Smith, 1979). .They calculated two pole positions for the early Jurassic, suggesting two separate periods of igneous activity at 190 m.y. and 175 m.y. These two pole positions have become known as the Newark trend I and II poles. These poles have been widely used in constraining the Early Jurassic part of the Mesozoic polar wander paths for North America. DeBoer (1968) and Smith (1976) also presented data that agree with two periods of igneous activity.

Unfortunately in the work on the Connecticut intrusives Smith (1976) averaged the southern extensions of the Holden, Pelham-Loudville and Ware systems together, leading to an erroneously young pole position for the Holden and Pelham-Loudville systems and an older pole position for the Ware system. It is also possible that the peak demagnetization levels used by Smith (1976) were not sufficient to remove all overprints. This also would have led to erroneous pole positions. In the present study overprinting was still present at 30 mT in the Ware system, whereas Smith (1976) used 20 mT peak demagnetization levels for the Ware system. 40 mT was needed to remove overprinting in some sites in the Holden and Pelham-Loudville systems but Smith only used 15 mT for the southern extension of the Holden and the Pelham-Loudville systems. Sutter (1979) determined an age for the Buttress (Ware) dike of 176.0 ± 3.8 by the $^{40}Ar/^{39}Ar$ method, and Smith and Noltimier (1979) inferred this age for Higganum and Bridgeport systems. Philpotts and Martello (1986) correlated the Massachusetts diabases with those in Connecticut (Higganum-Holden, Bridgeport-Pelham and Buttress-Ware). Smith and Noltimier (1979), using published data combined with their own results, calculated an older Newark Trend I pole ($63^0N, 83^0E$) and a younger Newark Trend II pole (65^0N, 103^0E).

Unfortunately a direct comparison of the pole positions from the present study to those determined for the dikes in Connecticut in earlier studies cannot be made. Most of the work of deBoer (1967) on intrusive diabases along the length of the Appalachians is not considered valid due to his excessive AF demagnetization (Smith and Noltimier 1979) The earlier work by DuBois (1957) and Bowker (1960) were largely reconnaissance surveys,

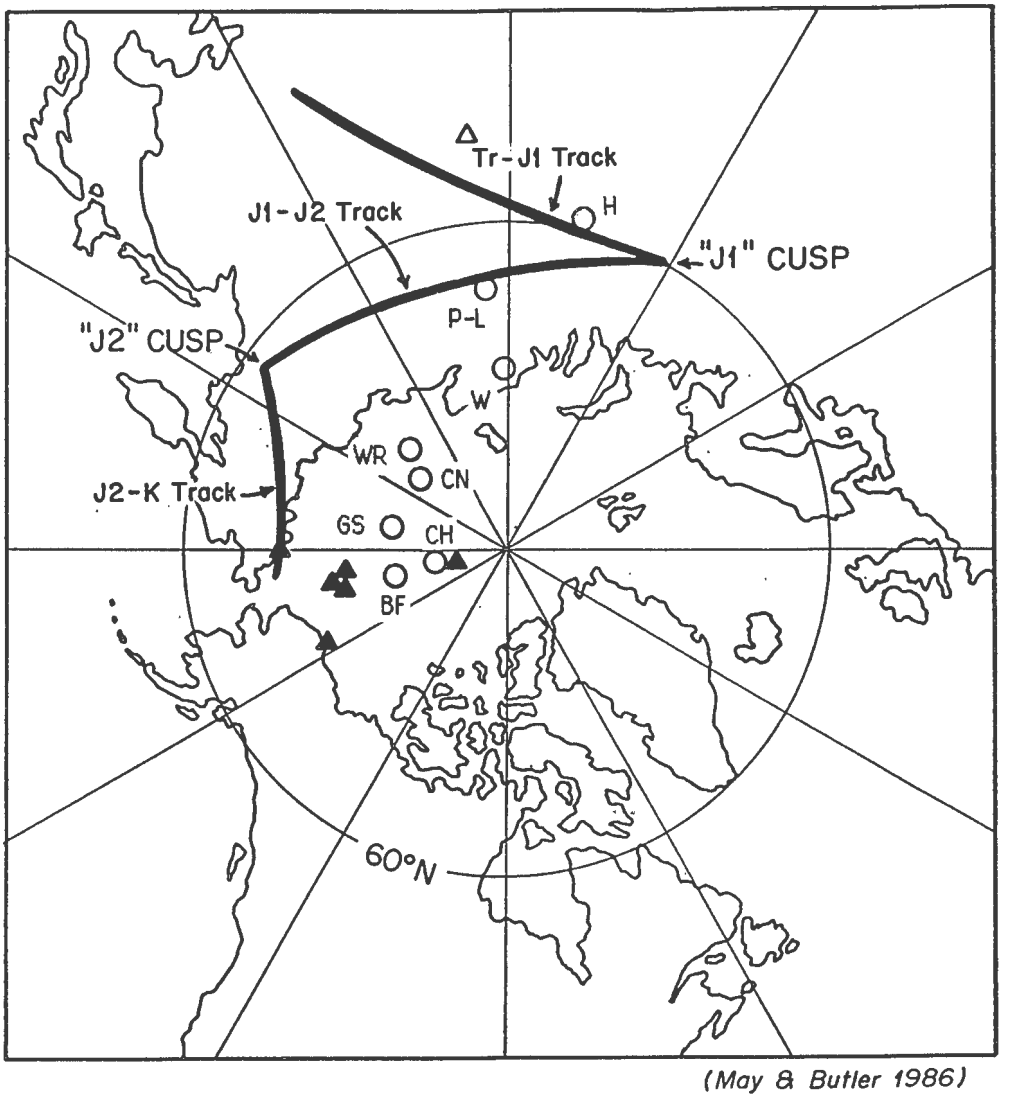

Figure 4.21 Mesozoic apparent polar wander path for North America, after May and Butler (1986). Paleopoles determined in this study shown by circles: H - Holden, P-L - Pelham-Loudville, W - Ware, WR - West Rutland, CN - Cape Neddick, GS - Gassetts, CH - Chapman Island, BF - Baffle Dam Island. Closed triangles indicate published Cretaceous paleopoles.

Table 4.4 Pole positions for northern and southern Appalachian Mesozoic igneous rocks.

	Lat.°N	Long°E	Source
Northern Appalachians			
Anticosti diabase dike, Anticosti Island, Quebec	75.7	84.7	Larochelle (1971)
Avalon dikes and sills, Newfoundland	72.9	87.8	Hodych and Hayatsu (1980)
Shelburne Dike, Nova Scotia	69.0	98.0	Larochelle and Wanless (1966)
North mountain basalt, Nova Scotia	66.0	113.0	Carmichael and Palmer (1968)
Caraquet diabase, dike(C), New Brunswick	78.0	143.0	Sequin et al.(1981)
Caraquet diabase, dike (N)	74.0	133.0	" " "
Caraquet diabase, dike (T)	62.0	82.0	" " "
Granby and Holyoke Lavas, Massachusetts	55.0	88.0	Irving and Banks (1961)
Diabase dikes and sills, Connecticut and Maryland	68.6	100.9	Smith(1976b)
Connecticut diabases Group 1	63.0	83.2	Smith and Noltimier(1979)
Connecticut diabases Group 2	65.3	103.2	" " "
Connecticut Valley dikes and sills	64.2	86.4	de Boer (1968)
Diabases and basalt flows New Jersey	63.6	98.5	Opdyke(1961)*
Watchung Basalts, New Jersey	63.0	90.1	McIntosh et al. (1985)
Palisades Sill, New Jersey	74.4	97.5	Rigotti and Schmidt(1976)
Holden diabase system, Massachusetts	59.7	77.9	This study
Pelham-Loudville diabase system, Massachusetts	65.2	95.0	" "
Ware diabase system, Mass.	73.3	90.8	" "
Bliss Hill south diabase (BH)	-4.2	359.4	" "
Bliss Hill north diabase(4I4)	83.9	63.2	" "
Quabbin Reservoir diabases (Chapman I. and Baffle Dam)	-81.7	25.2	" "
Southern Appalachians			
Gettysburg intrusive	76.9	161.2	Beck (1972)
Diabase dikes, Georgia and North Carolina	65.1	82.3	Watts(1975)
Haile-Brewer diabase dikes, South Carolina	64.5	75.7	Bell et al.(1980)**
Diabase dikes, South Carolina	67.9	95.3	Dooley and Smith (1982)**
Northwest diabase dikes, North Carolina	52.8	60.2	Smith(1987)
North-south diabase dikes, North Carolina	71.5	53.5	Smith(1987)

* Smith (1987) recalculated for the lavas and intrusives
**Smith (1987) recalculated for pole positions

with inappropriately low levels of demagnetization. Figure 4.22 is a histogram of the peak demagnetization levels from this study. As noted earlier the average is significantly higher than the levels used in most of the earlier studies.

Polar Wander Paths

The paleopoles from this study are compared to recently published paleopoles for North America in the Mesozoic and to a presently accepted APWP for North America in the Mesozoic. The present study has produced pole positions that are in some disagreement with the apparent polar wander path for North America in the Jurassic and Cretaceous. Plotted on Figure 4.21 is an apparent polar wander path for North America for part of the Mesozoic, after May and Butler (1984). Also plotted are paleopoles from this study and other recent published paleopoles. Smith (1987) has recently completed a study of the diabase dikes in the North Carolina piedmont region and has interpreted these as being emplaced during two different stress regimes in the early Mesozoic rifting of the North Atlantic margin. The two groups yield significantly different VGP'S of 52.8^{0}N, 60.2^{0}E and 71.5^{0}N, 53.5^{0}E. These pole positions fall east of the Jurassic track near the J1 cusp but removed south and north from it respectively. Van Fossen and Kent (1988) have produced a paleopole (74^{0}N, 189^{0}E) for the 120 m.y. intrusions in the White Mountain Magma series that is displaced north and east of the J2-K track. Lapointe (1979) worked on the 130 m.y. old lamprophyre dikes in Newfoundland which yield a north- and east-displaced paleopole (71^{0}N, 207^{0}E) (as cited by Globerman and Irving 1988). The 136 m.y. old peridotite dikes in New York have a paleopole of 85^{0}N, 207^{0}E (DeJournett and Schmidt,1975).

The pole positions determined for the Cretaceous intrusions in Massachusetts are displaced farther north in latitude than the presently accepted pole position for North America at this time. The pole positions from this study are plotted in Figure 4.21. These indicate a smoother and more northerly apparent polar wander path for North America from the Jurassic into the Early Cretaceous than presently accepted. Previous studies of the apparent polar wander path for North America by Irving and Irving (1982), Gordon et al. (1984) and May and Butler (1986) all indicate the critical need for additional paleomagnetic data for the Cretaceous. Gordon et al. (1984) concluded that the "number and quality of Cretaceous poles are inadequate to detect systematic motion along this track during the Cretaceous". The new data from the Massachusetts diabase intrusions indicate a more northerly latitude for the North America plate at 120 m.y. than previously thought and point to the critical need of additional paleomagnetic research from this period in areas such as New England that have been tectonically inactive after the Mesozoic. These results indicate that the apparent polar wander path for North America in the Jurassic needs to be reevaluated.

Rock Magnetic Properties

IRM Acquisition Study

Methods. An isothermal remanent magnetization (IRM) acquisition study of the Cape Neddick Gabbro and the Baffle Dam Island sites was run in the Phase Equilibria Laboratory at the University of Massachusetts. An IRM is a laboratory- induced magnetization that is very effective for distinguishing between the presence of Ti-poor titanomagnetites and Ti-poor ilmenohematites. This is due to the magnetic moment saturation of magnetite (by weight) which is two orders of magnitude greater than that of hematite (Tarling,1983).

The samples were first subjected to an alternating field of 80 mT on an AC Geophysical Specimen Demagnetizer. Demagnetized samples were subjected to an increasingly higher direct magnetic field in 17 incremental steps of 0.025, 0.05, 0.01, 0.02, 0.04, 0.06, 0.08, 0.1, 0.125, 0.2, 0.25, 0.3, 0.4, 0.6 and 0.8 Tesla using a Cahn

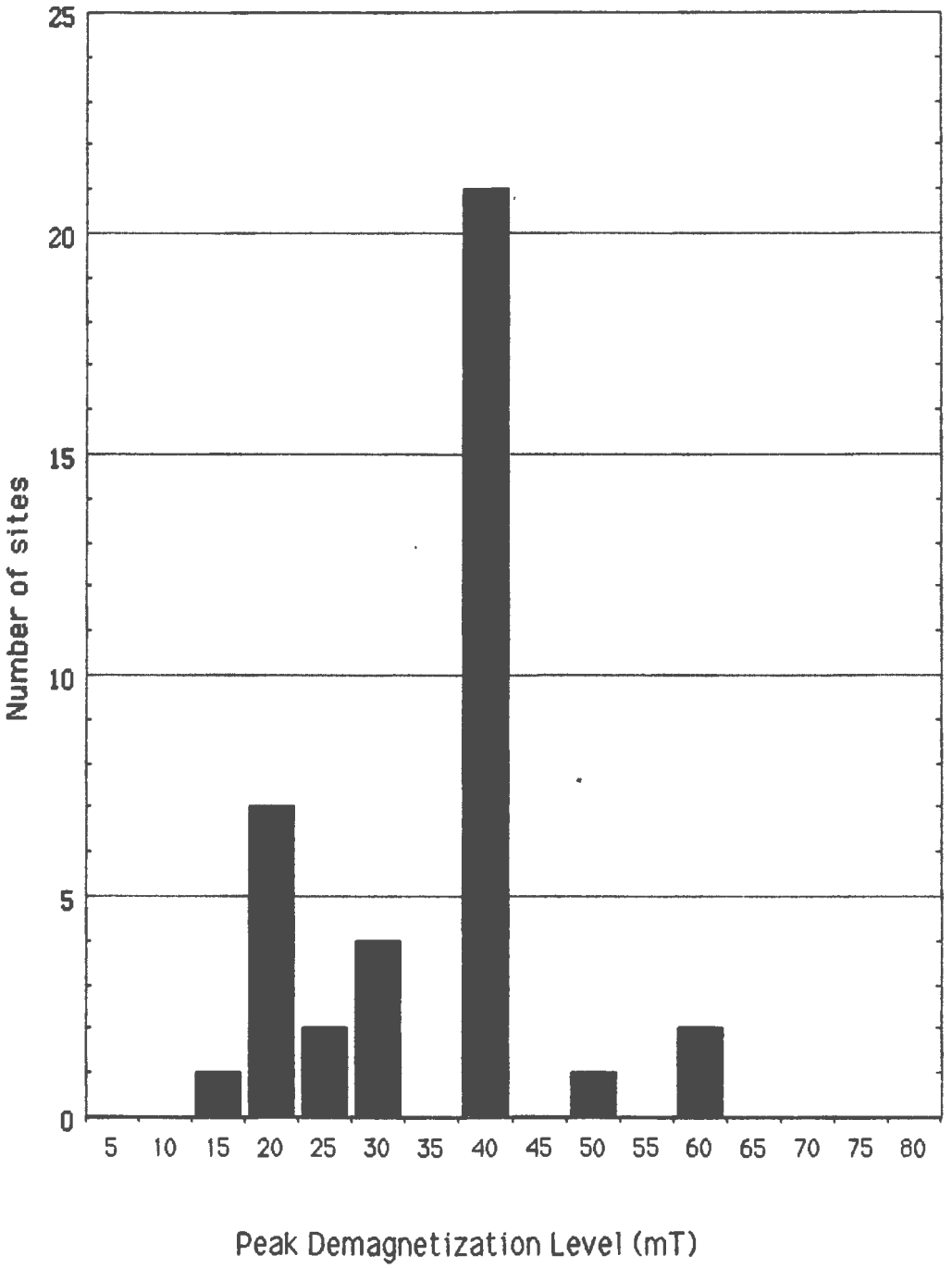

Figure 4.22 Histogram of peak alternating field demagnetization levels from the central Massachusetts diabases.

electromagnet. The intensity of the sample was measured on a Molspin fluxgate magnetometer after each step.

Results. The specimens from the Cape Neddick Gabbro and Baffle Dam Island are both saturated by 0.1 Tesla (Figures 4.23, 4.24). This indicates that magnetite is the dominant magnetic carrier in these sites. There is a break and a flattening of the curve for Baffle Dam Island at low fields. This may be due to incomplete cleaning by alternating-field demagnetization prior to the IRM acquisition. Because a field can be induced above the 80 mT level by AF demagnetizing, samples were not demagnetized above this level. The overall shape of the curves clearly indicate that magnetite is the dominant magnetic carrier.

Curie Temperature

Methods. A Curie temperature was determined for a sample from Baffle Dam Island . A gram of powder prepared for the XRF analysis was magnetically separated using a hand magnet. The magnetic residue was wrapped in a piece of platinum foil and placed in the sample holder of the Curie balance. The atmosphere was evacuated and replaced by argon. The sample was then subjected to a large magnetic field and heated in incremental steps. The sample was heated to 600^0C at a rate of approximately 500^0C per hour. A direct chart recording was made of the changes in apparent mass of the sample at incremental heating steps.

Results. The Curie temperature is determined by the inflection point on the heating curve. This temperature is approximately 280^0C (Figure 4.25). The Curie temperature is a function of the composition of the magnetite. This temperature is significantly lower than that of a pure Fe magnetite. A sample from Chapman Island, was studied using an electron-back-scatter image on the microprobe at RPI. The magnetites were found to be magnesium-rich. Petrographically the magnetites at Baffle Dam Island and Chapman Island are identical. They are a cool tan color with no visible exsolution at 90 power under oil immersion, and some contain blue cores of chromium spinel. These samples show little alteration and they decay in an orderly manner under both AF and thermal demagnetization.

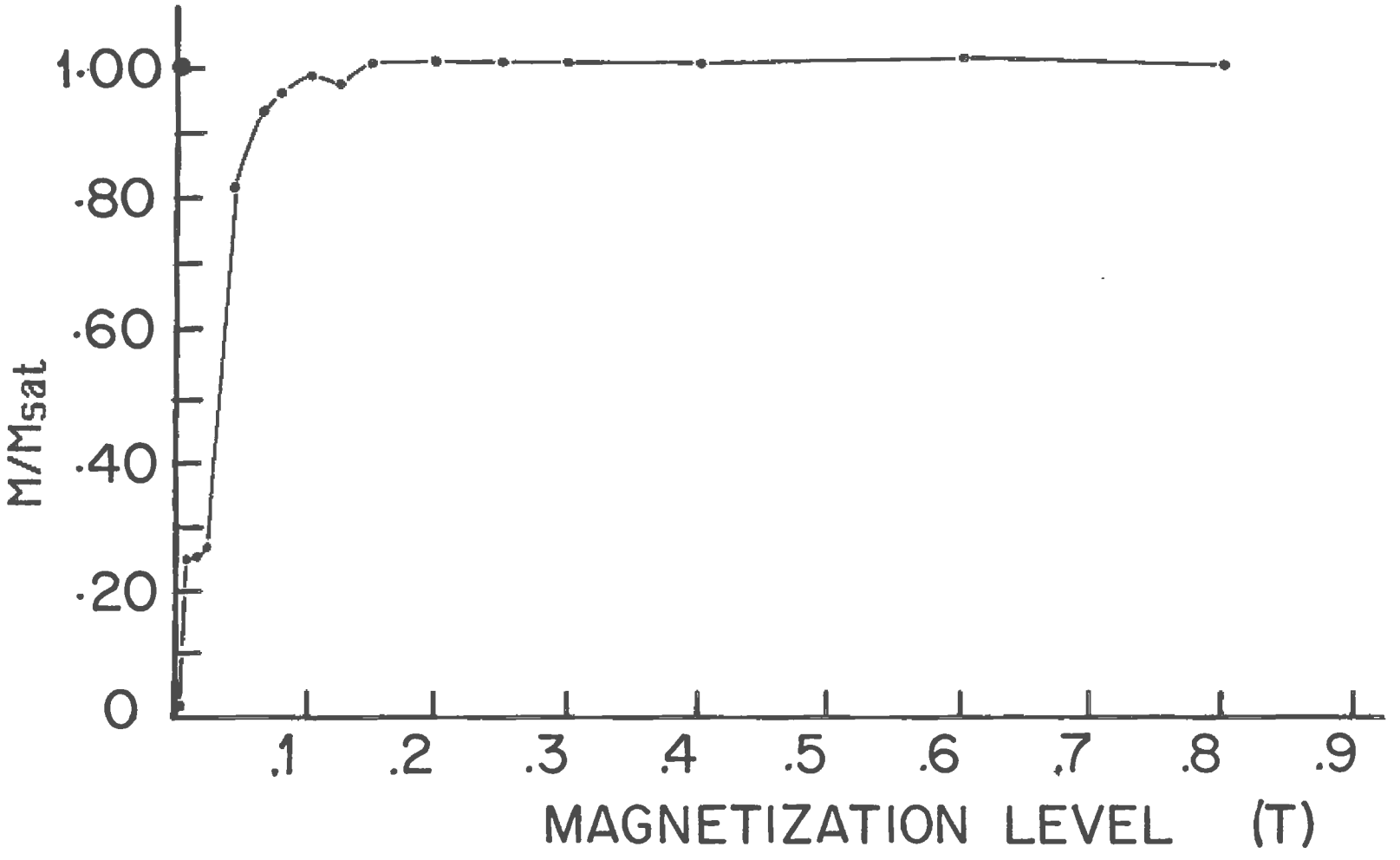

Figure 4.23 IRM saturation study of samples from Baffle Dam Island.

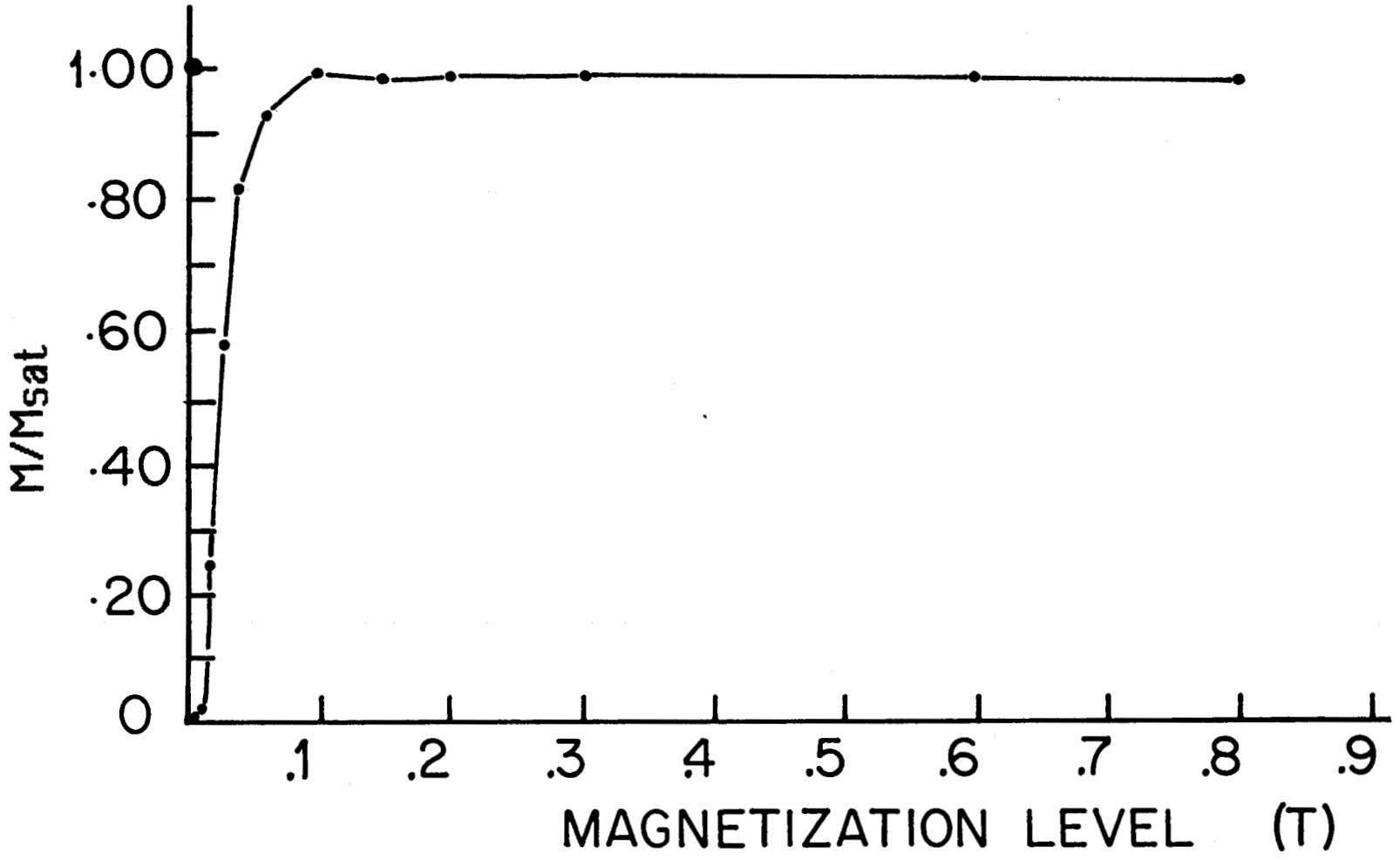

Figure 4.24 IRM saturation study of samples from Cape Neddick Gabbro, Maine.

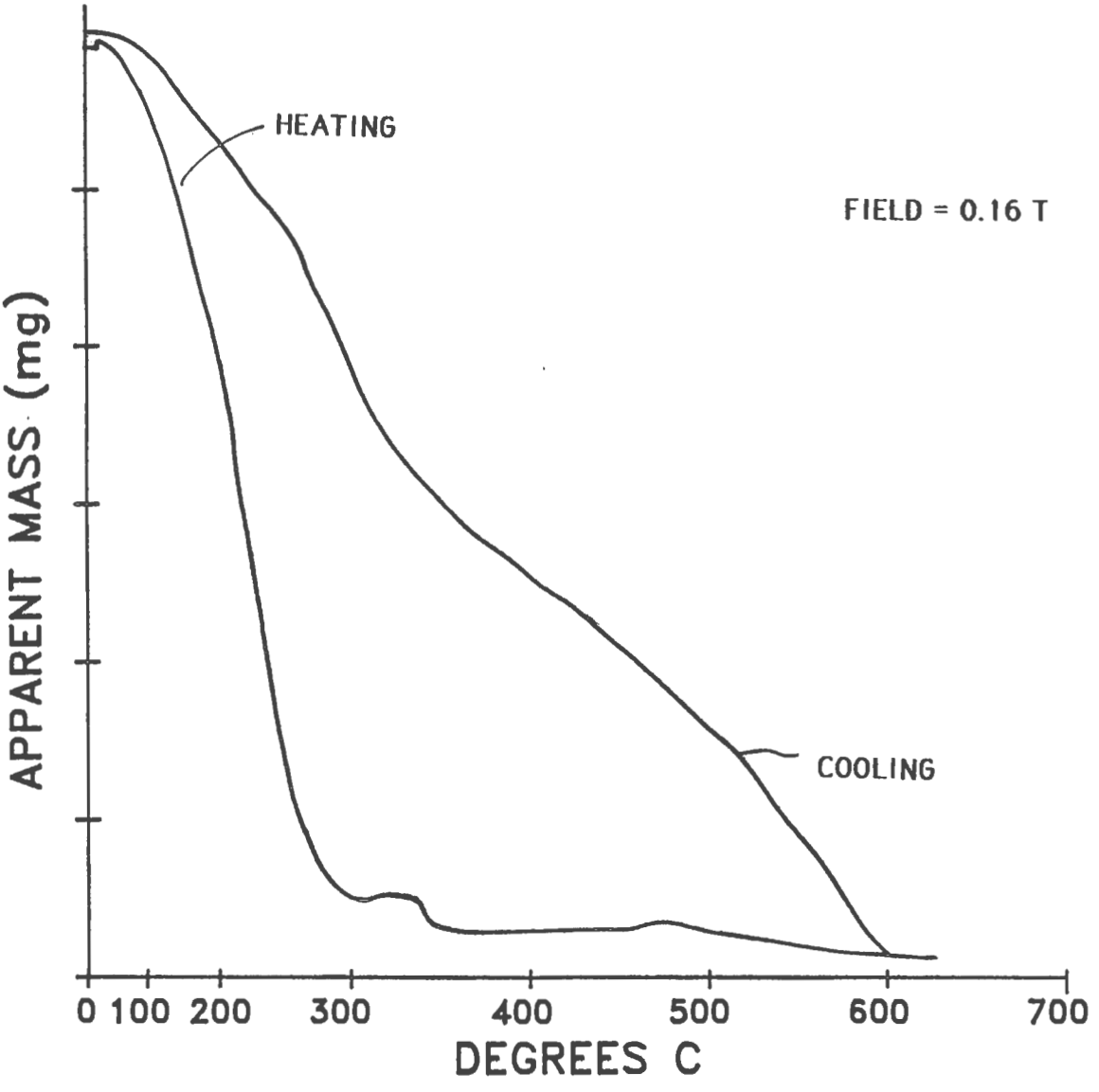

Figure 4.25 Curie determination curve of titanomagnetite from the Chapman Island diabase.

CHAPTER 5

K-Ar RADIOMETRIC AGES

Introduction

A crucial factor in any study of apparent polar wander paths is a program of absolute age determinations on the rocks being studied paleomagnetically. Because the pole positions from the present study are displaced from the currently used apparent polar wander paths for North America, it is important to obtain accurate geochronological data. Cooperation of Prof. Kenneth A. Foland of Ohio State University was enlisted in this study. Professor Foland has a long experience of geochemical and isotopic studies on igneous rocks of northeastern North America, and particularly the Jurassic White Mountain Magma series and the Cretaceous New England-Quebec igneous province (Foland and Faul, 1977; Foland et al., 1986; 1988) Thirteen samples were carefully selected for primary analytical material. These were sawed into chips and then split in half. One half was sent to Ohio State University for K-Ar analyses; from the other half a thin section was made and the remainder prepared for XRF analyses.

It is fully recognized that the history of K-Ar age dating of Mesozoic dikes in eastern North America has been complex and the problems with obtaining accurate dates has been severe. Armstrong and Besancon (1970) attributed the difficulties of K-Ar measurements to argon loss, possibly due to inhomogeneity in the distribution of K-Ar in the material, or a low grade metamorphic event after emplacement. Other authors (Dooley and Wampler,1983; Seidemann et al., 1984; Sutter and Smith 1979; Sutter.1985) have attributed the problem to excess radiogenic argon. This excess argon in the samples has been attributed to igneous assimilation of material from local country rocks, to igneous assimilation from a deep-seated crust or mantle source, or to the introduction of hydrothermal solutions following emplacement. In most instances the carrier of the excess argon is not known, and might include igneous glass or devitrified glass, secondary minerals replacing the glass or crystallized minerals, or a later low temperature secondary mineral filling the vesicles.

Results

The K-Ar results from the Quabbin diabases and from the Vermont lamprophyres, which were studied paleomagnetically for comparison with the Cretaceous Massachusetts diabases, are listed in Table 5.1. The problem of excess argon was encountered very severely in dating the Quabbin Reservoir diabases, where whole-rock K-Ar ages in geochemically and mineralogically similar sills ranged from 190 m.y. to 119 m.y. (Figure 5.1). Two obvious possibilities in this case are a) that the finer-grained more glassy samples from Baffle Dam Island (6I7) have captured and retained more excess argon than the other more crystallized samples or b) that this thinner sill at Baffle Dam Island did not permit degassing before it chilled. The coarser-grained samples from Chapman Island produced consistent ages of 136 m.y. Given the regional excess argon problem, it is believed that the youngest age of 119 m.y., given by the freshest coarser-grained sample from south Baffle Dam, represents the maximum age. A preliminary $^{40}Ar/^{39}Ar$ release spectrum on the sample from Baffle Dam Island confirms excess argon, giving an age of 190 m.y. falling of toward 120 m.y. in the high temperature fractions. The paleomagnetic directions obtained from the Quabbin Reservoir samples (Chapman Island and Baffle Dam Island) are similar to the directions obtained from other well dated Cretaceous intrusions in southern New England (Foland and Faul,1977; Foland et al. 1988, Zen 1972; and Foland, pers. comm. 1988). The new paleomagnetic and radiometric data on the Quabbin Reservoir and Bliss Hill diabases provide the first evidence of Cretaceous igneous activity in Massachusetts. This extends the New England - Quebec Cretaceous igneous province

Table 5.1 Summary of whole-rock K-Ar results. K. A. Foland, analyst.

Sample	K (wt.%)	$^{40}Ar_{rad}$ (10^{-10}mol/g)	Age (Ma)
Quabbin Reservoir Diabases			
C26N-1	0.4728	1.197	
	0.4901	1.183	
	0.4934	1.199	
	Av. 0.485	Av. 1.193	136 ± 2
C26Q-2	0.4837	1.188	
	0.4829	1.175	
	0.4728	1.177	
	Av. 0.480	Av. 1.180	136 ± 2
6I7-3	0.4249	1.465	
	0.4313	1.453	
	0.4141	1.456	
	Av. 0.423	Av. 1.458	188 ± 3
6I7-4	0.4177	1.461	
	0.4270	1.461	
		1.472	
	Av. 0.422	Av. 1.465	190 ± 3
B44	0.3625	0.7584	
	0.3535	0.7727	
	0.3557	0.7563	
	0.3481		
	Av. 0.358	0.7625	119 ± 2
Vermont Lamprophyres			
Wr-1	1.701	4.077	
	1.701	4.081	
	1.694		
	Av. 1.699	Av. 4.079	133 ± 2
GS-2	1.600	2.845	
	1.610	2.895	
	1.603		
	Av. 1.604	Av. 2.870	100 ± 2
BRM-3	1.482	3.735	
	1.468	3.717	
	1.468		
	Av. 1.472	Av. 3.726	140 ± 2

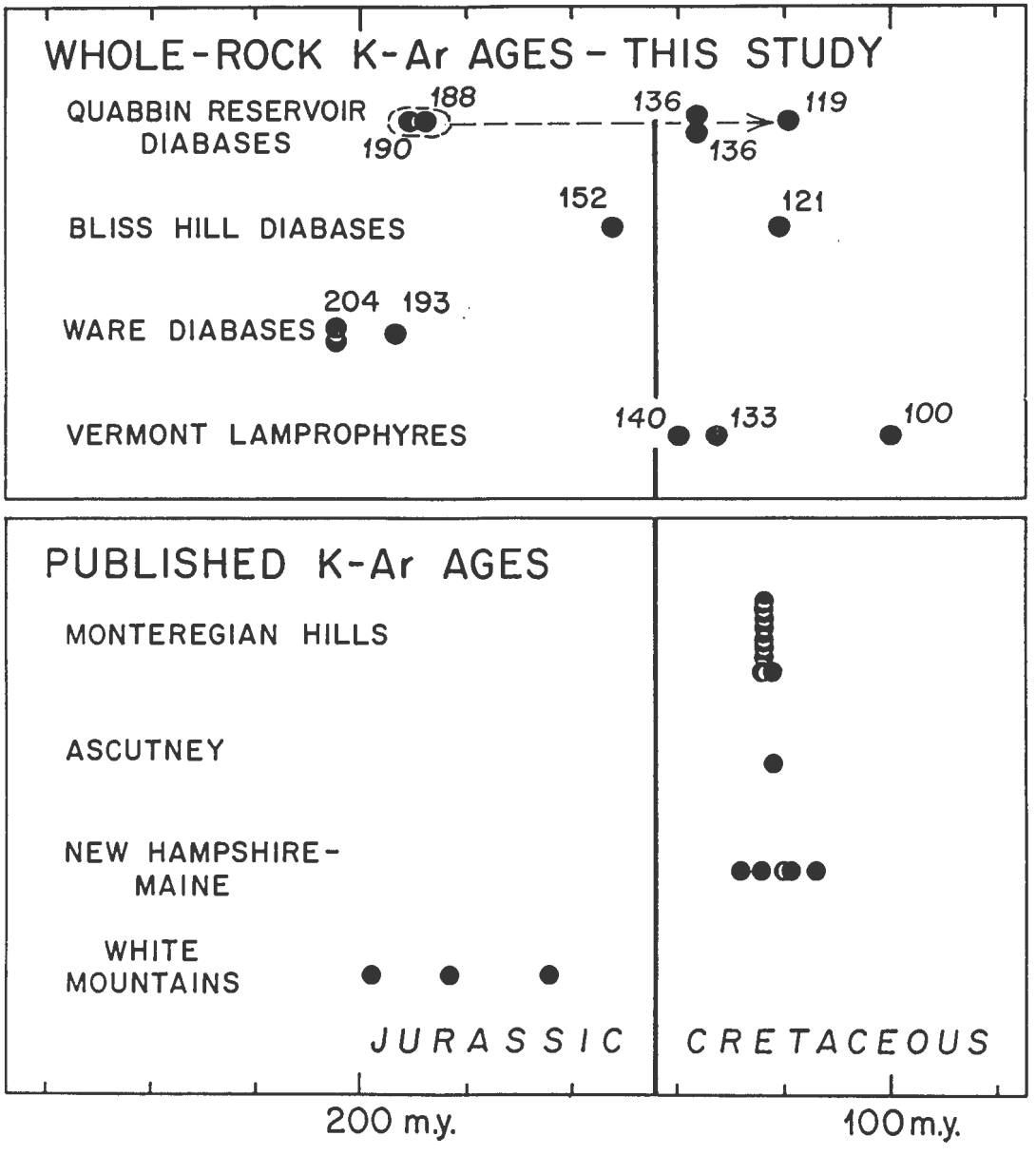

Figure 5.1 Diagram showing the K-Ar ages from this study and others recently published by Foland et al. (1987) for New England and adjacent Quebec. Dashed lines and arrow for Quabbin Reservoir diabases shows results of stepwise Ar release study of one of the samples, indicating excess argon giving an age of about 190 m.y. falling off toward 120 m.y. in the high temperature fractions.

south into Massachusetts (Figure 5.2). These diabases are the first tholeiites reported from the New England - Quebec Cretaceous igneous province.

The K-Ar results on the two samples from the Ware system do not agree with a Middle Jurassic age as indicated by the paleomagnetism. It is hoped that some of these samples will be studied by the $^{40}Ar/^{39}Ar$ release method. Sutter (1979) did have success in dating the Buttress dike from the Ware system in Connecticut by the $^{40}Ar/^{39}Ar$ method, and determined an age of 176 ± 3.8 m.y. Previous dates on the Buttress dike by Armstrong and Besancon (1970) using the K-Ar whole-rock method gave ages of 194-223 m.y.

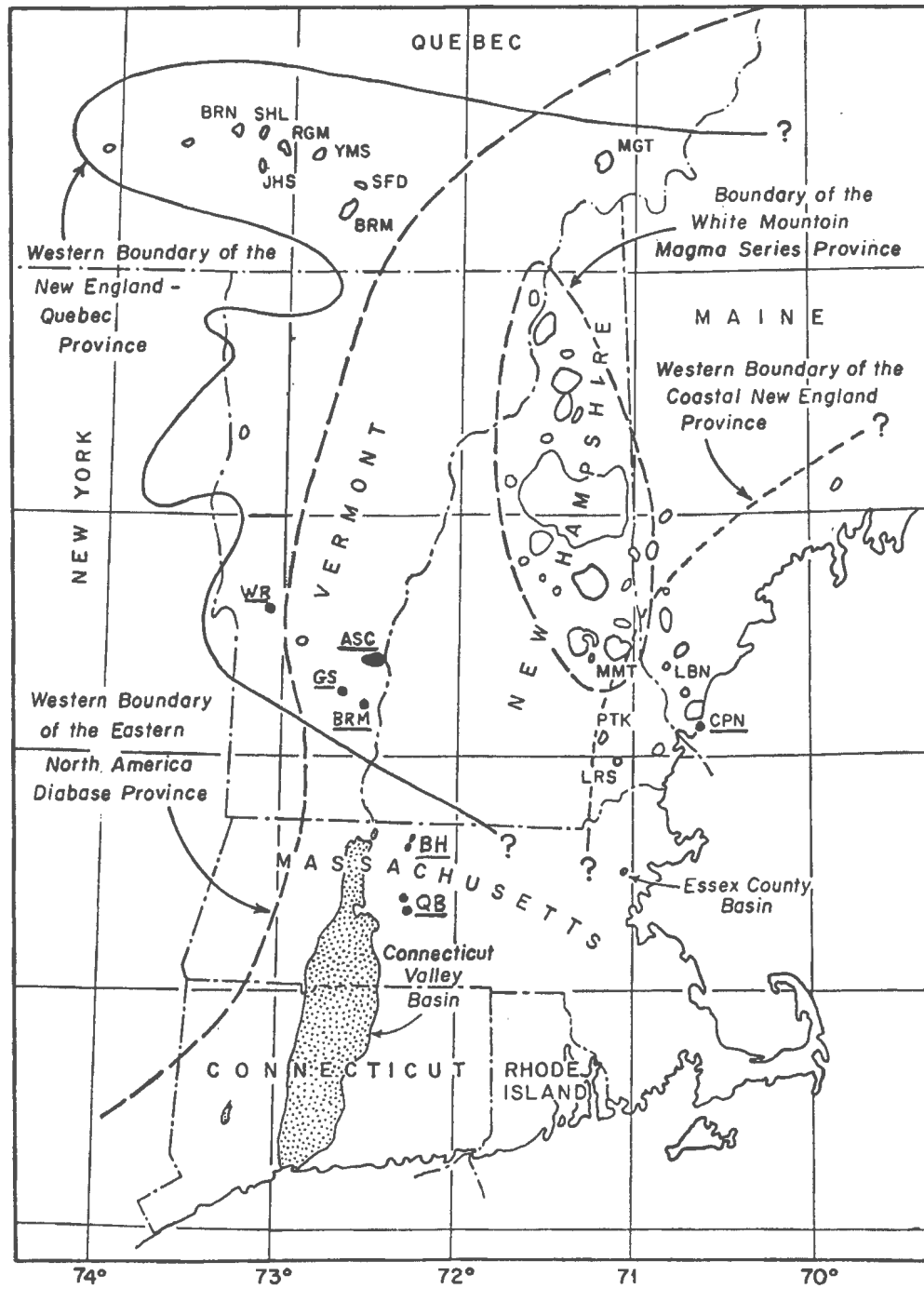

Figure 5.2 Mesozoic igneous provinces in New England, modified from McHone and Butler (1984). Shows the location of the Quabbin Reservoir (QB) and Bliss Hill (BH) Cretaceous sites , and also four Cretaceous sites mentioned in the present study, three Vermont lamprophyres at Brockways Mills (BRM), Gassetts (GS), and West Rutland (WR), and the gabbro at Cape Neddick, Maine (CPN).

CHAPTER 6

COMMENTS ON DIABASE PETROGENESIS

Although an investigation of the petrogenesis of the central Massachusetts diabases was not a primary objective of this study, the availability of major- and trace-element analyses, as well as detailed petrography, makes it possible to give some preliminary observations and comments on this topic. These comments are in two areas: on the use of major and trace elements as discriminants in helping to identify the tectonic settings of the diabases; and on patterns in the major-element concentrations in the various diabases in relation to their petrography and the bearing this may have on magma evolution.

Geochemical Discriminant Diagrams for Tectonic Settings

Discriminant diagrams for the assignment of tectonic settings of basaltic rocks have been widely used since Pearce and Cann (1971, 1973) developed a series of diagrams based on Sr, Ti, Zr, Y, and Nb. Most of the eastern North American (ENA) diabases plot outside of the continental basalt fields on many of these diagrams.

Pearce and Cann (1973) use Ti, Zr and Y as discriminators for tectonic fields of; ocean floor basalts and low-K tholeiites, calc alkaline basalts, and within-plate basalts. J. A. Philpotts (1985) plotted the data of Wiegand and Ragland (1970), Smith et al. (1975), Puffer et al. (1981) and his own unpublished data for ENA. These data plot in two of the established fields: the field of ocean floor basalts and low-K tholeiites , and the field of calc-alkaline basalt, but there is also a group that plots outside the boundaries of the four fields. The central Massachusetts diabases plot in three areas (Figure 6.1). The Holden diabases plot at a triple junction, where the fields of ocean floor basalts and low-K tholeiites, of calc-alkaline basalt and of with-in plate basalts come together. The Pelham-Loudville and Ware diabases are very well clustered and plot in the field of ocean floor basalts and low-K tholeiites with no overlap to any other field. The Quabbin Reservoir and Bliss Hill diabases are distinct for the ENA diabases because these plot in the with-in plate field.

Shervais (1982) uses the elements Ti and V as tectonic discriminants. Ti, Zr, P, Hf, Ta, and Nb are high field strength cations that are strongly incompatible and immobile during low-temperature alteration. The transition elements that are considered immobile during alteration and metamorphism are Ni, Co, Sc, Ti, V, and Cr, but only Ti and V are incompatible elements. The incompatible elements are partitioned into the liquid during melting, whereas the compatible elements are partitioned into the refractory residual phases in partial melting and into early liquidus mafic phases during crystallization. Shervais choose Ti and V as useful discriminators because these elements are neither compatible nor subject to alteration. This plot is based on the variation in the crystal-liquid partition coefficient for vanadium which is believed to be a function of oxygen fugacity. The partition coefficients range from greater than 1 to much less than 1 with increasing oxygen fugacity. Since the partition coefficients of Ti are much less than 1, the depletion of the vanadium relative to titanium is a function of the oxygen fugacity of the magma and its source, the degree of partial melting, and subsequent fractional crystallization (Shervais,1982). Shervais compiled 482 analyses of basalts from different geotectonic settings and determined that the trends of related samples can be clearly distinguished. Tholeiites and alkali basalts plot in distinct fields of Ti/V with minimum overlap separated by a Ti/V ratio of 50. Mid-ocean-ridge basalts and continental basalts have Ti/V ratios from 20 to 50 though continental basalts have greater absolute abundances. Alkaline basalts have ratios greater than 50.

All of the central Massachusetts diabases sampled plot within the Ti/V ratios of 18-50 (Figure 6.2). The Holden diabases (12 samples) plot on two trends with Ti/V ratios of 23 and 27. These plot in both the Jurassic Atlantic field, defined by 13 samples, and in the

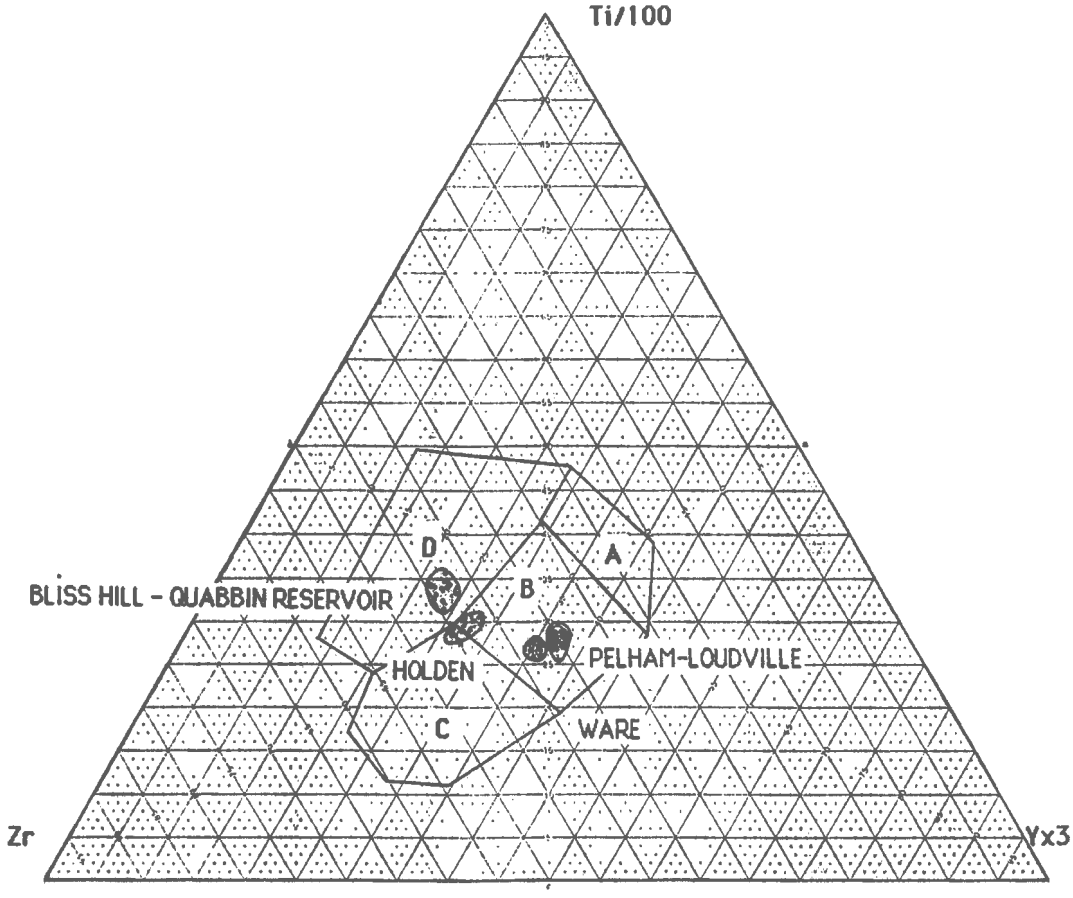

Figure 6.1 Ti-Zr-Y discriminant diagram, after Pearce and Cann (1973) with plot areas of Massachusetts diabase systems and groups shown. Basalt fields are as follows: A+B - low K tholeiites; B - ocean-floor basalts; B+C - calc-alkali basalts; D - continent and ocean island within-plate basalts.

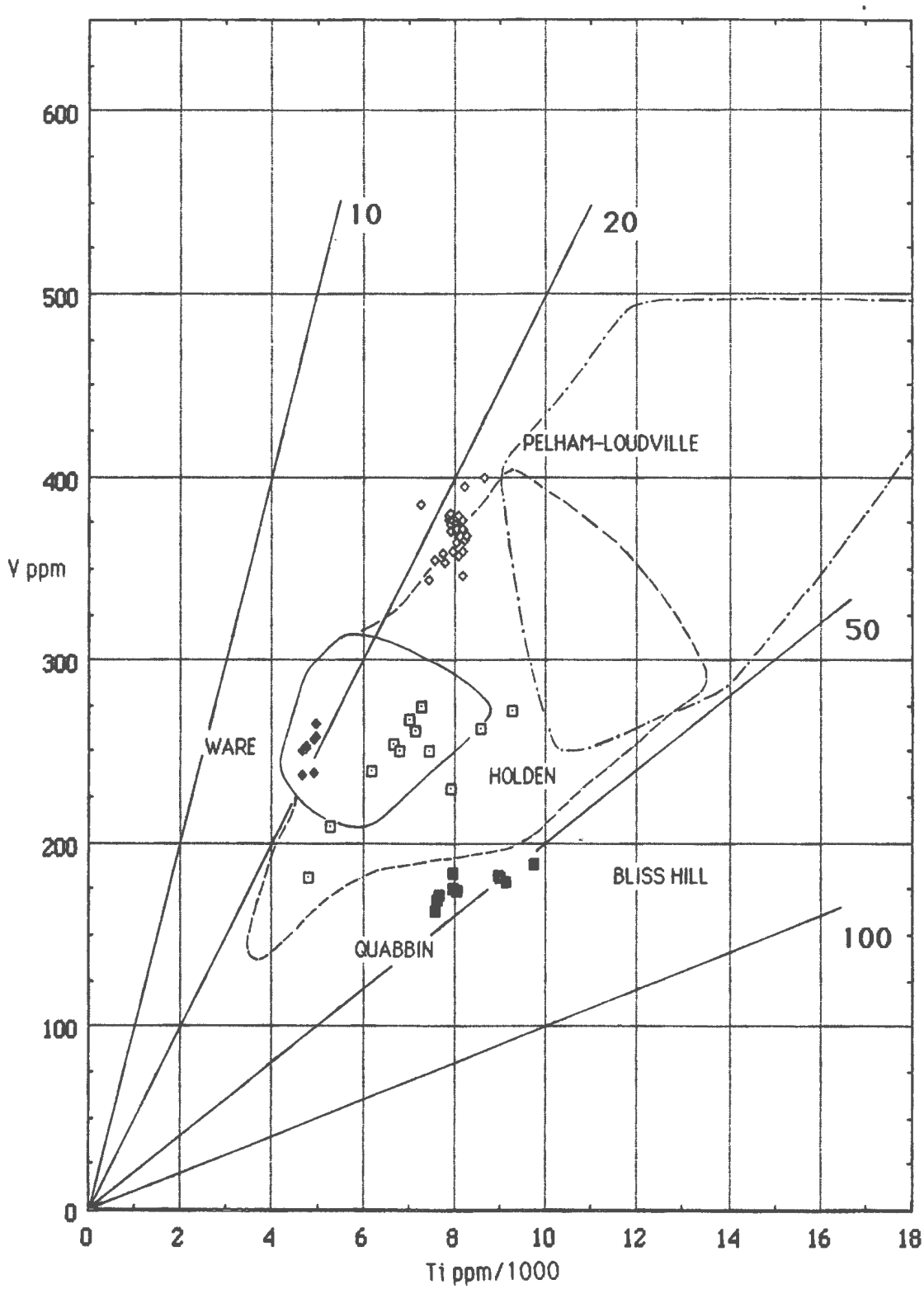

Figure 6.2 Discriminant diagram of Tippm/1000 versus V ppm, after Shervais (1985). All diabase analyses from this study are plotted. Symbols: Holden - open squares; Pelham-Loudville - open diamonds; Ware - closed diamonds; Bliss Hill Quabbin Reservoir diabases - closed squares. Solid line outlines area of Jurassic Atlantic basalts; dashed line, Atlantic basalts; dash-dot line, Columbia River flood basalts.

Atlantic ocean field, defined by 61 samples, respectively. There is no overlap with the Columbia River Basalt field which defines the continental flood basalt field (22 samples). The Pelham-Loudville diabases (23 samples) with one exception plot in the range of continental and mid-ocean-ridge basalts, with an average ratio Ti/V ratio of 23. These plot near or in the Atlantic ocean field and do not overlap into the Columbia River Basalt fields. The Ware system diabases (8 samples), with an average Ti/V ratio of 19, plot well within the field defined by the Jurassic Atlantic samples. More than half of the samples that define the Jurassic Atlantic have a Ti/V ratio of 20 or less. A field with Ti/V < 20 is characteristic of modern island arcs and calc-alkaline volcanics. The Bliss Hill diabases (4 samples) plot on the boundary of the tholeiite and alkali basalts (Ti/V > 50) field, and outside of the field boundary of MORB. The Quabbin Reservoir diabases (12 samples) plot in the tholeiite field (Ti/V=45), and outside any other field. The Holden, Pelham-Loudville and Ware diabases have an affinity with Atlantic ocean samples and do not overlap the fields for the Columbia River Flood basalts. Except for the Pelham-Loudville system, relative abundances of Ti and V are not higher than the MORB'S (135 samples) used by Shervais, as would be expected for continental basalts based on this discriminant diagram. The Bliss Hill and Quabbin Reservoir diabases are distinct and all fall outside the fields defined by MORB and continental Basalts.

J. A. Philpotts (1985) modified a log-log Ti ppm versus Cr ppm discriminant plot of Pearce (1975). Philpotts suggests that this is the best discriminant diagram for interpretation of eastern North America diabases. In Figure 6.3 the Holden dike system plots generally in the high-titanium field with some spread into other fields. The Pelham-Loudville system plots in the high-iron field. The Ware system is in the low-titanium field. The Bliss Hill and Quabbin Reservoir diabases plot outside the discriminant fields on the high titanium side.

Pearce and Norry (1979) use the immobile trace elements Zr and Y as discriminants for tectonic settings for basaltic rocks. Figure 6.4 uses their plot of Zr/Y versus Zr with their fields of mid-ocean ridge basalts (MORB), island arcs basalts, and with-in plate basalts. Superimposed on this diagram is the field boundary (thick horizontal line) separating continental arcs basalts from oceanic arcs after Pearce (1983).

In Figure 6.4 the Pelham-Loudville samples all lie in the MORB field, and all but one sample lie below the continental arc-oceanic arc boundary line. The Ware samples lie partially in the island arc field, close to the MORB field and just above the continental arc-oceanic arc field boundary. The Holden samples plot near and on the field boundary of within-plate basalts and distinctly away from the the other Jurassic intrusions. The Bliss Hill and Quabbin Reservoir samples plot in the within-plate field. Like the Holden samples, these plot well above the continental arc - oceanic arc field boundary. This diagram suggests a more oceanic type magma for the Pelham-Loudville system and the Ware system. The homogeneity in the major- and trace-element analyses from these two systems also suggests a large or a well mixed source for these magmas. This diagram would suggest a within-plate type setting for the Holden system, and for the Bliss Hill and Quabbin Reservoir diabases.

Meschede (1986) uses the immobile trace elements Nb, Zr, and Y to discriminate between N-type MORBs, P-type MORBs, within-plate tholeiites, and within-plate alkali basalts. He chose Nb because it is a sensitive indicator of mantle enrichment or depletion processes, and Zr and Y because they show these trends differently from Nb. This discriminant diagram (Figure 6.5) is based on more than 1800 analyses from different geotectonic settings of basaltic rocks. The suggested application is limited to tholeiites and all types of within-plate basalts. Meschede reevaluated data from ancient rocks that were known to be within-plate basalts, but in previous diagrams had plotted in the MORB field. Using this diagram these plot as within-plate basalts. The success of this discriminant diagram for ancient within-plate basalts makes the use of it pertinent. The Massachusetts

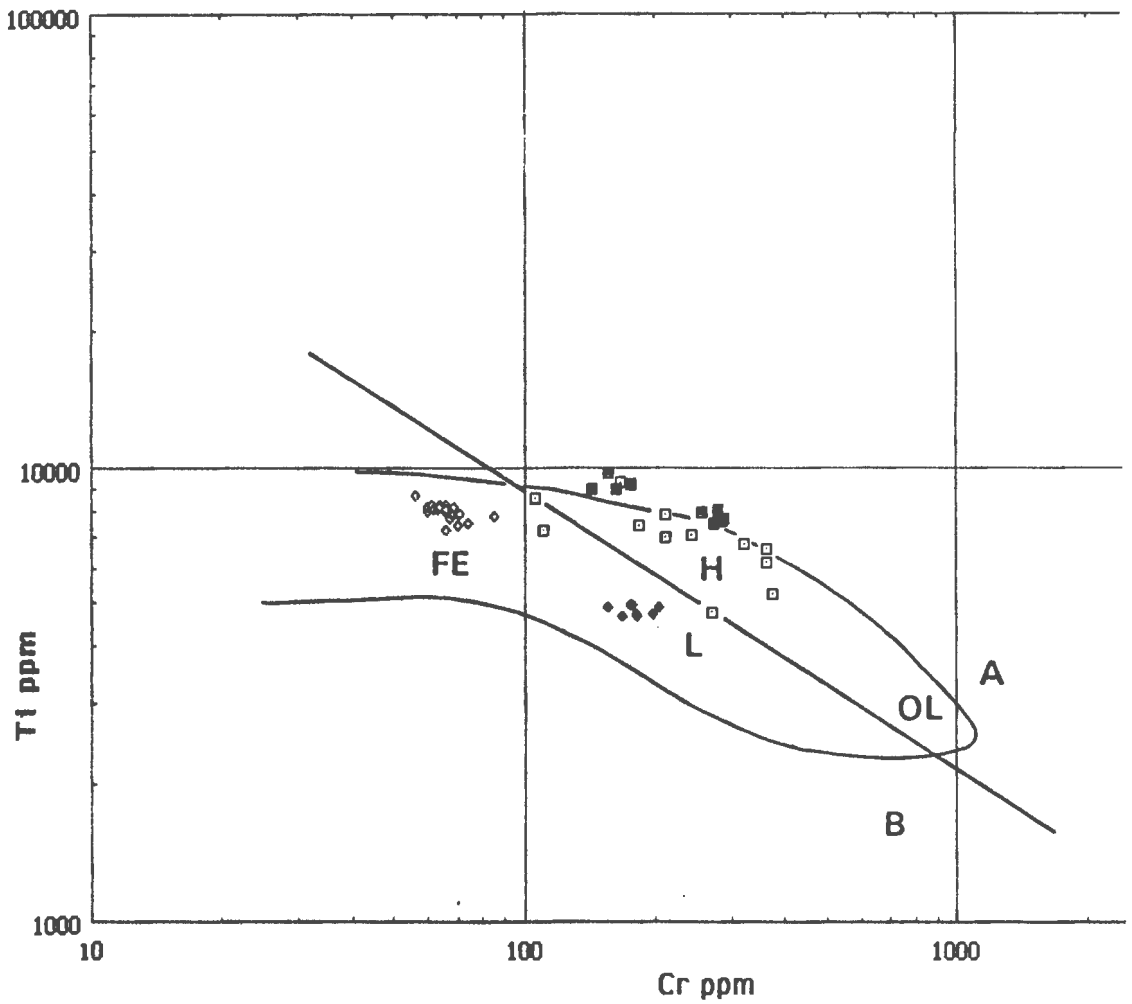

Figure 6.3 Log-log plot of Ti ppm versus Cr ppm. Fields for eastern North America diabases after J. A. Philpotts (1985). H, high-titanium diabase. L, low-titanium diabase. Ol, olivine-normative (or non-quartz-normative) diabase. Ocean-floor basalts plot in field A, island-arc tholeiites in field B. All diabase analyses from this study are plotted. Symbols: Holden - open squares; Pelham-Loudville - open diamonds; Ware - closed diamonds; Bliss Hill Quabbin Reservoir diabases - closed squares.

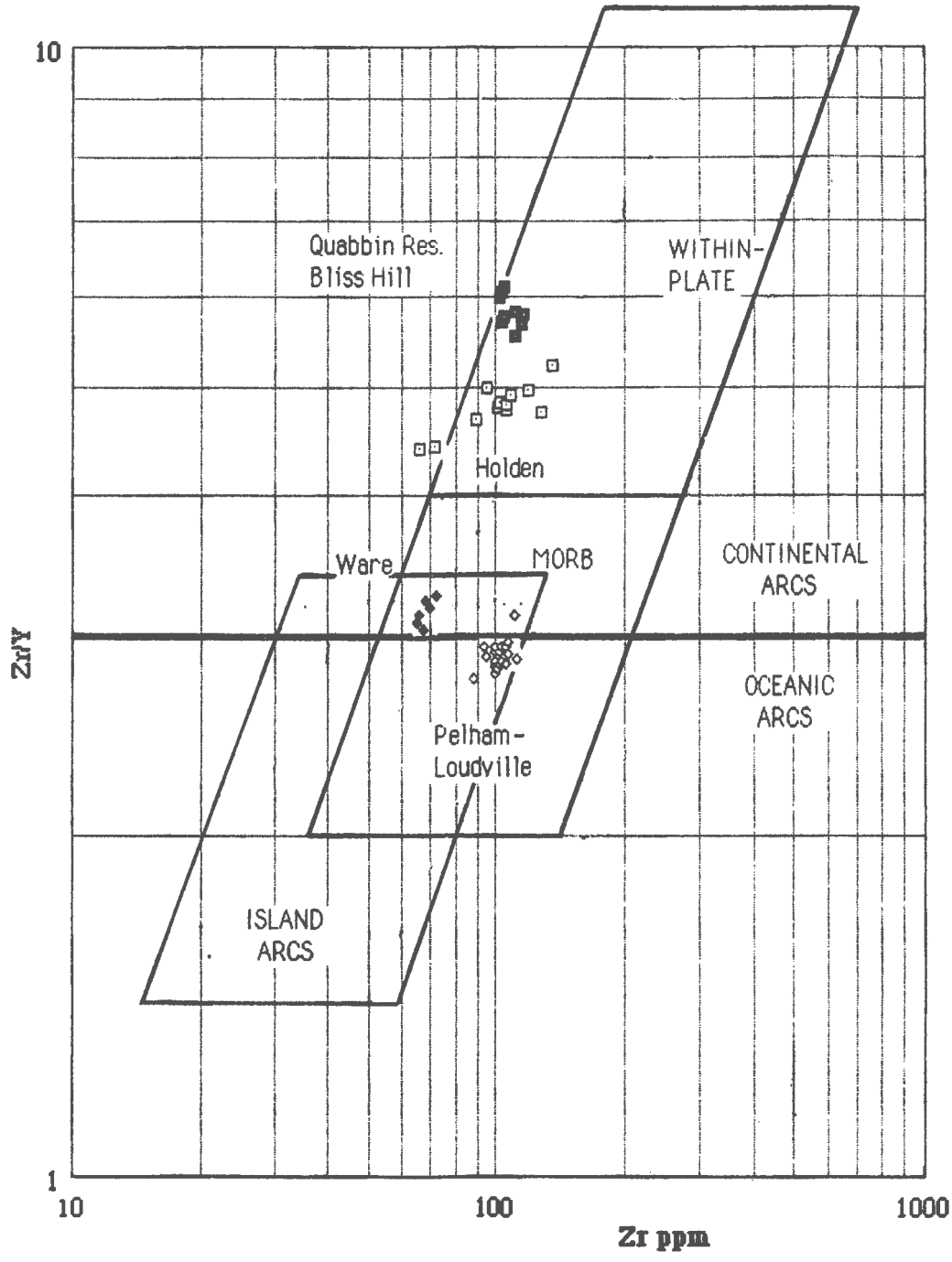

Figure 6.4 Discriminant diagram of Zr/Y versus Zr ppm after Pearce and Norry (1979) modified by Pearce (1983). Heavy horizontal line is the separation of continental arc basalts from oceanic arc basalts. All diabase analyses from this study are plotted. Symbols: Holden - open squares; Pelham-Loudville - open diamonds; Ware - closed diamonds; Bliss Hill Quabbin Reservoir diabases - closed squares.

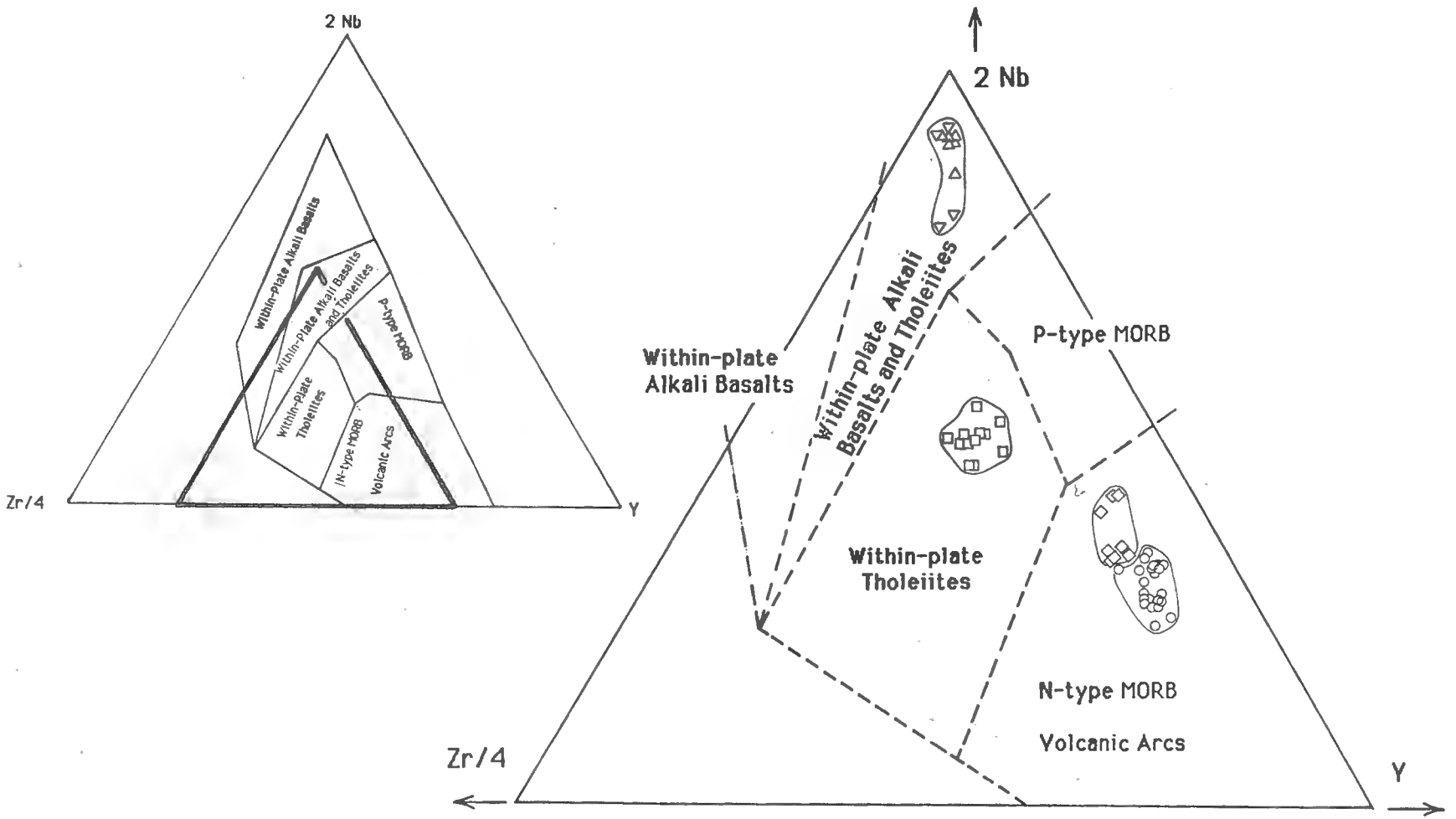

Figure 6.5 Discriminant diagram for the trace elements Nb, Zr, and Y (after Meschede, 1986) indicating tectonic settings for tholeiites and all types of within-plate basalts. All diabase analyses are plotted within the area of the enlarged inset. Symbols: Holden - squares; Pelham-Loudville - circles; Ware - diamonds; Quabbin Reservoir diabases - triangles; and Bliss Hill diabases inverted triangles.

Mesozoic diabases plot in three fields, and are discussed in order of relative age based on the paleomagnetic data. The oldest, the Holden dikes, all plot in the field of within-plate tholeiites. The Pelham-Loudville intrusions fall in the field of N-type MORB as do the Ware diabases. The youngest, the Bliss Hill and Quabbin Reservoir Cretaceous diabases plot in the field of within-plate alkali basalts and tholeiites.

The question arises whether the discriminant diagram of Figure 6.5 fails, or succeeds. Obviously the Pelham-Loudville and Ware diabases were intruded into continental crust even though they have some trace-element characteristics of N-type MORB. Based on thermal modelling of the structural evolution of the Newark basin, Steckler and Karner (1988) suggest that the source of the Jurassic basalts in the Newark basin may not have been beneath the basin, and that the magmas possibly migrated from a region of greater crustal extension offshore, where the birth of the modern Atlantic was about to take place. The oldest Jurassic diabases of the Holden system, and the Cretaceous groups plot well inside the within-plate fields. These differences may well reflect the significant changes in the thermal-tectonic regime over the extended period from earliest Jurassic through the early Cretaceous. In this connection J. A. Philpotts (1985) states that perhaps the best current interpretation for the eastern North American diabases calls for a number of mantle source regions, perhaps subduction-related as proposed by Pegram (1983) to account for his Nd, Sr, and Pb isotopic data. The low Nb contents of the Jurassic diabases from the present study also imply a mantle source that has been involved in subduction-related magmatic processes. Similar unusual isotopic data were also recently reported by Lambert et al. (1988) for Mesozoic volcanic suites in the Canadian segment of the eastern North American margin. Philpotts suggests that the conflicting results of the discriminant diagrams, including the Ti/Cr diagram of Figure 6.3, may indicate a relatively unusual and little sampled thermal-tectonic regime during the generation of some of the Mesozoic diabases.

Based on these discriminant diagrams and the relative age constraints from the paleomagnetic pole positions, a possible scenario for the emplacement of the central Massachusetts diabases could be as follows:

1. Emplacement of the Holden dike system into a thick continental crust, as characterized by the with-in plate chemical signature, prior to the opening of the Atlantic (pre-J1 cusp).

2. Thinning of the continental crust, and development of a large offshore magma source in the location of the newly forming Atlantic spreading center. The emplacement of the Pelham-Loudville system (post-J1 cusp), possibly by migration from this large magma source. This would account for the striking homogeneity in the chemistry and the oceanic affinities in discriminant diagrams of this system. The migration of magma along fractures from offshore in the Early Jurassic (post-J1 cusp) is supported by thermal and gravity modelling of the Newark basin (Steckler and Karner 1988, Bell et al. 1989).

3. Change from a rifting to a drifting environment is thought to have occurred around 175 m.y. (Klitgord and Schouten, 1986). The Ware system diabases may be related to this tectonic event. The chemistry of the Ware samples has oceanic affinities and there is a strikingly similarity to the Early Jurassic Atlantic samples in Ti and V contents. The pole position for the Ware system would indicate a younger age than the Holden or Pelham-Loudville systems. The possibility of an unusual magnetic signature due to secular variation must be considered, however, because the K-Ar ages are inconclusive. This could lead to an older age assignment for the Ware system than 175 m.y.

4. By 120 m.y. the thermal regime had changed. There was a well established spreading center at the mid-Atlantic ridge far offshore. There was a return to with-in plate igneous activity. The Bliss Hill and Quabbin Reservoir diabases are tholeiites, but are far more enriched in Ni, Cr, Sr, Ba, Zr, and Nb than the Jurassic diabases. The stress orientations at this time were possibly related to the separation of Newfoundland and Great Britain, but

the igneous activity in Massachusetts may be related to a hot spot, as is postulated for the Cretaceous intrusions in the White Mountains (Foland pers. comm. 1988).

Major Element Concentrations in Relation to Petrography and Magma Evolution

Grove et al. (1982) devised a method for comparing the compositions of basalts with experimental data on liquidus phase relations, particularly based on experiments with mid-ocean-ridge basalts. Both the composition and experimental data are treated in a normative tetrahedron olivine - calcic pyroxene - plagioclase - quartz, and are then plotted on a projection from plagioclase onto the olivine (Oliv) - calcic pyroxene (Cpx) - quartz (Qtz) base as in Figure 6.6. This shows fields of primary co-saturation of liquids with plagioclase and each of the phases olivine (oliv), augite (aug), pigeonite (pig), and orthopyroxene (opx). The 1 atmosphere field boundaries are the dark solid curves and the fields of primary crystallization at 1 kbar p_{H2O} are shown dashed. The plagioclase-orthopyroxene- calcic pyroxene plane that separates olivine-normative from quartz-normative tholeiites appears in the plagioclase projection of Figure 6.6 as the orthopyroxene - calcic pyroxene line. The approximate compositions of augite (Aug), pigeonite (Pig), and orthopyroxene (Opx) coexisting with plagioclase, olivine, and liquid at 1 atmosphere are also plotted.

All except one analysis (CS) of the central Massachusetts diabases plot within the triangle olivine-clinopyroxene-quartz and hence are tholeiites, but are clearly split into those that are quartz-normative and those that are olivine-normative. The analyses from the Holden, Pelham-Loudville and Ware systems all plot in the projected olivine field of primary crystallization, yet show little to no olivine in their mineralogy. No olivine was found at all in thin section in the Holden system. In the Pelham-Loudville and Ware systems olivine was found in a few samples and there is the suggestion of a pertectic reaction relationship in which olivine appears to have reacted with liquid to produce augite and pigeonite. The presence of biotite could explain some normative olivine, because it is a silica undersaturated mineral. The Bliss Hill diabases plot in two distinct areas. The northern diabase (4I4) is olivine-normative and contains relict olivine. The southern diabase (BH) is quartz-normative. The Quabbin Reservoir diabases are the only diabases with abundant phenocrysts of olivine and with one exception all plot in the olivine-normative field. The exception is from a chilled margin, which may not have contained any phenocrysts of olivine. The Quabbin Reservoir diabases also have abundant augite in the matrix.

Curiously, the Holden, Pelham-Loudville, and Ware diabases lie on trends that are parallel to the olivine-clinopyroxene boundary suggesting that the chemistry in these systems was controlled by co-saturation with both these phases. This fact is puzzling for the Holden system in that the dominant primary phenocryst phase is orthopyroxene. The Pelham-Loudville and Ware systems plot nearly perfectly on the olivine-clinopyroxene (+plagioclase) boundary at 1 kbar p_{H2O}. At 1 kbar p_{H2O} the Holden system plots above the olivine-clinopyroxene boundary and in the field of augite (+plagioclase). Biotite is present in the thin sections from these systems that appears to be magmatic. This would support some H_2O present in the system. A completely different suggestion is presented by the studies of McKenzie and Bickle (1988) on the composition of melt generated by lithospheric extension. The suggestion is that these linear trends are unrelated to crystal saturation during cooling, but represent mixing lines between early liquids of deep-seated origin and later liquids of shallower origin, all produced by continuous decompressive melting of the same mantle source (see especially their Figures 11 and 20).

These brief observations plus other features in the geochemistry, particularly in the Holden system, suggest there is a range of intriguing petrogenetic problems yet to be solved in these diabases.

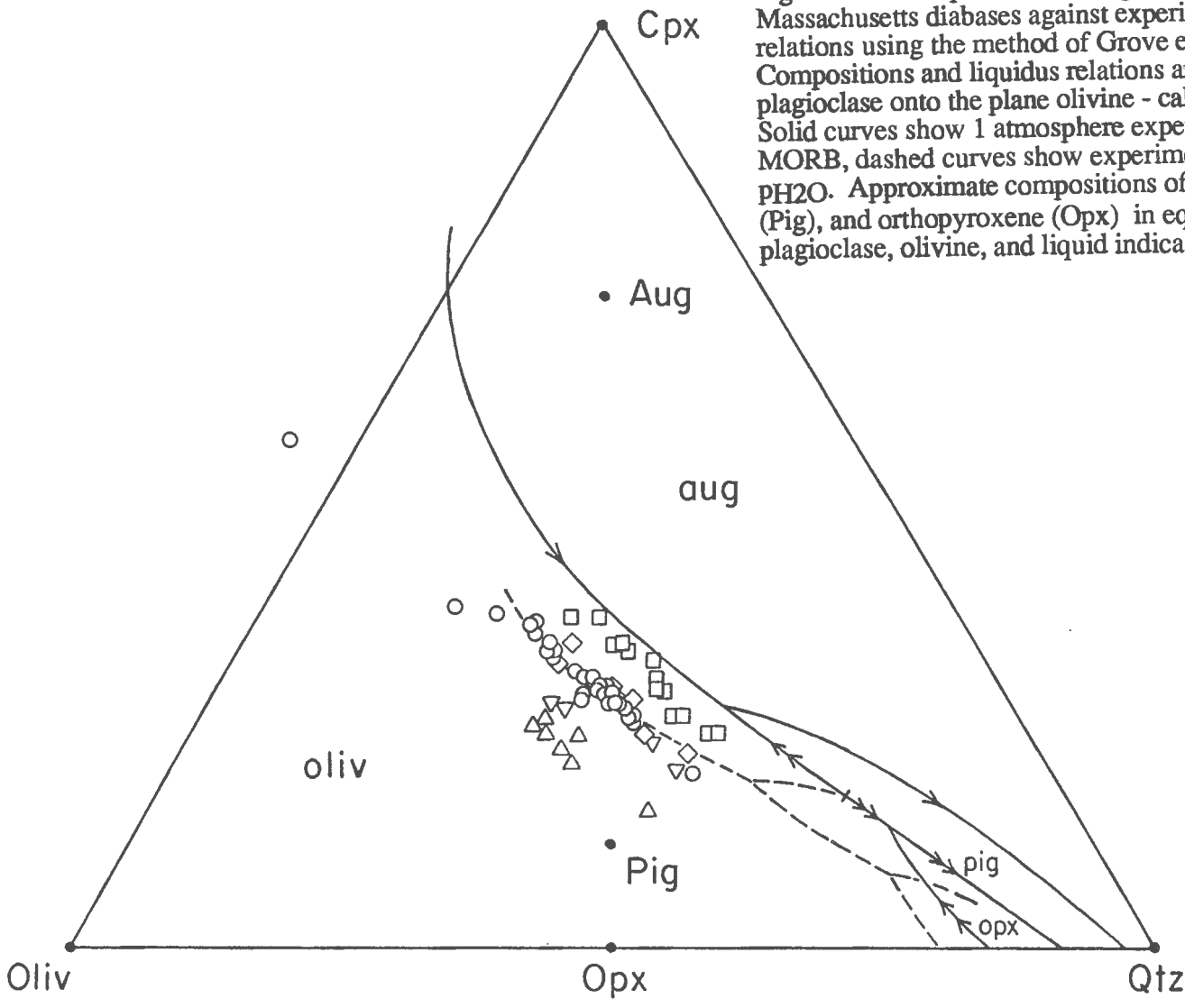

Figure 6.6 Comparison of compositions of central Massachusetts diabases against experimental liquidus phase relations using the method of Grove et al. (1982). Compositions and liquidus relations are projected from plagioclase onto the plane olivine - calcic pyroxene - quartz. Solid curves show 1 atmosphere experimental data for MORB, dashed curves show experimental data for 1 kbar pH2O. Approximate compositions of augite (Aug), pigeonite (Pig), and orthopyroxene (Opx) in equilibrium with plagioclase, olivine, and liquid indicated.

CHAPTER 7

CONCLUSIONS

The present study has led to the following conclusions.

1. The central Massachusetts diabases fall into five petrographically distinct systems or groups, the Holden system, the Pelham-Loudville system, the Ware system, the Bliss Hill group and the Quabbin Reservoir group. All are are quartz-normative or olivine-normative tholeiites.

Chilled margins of the Holden system contain phenocrysts of plagioclase, Mg-rich orthopyroxene, augite and pigeonite in a matrix of plagioclase, clinopyroxene, red-brown biotite, skeletal to euhedral grains of titanomagnetite (C1 to C2), discrete grains of ilmenite, pyrite and chalcopyrite. The interiors contain grains of pigeonite rimmed by augite, indicating a peritectic relationship. The local micrographic intergrowths of quartz and alkali feldspar, common to all the interior samples, probably represent interstitial residual liquid of granitic composition.

Chilled margins of the Pelham-Loudville diabases contain phenocrysts of plagioclase, augite and pigeonite, and microphenocrysts of olivine rimmed by augite and pigeonite, in a matrix of plagioclase, augite, pigeonite, titanomagnetite, ilmenite,.pyrite, chalcopyrite, and biotite. Titanomagnetites are classified C1-C3, and range from skeletal arrangements with herring-bone texture, to euhedral crystals to fine-grained titanomagnetite dust. The internal titanomagnetite textures include lit-par-lit, and "vermiform". Locally there are thin veins or dikelets containing red-brown high temperature biotite and olive-green hornblende.

Chilled margins of the Ware system contain phenocrysts of plagioclase, augite and pigeonite, and microphenocrysts of olivine rimmed by clinopyroxene, indicating a reaction relationship between olivine and liquid. The matrix is composed of plagioclase, augite and pigeonite, devitrified glass, straw-colored oxidized glass and fine-grained herring-bone skeletal titanomagnetite (C1). Most of the titanomagnetite grains in the interior of the diabases are classified as C3. There are rare discrete grains of ilmenite and common sulfides. A distinguishing feature of this system, as compared to other systems is the marked abundance of pigeonite relative to augite.

The northern Bliss Hill dike contains phenocrysts of plagioclase, augite, orthopyroxene, and relict olivine. The matrix consists of plagioclase, clinopyroxene, titanomagnetite (C2 to C3), oxide-charged devitrified glass, amygdules filled with calcite or devitrified glass, ilmenite and pyrite. The southern Bliss Hill dike contains phenocrysts plagioclase, augite and orthopyroxenes. The matrix consists of plagioclase, titanomagnetite (C1 to C2), devitrified glass, amygdules and trace amounts of pyrite, pyrrhotite, and ilmenite.

The chilled margins of the Quabbin Reservoir diabases contain phenocrysts of plagioclase, and skeletal olivines. The matrix consists of plagioclase laths, clinopyroxenes, amygdules, and magnesium-rich titanomagnetites of several generations, some with blue-gray chrome spinel cores. Very few oxidation exsolution lamellae are present and the titanomagnetites are classified C1 to C2. Petrographically, these Quabbin Reservoir diabases are distinct from the other Massachusetts diabases in the presence of abundant phenocrystic olivine, and the chrome spinel cores in titanomagnetites. The presence of amygdules in the Bliss Hill and Quabbin Reservoir diabases as contrasted to the more abundant Jurassic diabases, may be characteristic of a shallower level of intrusion in the Cretaceous than in the Jurassic.

2. Instead of a few isolated occurrences, there is a swarm of Jurassic dikes near Loudville, west of the Hartford basin, belonging to the Pelham-Loudville system.

3. One sill near French King Bridge in the Millers Falls area of the Pelham-Loudville system is geochemically and paleomagnetically a part of the Ware system that is mainly exposed 35 km to the southeast.

4. The Holden, Pelham-Loudville, and Ware systems of Jurassic age have distinct chemical signatures that represent different magmatic sources.

5. The diabases of Bliss Hill north and Quabbin Reservoir groups of Early Cretaceous age are chemically more enriched and possibly implying a deeper source.

6. The Bliss Hill south diabase may represent a Late Jurassic intrusion. The K-Ar age is 152 m.y., though it is geochemically similar to the Bliss Hill north diabase. The paleomagnetic pole is not conclusive and may be transitional in nature. It is petrographically distinct from the Bliss Hill north diabase.

7. Of the forty sites sampled, thirty-two sites yield stable directions after alternating field cleaning techniques. These directions were confirmed by representative samples from each system that were thermally cleaned.

8. The new paleomagnetic and radiometric data on the Quabbin Reservoir and Bliss Hill diabases provide the first evidence of Cretaceous igneous activity in Massachusetts. This extends the New-England - Quebec Cretaceous igneous province south into Massachusetts.

9. All the Jurassic diabases are of normal polarity. The Cretaceous diabases are of mixed polarity. The reversed Quabbin Reservoir sites have directions that are consistent with other well dated igneous intrusions in New England (McEnroe et al 1987).

10. There are four distinct paleopole positions found for the diabases in this study. The two Early Jurassic poles from the Holden and Pelham-Loudville systems are in good agreement with May and Butler's (1986) APWP and fall on opposite sides of the J1 cusp. The Middle Jurassic pole would be in agreement with Irving and Irving's (1982) APWP for North America , but not with May and Butler's APWP (1986). The Cretaceous intrusions are all displaced north of all APWP for North America. These pole positions are supported by recent work in Cretaceous intrusions in the White Mountains by Van Fossen and Kent (1988) and other workers. If these pole positions are accurate and correct, then they would indicate a short and smoother track for North America from the Early Jurassic to the Cretaceous. This would also imply that North America arrived near to the present day position in the Cretaceous.

11. The conflicting results of the geochemical discriminant diagrams, may indicate relatively unusual and little sampled thermal-tectonic regimes during the generation of some of the eastern North America Mesozoic diabases. The differences may well reflect significant changes of regime over the extended period from earliest Jurassic through the early Cretaceous. Perhaps the best current interpretation for the eastern North American diabases, as stated by J. A. Philpotts (1985), calls for a number of mantle source regions. This would be in agreement with the diversity of Mesozoic diabases in central Massachusetts.

12. This study points to the need to reevaluate the Newark trend I and II paleomagnetic data and group these data by rock geochemistry, and not by geographic trend as done by previous workers. This study also points to the critical need for additional Early Jurassic through Cretaceous paleomagnetic data to constrain the Mesozoic APWP for North America.

REFERENCES

Armstrong, R.L. and Besancon, J., 1970, A Triassic time scale dilemma: K-Ar dating of Upper Triassic mafic igneous rocks, eastern U. S. A. and Canada and post Triassic plutons, Western Idaho, U. S. A.: Eclogae Geologicae Helvetiae, 63, p.15-38.

Ashenden, D.D., 1973, Stratigraphy and structure, northern portion of the Pelham Dome, north-central Massachusetts: Contribution No. 16 (M.S. thesis) Dept. of Geology, University of Massachusetts, Amherst, 132 p.

Balk, R., 1940, Preliminary report on the geology of the Quabbin Reservoir area, Massachusetts: U.S. Geological Survey open-file report, 58.p.

Beck, M.E., Jr., 1972, Paleomagnetism of Upper Triassic diabase from Pennsylvania: further results: Journal of Geophysical Research, v. 77, p. 5673-5687.

Bell, H., Brooks, K.G., Daniels, D.L., Hoff, W.E., Jr., and Popenoe, P., 1980, Diabase dikes in the Haile-Brewer area, South Carolina and their magnetic properties: U.S. Geological Survey Professional Paper 1123A-D, p. C 1-17.

Bell, R.E., Karner, G.D., and Steckler, M.S., 1989, Gravity anomalies, detachments and the source of mafic materials associated with the Early Mesozoic basins of eastern North America: Geological Society of America Abstracts with Programs, v. 21, p. 4.

Bougault, H.,1980, Contribution des elements de transition a la comprehension de la genese des basalts oceaniques: Ph.D. thesis, Universite de Paris VII, 221p.

Bougault , H., and Treuil, M., 1980, Mid-Atlantic ridge: zero-age geochemical variations between Azores and 22^{0}N: Nature, V. 286, p. 209-212.

Bowker, D.E., 1960, Remanent magnetization of eastern United States Triassic rocks: Ph.D. thesis, Massachusetts Institute of Technology, Cambridge Massachusetts, 186 p.

Brown, L.L., 1979, Magnetic observations of the red beds of the northern Connecticut Valley-DRM or CRM? (abstract): EOS, v. 60, p. 815.

Brown, L.L., 1988, Multicomponent paleomagnetic directions from the Sugarloaf Arkose, Deerfield basin, Massachusetts: Geological Society of America Abstracts with Programs, v. 20, p. 10.

Carmichael, C.M., and Palmer, H.C., 1968, Paleomagnetism of the Late Triassic North Mountain Basalt of Nova Scotia: Journal of Geophysical Research, v. 73, n. 8, p. 2811-2822.

De Boer, J. Z., 1967, Paleomagnetic-tectonic study for Mesozoic dike swarms in the Appalachians: Journal of Geophysical Research, 72, p. 2237-2250.

De Boer, J. Z., 1968, Paleomagnetic differentiation and correlation of the Late Triassic volcanic rocks of the central Appalachians (with special reference to the Connecticut Valley): Geological Society of America Bulletin, v. 79, p. 609-626.

DeJournett, J.D., and Schmidt, V.A., 1975, Paleomagnetism of some peridotite dikes near, Ithaca, New York (abstract): EOS, v. 56, p.354.

Dooley, R.E., and Smith, W.A., 1982, Age and magnetism of diabase dikes and tilting of the Piedmont: Tectonophysics, v. 90, p. 283-307.

Dooley, R.E., and Wampler, J.M., 1983, Potassium-argon relations in diabase dikes of Georgia: the influence of excess ^{40}Ar on the geochronology of the early Mesozoic igneous and tectonic events: U.S. Geological Survey Professional Paper 1313, M1-M24.

DuBois, P. M., Irving, E., Opdyke, N.D., Runcorn, S.K, and Banks, M.R.,1957, The geomagnetic field in the Upper Triassic times in the United States: Nature, v.180, p. 1186-1187.

Dungan, M.A., and Rhodes, J.M., 1978, Residual glasses and melt inclusions in basalts from DSPD leg 45 and 46: evidence for magma mixing: Contributions to Mineralogy and Petrology, v.67, p. 417-431.

Elbert, D. C., 1986, Recognition and implications of a structurally inverted Monadnock-Western Maine stratigraphy directly above the core of the Bernardston Nappe, Hinsdale, New Hampshire: Geological Society of America Abstracts with Programs, v. 18, p.15.

Fahlquist, F., 1935, Geology of region in which Quabbin Aqueduct and Quabbin Reservoir are located: Appendix of Chief Engineer, Annual Report of the Metropolitan District Water Supply Commission, Commonwealth of Massachusetts, Public Document No. 147.

Field, M.T., 1975, Bedrock geology of the Ware area, central Massachusetts: . Contribution No. 22, (Ph.D. thesis), Department of Geology, University of Massachusetts, Amherst, 186p., 6 plates.

Fisher, R., 1953, Dispersion on a sphere: Proceedings of the Royal Society, Ser. A., v. 217, p.295.

Foland, K.A., and Faul, H., 1977, Ages of the White Mountain intrusives - New Hampshire, Vermont, and Maine, U.S.A.: American Journal of Science, v. 277, p. 888-904.

Foland, K.A., Gilbert, L.A., Sebring, C.A., and Jiang-Feng, C., 1986, $^{40}Ar/^{39}Ar$ ages for plutons of the Monteregian Hills, Quebec: evidence for a single episode of Cretaceous magmatism: Geological Society of America Bulletin, v. 97, p.966-974.

Foland, K.A., Jiang-Feng,C., Gilbert, L.A., and Hoffman, A.W., 1988a, Nd and Sr isotopic signatures of Mesozoic plutons in north-eastern North America: Geology, v. 16, p. 684-687.

Globerman, B.R., and Irving, E., 1988, Mid-Cretaceous paleomagnetic reference field for North America: Restudy of 100 Ma intrusive rocks from Arkansas: Journal of Geophysical Research, v. 92, 11,721 - 11,733.

Gordon, R.G., Cox, A., and O'Hare, S., 1984, Paleomagnetic Euler poles and apparent polar wander and absolute motion of North America since the Carboniferous: Tectonics, v. 3, 499-537.

Grove, T.L., and Bryan, W.B., 1983, Fractionation of pyroxene-phyric MORB at low pressure: an experimental study: Contributions to Mineralogy and Petrology, v. 84, p. 293-309.

Grove, T.L., Gerlach, D.C., and Sando, T.W., 1982, Origin of calc-alkaline series lavas at Medicine Lake volcano by fractionation, assimilation and mixing: Contributions to Mineralogy and Petrology, v.80, p. 160-182.

Haggerty , S.E., 1976, Oxidation of opaque mineral oxides in basalts: in Rumble, D. III, editor, Reviews in Mineralogy, V. 3, Oxide Minerals: Mineralogical Society of America, Blacksburg, VA., p. Hg.1- Hg.100.

Heinrich S.M., 1980, Chemistry and mineralogy of the Holyoke Basalt at East Mountain, Holyoke Massachusetts: Senior honors thesis (unpub.), Department of Geology, University of Massachusetts, 47 p.

Hermes, O.D., Rao, J.M., Dickenson, M.P., and Pierce, T.A., 1984, A transitional alkalic dolerite suite of Mesozoic age in southeastern New England: Contributions to Mineralogy and Petrology, v. 86 p. 386-397.

Hodych, J.P., and Hayatsu, A., 1980, K-Ar isochron age and paleomagnetism of diabase along the trans-Avalon aeromagnetic lineament of Late Triassic rifting in Newfoundland: Canadian Journal of Earth Sciences, v. 17, p. 491-499.

Hubert, J.H., Reed, A.A., Dowdall, W.L., and Gilchrist, J.M., 1978, Guide to the Mesozoic redbeds of central Connecticut: Guidebook No.4, State Geological and Natural History Survey of Connecticut, Dept. of Environmental Protection, 129p.

Husch J.E., and Roth, E.A., 1988, Multiple magma pulses and the petrogenesis of the early Jurassic diabases in the Newark Basin: Geochemical and petrographic evidence from the Lambertville sill, New Jersey: Geological Society of America Abstracts with Programs, v. 20, , p. A156.

Husch, J.M. Sturgis, D.S., and Bambrick, T.C.,1984, Mesozoic diabases from west-central New Jersey: Major and trace element geochemistry of whole-rock samples: Northeastern Geology, v. 6, p. 51-63.

Irving, E., and Irving G.A., 1982, Apparent polar wander paths: Carboniferous through Cenozoic and the assembly of Gondwana: Geophysical Survey, v. 5, p.141-188.

Jansa, L.F., and Pe-Piper, 1988, Middle Jurassic to Early Cretaceous igneous rocks along eastern North American continental margin: American Association of Petroleum Geologists Bulletin, v. 72, p. 347-366.

King, P.B., 1961, Systematic pattern of Triassic dikes in the Appalachian region: U.S. Geological Survey Professional Paper 424-B, p. B93-B95.

Klitgord, K.D., and Schouten, H., 1986, Plate kinematics of the central Atlantic: in Vogt, P.R., and Tucholke, B.E., Editors: The Geology of North America, Volume M,The Western North Atlantic Region, Geological Society America, Boulder, Colorado, p. 351-378.

Lambert, R.St.J., Pe-piper, G., and Jansa, L.F., 1988, Sr, Nd, and Pb isotopic data from Mesozoic volcanic suites on the eastern North American continental margin: Geological Association of Canada Programs with Abstracts, v. 13, p. A71.

Lapointe, P.L., 1979, Paleomagnetism of the Notre Dame bay lamphrophyre dikes, Newfoundland, and the opening of the North Atlantic Ocean: Canadian Journal of Earth Sciences, v., 16, p. 1823-1831.

Larochelle, A., and Wanless, R.K., 1966, The paleomagnetism of a Triassic diabase in Nova Scotia: Journal of Geophysical Research, v.71, p. 4949

Lofgren, G., 1974, An experimental study of plagioclase crystal morphology: Isothermal crystallization: American Journal of Science, v. 274, p. 243-273.

Macdonald, G.A., and Katsura, T., 1964, Chemical composition of Hawaiian lava: Journal of Petrology, v.5, p. 82-133.

Manspeizer, W., 1988, Triassic-Jurassic rifting and opening of the Atlantic: An overview: in Manspeizer, W., editors, Triassic-Jurassic rifting: North America and North Africa: Elsevier Science Publishers,.Amsterdam.

Manspeizer, W., and Cousminer H.L., 1988, Late Triassic-Early Jurassic synrift basins of the U.S. Atlantic margin: in Sheridan R.E., and Grow, A.J., editors., The geology of North America vol. 1-2, The Atlantic continental margin: The Geological Society of America p.197-216.

May, S. R., and Butler, R.F., 1986, North American Jurassic apparent polar wander: implications for plate motion, paleogeography and Cordilleran tectonics: Journal of Geophysical Research, v. 91, p. 11519-11544.

McEnroe, S. A., 1988, Diversity in paleomagnetism, geochemistry and age in Mesozoic diabase intrusions, central Massachusetts: Geological Society of America Abstracts with Programs, v. 20, p. 55.

McEnroe, S.A. and L.L. Brown, 1987, Paleomagnetism of diabase dikes and sills intruding pre-Mesozoic basement rocks near and east of the Connecticut Valley Mesozoic basins, west-central Massachusetts (abstract): EOS, v. 68, p. 295.

McEnroe, S.A. and L.L. Brown, 1988, Paleomagnetism of Mesozoic diabase intrusions and redbeds in central Massachusetts: Relations to the APWP for North America: Geological Society of America Abstracts with Programs, v. 20, p. A351.

McEnroe, S.A., Robinson, Peter., Brown, L.L., and Foland, K.A., 1987, Paleomagnetic discovery of Cretaceous diabase dikes in central Massachusetts: Geological Society of America Abstracts with Programs, v. 19, p.765.

McHone, J.G, and Butler, J.R., 1984, Mesozoic igneous province of New England and the opening of the Atlantic Ocean: Geological Society of America Bulletin, v. 94, p. 757-765.

McHone, J.G., and Trygstad, J.C., 1982, Mesozoic mafic dikes of southern Maine: Maine Geological Bulletin, v. 2, p.16-32.

McKenzie, D. and Bickle, M.J., 1988, Melt generated by lithospheric extension: Journal of Petrology, v.29, p. 625-679.

McIntosh, W.C., Hargraves, R.B., and West, C.L., 1985, Paleomagnetism and oxide mineralogy of Upper Triassic to Lower Jurassic red beds and basalts in the Newark Basin: Geological Society of America Bulletin, v. 96, p. 463-480.

Menzies, M. A.and Hawkesworth, C. J., 1987, Mantle Metasomatism: Academic Press, New York, 472 p.

Meschede, M., 1986, A method of discriminating between different types of mid-Ocean ridge basalts and Continental tholeiites with the Nb-Zr-Y diagram: Chemical Geology, v. 56, 207-218.

Norrish, K., and Chappell, B.W., 1967, X-Ray fluoresence spectrometry: in Zussman, J., ed., Physical Methods in Determinative Mineralogy, Academic Press, p. 201-272.

Norrish, K., and Hutton, J.T., 1969, An accurate X-Ray spectrographic method for the analysis of a wide range of geological samples: .Geochimica et Cosmochimica Acta, v. 33, p. 431-454.

Olsen, P.E., 1986, A 40 - million - year lake record of Early Mesozoic orbital climate forcing: Science, v. 234, p. 789-912.

Opdyke, N.D., 1961, The paleomagnetism of the New Jersey Triassic: a field study of the inclination error in red sediments: Journal of Geophysical Research, v. 66, p. 1941-1949.

Opdyke, N.D., and Wensink, 1966, Paleomagnetism of rocks from the White Mountain plutonic-volcanic series in New Hampshire and Vermont: Journal of Geophysical Research, v. 71, p. 3045-3051.

Peachy, C., 1983, Geochemistry of basaltic tholeiitic dikes in the basement rocks adjacent to the Connecticut Valley: A special studies thesis (unpublished), Smith College, Northampton, Massachusetts, 43p.

Pearce J. A., 1975, Basalt geochemistry used to investigate past tectonic environments on Cyprus: Tectonophysics, v. 25, p. 41-67.

Pearce, J.A., 1983, Role of the sub-continental lithosphere in magma genesis at active continental margins: in Hawkesworth, C.J. and Norry, M.J., Editors, Continental Basalts and Mantle Xenoliths, Shiva Publishing Co., Cheshire, U.K., p. 290-300.

Pearce, J.A., and Cann, J.R., 1971, Ophiolite origin investigated by discriminant analysis using Ti, Zr, and Y: Earth and Planetary Science Letters, v. 12, p. 339-349.

Pearce, J. A., and Cann J. R., 1973, Tectonic setting of basic volcanic rocks determined using trace element analyses: Earth and Planetary Science Letters, v. 19, p. 290-300.

Pearce, J.A., and Norry, M.J., 1979, Petrogenetic implications of Ti, Zr, Y, and Nb variations in volcanic rocks: Contributions to Mineralogy and Petrology, v. 69, p. 33-47.

Pegram, W. J., 1983, Isotopic characteristics of Mesozoic Appalachian tholeiites: Geological Society of America Abstracts with Programs, v. 15, p.660.

Pegram, W. J., 1986, The isotope, trace element, and major element geochemistry of the Mesozoic Appalachian tholeiite province: Ph.D. thesis, Massachusetts Institute of Technology,Cambridge, Massachusetts, 622 pp.

Peper, J.D., 1966, Stratigraphy and structure of the Monson area, Massachusetts and Connecticut: Ph.D. thesis, University of Rochester, Rochester, N.Y., 127p.

Philpotts A.R., and Reichenbach, Ingrid, 1985, Differentiation of Mesozoic basalts of the Hartford basin,Connecticut: Geological Society of America Bulletin, v.96, p. 1131-1139.

Philpotts, A.R., and Martello, A., 1986, Diabase feeder dikes for the Mesozoic basalts in southern New England: American Journal of Science, v. 286, p. 105-126.

Philpotts, J.A., 1985, Pearce-Cann discriminant diagrams applied to the North American Mesozoic diabases: in Robinson, G.R., and Froelich, A.J., Editors, Proceedings of the Second U.S. Geological Survey Workshop on the Early Mesozoic Basins of the Eastern United States: U. S. Geological Survey Circular 946, p.114-117.

Pierce, T.A., 1970, Petrology of dolerite-metadolerite dikes of southeastern New England: M.S. thesis, University of Rhode Island, Kingston, 128 p.

Puffer J.H., Hurtubise, D.O., Geiger, F.J., and Lecher, Paul, 1981, Chemical composition and stratigraphic correlation of the Mesozoic basalt units of the Newark basin, New Jersey and the Hartford basin, Connecticut: Geological Society of America Bulletin, v. 93, p. 515-553.

Ratcliffe N. M., and Burton B. C., 1985, Fault reactivation models for the origin of the Newark Basin and studies related to eastern U. S. seismicity: in Robinson, G. R. and Froelich, A.J., Editors, Proceedings of the Second U.S. Geological Survey Workshop on the Early Mesozoic basins of the Eastern United States: U. S. Geological Survey Circular 946, p.36-45.

Rigotti, P.A., 1976, The paleomagnetism of the Palisade Sill and the development of the ARM correction method of paleointensity determination: Ph.D. thesis, University of Pittsburg, Pittsburg, Pennsylvania, 258 p.

Robinson, Peter, 1963, Gneiss domes of the Orange area, Massachusetts and New Hampshire: Ph.D. thesis, Harvard University, 253 p.

Robinson, Peter, 1986, Introduction: in Robinson and Elbert, Editors, Field trip guidebook: regional metamorphism and metamorphic phase relations in northwestern and central New England: Field Trip B-5, International Mineralogical Association, 14th General Meeting at Stanford University, Contribution No. 59, Department of Geology and Geography, University of Massachusetts, Amherst, Massachusetts, p. 1-10.

Seidemann, D.E., Masterson, W.D., Dowling M.P., Turekian, K.K., 1984, K-Ar dates and $^{40}Ar/^{39}Ar$ age spectra for the Mesozoic flows of the Hartford basin, Connecticut, and the Newark basin, New Jersey: Geological Society of America Bulletin, v. 95, p. 594-598.

Sequin, M.K., Rao, K.V., Venugopal, D.V., and Gahe, E., 1981, Paleomagnetism of parts of the late Triassic diabase dike system associated with the trans-New Brunswick aeromagnetic lineament: Canadian Journal of Earth Sciences., v. 18, p.1776-1786.

Shervais, J.W., 1982, Ti-V plots and the petrogenesis of modern and ophiolitic lavas: Earth and Planetary Science Letters, v.59, p.101-118.

Smith W.A., 1987, Paleomagnetic results from a crosscutting system of northwest and north-south trending diabase dikes in the North Carolina Piedmont: Tectonophysics, 136, p. 137-150.

Smith, R.C., II, Rose, A.W., and Lanning, R.M., 1975, Geology and geochemistry of Triassic diabase in Pennsylvania: Geological Society of America Bulletin, v. 86, p. 943-955.

Smith, T.E., 1976, Paleomagnetic reversal in the Lower Mesozoic Medford diabase of eastern Massachusetts (abstract): EOS, v. 58, p. 376.

Smith, T.E., 1976, Paleomagnetic study of lower Mesozoic diabase dikes and sills of Connecticut and Maryland: Canadian Journal of Earth Sciences, v. 13, 567-609.

Smith, T.E., and Noltimier, H.C., 1979, Paleomagnetism of the Newark trend igneous rocks of the north-central Appalachians and the opening of the central Atlantic Ocean: American Journal of Science, v. 279, p. 778-807.

Steckler, G.R., and Karner G,D., 1988, The distribution of extension with depth in the Newark basin: Geological Association of Canada Programs with Abstracts, v. 13, p. A117.

Sutter, J.F., 1985, Progress on geochronology of Mesozoic diabases and basalts, in Robinson, G.R., and Froelich, A.J., Editors, Proceedings of the Second U.S. Geological Survey Workshop on the Early Mesozoic Basins of the Eastern United States: U. S. Geological Survey Circular 946, p. 110-113.

Sutter, J.F. and Smith, T.E., 1979, $^{40}Ar/^{39}Ar$ ages of diabase intrusions from the Newark basins in Connecticut and Maryland: initiation of central Atlantic rifting: American Journal of Science, v. 279, p. 808-831.

Tarling, D., 1983, Paleomagnetism: Chapman and Hall Limited, London.

Tucker, R.D., 1977, Bedrock geology of the Barre area, central Massachusetts: Contribution No. 30 (M.S. thesis), Department of Geology and Geography, University of Massachusetts, Amherst, 132 p., 5 plates.

Van Fossen, M.C., and Kent, D.V.,1988, New paleomagnetic results from Jurassic and Cretaceous White Mountain igneous rocks of New England (abstract): EOS, v. 69, p.342.

Watts, D., and Noltimier, H.C., 1974, Paleomagnetic study of diabase dikes in the inner Piedmont of North Carolina and Georgia (abstract): EOS, v. 55, p. 675.

Weigand, P. W., and Ragland P. C., 1970, Geochemistry of Mesozoic dolerite dikes from eastern North America: Contributions to Mineralogy and Petrology, v. 29, p. 195-214.

Yoder, H.S., and Tilley, C.E., 1962, Origin of basaltic magmas: An experimental study of natural and synthetic rock systems: Journal of Petrology, v. 3, p. 342-532.

Zen, E-an, Goldsmith, R., Ratcliffe, N.M., Robinson, P., and Stanley, R.S., 1983, Bedrock geological map of Massachusetts, U.S. Geological Survey, Washington, D. C.